L'histoire de la pollution atmosphérique européenne déduite des carottes glaciaires alpines

Susanne Preunkert

CENTRE NATIONAL DE LA RECHERCHE SCIENTIFIQUE

LABORATOIRE DE GLACIOLOGIE ET GEOPHYSIQUE DE L'ENVIRONNEMENT

Associé à l'UNIVERSITE JOSEPH FOURIER - GRENOBLE I

History of European air pollution inferred from Alpine ice cores

Susanne PREUNKERT

Thèse de doctorat de l'Université Joseph Fourier - Grenoble I
(Arrêtés ministériels du 5 Juillet 1984 et 30 mars 1992)

Spécialité : Sciences de la Terre et de l'Univers

Date de la soutenance : 27 juillet 2001

Composition du jury :

M.	Michel Campillo	President
M.	Eric Wolff	Reviewer
M.	Hans Puxbaum	Reviewer
M.	Dietmar Wagenbach	Examinator
M.	Michel Legrand	Director of Thesis

Laboratoire de Glaciologie et Géophysique de l'Environnement - CNRS
Tél (33) 04.76.82.42.00 - Fax (33) 04.76.82.42.01
54, Rue Molière - BP 96 - 38402 Saint Martin d'Hères Cedex France

Contents

Résumé

La possibilité de reconstruire l'histoire de la pollution atmosphérique Européenne a été exploré au Col du Dôme (CDD) (4250 m d'altitude, Massif du Mont Blanc). Pour cela une carotte de 126 m a été analysé à haute résolution pour les ions majeurs, le F^- et les carboxylates, et des mesures atmosphériques continues de l'aérosol effectuées sur le site (Observatoire Vallot). Ceci a montré que des informations atmosphériques peuvent être obtenues avec une résolution saisonnière à partir de la glace du CDD et ce au moins sur les 80 dernières années mais que des précautions sont à prendre pour tenir compte du fluage de la glace lors de l'interprétation de ces signaux en terme de changements atmosphériques.

Les enregistrements "glace" montrent que les valeurs estivales de SO_4^{2-} suivent l'évolution des émissions anthropiques de SO_2 des pays situés à 1000 km autour des Alpes tandis qu'en hiver elles reflètent plus la contamination diffuse de la troposphère libre à l'échelle de l'Europe entière. En utilisant la relation "air/neige" obtenue à Vallot, les concentrations atmosphériques passées de SO_4^{2-} ont été reconstituées et comparées aux simulations des modèles de chimie. Nous avons estimé que les émissions naturelles représentent environ 20% des émissions actuelles de NO. L'évolution passé de NO_3^- est en bon accord avec l'histoire des émissions anthropiques de NO de l'Europe, il n'en va pas de même pour NH_4^+ dont la tendance apparait plus importante que ce que l'on peut attendre avec les estimations actuelles d'émission anthropique de NH_3. Notre examen du budget de F^- et HCl montrent qu'en plus de la combustion du charbon, l'industrie de l'aluminium et l'incinérarion des déchets ont été les sources anthropiques majeures de ces composés entre 1935 et 1975, après 1960, respectivement. Finalement les sources naturelles semblent dominer le budget de l'oxalate depuis 80 ans tandis que le formate et l'acétate indiquent une tendance anthropique entre 1950 et 1980.

Abstract

The Col du Dôme (CDD) glacier site (4250 m asl, Mont Blanc massif), was investigated for its suitability to reconstruct the anthropogenic atmospheric perturbation over Europe. For that: (1) a 126 m long ice core was analysed in high resolution for major ions, fluor, and light carboxylates, (2) continuous year round measurements of key aerosol species were performed at the CDD site (Vallot Observatory). It is shown that atmospheric relevant information can be extracted in seasonal resolution from the CDD ice at least over the last 80 years, but also that special attention has to be paid on glacier flow effects when interpreting ice records from such a small scaled glacier site in terms of atmospheric changes.

The interpretation of the chemical CDD ice core records revealed that summer SO_4^{2-} changes at CDD follow closely the course of anthropogenic SO_2 emissions released within 1000 km around the Alps, while winter SO_4^{2-} changes reflect a more limited contamination of the free troposphere at the scale of total Europe. Using the firn/air relation established at CDD, past atmospheric SO_4^{2-} concentrations at 4300 m asl over Europe were reconstructed and compared to current atmospheric model simulations. The natural NO emissions was estimated to amount for ≈20% of the present-day NO budget. While temporal changes of CDD NO_3^- levels are in agreement with estimated NO emissions in western Europe, this is not true for NH_4^+ which appears to increase significantly stronger over the last 80 years than current ammonia emission estimates. The examination of the F^- and HCl budget revealed that in addition to coal burning, aluminium smelters and waste incineration were the major anthropogenic sources of these species between 1935 and 1975, after 1960, respectively. Finally it was shown that natural inputs dominate here the oxalate budget over the last 80 years, whereas for acetate and formate a significant anthropogenic contribution occurred between 1950 and 1980.

Introduction

1. Remarques générales

De nombreuses espèces chimiques, dérivées des cycles du carbone (CO_2, CO, CH_4, hydrocarbures non méthaniques (NMHC), aérosols organiques), de l'azote (N_2O, NH_3, et NO_X), des halogènes (fluor et chlore) et des métaux, conditionnent le fragile équilibre des écosystèmes terrestres, de la composition chimique de l'atmosphère et du système climatique. Depuis le début de l'ère préindustrielle, l'activité humaine croissante (consommation des carburants fossiles, activités agricoles intensives, combustion de déchets et de biomasse, production de métaux) a modifié de façon significative le niveau naturel des espèces dérivées de ces cycles biogéochimiques.

En plus des gaz à effet de serre à longue durée de vie (comme par exemple CO_2, CH_4, N_2O et les CFCs), il est maintenant accepté que les espèces à durée de vie plus courte, comme par expemple l'ozone et les aérosols jouent un rôle clef dans le climat, en particulier aux échelles régionales. Par exemple, l'ozone, un gaz à effet de serre dont les concentrations sont contrôlées par les niveaux respectifs de NO_X, CO, CH_4 et des NMHCs, influence la capacité oxidante de l'atmosphère et contribue ainsi à déterminer la durée de vie atmosphérique de nombreuses espèces chimiques. Par leur effets directs (adsorption et diffusion du rayonnement solaire) et indirects (microphysique nuageuse), les aérosols jouent un rôle important sur le transfert radiatif et donc sur le climat. Ainsi, l'augmentation des concentrations d'aérosols due aux activitées humaines a probablement, en tout cas dans certaines régions, compensé l'augmentation parallèle du forçage radiatif par les gaz à effet de serre.

Pour quantifier l'impact des émissions anthropiques sur l'équilibre naturel de notre environnement, que ce soit le climat ou la composition de l'atmosphère, et pour prédire les changements futurs aux échelles globale et régionale, il est indispensable de connaître suffisamment bien les conditions naturelles (préindustrielles) et de savoir comment ces conditions ont été progressivement modifiées par l'homme pendant l'ère industrielle. Des mesures directes et de bonne qualité de la composition chimique de l'atmosphère et des précipitations n'existent que pour les dernières 10 à 40 années. A cette époque, les activités humaines avaient déjà commencé à modifier fortement les conditions naturelles. Ainsi, de grands efforts de recherche ont été entrepris pour extraire des paramètres environnementaux passés des cernes de croissance des arbres, des sédiments océaniques et lacustres, et des glaciers. Parmi ces archives, les glaciers froids jouent un rôle unique de par le fait qu'ils archivent, à haute résolution temporelle, de l'information climatique (par exemple des proxies de la précipitation et des températures) et atmosphérique (gaz dans les bulles d'air, aérosols piégés dans la glace) et ceci parfois sur des périodes allant jusqu'à des centaines de milliers d'années (Dansgaard et al., 1973; Delmas, 1992; Legrand et Mayewski, 1997).

Depuis 1965, la plupart des études dans ce domaine ont été concentrées sur les carottes de glace polaire provenant du Groenland et de l'Antarctique, qui ont le double avantage d'une géométrie glaciaire simple, représentative d'une grande échelle temporelle, et de températures de névé très basses. Des mesures des isotopes stables de l'eau (Dansgaard, 1954; Johnsen et al., 1972; Lorius et al., 1985; Jouzel et al., 1987; Dansgaard et al., 1993) du CO_2 (Delmas et al., 1980; Barnola et al., 1987) du CH_4 (Chappellaz et al., 1990 et 1997; Blunier et al., 1995) du N_2O (Flückiger et al., 1999) ainsi que du contenu en aérosols (voir Legrand et Mayewski, 1997 pour une synthèse) ont surtout été utilisées pour étudier l'histoire du climat et de l'environnement atmosphérique sur les derniers cycles climatiques. En ce qui concerne les enregistrements des 200 dernières années, les carottes de glace Groenlandaises ont archivé le changement de l'acidité de la précipitation. Par exemple, les données provenant du Groenland montrent une forte augmentation des concentrations de SO_4^{2-} et de NO_3^- pendant le 20e siècle (Neftel et al., 1985; Mayewski et al., 1986; Fischer et al., 1998b) ainsi qu'un doublement du niveau de CH_4 dans l'atmosphère depuis 1800 (Etheridge et al., 1998). Ces résultats ont clairement montré que des régions reculées et très faiblement peuplées de l'hémisphère Nord ont été perturbées depuis le début de l'ère industrielle. Néanmoins, des ambigüités importantes existent en ce qui concerne l'attribution des sources des espèces chimiques à courte durée de vie dans les dépôts de neige au Groenland. Ceci est dû aux interactions complexes entre le transport à longue distance vers le site de dépôt, le sort des précurseurs atmosphériques et les processus de déposition des produits finaux d'oxydation. Pour les aérosols soufrés, la comparaison entre les tendances à long terme dans la neige Groenlandaise avec les inventaires d'émissions de dioxyde de soufre d'origine anthropique suggère des contributions d'émissions d'Europe, de l'Asie et d'Amérique du Nord à travers de transport à longue distance (Fischer et al., 1998b). Comme le transport à longue distance depuis les régions industrialisées de l'hémisphère Nord vers le Groenland reste toujours assez mal simulé par les modèles globauw de transport, ces archives glaciaires Groenlandaises restent d'un intérêt limité pour celui qui veut contraindre les inventaires d'émission depuis les régions émettrices possibles. De ce point de vue, d'autres tendances à long terme, archivées dans des glaciers dans des régions qui sont plus directement influencées par les émissions provenant d'un continent donné, seraient plus adéquates pour contraindre précisément les inventaires d'émissions. De plus, afin de quantifier l'impact climatique des variations du contenu en aérosol au-dessus des régions tempérées et habitées, il est nécessaire de disposer d'enregistrements glaciaires aux latitudes moyennes. En ce qui concerne les sulfates, on pense que l'Europe occidentale et centrale, avec l'Est des Etats-Unis, est l'une des régions di globe où l'impact radiatif des aérosols est le plus important. De manière plus générale, des enregistrements passées d'espèces chimiques à durée de vie courte à différents sites glaciaires dans l'hémisphère Nord (mais aussi dans le Sud) seraient utile pour bon nombre d'études portant sur la quantification des changements climatiques régionaux, ainsi que pour

l'amélioration de notre faible connaissance des cycles atmosphériques de certaines espèces chimiques (par exemple les acides hydrochlorique, fluorhydrique, et carboxyliques) au-dessus des continents.

2. Le potentiel des carottages dans les glaciers froids de moyennes latitudes

En plus du Groenland et de l'Antarctique, certains glaciers en montagne sont froid (c'est à dire qu'ils ont des températures de névé à 10 mètres inférieures au point de fusion de la glace). Ils enregistrent ainsi convenablement (sans fonte) des paramètres environnementaux, ce qui rend possible la reconstruction de plusieurs aspects de la chimie passée dans plusieurs régions du monde. Ceci inclue des glaciers tropicaux comme par exemple la calotte du Huascaran dans les Andes Péruviennes (Thompson et al., 1995b), les calottes de Guliya (Thompson et al., 1995a) et de Dunde (Thompson et al., 1988) au Tibet, ainsi que la calotte de glace de Devon Island dans l'Arctique Canadien (Koerner, 1977), Mount Logan (Holdsworth et Peak, 1985) dans l'Ouest du Canada, et des sites alpins (Wagenbach, 1993b).

Plus spécifiquement, les enregistrements glaciaires provenant de glaciers froids des Alpes pourraient aider à quantifier l'impact des activités humaines sur les variations du climat et de l'environnement ainsi que les changements lents à l'échelle Européenne, car ces archives sont probablement intimement liées aux émissions provenant de l'Europe. Dans les Alpes, les glaciers convenables (c'est à dire non influencés de façon substantielle par la percolation d'eau de fonte) sont presqu'exclusivement situés bien au-dessus de 4000 m d'altitude donc très rares. Ils sont restreint à des petites surfaces dans les régions sommitales des massifs du Mont Rose, des Alpes Bernoises, du Grand Combin et du Mont Blanc (Funk, 1993).

Actuellement, de l'information obtenue à partir d'enregistrements glaciaires long-terme dans les Alpes provient surtout de la région du Mont Rose (Colle Gnifetti, 4450 m d'altitude) (Haeberli et al., 1983; Wagenbach, 1989). A cause du bilan de masse en surface relativement faible de l'ordre de 0.2 à 0.4 m d'équivalent en eau à ce petit site glaciaire, l'enregistrement s'étend sur plusieurs siècles. Les études portant sur la glace du Colle Gnifetti ont entre autres révelé une augmentation des concentrations de sulfate, de nitrate et d'ammonium au cours du 20e siècle (Wagenbach et Preunkert, 1996 (données de Jung, 1993); Döscher et al., 1996) ainsi qu'un signal anthropique clair dans les concentrations de plomb (Wagenbach et Preunkert, 1996 (données de Schajor, 1993)). Néanmoins, des problèmes liés au site de forage limitent une interprétation directe de ces enregistrements en termes d'environnement et climat passés (Wagenbach, 1993a):

- A cause de la faible surface du glacier (0.3 km^2) et une forte variabilité des caractéristiques de déposition au site (Preunkert, 1994), l'enregistrement glacaire est probablement affecté par l'écoulement du glacier.

- L'accumulation nette de neige sur le site est contrôlée par l'érosion éolienne, ce qui favorise l'accumulation de la neige à la fin du printemps et en été, la précipitation d'automne et d'hiver contribuant au mieuw à 20% de l'accumulation annuelle, Preunkert, 1994). Le signal d'hiver est donc plus ou moins absent.
- Des observations atmosphériques récentes menées sur des sites d'altitude au-dessus de 3000 m (Preunkert et Wagenbach, 1998; Baltensperger et al., 1997; Kasper et Puxbaum, 1998) ont montré que les teneurs en impuretés en hiver sont très faibles dû à la contamination très limitée des masses d'air d'altitude par celles de la couche limite à cette saison. Par contre, au printemps et en été, le transport convectif affecte de façon significative les sites d'altitude Alpins et conduit donc à des contenus en impuretés bien plus élevés. A cause de ces variations saisonnières des conditions atmosphériques et de l'accumulation irrégulière de neige, la représentativité de ces enregistrements glaciaires enterme de changements atmosphériques est parfois délicate.

Le programme de recherche Européen ALPCLIM visait à examiner la qualité de ces enregistrements Alpins en vue de leur interprétation en terme de signaux environmentaux. Les objectifs de ce programme étaient d'examiner plusieurs enregistrements glaciaires Alpins et d'évaluer validité pour en extraire des informations atmosphériques fiables. En plus des carottes de glace provenant du Col del Lys et du Colle Gnifetti dans le massif du Mont Rose, ce projet incluait aussi le site glaciaire du Col du Dôme à 4250 m d'altitude dans les régions sommitales du massif du Mont Blanc.

Dans le passé, des études glaciologiques (e.g. Lliboutry et al., 1976; Vincent et al., 1997) et des analyses de carottes de glace (e.g. Briat et al., 1978; Jouzel et al.,1984; De Angelis et Gaudichet, 1991) ont montré que le site du Col du Dôme, caractérisé par une accumulation annuelle de neige assez élevée (de l'ordre de 0.5 à 2.5 m d'eau equivalent), est potentiellement un endroit convenable pour des études de carottage glaciaires. Lors d'une étude pilote, entreprise à ce site en 1991 (Maupetit et al., 1995), la partie soluble des espèces chimiques a été analysée à haute résolution spatiale dans la neige des années 1988 à 1991. Cette étude a confirmé l'accumulation importante de neige et a montré des couches hivernales bien préservées. Contrairement au Colle Gnifetti, on s'attend ainsi à ce que ce site permette l'analyse des changements passés de la chimie atmosphérique sur au moins quelques décennies et ce avec une résolution temporelle saisonnière. Dans le cadre du programme ALPTRAC, deux forages profonds ont été effectués à ce site jusqu'au socle rocheux en 1994. L'une des deux carottes était destinée à l'étude des isotopes stables et à l'analyse des impuretés piégées dans la matrice de glace, tandis que l'autre était utilisé pour des mesures de gaz trace dans le cadre du programme ALPCLIM.

3. Etudes glaciochimiques effectués au Col du Dôme dans le cadre de ce travail

Dans ce contexte, le travail présent se focalise sur une étude glaciochimique d'une carotte de glace du Col du Dôme (CDD), ce qui inclue:

- l'étude des caractéristiques glaciologiques du site de forage du CDD afin d'établir s'il est convenable à des études de carottes de glace en relation avec la chimie atmosphérique au-dessus de l'Europe,
- l'établissement de la relation pour les espèces importantes qui lie les concentrations dans la neige récente à celle de l'atmosphère actuelle,
- la reconstruction détaillée (c'est à dire saisonnière) de la composition chimique de la neige et de ses variations sur les dernières décennies, et
- la discussion de ces résultats en termes d'information relevante pour l'environnement.

Ces objectifs ont été atteint en analysant de nombreux échantillons de neige obtenus au CDD à l'aide de forages de surface, de puit, de la carotte profonde obtenue en 1994 ainsi que de filtres à aérosols (environ 2500 échantillons). Les analyses chimiques étaient ciblées sur les ions minéraux majeurs (F^-, Cl^-, NO_3^-, SO_4^{2-}, Na^+, NH_4^+, K^+, Mg^{2+} et Ca^{2+}) ainsi que sur les carboxylates légers (acétate (CH_3COO^-), formate ($HCOO^-$) et oxalate ($C_2O_4^{2-}$)).

Des mesures continues, à toutes saisons, d'aérosols au site glaciaire du CDD sont nécessaire pour établir la relation liant la concentration dans l'atmosphère et dans la neige. Dans ce but, le prototype d'un échantillonneur automatique d'aérosols qui avait déjà été déployé au Colle Gnifetti (Preunkert et Wagenbach, 1998) a été substantiellement modifié pour obtenir des données fiables durant toute l'année à l'Observatoire Vallot (4361 m) situé au site du CDD. Comme détaillé dans le Chapitre 1 de la thèse, une attention particulière a dû être faite pour régler des problèmes existant du prototype, en particulier pour améliorer la protection de l'appareil contre la foudre ou l'électricité statique de l'air, et pour améliorer les limites de détection.

Dans notre discussion de l'intérêt des enregistrements glaciaires du CDD pour recontruire les changements atmospheriques passés, nous avons examiné les propriétés glaciologiques déjà connues de ce site du CDD en complément d'une étude à haute résolution resolution (saisonnière) des carottes de glace. Ceci incluait un examen détaillée de la variabilité spatiale locale et régionale des enregistrements dans la glace, l'échelle de temps couverte par la glace de ce site et avec résolution temporelle (saisonnière), ainsi que la possibilité d'étendre les enregistrements jusqu'à l'ère préindustrielle. En plus, une attention particulière a été dédié ici à la déconvolution des signaux enregistrés dans la glace (signal atmosphérique net et effets locaux liés à l'écoulement de la glace) (Chapitre 2).

Les enregistrements glaciaires à résolution saisonnière ainsi obtenus (Chapitre 3) ont ensuite été discutés dans les Chapitres 4, 5 et 6 en termes d'implications géochimiques pour le climat et l'environnement. Ceci inclue une tentative d'estimation des régions sources influencant le site du CDD ainsi que l'identification des différentes sources (naturelles ou

anthropiques). Notre effort atout d'abord porté sur les changements à long terme de SO_4^{2-} car il est connu que l'aérosol de sulfate exerce une influence significative sur le budget radiatif global et régional, et qu'il pourrait être l'un des acteurs les plus importants à l'échelle européenne (Chapitre 4). Le Chapitre 4 examine lui en détail les budgets (et les variations passées) des espèces azotées (NO_3^- et NH_4^+), qui sont deux contributeurs clefs du cycle d'azote qui lui-même représente l'un des cycles biogéochimiques les plus importants déjà perturbés par l'homme.

Enfin nous avons porté notre attention sur quelques espèces mineures, par exemple les espèces halogénées (F^- et HCl) (Chapitre 5). En fait, leurs budgets atmosphériques sont encore mal connus (Cicerone, 1981; Graedel et Keene, 1995; Graedel et Keene, 1996), en particulier en ce qui concerne l'importance relative des processus naturels par rapport aux processus anthropiques. Enfin, les changements à long terme des composés organiques (oxalate, acetate et formate) ont été examinés dans les dépots de neige au Col du Dôme (Chapitre 6). Les variations à long terme d'oxalate ont un intérêt particulier car cet aérosol contribue à la fraction organique des aérosols atmosphériques. En plus du sulfate, il interagit certainement sur le budget radiatif. L'acétate et le formate sont produits lors de l'oxydation atmosphérique de divers hydrocarbures naturels et anthropiques (Chebbi et Carlier, 1996). Malgré leur contribution potentielle à l'acidité de la précipitation dans des régions reculées, leurs budgets globaux sont totalement inconnus.

Introduction

1. Background

Numerous chemical species derived from the carbon (CO_2, CO, CH_4, non methane hydrocarbons (NMHC), organic aerosols), nitrogen (N_2O, NH_3, and NO_x), halogen (chlorine and fluorine derived species), and metal cycles are controlling the fragile equilibrium of the Earth's ecosystems, the chemical composition of the atmosphere and the climate. Since the beginning of the pre-industrial era, growing man-made activities (consumption of fossil fuel, intensive agricultural activities, waste- and biomass burning, metal production) have significantly modified the atmospheric natural level of species derived from these biogeochemical cycles.

In addition to long lived greenhouse gases such as CO_2, CH_4, N_2O, and chlorofluorocarbons (CFCs), it is now well recognized that other short lived species such as ozone and aerosols can play a key role on the climate, particularly at a regional scale. For instance, ozone, a greenhouse gas whose concentrations are strongly controlled by NO_x, CO, CH_4 and NMHC levels, contributes to the oxidative capacity of the atmosphere and thus influences the lifetime of numerous atmospheric species. Through their direct (adsorption and diffusion of solar radiation) and indirect (cloud microphysics) effects, aerosols play an important role on the radiative transfer and the climate. In this way, the anthropogenic enhancement of aerosols over the past century may have regionally compensated the parallel increase in greenhouse radiative forcing.

To assess the impact of anthropogenic emissions on the natural equilibrium of our environment (climate and atmospheric composition) and to predict future changes at both global and regional scales, it is mandatory to gain a knowledge of natural (preindustrial) conditions and how these later conditions have been progressively modified by man-made emissions since the pre-industrial era. Reliable direct measurements of the chemical composition of atmosphere and precipitation are only available for the last 10 to 40 years, a period over which man-made activities have already started to modify strongly the natural conditions. Therefore extensive investigations were made to extract environmental parameters from records in tree rings, lake and sea sediments, and glaciers. Among these archives, cold glaciers play an unique role since they store climatic information (e.g. proxy of precipitation rate, temperature) as well as atmospheric ones (trace gas in air bubbles, aerosol trapped in ice) in high temporal resolution, sometimes back to several hundred of thousands years (Dansgaard et al., 1973; Delmas, 1992; Legrand and Mayewski, 1997).

Since 1965, most of ice studies were performed on ice cores extracted from the polar ice sheets of Greenland and Antarctica which unify the advantages of a rather simple and large scale glacier geometry and very low firn temperatures. Measurements of stable water isotopes (Dansgaard, 1954; Johnsen et al., 1972; Lorius et al., 1985; Jouzel et al., 1987;

Dansgaard et al., 1993), CO_2 (Delmas et al., 1980; Barnola et al., 1987), CH_4 (Chappellaz et al., 1990 and 1997; Blunier et al., 1995), N_2O (Flückiger et al., 1999) as well as the aerosol related chemical composition (see Legrand and Mayewski, 1997 for a review) were mainly used to investigate the history of climate and atmospheric environment over the last climatic cycles. Concerning the records of the last 200 years, Greenland ice cores have recorded the change in acidification of precipitation. For example ice core data from Greenland showed a marked increase of SO_4^{2-} and NO_3^- in the course of the 20th century (Neftel et al., 1985; Mayewski et al., 1986; Fischer et al., 1998b) as well as a doubling of atmospheric methane concentrations since 1800 AD (Etheridge et al., 1998). These findings clearly demonstrated that very remote (unpopulated) areas of the northern hemisphere have been disturbed since the beginning of the 19th century by man made activities. However, for Greenland snow deposits large ambiguities exist in the source region apportionment for short lived species due to the complex interplay between long-range transport from source regions toward the deposition site, the atmospheric fate of precursors and removal processes of end-oxidation products. For the sulfate aerosol, the comparison of long term SO_4^{2-} trends revealed in Greenland snow deposits and anthropogenic SO_2 emission inventories suggested a contribution of emissions from Europe, Asia and North America (via long range transport) (Fischer et al., 1998b). Since the long-range atmospheric transport between major industrialized continents of the northern hemisphere and the Greenland ice cap remains still poorly simulated by global circulation transport models, these Greenland ice core records remain of limited interest to constrain emission inventories from the various source regions of concern. From this point of view, other long term trends recorded at glacier sites located in regions more directly influenced by emissions from a given continent would be more adequate to accurately constrain existing emission inventories of the region of concern. Furthermore, in view to quantify the climatic impact of changing aerosol load over temperate (populated) regions, there is a strong need to gain ice core records at mid-latitudes. For sulfate, together with eastern USA, western and central Europe are regions where the radiative effect of anthropogenic sulfate aerosol is believed to be the largest. More generally, long term ice records of short lived species at various glacier sites of the northern (but also southern) hemisphere would be useful for many environmental studies dealing with the evaluation of regional climate change, and the knowledge of the still poorly understood atmospheric cycle of some atmospheric species (hydrochloric and fluorhydric acids, light carboxylic acids, and organic aerosols, for instance) over continents.

2. The potential of mid-latitude cold glacier ice cores

Experiencing 10 m firn temperatures below the water freezing point, some mountain glaciers in addition to the polar ice sheets (Greenland and Antarctica), store adequately (without melting) environmental parameters, opening the possibility to reconstruct several

aspects of the past atmospheric chemistry over various regions of the world. This includes glaciers located in tropical regions such as the Huascaran ice cap in the Peruvian Andes (Thompson et al., 1995b), the Guliya (Thompson et al., 1995a) and Dunde (Thompson et al., 1988) ice caps located in Tibet, as well as Devon Island ice cap in the Canadian Arctic (Koerner, 1977), Mount Logan (Holdsworth and Peak, 1985) in western Canada, and Alpine sites (Wagenbach, 1993b).

More specifically, long term ice core records from cold Alpine glaciers may help to infer the impact of human activities on climate and environmental variabilities and long term changes at the European scale since here the glacier archives may be intimately connected to emissions from Europe. In the Alps, suitable glaciers (not substantially disturbed by melt water percolation) are almost exclusively located well above 4000 m asl and are therefore very rare and restricted to small areas in the summit ranges of the massifs of Monte Rosa, Bernese Alps, Grand Combin, and Mont Blanc (Funk, 1993).

At present, information gained from long term Alpine ice core records are mainly available from the Monte Rosa region (Colle Gnifetti, 4450 m asl) (Haeberli et al., 1983; Wagenbach, 1989). Due to the relatively low annual net snow accumulation of 0.2-0.4 m of water equivalent (w.e.) at this small glacier site, the ice records span more than several centuries. These Colle Gnifetti ice core studies have for instance already revealed an enhancement of sulphate, nitrate and ammonium concentrations over the 20th century (Wagenbach and Preunkert, 1996 (data from Jung, 1993); Döscher et al., 1996) as well as a clear anthropogenic signal for lead (Wagenbach and Preunkert, 1996 (data from Schajor, 1993)). However drill site related shortcomings still strongly limit a straightforward interpretation of these records in terms of past environment and climate (Wagenbach, 1993a):

- Due to the small area of the glacier (0.3 km^2) and a strong spatial variability of the deposition characteristics at the site (Preunkert, 1994), the ice core records underlying net atmospheric signals are likely biased by glacier flow effects.
- The net snow accumulation at the site is controlled by wind erosion favouring snow accumulation primarily built up by late spring and summer precipitation (winter and fall precipitation contributes only to 20 % at the best; Preunkert, 1994) leading to a more or less missing winter signal.
- Recent atmospheric observations made on high Alpine sites above 3000 m asl (Preunkert and Wagenbach, 1998; Baltensperger et al. 1997; Kasper and Puxbaum, 1998) showed low impurity contents in winter due to the very limited contamination of these high altitude regions by polluted boundary layer air masses during that season. Conversely, in spring and summer, upward advection by convective transport significantly affects high Alpine sites and leads to significantly increased atmospheric impurity contents during this season. These seasonal variations of atmospheric conditions and the seasonal irregular

snow accumulation therefore leads to a virtually unknown spatial representativeness of the ice core records from this site.

These present interpretation limits were aimed to overcome within the framework of the European research program ALPCLIM whose principal objectives are to explore several Alpine glacier records and to evaluate and validate these records in view of their reliability, representativeness and inherent net atmospheric signals. In addition to the high Alpine ice core drill sites of Col del Lys, and Colle Gnifetti located in the Monte Rosa massif, the ALPCLIM project includes also the Col du Dôme glacier site situated at 4250 m asl in the summit range of the Mont Blanc massif.

From previous glaciological studies (e.g. Lliboutry et al., 1976; Vincent et al., 1997) and ice core investigations (e.g. Briat et al., 1978; Jouzel et al., 1984; De Angelis and Gaudichet, 1991) the Col du Dôme glacier site characterized by a rather high accumulation rate (≈ 0.5 to 2.5 m w.e.) is known to be potentially suitable for ice core studies. In 1991, a pilot study (Maupetit et al., 1995) was performed at the Col du Dôme site in which the soluble part of chemical species was investigated with a high temporal resolution in snow deposited from 1988 to 1991. This study confirmed the rather high snow accumulation rate and revealed well-preserved winter snow layers at that site. In contrast to Colle Gnifetti, this site is expected therefore to permit the examination of past changes of atmospheric chemistry at a seasonal (winter/summer) resolution at least over the last few decades or so. In the framework of the ALPTRAC project, two deep ice cores were drilled close to bedrock at Col du Dôme in 1994. Within the framework of ALPCLIM one of them was dedicated to the study of stable isotopes and the investigation of impurities trapped in the ice lattice, the other one to trace gas measurements.

3. Glaciochemical studies achieved in this work at the CDD site

In this context the present work is focused on a glaciochemical ice core study at the Col du Dôme glacier site which included:

- the examination of the Col du Dôme glacier site in view of its suitability for ice core studies in relation with past atmospheric chemistry over Europe,
- the establishment of the relationship linking the concentration of key species in recent snow deposits to those of the atmosphere at this site,
- the reconstruction of detailed (seasonal resolved) trends of the chemical snow composition and its change over the last decades,
- ultimately, to discuss these findings in terms of relevant environmental information.

This work was achieved by investigating numerous snow samples collected at Col du Dôme in snow pits, shallow firn cores and down the length of the deep ice core drilled in

1994, as well as aerosol filter samples (total ≈ 2500 samples). Chemical investigations were focused on major mineral ions (F^-, Cl^-, NO_3^-, SO_4^{2-}, Na^+, NH_4^+, K^+, Mg^{2+} and Ca^{2+}) as well as on light carboxylates, namely acetate (CH_3COO^-), formate ($HCOO^-$) and oxalate ($C_2O_4^{2-}$).

To establish the relationship linking concentration changes in snow to the ones in the atmosphere at the CDD site, continuous year round aerosol measurements at the Col du Dôme glacier site are here needed. For this purpose, an automatic prototype aerosol sampler already deployed at the Colle Gnifetti glacier site (Preunkert and Wagenbach, 1998) had been substantially modified to gain reliable year round aerosol data at the Vallot Observatory (4361 m asl) situated at the border of the Col du Dôme glacier site. As developed in Chapter 1, special attention had to be paid to overcome existing problems of the prototype device, in particular to harden the new device against lightning and air electricity disturbances, and to improve its detection limits.

To discuss the usefulness of Col du Dôme ice core records for atmospheric relevant chemical time records, we have used already known basic glaciological properties of the Col du Dôme glacier site as well as highly temporal resoluted ice core records gained in this work. This included a detailed examination of Col du Dôme ice core records with respect to their local and regional spatial variability, their accessible time resolution, as well as their potential to extend records back to the pre-industrial era. In addition special attention had to be paid to deconvolute the net atmospheric signal embedded in the ice core records from non-atmospheric local glaciological effects (Chapter 2).

The obtained seasonally resolved ice core records (Chapter 3) were then discussed in Chapters 4, 5 and 6 in terms of geochemical implications for climate and environmental. This includes an attempt to estimate relevant source areas as well as the impact of different sources influencing the snow deposits of these species at Col du Dôme. First, special attention was paid to the long term changes of SO_4^{2-} since the sulfate aerosol is known to exert a significant influence on the global and regional radiation budget, and may be one of the most important climatic actor at the scale of Europe (Chapter 4). The budgets (and their variations over the past) of the nitrogen species (NO_3^- and NH_4^+), two key contributors of the N-cycle which represents one of the most important global biogeochemical cycles already significantly disturbed by human impact, are examined in details (Chapter 4).

In addition to these major atmospheric species, attention was also paid to some minor ones as the halogen species (F^- and HCl) (Chapter 5). Indeed, their atmospheric budgets remain still poorly understood (Cicerone, 1981; Graedel and Keene, 1995; Graedel and Keene, 1996) and in particular the relative importance of natural versus anthropogenic processes. Finally the long term changes of organic compounds (oxalate, acetate and formate) were investigated in snow deposits of Col du Dôme (Chapter 6). The long term temporal variations of oxalate is of interest since this aerosol species contributes to the organic fraction of atmospheric organic aerosol which, in addition to sulfate, certainly exerts also an influence

on the radiation budget. Acetate and formate are produced along with the atmospheric oxidation of various natural and anthropogenic hydrocarbons (Chebbi and Carlier, 1996). In spite of their potential contribution to the acidity of precipitation in remote regions, their global budgets are still totally unknown.

Chapter I

Continuous automatic aerosol sampling at the Vallot Observatory

1.1 State of the art

Clearly the interoperation of records of short lived species like aerosols and reactive trace gases in ice cores in terms of past atmospheric changes requires the knowledge of the relationship linking the composition of firn and air at the respective ice core drill sites (e.g. Bales and Wolff, 1996).

However, due to logistical constraints at remote ice core drill sites, year round information of this local firn/air relation is presently only available for Dye 3 (South Greenland) through the DGASP campaign (Jaffrezo and Davidson, 1993) and for the central Greenland Summit site. At the latter site atmospheric data were obtained by running a manual 10-month aerosol sampling program (Jaffrezo et al., submitted), as well as by deploying an automatic streaker sampler (Wåhlin, 1996) which delivers year round records of the elemental aerosol composition with a weekly resolution. The subsequent PIXE-analyses applied to this automatic streaker samples provide however only semiquantitative information on Cl^- and Na^+, no information on nitrogen derived species (NO_3^- and NH_4^+), and only global sulfur content without chemical speciation of sulphur derived species (SO_4^{2-}, $CH_3SO_3^-$).

With the attempt to partly overcome such an information lack at high Alpine sites, an automatic device comprising filter pack sampling and snow height monitoring was developed at the Institut für Umweltphysik (Heidelberg, Germany). The complete station was operated during two years (1993-1995) at the Colle Gnifetti (4450 m asl, Swiss Alps) ice core drill site (Preunkert and Wagenbach, 1998) (see Annex I)). The aerosol sampler was then set up for a half year (1997/1998) at the Vallot Observatory (4361 m asl, French Alps). Despite the harsh environmental conditions, the device was working quite well most of time with the exception of data logger break downs induced by lightning activities and electrostatic discharges (which occurred even when runs were achieved inside the Vallot Observatory).

1.2 Summary of the work achieved to run the newly developed aerosol sampler at the Vallot Observatory

Because of the above mentioned failures related to lightning activities and electrostatic decharges which appeared too frequently to ensure continuous atmospheric observations, the prototype sampling device was basically revised in 1998/99 to ensure more continuous atmospheric observations at the Vallot site. With respect to the restricted energy availability

and the extreme environmental conditions taking place there, a concept was developed to realize a maximal hardening of the sampler with respect to lightning and air electricity. In addition, to overcome the relative high detection limits of the prototype, an isolation of the filter packs from ambient air during their storage time in the device was designed. Details on the technical improvements made on the new device and on developments made to decrease its detection limit by reducing blank filter values and modifying sampling characteristics are given in section 1.3.

In 1999 the updated aerosol sampler was set up at the Vallot Observatory (Figure 1.1). With respect to the inner geometry of the hut, ambient air is sucked through a tube from the air intake point outside (Figure 1.2) to the sampler unit placed inside the hut (Figure 1.3). The achieved system was working very well until now, demonstrating the robustness of the new system despite the strong lightning activities, occurring regularly during summer at such high elevated sites. Furthermore, using the closure device of filter holders, the obtained filter blank levels (and subsequently the detection limits) of the new device have been significantly decreased, compared to the ones of the prototype (see details in section 1.3).

Figure 1.1: The Vallot Observatory (4361 m asl). With a nominal power of 100 W the solar panels set up on the roof of the hut provide ~7 W to the aerosol sampling device at any time of the year.

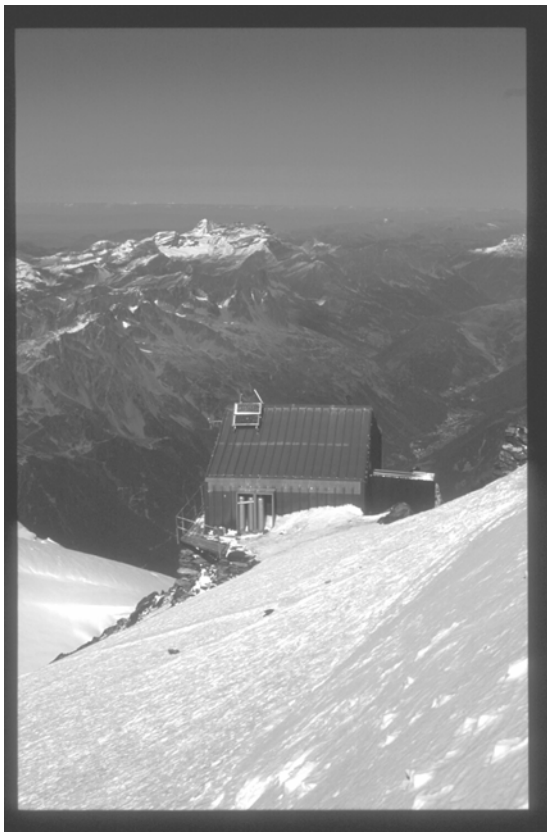

Figure 1.2: The air intake point arrangement of the aerosol sampling device is situated 3 m above ground at a distance of 60 cm to the wall of the hut. The swinging steel bell is aimed to prevent a blocking of the air inlet by blowing snow and riming.

Figure 1.3: The aerosol sampling unit inside the hut is divided into two parts (top: pump box, bottom: logger box) with the aim to avoid failures due to lightning activities and electrostatic discharges.

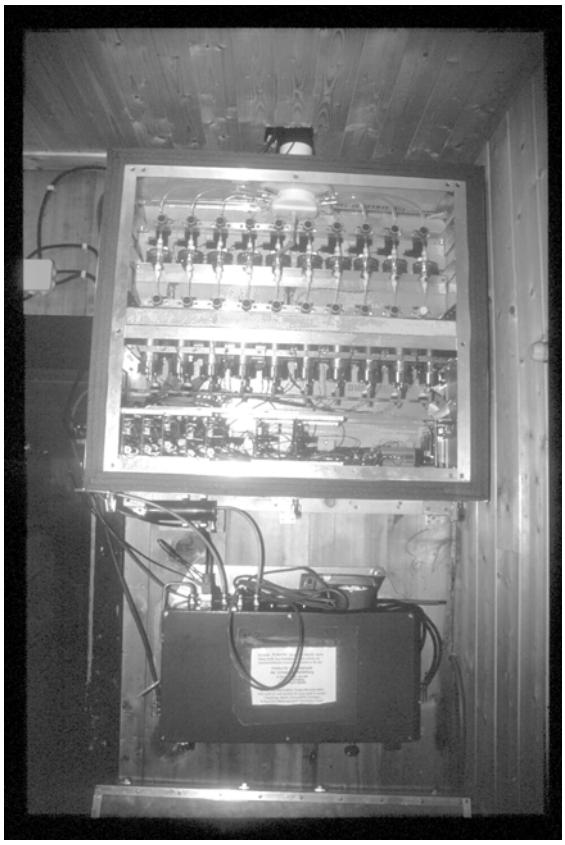

Based on the atmospheric data set obtained during one year of aerosol sampling with the new device at the Vallot Observatory and regular snow pit sampling carried out at CDD, a preliminary investigation of the relation between the composition of the air and the one of firn has been performed for NH_4^+, SO_4^{2-}, oxalate and total NO_3^- components. Different from the so-called scavenging ratios, the here calculated firn air relation (FAR) ratios correspond to the ratio between the mean seasonal concentrations observed in the snowpack and the corresponding mean seasonal air concentrations. The FAR values obtained at the Vallot

Observatory site are reported in Table 1.1. Despite the limited time period (one year) of these investigations, the obtained FAR values are in rather good agreement with the ones gained at other high elevated ice core drill sites. Thus these preliminary FARs from the Vallot Observatory will be used within this work to translate Col du Dôme ice core data in terms of atmospheric concentrations at this site. Note that these FAR values represent an empirical way immediately useful to invert ice core records in terms of past atmospheric changes, but are in no way useful to investigate the physic and chemistry of parameters responsible for the observed air-snow relationship. The study of these processes is out of the scope of the present work.

Table 1.1: Seasonal averaged Firn/Air Ratios (FAR) obtained at Vallot Observatory (this study) for sulfate, ammonium, total nitrate at Colle Gnifetti (Preunkert and Wagenbach, 1998), Sonnblick Observatory (Kasper-Giebl et al., 1999) and Summit (Jaffrezo et al., in press; Dibb et al., 1994; Aymoz, 1999).

	Vallot Observatory (4361 m asl)		Colle Gnifetti (4450 m asl)		Sonnblick Observatory (3106 m asl)		Summit (Greenland) (3200 m asl)	
Species	winter	summer	winter	summer	winter	summer	winter	summer
total NO_3^-	5.2	3.7	2.3	1.3	4.9	1.6	n.d.	2.2
SO_4^{2-}	2.6	1.3	1.8	1.5	2.5	0.9	0.87	0.54
NH_4^+	1.1	1.7	1.6	1.6	2.8	1.0	2	1.44

all values $\times 10^6$

1.3 Improvement and characterization of an automatic aerosol sampler for remote (glacier) sites

Improvement and characterization of an automatic aerosol sampler for remote (glacier) sites

Susanne Preunkert[1,2,*], Dietmar Wagenbach[2], and Michel Legrand[1]

1. Laboratoire de Glaciologie et Géophysique de l'Environnement, CNRS, BP96, 38402 St. Martin d'Hères, France.

2. Institut für Umweltphysik, Universität Heidelberg, INF 229, 69120 Heidelberg, Germany.

* Corresponding author. Phone: +33/(0)476824207; Fax: +33/(0)476824201; e-mail: ps@glaciog.ujf-grenoble.fr

In press at "Atmospheric Environment"

Abstract

An automatic prototype aerosol sampler has been specifically revised to gain reliable year round data sets of the chemical aerosol composition at high Alpine ice core drill sites. An unattended deployment of the new aerosol sampler at the Vallot Observatory (4361 m asl, French Alps) showed that previous shortcoming such as sensitivity to lightning activities and strong passive sampling effects were successfully overcome. The latter effect was almost eliminated, leading to an improvement of the detection limits by up to a factor of 30. Detailed investigations of the blank variability and sampling characteristics revealed that the new sampler allows to quantify the aerosol species NH_4^+, SO_4^{2-}, K^+, oxalate as well as total Cl^- and total NO_3^-. In addition records of Na^+, Mg^{2+} and Ca^{2+} can be provided though systematically underestimated. On the other hand unreliable results are derived for formate, acetate and SO_2. Considering a bi-weekly sampling interval, detection limits range from 0.2 to 2 ng m^{-3} STP (except for Na^+ : 16 ng m^{-3} STP). Such a detection limit is also accessible for Na^+ if PTFE filters are used. The aerosol data set gained at Vallot Observatory allowed preliminary estimates of mean firn/air ratios for NH_4^+, SO_4^{2-} and total NO_3^-. The air/firn relationship appeared to be consistent compared to other high elevation ice core drilling sites. With the improved detection limits at still minimized energy consumption, a year round deployment of the automatic aerosol sampler appears now to be feasible even at polar glacier sites.

Key word index: automatic aerosol sampler, high Alpine aerosol chemistry, firn/air relationship, Vallot Observatory

1 Introduction

Since several decades ice cores from polar ice sheets and cold mountain glaciers have been investigated (Oeschger and Langway, 1989; Legrand and Mayewski, 1997; Wagenbach, 1997) to reconstruct anthropogenic and natural changes of bio-geochemical cycles over time scales from decades (Wagenbach and Preunkert, 1996) to several climatic cycles (e.g., for the sulfur cycle, Legrand et al., 1997). Concerning short-lived aerosols and reactive trace gases, site specific relationships linking concentration changes in snow to the respective net atmospheric signals are needed (see Bales and Wolff, 1996 for a review). Ice core related attempts to establish such an empirical relationship were mainly performed during over wintering campaigns at Greenland drilling sites (Davidson et al. 1993). However at other drill sites e.g. in Antarctica (Harder et al., 2000) or on high elevation mountain glaciers almost no year round observations of atmospheric constituents are available yet.

To overcome this lack, we have developed an automatic, solar panel powered aerosol sampler to be deployed unattendedly at remote glacier sites (Preunkert and Wagenbach, 1998). The system provides individual aerosol and (nylon) trace gas filter samples for subsequent analyses of ionic species. Thus, different to the approach developed in Greenland for trace

element records using PIXE-analyses of streaker samples (Wåhlin, 1996), important species like NO_3^-, NH_4^+ or MSA are covered as well. The device has been set up for two years at the ice core drill site Colle Gnifetti (CG, Monte Rosa, Swiss Alps, 4450 m asl) and later on for one year in the Vallot Observatory (VO, 4361 m asl) located close to the Col du Dôme drilling site in the Mont Blanc summit range. Although the system was shown to cope well with the highly adverse local conditions (high wind speeds, riming etc), failures due to lightning activities and electrostatic discharges appeared too frequently to ensure continuous atmospheric observations. The second major shortcoming was found to be related to passive sampling, which may lead to unnecessarily increased detection limits and inadequate control of the blank filter levels. Maintaining the basic principle, we thoroughly revised the sampler to overcome these major problems. In addition, attempts were made to increase the flow rate, to further avoid ice crystal entrainments and to explore the possibility of sampling light carboxylic acids as well. Here we report on the respective developments and dedicated experiments aimed at characterising the sampling performance of the improved system. Based on atmospheric records obtained during a one year deployment at VO within the EU project ALPCLIM, an exemplary inspection of the relation between mean seasonal air and snow concentrations is presented along with the perspective to run this system at polar glacier drill sites as well.

2 Technical design and deployment at Vallot Observatory

2.1 Technical design

The prototype device is described in detail by Preunkert and Wagenbach (1998). In brief, through a single inlet, connected to a small chamber acting as a sedimentation sink for ice crystals and cloud droplets, air is sucked to 10 sampling units each consisting of an inline filter holder, a pump and a one way valve. The pumps are activated consecutively for a (constant) pre-selected sampling time. The one-way valves are placed to ensure the air flow direction and to minimize the contact of the stand by aerosol filters with ambient air. The prototype sampler ran successfully at CG from 1993 to 1995 but showed frequent failures of the data logger by electrostatic discharges and lightning activities, and relatively high detection limits probably due to passive sampling. The new device is therefore mainly improved with respect to lightning/air electricity disturbances, and the long term filter sealing.

The principal sketch of the updated aerosol sampler is illustrated in Figure 1. To avoid damages from electrostatic discharges and lightning activities, the device is separated into two metal-boxes (housed in a field container). Using rugged AD and DA converters connected via fibre optic lines, we could avoid that any electric cable enters directly in the sensitive signal input unit of the data logger from outside the logger box. The pump activation is controlled by the data logger connected with an electro-mechanical counting switch. The

prevention of permanent electrical connection of the data logger output unit with the pump control unit (placed in the pump box), is realized by reed relays. As electrical cables of the power supply enter into both boxes, a three component high frequency protection has been placed between the two potentials of the power supply using noble gas shunts, voltage dependent resistors and Transzorb-diodes. The negative potential of the power supply and the mass-ground of the two boxes are connected to the electrical potential of the metallic envelope of VO, serving as a low resistance capacitor with high capacitance. The metal envelope itself is not connected to the rock ground to avoid an antenna-effect, since no protection would be possible against a direct lightning strike (H. Vogelmann, personal communication).

To avoid permanent contact of the filters with ambient air, each filter pack unit is isolated via two specially designed (tube squeezing) magnetic valves (ASCO Joucomatic, Germany). The magnetic valves operate in a flip-flop mode and thus consume energy only during the switching phase. Carbon vane pumps (Fuergut company, Germany), driven by ironless precision 24 DC servomotors were selected, which provide a 50 % higher flow rate than the pumps used in the prototype at similar power consumption.

Further, essential attention is paid to the following occurrences:

- To minimize the energy consumption, the pump is stopped when the line is blocked.
- To ensure functioning of the data logger when the energy supply is interrupted it is equipped with an autonomous “security” battery pack.
- To avoid water condensation and freezing inside the air lines, the filter containing part of the device is thermally isolated, and condensation traps are placed where the air line is subject to a (potential) negative temperature gradient.
- To minimize losses of HNO_3, Teflon inlet lines are used.

The system shows a total energy consumption of 7 W (pump: 5 W, flow meter: 0.6 W, data logger: 1.3 W). If the data logger operates non-continuously, the overall power supply may be reduced to slightly less than 6 W. The typical flow rate of the device, achieved at 12 V, using a quartz followed by a nylon filter, is about 5.0 l STP min^{-1} at low altitude and 3.0 l STP min^{-1} at 4461 m asl. The dimension (pump box: 140 l, 40 kg; logger box: 30 l, 25 kg) of the new device is still relatively small, and easy to move.

2.2 Deployment at Vallot Observatory

In August 1999 the new device was set up at the VO. Situated at 4361 m asl, this site experiences precipitation almost exclusively as snow, frequently riming, winter daily mean air temperatures lower than –20 °C, and hourly mean wind speeds higher than 20 m s^{-1}. The

observatory consists of a simple mountain shelter hut exclusively dedicated to scientific research (almost no contamination from alpine tourist activities). The Observatory did not allow to place the filter holders close to the air intake. Thus, the ambient air is sucked through a 2 m long tube (inner diameter 5 mm) from the air intake point situated 3 m above ground at 60 cm distance to the wall to the sampler unit inside the hut. To minimize losses of aerosol and HNO_3 within the inlet line, a silica covered steel tube (Restek company, France) was used. Note that HNO_3 adsorption is expected to be not critical for our application since it will be decreased at longer sampling periods (Neumann et al., 1999). Blocking of the air inlet by blowing snow and riming is counteracted by a swinging steel bell. Electrical energy is provided by two 50 W solar panels mounted on the roof of the hut and backed up with two 1000 VAh buffer batteries.

Since September 1999 the device was run unattended over four periods lasting 1 to 5 months, until end of August 2000. Individual sampling intervals ranged from 4 to 10 days except one sample covering 45 days. As for the prototype, aerosols were collected on a high purity quartz fibre filter (Whatman, QM-A) placed in front of a single nylon membrane filter (Gelman, Nylasorb) to collect gaseous HNO_3 including the fraction eventually remobilized from the quartz filter (Talbot et al., 1990). The four sampling runs showed an excellent reliability of the whole system including no malfunctions of the data logger. Note also that during regular visual inspections neither ice crystals nor traces of (refrozen) water were observed upstream or on the filters.

3 Analytical methods

Polycarbonate inline filter holders of 47 mm diameter, sealed with a silicon o-ring, were used. The exposed filter area was reduced with a PTFE ring to 36 mm diameter. The key steps of the filter handling protocol are given below:

- Filters were cleaned by several soakings in high purity (18 MΩ) water. For Nylon filters the last soaking was done in high purity water which was adjusted to pH 8 by NaOH.
- Cleaned filters were dried in a dessicator and loaded on filter holders under a laminar flow.
- Storage of filters during transport was done in closed filter holders which were sealed in plastic bags. Filter samples were transported (2 days) at below 0 °C and stored for several days at –15 °C before analysis.
- Extraction of filters (after discarding of the unexposed area) was done several hours before ion chromatography analyses in 20 ml high purity water. For nylon filters, the extraction solution was adjusted at pH 8 with NaOH.

Subsequent analyses of the filter extracts were achieved for major ions (Cl^-, NO_3^-, SO_4^{2-}, Na^+, NH_4^+, K^+, Mg^{2+}, Ca^{2+}) as well as for light carboxylates (acetate: CH_3COO^-, formate: $HCOO^-$,

oxalate: $C_2O_4^{2-}$) using ion chromatography working conditions developed for trace levels by Legrand et al. (1993). According to this analytical protocol liquid concentrations of ion chromatography blank levels are below 0.3 ng g^{-1} for anions (except acetate: 0.7 ng g^{-1}) and below 0.7 ng g^{-1} for cations.

4 Filter blank variability and post sampling artefacts

4.1 Blank variability

The detection limit of the sampling device is generally controlled, for a given flow rate and sampling time, by the blank filter variability as well as by post sampling artefacts. Here most critical may be passive sampling effects or losses occurring during the relative long storage of blank and loaded filters in the sampling device. During the deployment of the sampler at VO, 8 blank filter pairs were obtained and treated identically to the loaded filter packs except that no air was sucked through them. They represent the maximum blank contribution associated with the four individual sampling campaigns, during which filters were stored between 1 and 5 months in the sampler (for respective blank results see Table 1). To improve the statistical significance of this data set, 5 additional quartz/nylon filter packs and 3 PTFE/nylon filter packs, were stored over one month at -12 °C before they were extracted and analysed. Since these simulated quartz and nylon field blanks show no systematic difference compared to the true field blanks, we assume that this laboratory experiment mimics field conditions quite well. The simulated field blanks were included therefore in the mean field blank value reported in Table 1. The fraction of the field blank which is not linked with the previously cleaned filter matrix (Table 1) was calculated on the base of filters extracted and analysed immediately after drying.

For all species except Ca^{2+}, field blank are higher than laboratory blank levels. No systematic change of field blank values with storage time is observed however for all investigated species on the quartz filter (except for acetate and formate), and for SO_4^{2-} on the nylon filter. In contrast, a systematic increase with storage time was detected on quartz filter field blanks for acetate (150 ng $filter^{-1}$ $month^{-1}$), and formate (48 ng $filter^{-1}$ $month^{-1}$), as well as on nylon filter field blanks for acetate (170 ng $filter^{-1}$ $month^{-1}$), formate (280 ng $filter^{-1}$ $month^{-1}$), Cl^- (20 ng $filter^{-1}$ $month^{-1}$), NO_3^- (11 ng $filter^{-1}$ $month^{-1}$), and oxalate (10 ng $filter^{-1}$ $month^{-1}$). These remaining passive sampling effects on the blank filters are assumed to be due to a degassing of the filter holder material (polycarbonate, silicon and polysulfone) or/and due to gas diffusion through the 4 cm long silicon tubes used in the magnetic valves. To evaluate the efficiency of the filter pack sealing during storage in the sampler, we compare in Table 1 the field blanks achieved with the new device to the ones achieved with the prototype for which a total separation of filter packs from ambient air was not ensured. In general the level of the new field blanks as well as their variability are significantly decreased (except for quartz

related Na^+ and Ca^{2+}). Note that passive SO_2 and HNO_3 sampling of nylon field blanks in the prototype are reduced by up to 90 % now.

4.2 Detection limits

The detection limits given in Table 1 are taken as three times the field blank variability and refer to a sampling period of two weeks at 4360 m asl (i.e. for 60 m^3 STP). Compared to the prototype version a significant decrease is observed for all species, but especially for the ones trapped on the nylon filter and for NO_3^-, SO_4^{2-} and NH_4^+ on the quartz filter. The corresponding decrease of the detection limits ranges between a factor of 1.5 for Na^+ on quartz filters to 30 for SO_4^{2-} (SO_2) on nylon filters. Note that this significant improvement of detection limits is due to the reduced variability of the field blanks as well as to the 50% larger flow rate of the new device. The relative high detection limit for Na^+ can be significantly reduced by using PTFE instead of quartz filters, now possible due to the stronger pumps employed in the new device. Based on three simulated PTFE field blanks, we calculated a Na^+ detection limit of 0.2 ng m^{-3} STP for a bi-weekly sampling time. Hence the Na^+ sensitivity has increased by a factor of 80, although PTFE filters led to a up to 20% decrease of the flow rate. In addition, the detection limit of NH_4^+, K^+, Mg^{2+}, Ca^{2+} and oxalate will decrease by a factor of 5, 11, 20, 10 and more than 10, respectively, if PTFE filters are used, while the detection limits of Cl^-, NO_3^- SO_4^{2-} will remain unchanged. Note that detection limits given here, have been calculated for 4360 m asl, and would be further decreased by about a factor of 1.7, if the device is deployed at sea level.

4.3 Post sampling artefacts

Since passive sampling effects are still observed on field filter blanks achieved with the new sampler (see section 4.1), it is important to evaluate the potential post sampling gains or losses from loaded filter packs. To do so, four inline filter holders equipped with pre-cleaned quartz and nylon filters were loaded with ambient air at the LGGE laboratory to obtain a similar load than the VO samples. Two filter packs were extracted and analysed immediately, while the two others were closed and stored for one month serving as simulated filter samples. For SO_4^{2-}, oxalate, NH_4^+ and K^+ on quartz filters, as well as for SO_4^{2-} and oxalate on nylon filters, no systematic changes are seen between stored and immediately extracted filters (less than 15% difference). For NO_3^-, a systematic remobilization (up to 30 %) from the quartz filter to the nylon filter during storage is observed but no change of the total NO_3^- load (sum of quartz and nylon filter loads) as confirmed by the good agreement (± 4%) between the total NO_3^- load of stored and immediately analysed filters. Furthermore our test shows that the Cl^- loss from the quartz filter (47 %) after storage of the filter stacks is counterbalanced by an increase (16 %) on the nylon filter. The resulting slight decrease of the total Cl^- load (9 %) remains insignificant with respect to analytical uncertainties, and supports the assumption of a

Cl^- remobilization between the two filters during storage. Since a separated real conservation of NO_3^- and Cl^- gaseous and aerosol fractions is not given, we will discuss in the following only total Cl^- and total NO_3^- values. Finally, significant net losses found for acetate and formate on the quartz and nylon filters after storage prevent a quantification of these species.

5 Sampling characteristics

To estimate sampling artefacts due to wall effects for HNO_3, gravitational settling and inertial deposition for aerosols, we carried out a field study during which we compared an air aspiration arrangement (similar to our new sampler at VO) with: 1) a sampling line with a triple denuder (mounted in series and backed up by an aerosol filter), 2) a sampling line with a double mist chamber (mounted in series) and an aerosol filter in front. Denuder and mist chamber were set up using working conditions detailed by Voisin et al. (2000), except that we used quartz instead of Teflon filters for the aerosol collection. The simulated air aspiration line (SIM) consisted of a 2 m silicon steel tube (6 mm inner diameter) which was connected to a sedimentation chamber of similar size as the one used in the new device. Behind the sedimentation chamber, a filter stack with quartz and two nylon filters was deployed. To mimic conditions encountered at VO, this experiment was carried out at Refuge Cosmiques (3620 m asl, Mont Blanc massif). Three sample runs of about one day were performed. Samples were extracted and analyzed two days after collection to minimize post sampling effects. Since denuder and mist chamber data are in an acceptable agreement, we compared (Table 2) the air concentrations derived from the SIM with the respective averages from the denuder and the mist chamber lines (taken as references).

For all aerosol species which were present at levels clearly exceeding their blank values (NO_3^-, SO_4^{2-}, NH_4^+, K^+, and oxalate), a very good agreement could be seen between SIM and the references values. Although only based on one run, the values derived from the nylon filters of the SIM for gas phase Cl^- and NO_3^- are in perfect agreement with the respective reference values (-8 ± 4 % for Cl^-, and an identical value for NO_3^-). In addition, the back up nylon filter placed in the SIM filter pack showed that almost 100 % of Cl^- and NO_3^- was retained on the first nylon filter, as already observed by Preunkert and Wagenbach (1998). An overall agreement within some 10 % difference is also found when comparing levels of total Cl^- and total NO_3^- between SIM and references lines. We conclude therefore that no significant aerosol loss (at least for sub micronic size) takes place in the intake line of the automatic aerosol sampler and that a reliable sampling of total Cl^- and NO_3^- can be assumed.

Data obtained from the reference lines indicate also that more than 98 % of formate and acetate (about 50 % of oxalate) were present in the gas phase with average values of about 300 ng m^{-3} STP for acetate and formate and 5 ng m^{-3} STP for oxalate. With respect to these

values, we found that only about 5 % acetate and formate and 10 % oxalate were collected on the SIM nylon filter. Since an important loss of these species on the aspiration tube wall is unlikely, we conclude that nylon filters do not collect efficiently gaseous acetate, formate and oxalate. Also for SO_2 a low collection efficiency (< 10%) is found for the SIM unit, confirming a highly uncertain and variable SO_2 collection of nylon filters (Chan et al., 1986). No quantification of SO_2 and light carboxylic acids in the gas phase could be achieved therefore with our sampler.

High blank contributions for Na^+, Mg^{2+} and Ca^{2+} did prevent us from gaining conclusive results on the overall sampling efficiency of our device with respect to supra micron particles (e.g. mineral dust). The overall losses of such large particles are expected to be controlled on the one hand by the aspiration efficiency at the air intake (sensitively depending on the wind velocity) and on the other hand by the transmission probability. The latter is mainly driven here by gravitational and inertial deposition within the sampling tube, sedimentation chamber and the condensation trap. While the aspiration efficiency could not be estimated yet (lack of wind statistics, complicated flow field around the roof-sampling head arrangement), we made a crude estimate of the transmission efficiency based on respective works from Fuchs (1964), Crane and Evans (1977), and Ye and Pui (1990).

For large particle aerosol characterized by a mass mean diameter (MMD) of 2.5 μm we arrived (for actual working conditions) at about 90 % transmission probability. This value, which may be typically for the mineral dust background concentration, decreases down to 70 %, approximately for a MMD of 4.5 μm particles, which are typically found in long range transported desert dust plumes (Wagenbach and Geis, 1989). Considering in addition the large particle aspiration efficiency, which may easily drop down to 50 % or so, it becomes clear, that any respective firn to air concentration ratios would be strongly biased towards unrealistically high values. A proper examination of the large particle sampling efficiency will be mandatory therefore in gaining quantifiable air/firn transfer information for large particle aerosol. Nevertheless, the seasonal cycle as well as episodic events associated with mineral dust species could be clearly identified at Vallot Observatory. For example short Saharan dust events occurring in October 1999 and April 2000 led to bi-weekly Ca^{2+} means about 7 times above the typical level.

In summary, such kind of experiments as made at Refuge Cosmiques (see section 5.1) are strongly needed to determine reliable sampling characteristic of the automatic aerosol sampler for all investigated species, including supra–micron particles. Dedicated high Alpine field experiments will be performed therefore in more extent as to obtain filter loads well above the

detection limit for all species, and a sufficient number of comparisons for statistically significant results.

6 Vallot Observatory records

6.1 The aerosol data set

Since atmospheric observations obtained at VO cover only one year, the results will not be discussed here in terms of high Alpine atmospheric chemistry. Instead they are used to evaluate the reliability of the year round automatic measurements, and to illustrate their application for ice core relevant air/firn transfer investigations. Figure 3 illustrates the change of SO_4^{2-}, NH_4^+, oxalate, and total Cl^- and NO_3^-, over the April – October period on the base of aerosol samples achieved in September - October 1999 and April - August 2000. Because several night time sampling interrupts occurred from November 1999 to February 2000 (due to energy lack), only mid-winter levels and their ranges are reported in Figure 3. Since for these species no significant diurnal variation is expected during mid-winter at high elevation Alpine sites (Baltensperger et al. 1991; Kasper and Puxbaum, 1994) our mean winter levels may not be biased systematically towards higher values due to missing night time samplings. The seasonal patterns as well as the summer/winter contrast are in good agreement with seasonally changing snow chemistry seen before at high Alpine sites (Maupetit et al. 1995; Preunkert et al., 2000).

In Table 3, the mean summer and mid-winter air concentrations gained with the new device are reported together with respective values observed with the prototype sampler at CG in the years 1993 to 1995 (Preunkert and Wagenbach, 1998) and with an unique continuous data set (1991 to 1993), performed at the high Alpine Sonnblick Observatory (SBO, 3106 m asl) by Kasper and Puxbaum (1998). At the latter (manned) site sampling was achieved with a multistage open face filter pack, containing a Zefluor (PTFE) for aerosol and a nylon filter for HNO_3 sampling. Summer as well as winter levels from VO are in very good agreement with the values measured six years before with the prototype sampler at CG except for total NO_3^-, for which the concentrations found at VO are systematically lower by about a factor of two. This discrepancy is most likely due to an underestimated HNO_3 passive sampling of the prototype device at CG, or (less obvious) to significantly different air conditions. Detection limit problems and unknown sampling efficiencies for large particles (likely different for both sampler versions) hamper a detailed intersite comparison of crustal species, though Na^+ summer as well as summer and winter Ca^{2+} values at VO are similar to those found with the prototype device at CG. As expected, atmospheric concentrations observed at VO and CG in summer and winter are considerably lower than the respective ones at SBO. This may be due to the 1400 m lower elevation of SBO, the increasing atmospheric pollution levels towards

the eastern part of the Alps (Puxbaum and Wagenbach, 1994), and possibly also the result of a stronger influence by tourists and permanent staff activities at SBO.

The new aerosol sampling device permitted for the first time continuous measurements of particulate oxalate at a high Alpine site, showing seasonal mean concentrations of 8 ng m^{-3} STP in winter and 44 ng m^{-3} STP in summer. At SBO 215 ng m^{-3} STP were measured during an event study in May 1997 (Limbeck and Puxbaum, 1999), and 7 ng m^{-3} STP have been observed end of September 2000 at Refuge Cosmiques (see Table 2). At the latter site low SO_4^{2-} (150 ng m^{-3} STP) and NH_4^+ (50 ng m^{-3} STP) concentrations suggest that almost winter like conditions prevailed (i.e. decoupled boundary layer), which confirms our mean winter oxalate value 8 ng m^{-3} STP at VO. The 215 ng m^{-3} STP oxalate measured in spring at SBO is about five times higher than the mean summer value at VO, what is consistent with the respective enhancement factors observed for SO_4^{2-} (6.5), NH_4^+ (5.6) and total NO_3^- (5.7).

6.2 Seasonal mean firn/air relations

To illustrate the application of our automatic sampler results for air/firn transfer studies, we inspected the relation between the mean seasonal air concentrations $\overline{C}_A$ expressed in g m^{-3} (ambient) and the corresponding mean seasonal concentrations observed in the snow pack $\overline{C}_F$ (in g g^{-1}). To do so, long term, volume based firn/air ratios (hereafter denoted as FAR) were calculated accordingly to:

$$FAR = \rho_w \frac{\overline{C}_F}{\overline{C}_A} \qquad \text{(dimensionless)} \qquad (1)$$

with ρ_w denoting water density. This ratio should not be confused with the -so called- scavenging ratio, which in general, refers to the impurity concentration of precipitation (falling snow) and the concurrent pollutant concentration in the precipitating air mass. Thus, different to scavenging ratios, FARs include periods without precipitation and are thus also related to the whole series of dry deposition fluxes (positive and negative ones). Obviously, long term

FAR values depend on the time fraction without snow falls and hence on the mean precipitation rate and frequency. FAR values obtained at VO and comparable sites are listed in Table 4. Concurrent mean concentrations in the snow pack are only available for the summer data set from VO, and were calculated as the water equivalent weighted mean concentration in the snow pack, accumulated during the time interval of aerosol measurements. For other periods and sites, $\overline{C}_F$ at VO and CG was calculated using for each site the representative mean summer or winter concentration values found over the time period from 1981 to 1991 (Preunkert et al., 2000). Since these snow concentrations do however not correspond to the years in which air measurements were made (1993/1994 at CG

and 1999/2000 at VO), they have been corrected with regard to the respective mean concentration changes observed in the Col du Dôme and CG snow pack from the 1980's to 1993, 2000, respectively (Wagenbach and Preunkert, 1996; Preunkert in prep). Note that no significant deviations are obtained when this extrapolation is applied to the well known summer 2000 snow impurity content at VO. The seasonal FAR values given for SBO in Table 4 are derived from monthly averaged precipitation concentrations and monthly averaged air concentrations (thus including also days without precipitation) from the years 1991 to 1993 (Kasper-Giebl et al., 1999). Hence, the SBO data are not pure FARs but rather a mixture of scavenging ratios and FARs. The NH_4^+ and SO_4^{2-} values given for Summit (Greenland) are based on seasonal means of monthly median air concentrations from 1997 (Jaffrezo et al., submitted) and seasonal means of monthly averaged concentrations in the surface snow of the years 1990 to 1995 (Aymoz, 1999). Since for total NO_3^- no continuous measurements exist for Summit, the NO_3^- summer FAR in Table 4 is only based on discontinuous air measurements of total NO_3^- obtained in summer 1993 at Summit (Dibb et al., 1994). The Alpine FAR values have been averaged over the same periods as the seasonal mean air concentrations presented in Table 3. The Greenland FAR data correspond to November to January means (winter) and June to August means (summer) in order to minimize the influence of interannual changes in the occurrence of the Arctic Haze.

Different to the highly variable scavenging ratios, the FAR values obtained at all sites are quite comparable reflecting the fact that FARs are built on long term mean air and snow concentrations. Since the FARs are however biased by the precipitation climatology (see above), a detailed intersite comparison would be not straightforward. We confine therefore the discussion of FAR values on the seasonal contrast and differences between aerosol and gas phase related species. At VO total NO_3^- FAR values of 5.2 10^6 and 3.2 10^6 were found in winter and summer, respectively. The seasonal change at VO (higher values in winter than in summer) is in agreement with the finding at SBO. At both sites, the total NO_3 FAR are in summer as in winter significantly larger than those of SO_4^{2-} and NH_4^+, suggesting a more efficient scavenging for gaseous HNO_3 than for aerosol derived species (Kasper-Giebl et al., 1999). A similar seasonal behaviour is seen at Summit for the total NO_3^- summer value (no winter value is available here). For measurements done with the prototype sampler at CG, total NO_3^- FAR values of 2.3 10^6 and 1.3 10^6 were found for winter and summer, respectively. Again the same seasonal difference could be observed as for VO and SBO, but probably due to HNO_3 passive sampling problems with the prototype device (see section 4.1), FAR values are artificially decreased at CG.

SO_4^{2-} FARs observed at all sites (including Summit) indicate also higher values in winter than in summer. At the three Alpine sites, in summer and to a lesser extent in winter, SO_4^{2-} and

NH_4^+ FARs are similar, while at Summit NH_4^+ FARs are almost three times higher than SO_4^{2-} ones. NH_4^+ FARs observed at SBO and Summit show again higher values in winter than in summer, which is not seen at VO and CG where summer and winter FAR values are quite similar. Such an intersite seasonal difference in NH_4^+ FARs cannot be attributed to a systematic overestimation of NH_4^+ air levels measured with the automatic devices, since the atmospheric molar ratio of NH_4^+ to SO_4^{2-} at SBO fits well with the VO one (see above) or is even higher than at CG (Preunkert and Wagenbach, 1998). On the other hand, in spite of the strong irregularities of snow deposition at high Alpine sites, FAR values at VO and CG are in rather good agreement. The presently limited length of the temporal atmospheric data sets at VO and CG needs to be extended by further continuous long term air and snow investigations to elucidate the seasonal difference in the NH_4^+ FARs and to confirm the SO_4^{2-} and total NO_3^- observations. Such extended investigations would also permit to evaluate the possible reasons responsible for the observed FAR differences between NH_4^+, SO_4^{2-}, and total NO_3^-.

7 Summary and prospectives

With respect to document continuously the year round aerosol load and composition at remote high Alpine glaciers sites, following state has been reached with the revised automatic aerosol sampler:

- an autonomous, long term operation at extremely adverse glacier sites is possible
- the importance of total filter holder sealing in controlling blank and post sampling artefacts is evident
- reliable data are ensured for SO_4^{2-}, NH_4^+, K^+, and oxalate as well as for total Cl^- and total NO_3^-, only underestimated values can be obtained for Na^+, Mg^{2+} and Ca^{2+}
- the knowledge of the collection efficiency of the device with respect to large particles need to be improved to gain reliable FAR data for crustal species
- an improvement of the filter holder inertness is required

Since it is not necessary to set up the aerosol sampler in a hut, the self-contained sampling device may be deployed at other ice core drill sites. On the base of the present sampler state, perspectives for other high elevation mountain and polar sites are given below.

a) High elevation sites (Himalaya, Andes): The deployment at these sites will be more restricted by logistical constraints (lacking infrastructure, difficult transport and adverse climatic conditions), than by low atmospheric aerosol loads. Based on available snow data (e.g. Sichang, et al., 2000; Thompson et al., 1998) no detection limit problems are expected here for inorganic species.

b) Polar regions: A major problem for deploying the device at these sites would be the energy supply during polar night. Assuming for simplicity half a year without sunlight, a buffer battery pack with a capacity of 2200 Ah (≈1600 kg of lead/sulfate cells operated at -30°C) would be required to run the sampler continuously at the given flow rate. In view of the good infrastructure and transport logistics available at the prominent polar drill sites, the installation of such an heavy battery pack may be not a major problem. On the other hand, using disposable but expensive lithium batteries only a 100 kg battery pack is needed at drill sites with limited transport logistics. An adequate power supply may be achieved here by a solar panel - buffer battery energy system (running when sunlight is available regularly), in combination with a lithium battery pack, dimensioned for the duration of the polar night at the respective sampling site. To cope with the low atmospheric levels at polar sites, sampling on PTFE filters is required which is now possible with the new device.
North polar sites (Greenland, North Canada): Assuming (for the sake of simplicity) a FAR of 1 10^{-6} , bi-weekly samples correspond to equivalent amounts of impurities in 100 g of firn, thus sufficiently large for reliable analyses of all inorganic species and MSA (e.g. Legrand and Mayewski, 1997; Fischer, 1997; Holdsworth and Peake, 1985). Note that during the Arctic Haze time period, rather high concentrations prevail, while on the other hand, the power supply may be critical during this final stage of the polar night. Since the energy consumption is strongly depending on the flow rate, which again controls the detection limits, energy consumption could be minimized by automatically decreasing the flow rate during the polluted Arctic Haze period.
Antarctica: The most important period at Antarctic sites lies between the equinox (i.e. September – March), where relative high air concentrations prevail, and the energy supply is ensured by sunlight. Specific problems may appear here in relation with temperatures down to –60 °C which may be overcome by an internal heating source (e.g. catalytic combustion) within a thermally well isolated container. Probably no problems will arrive concerning the detection limits at more coastal sites (e.g. Wagenbach , 1996; Legrand et al., 1998) with the exception of NH_4^+, for which an assessment may be critical in view of passive sampling effects on acidic filters. It is not assumed that the high wind speeds and the riming occurring at these sites restrict the deployment of the sampler, since no serious problems occurred during the deployment at VO and CG. In Central Antarctica (Legrand and Mayewski, 1997) detection limit problems may arrive perhaps for Ca^{2+} and K^+ species during the polar night and for NH_4^+ (see above). Except for MSA, no assessment is possible yet for organic species.

In future, the aerosol sampler will be run at VO, to overcome the existing information lack concerning the firn/air relation at high Alpine ice core drill sites. Note that this opens also the possibility to get reliable long term year round data of the aerosol composition above 4000 m

asl over Europe. In addition, it is planned to build up an adequate version of the aerosol sampler for continuous, year round deployment at polar drill sites.

8 Acknowledgements

This paper is a contribution to the European Environment and Climate Programme ALPCLIM. Funding was provided by the European Community via contract ENV4-CT97-0639 (ALPCLIM) and ENV4-CT96-5051 (Environment and Climate Research Training Grant). We could not do without the ingenious electro technical ideas provided from H.G. Junghans and S. Grabert. We thank A. Manouvrier, C. Rado and J.P. Balestrieri for their invaluable help in constructing the device. We are grateful to B. Jourdain and numerous other colleagues for their commitment in the field. We particularly acknowledge the logistical support provided by the staff of Refuge Cosmiques and Chamonix Mont Blanc Helicopter. The helpful comments of J. Dibb and an anonymous referee were very greatly acknowledged.

References

Aymoz, G. (1999) *Etude de la composition chimique de la neige de surface de Groenland*. MS thesis, Laboratoire de Glaciologie et Géophysique de l'Environnement, University Joseph Fourier, Grenoble 1, 45p.

Bales, R.C. and Wolff, E.W. (1996) Interpreting natural climate signals in ice cores. *EOS* **76**, 477,482-483.

Baltensperger, U., Gäggeler, H.W., Jost, D.T., Emenegger, M. and Nägeli, W. (1991) Continuos background aerosol monitoring with the Epiphaniometer. *Atmospheric Environment* **25A**, 629-634.

Chan, W.H., Orr, D.B. and Chung, D.H.S. (1986) An evaluation of artifact SO_4^{2-} formation on nylon filters under field conditions. *Atmospheric Environment* **20**, 2397-2401.

Crane, R.I. and Evans, R.L. (1977) Inertial deposition of particles in a bent pipe. *Journal of Aerosol Science* **8**, 161-170.

Davidson, C.I., Jaffrezo, J.-L., Mosher, B.W., Dibb, J.E., Borys, R.D., Bodhaine, B.A., Rasmussen, R.A., Boutron, C.F., Gorlach, U., Cachier, H., Ducret, J., Colin, J.-L., Heidam, N.Z., Kemp, K. and Hillamo, R. (1993) Chemical constituents in the air and snow at Dye 3, Greenland - I. Seasonal variations. *Atmospheric Environment* **27A**, 2709-2722.

Dibb, J.E., Talbot, R.W. and Bergin, M. (1994) Soluble acidic species in air and snow at Summit, Greenland. *Geophysical Research Letters* **21**, 1627-1630.

Fischer, H. (1997) *Räumliche Variabilität in Eiskernzeitreihen Nordostgrönlands - Rekonstruktion klimatischer und luftchemischer Langzeittrends seit 1500 A.D.*. PhD-Thesis, Institut für Umweltphysik der Universität Heidelberg, 135p.

Fuchs, N.A. (1964) *The Mechanics of Aerosols*. Oxford, Pergamon.

Harder, S., Warren, S.G. and Charlson, R.J. (2000) Sulfate in air and snow at the South Pole: implications for transport and deposition at sites with low accumulation. *Journal of Geophysical Research* **105**, 22825-22832.

Holdsworth, G. and Peake, E. (1985) Acid content of snow from a mid-troposphere sampling site on Mount Logan, Yukon Territory. *Annals of Glaciology* **7**, 153-160.

Jaffrezo, J.L., Davidson, C.I., Kuhns, H.D. and Strader, R. Seasonal variations in aerosol chemical species on the Greenland ice sheet. *Atmospheric Environment*, submitted.

Kasper, A. and Puxbaum, H. (1994) Determination of SO_2, NHO_3, NH_3 and aerosol components at a high Alpine background site with a filter pack method. *Analytica Chim. Acta* **291**, 297-304.

Kasper, A. and Puxbaum, H. (1998) Seasonal variation of SO_2, HNO_3, NH_3 and selected aerosol components at Sonnblick (3106 m asl). *Atmospheric Environment* **32**, 3925-3939.

Kasper-Giebl, A., Kalina, M.F. and Puxbaum, H. (1999) Scavenging ratios for sulfate, ammonium and nitrate determined at Mt. Sonnblick (3106 m a.s.l.). *Atmospheric Environment* **33**, 895-906.

Legrand, M., De Angelis, M. and Maupetit, F. (1993) Field investigation of major and minor ions along Summit (central Greenland) ice cores by ion chromatography. *J. Chromatogr*. **640**, 251-258.

Legrand, M. and Mayewski, P. (1997) Glaciochemistry of polar ice cores: A review. *Reviews of Geophysics* **35**, 219-243.

Legrand, M., Hammer, C., de Angelis, M., Savarino, J., Delmas, R., Clausen, H. and Johnsen, S. (1997) Sulfur-containing species (methanesulfonate and SO_4^{2-}) over the last climatic cycle in the Greenland Ice Core Project (central Greenland) ice core. Journal of Geophysical Research 102, 26663-26679.

Legrand, M., Ducroz, F., Wagenbach, D., Mulvaney, R. and Hall, J. (1998) Ammonium in coastal Antarctic aerosol and snow: Role of polar ocean and penguin emissions. *Journal of Geophysical Research* **103**, 11043-11056.

Limbeck, A. and Puxbaum, H. (1999) Organic acids in continental background aerosols. *Atmospheric Environment* **33**, 1847-1852.

Maupetit, F., Wagenbach, D., Weddeling, P. and Delmas, R.J. (1995) Recent chemical and isotopic properties of high altitude cold Alpine glaciers. *Atmospheric Environment* **29**, 1-9.

Neumann, J.A., Huey, L.G., Ryerson, T.B. and Fahey, D.W. (1999) Study of inlet materials for sampling atmospheric nitric acid. *Environ. Sci. Technol.* **33**, 1133-1136.

Oeschger, H. and Langway, C.C. (eds) (1989) *The environmental record in glaciers and ice sheets.* Dahlem Konferenzen, John Wiley and Sons, Chichester.

Preunkert, S. *History of the European air pollution inferred from Alpine ice cores*. PhD-Thesis, Laboratoire de Glaciologie et Géophysique de l'Environnement, University Joseph Fourier, Grenoble 1, in preparation.

Preunkert, S. and Wagenbach, W. (1998) An automatic recorder for air/firn transfer studies of chemical aerosol species at remote glacier sites, *Atmospheric Environment* **32**, 4021-4030.

Preunkert, S., Wagenbach, D., Legrand, M. and Vincent, C. (2000) Col du Dôme (Mt Blanc Massif, French Alps) suitability for ice-core studies in relation with past atmospheric chemistry over Europe. *Tellus* **52B**, 993-1012.

Puxbaum, H. and Wagenbach, D. (1994) High alpine precipitation chemistry. In *The Proceedings of EUROTRAC Symposium 1994,* eds. P.M. Borell *et al*., pp. 597-605. SPB Academic Publishing bv, The Hague, The Netherlands.

Shichang, K., Wake, C.P., Dahe, Q., Mayewski, P.A. and Tandong, Y. (2000) Monsoon and dust signals recorded in Dasuopu glacier, Tibetan Plateau. *Journal of Glaciology* **46**, 222-226.

Talbot, R.W., Vijgen, A.S. and Harriss, R.C. (1990) Measuring tropospheric HNO_3: Problems and prospects for nylon filter and mist chamber techniques. *Journal of Geophysical Research* **95**, 7553-7561.

Thompson, L.G., Davis, M.E., Mosley-Thompson, E., Sowers, T.A., Henderson, K.A., Zagorodnov, V.S., Lin, P.N., Mikhalenko, V.N., Campen, R.K., Bolzan, J.F., Cole-Dai, J., Francou, B. (1998) A 25,000-year tropical climate history from Bolivian ice cores. *Science* **282**, 1858- 1864.

Voisin, D., Legrand, M. and Chaumerliac, N. (2000) Scavenging of acidic gases (HCOOH, CH_3COOH, HNO_3, HCl, and SO_2) and ammonia in mixed liquid-solid water clouds at the Puy de Dôme mountain (France). *Journal of Geophysical Research* **105**, 6817-6835.

Wagenbach D. (1996) Coastal Antarctica: Atmospheric chemical composition and atmospheric transport. In *NATO ARW Workshop: Process of chemical exchange between the atmosphere and polar snow (Il Chiocco, Italy 1995),* eds. E. Wolff and R. Bales, NATO-ASI Series I: Chemical Exchange Between the Atmosphere and Polar Snow, Vol. 43, 173-199. Springer, Berlin.

Wagenbach, D. (1997) High Alpine Air and Snow Chemistry. In *Cloud multi-phase processes and high Alpine air and snow chemistry,* eds. S. Fuzzi and D. Wagenbach, pp. 163 – 282. Transport and chemical transformation of pollutants in the troposphere Volume 5, Springer.

Wagenbach D. and Geis K. (1989) The mineral dust record in a high altitude glacier (Colle Gnifetti, Swiss Alps). In *Paleoclimatology and Paleometeorology: Modern and Past Patterns of Global Atmospheric Transport,* eds. M. Leinen and M. Sarnthein, pp.543-564. Kluwer Academic Publishers, Dordrecht.

Wagenbach, D. and Preunkert, S. (1996) The History of European Pollution Recorded in Alpine Ice Cores. In *Proceedings of the EUROTRAC Symposium 1996, G.-Partenkirchen,* ed. P.M. Borell *et al*., pp 273-281. Computational Mechanics Publications, Southampton.

Wåhlin, P. (1996) One year's continuous aerosol sampling at Summit in central Greenland. In *Chemical Exchange Between the Atmosphere and Polar Snow*, eds. E.W. Wolff and R.C. Bales, pp. 131-143. Springer, New York.

Ye, Y. and Pui, D.Y.H. (1990) Particle deposition in a tube with an abrupt contraction. *Journal of Aerosol Science* **21**, 29-40.

Tables

Table 1: Blank filter variability and associated detection limits for the new and the prototype aerosol sampler. $(\Delta C/C)_{new}$ corresponds to the relative blank enhancement with respect to laboratory filter blanks; all blank values refer to a filter area of 10 cm^2 and detection limits (DL) to bi-weekly samples of 60 m^3 STP.

	$C_{new} \pm SD$ (ng)	$(\Delta C/C)_{new}$ (%)	C_{proto} (ng)	DL_{new} (ng m^{-3}STP)	DL_{proto}/DL_{new}
Quartz Filter (36 mm)					
Acetate	890 ± 93*	73	n.a.	4.6	-
Formate	280 ± 38*	88	n.a.	1.8	-
Cl^-	43 ± 265	7	59 ± 65	1.3	3.8
NO_3^-	19 ± 6.4	48	160 ± 70	0.3	17
SO_4^{2-}	61± 19	57	140 ± 110	1.0	8
Oxalate	11 ± 5	68	n.a.	0.3	-
Na^+	1610 ± 310	49	1170 ± 350	16	1.6
NH_4^+	62 ± 26	83	260 ± 170	1.3	10
K^+	60 ± 13	14	64 ± 70	0.7	7.1
Mg^{2+}	13 ± 4	13	24 ± 9	0.2	3.5
Ca^{2+}	130± 39	-63	130 ± 35	2.0	1.5
Nylon Filter (36 mm)					
Acetate	970 ± 64*	82	n.a.	3.2	-
Formate	1800 ± 430*	90	n.a.	22	-
Cl^-	140 ± 26*	86	370 ± 320	1.3	19
NO_3^-	76 ± 18*	92	190 ± 88	0.9	8
SO_4^{2-}	53 ± 16	94	400 ± 310	0.8	30
Oxalate	33 ± 6*	30	n.a.	0.2	-

* temporal increase of field blank, adjusted to six months storage time

Table 2: Field comparison of a simulated aspiration/sampling configuration versus denuder and mist chamber sampling lines at Refuge Cosmiques (see text).

N denotes the number of runs, C_{ref} the mean reference concentration obtained by denuder and mist chamber lines, respectively. C_{ref} for aerosols is obtained by averaging the air concentrations achieved form the quartz filters of the denuder and the mist chamber lines. If not marked otherwise, C_{ref} for gas phase species is obtained by averaging denuder tubes and the mist chambers data.

	N	C_{SIM} /C_{ref} (range)		C_{ref} (ng m^{-3} STP)
Aerosol				
Acetate [a, b]	3	2.9 ± 0.8	2.1 - 4.1	5 - 15
Formate [a, b]	3	1.8 ± 2.2	0.9 - 3.5	1 - 5
Cl^- [a, b]	1	≈ 0.2	-	2
NO_3^-	1	0.9 ± 0.01	-	50
SO_4^{2-}	3	1.1 ± 0.01	1.0 - 1.2	150 - 500
Oxalate	3	0.9 ± 0.04	0.8 - 1.2	5 - 30
Na^+ [a, b]	2	0.7 ± 1.2		10 - 30
NH_4^+	3	1.0 ± 0.03	0.8 - 1.0	50 – 150
K^+	3	0.9 ± 0.2	0.7 - 1.0	4 – 16
Gas phase				
Acetate [a]	1	0.04 ± 0.02	-	300
Formate [a]	1	0.06 ± 0.1	-	300
Cl^-	1	1.3 ± 0.3	-	10
NO_3^-	1	1.0 ± 0.1	-	25
SO_4^{2-} [a]	1	< 0.1	-	50
Oxalate [a]	1	0.1 ± 0.04	-	5 [c]
Total				
Cl^- [(a, b)]	1	1.1 ± 0.4	-	12
NO_3^-	1	0.9 ± 0.04	-	75

a: C_{SIM} below double blank level
b: C_{ref} below double blank level
c: C_{ref} only from denuder

Table3: Comparison of seasonal mean atmospheric concentration of ionic species observed at high Alpine sites.

(1) updated automatic sampler, this work

(2) prototype sampler (Preunkert and Wagenbach, 1998)

(3) attended samplings (Kasper and Puxbaum, 1998)

	Vallot Observatory (1) (4361 m asl)			Colle Gnifetti (2) (4450 m asl)			Sonnblick Observatory (3) (3106 m asl)		
Species	winter (ng m^{-3} STP)	summer (ng m^{-3} STP)	summer/ winter	winter (ng m^{-3} STP)	summer (ng m^{-3} STP)	summer/ winter	winter (ng m^{-3} STP)	summer (ng m^{-3} STP)	summer/ winter
total Cl^-	<10	58	> 5.8	19	85	4.5	-	-	-
total NO_3^-	34	192	5.6	83	420	5	210	1090	5.2
SO_4^{2-}	101	533	5.2	110	630	5.7	410	3480	8.5
Oxalate*	8	44	5.5	-	-	-	-	-	-
Na^+	<50	<25	-	<15	26	>1.7	-	-	-
NH_4^+	21	190	9	20	180	9	96	1060	11
K^+	<7	12	>1.7	-	-	-	-	-	-
Mg^{2+}	<0.7	2.2	>3.1	-	-	-	-	-	-
Ca^{2+}	<9	27	>3	4.3	37	8.6	-	-	-

* particulate fraction

Table 4: Comparison of seasonal averaged Firn Air Ratios (FAR) at high Alpine sites and Greenland (see text).

	Vallot Observatory (4361 m asl)		Colle Gnifetti (4450 m asl)		Sonnblick Observatory (3106 m asl)		Summit (Greenland) (3200 m asl)	
Species	winter	summer	winter	summer	winter	summer	winter	summer
total NO_3^-	5.2	3.7	2.3	1.3	4.9	1.6	n.d.	2.2
SO_4^{2-}	2.6	1.3	1.8	1.5	2.5	0.9	0.87	0.54
NH_4^+	1.1	1.7	1.6	1.6	2.8	1.0	2	1.44

all values × 10^6

Figures

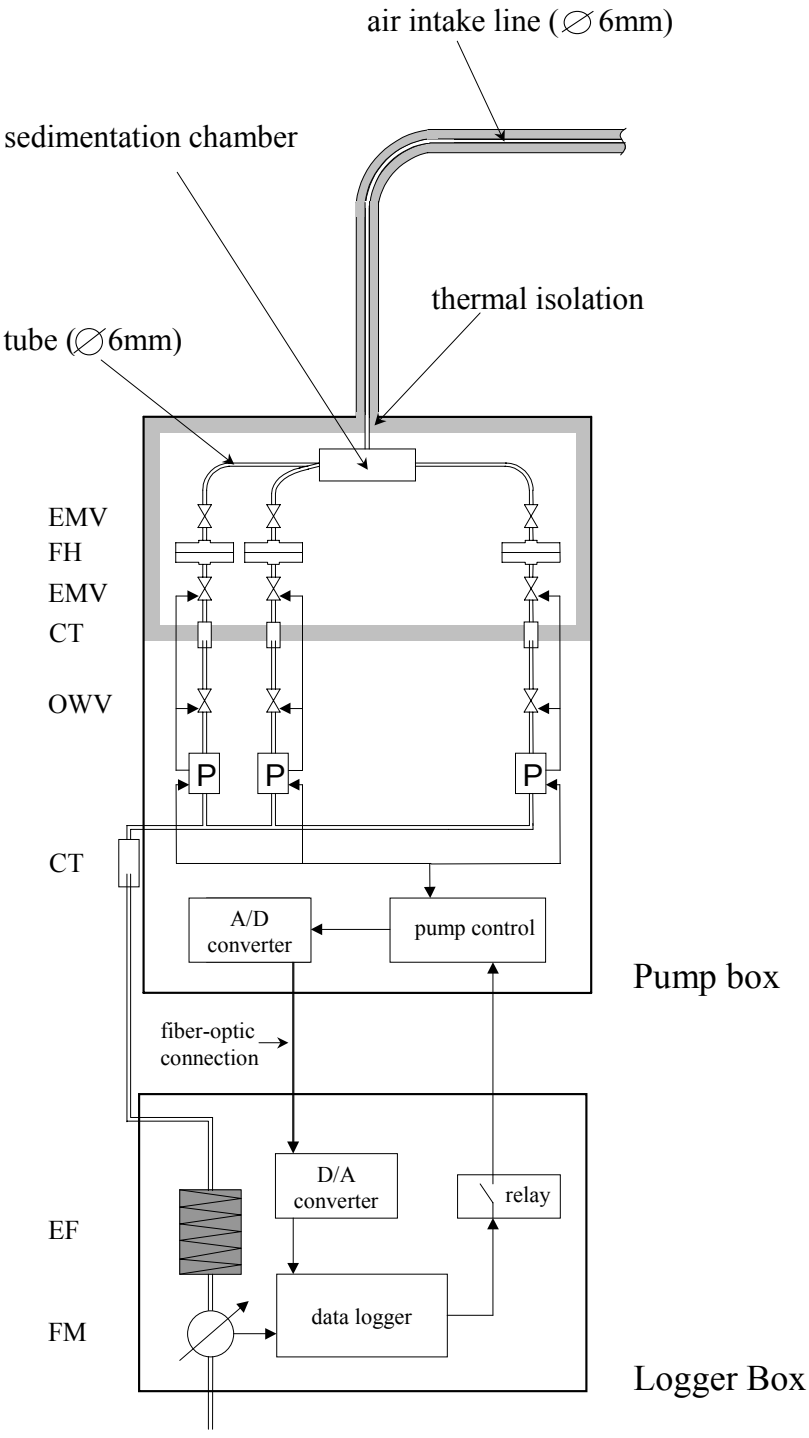

Figure 1: Setup principle of the new aerosol sampling device. Abbreviations: EMV: electro magnetic valve; FH: filter holder; CT: condensation trap; OWV: one way valve; P: pump; EF: exhaust filter; FM: flow meter.

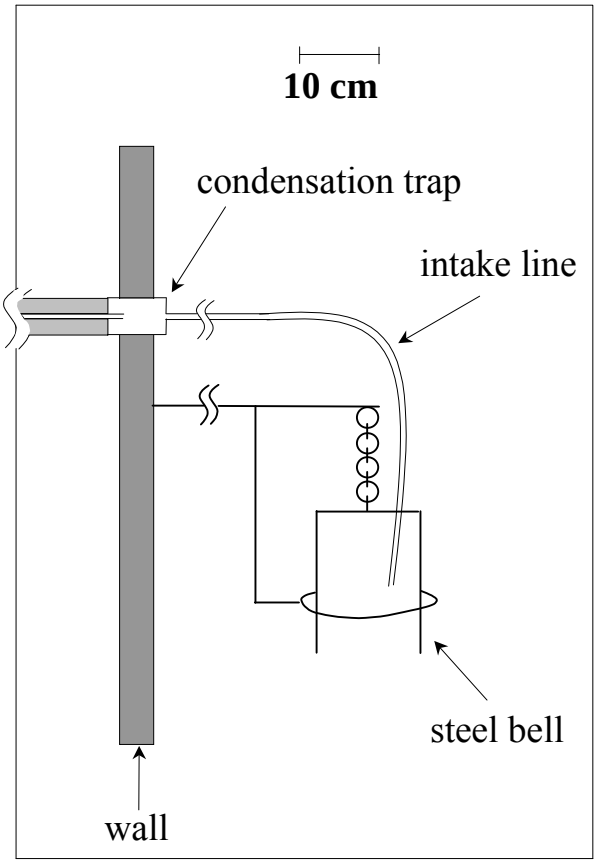

Figure 2: Design of the air aspiration arrangement installed at Vallot Observatory for automatic aerosol sampling.

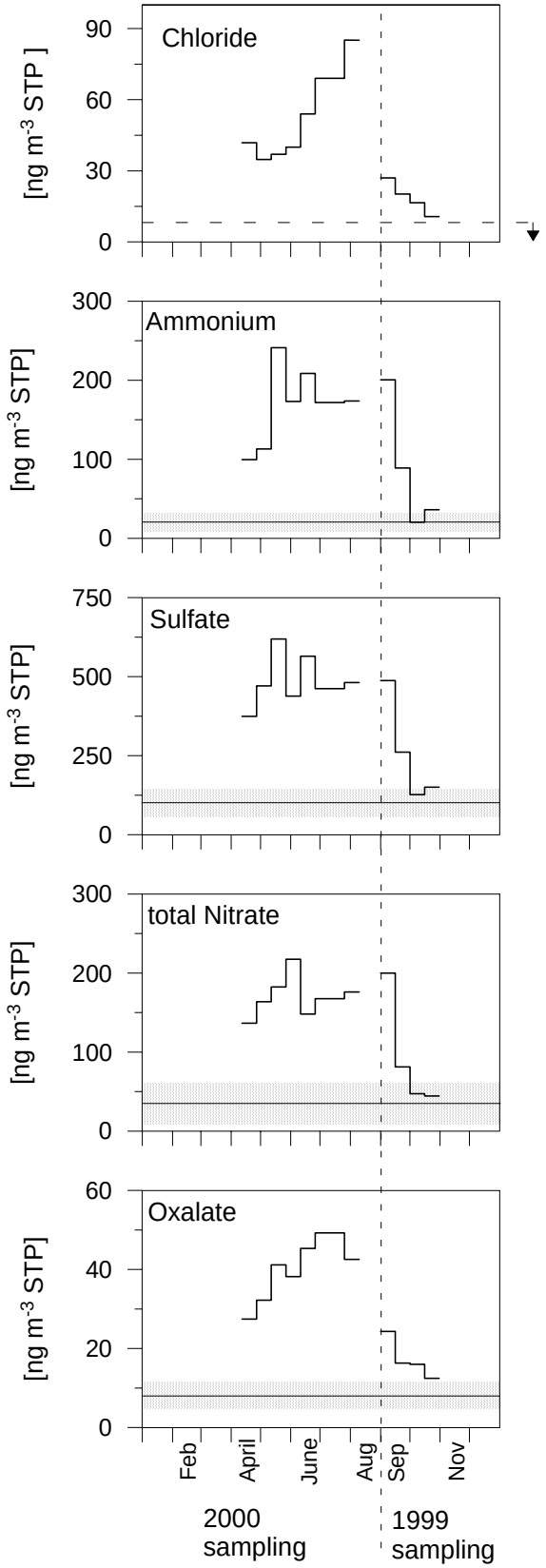

Figure 3: Seasonal pattern of NH_4^+, SO_4^{2-}, total NO_3^-, total Cl^-, and oxalate observed at Vallot Observatory during end of summer 1999 and summer 2000 (averages over 15 days). Dashed horizontal lines and shaded area denote the mean levels and ranges, respectively, obtained during the mid-winter period (November 1999 – February 2000).

Chapter II

Suitability of the Col du Dôme site for ice core records of past atmospheric chemistry over Europe

With the aim to reconstruct the long term changes of the atmospheric chemistry over Europe, a 126 m long ice core (C10) was drilled in 1994 close to bedrock at the Col du Dôme site (see *Figures 1* and *2* in section 2.4). To assess the quality, and to achieve an appropriate interpretation of the ice core signals extracted from this core in terms of atmospheric changes, investigations were made concerning (1) the dating of the C10 core, (2) systematic changes in the snow deposition characteristics upstream to the C10 drill site, and (3) the seasonal variation and the spatial representativity of the chemical signal in the recent snow pack.

2.1 Dating of the C10 core

As detailed in section 2.4 (*4.1*) the establishment of the chronology of the C10 ice core was achieved by using a stratigraphical method based on the strong seasonal change in the concentrations of ammonium. In this way, a precise dating of the core has been obtained by annual layer counting using the ammonium profile. The hereby applied protocol is detailed in section 2.4. The complete ammonium depth profile is reported in the Annex II along with the annual dating marks. The comparison of the time scale derived from this ammonium stratigraphical method with different absolute time horizons (^{137}Cs radioactive layers and well-known Saharan dust inputs) found in the C10 ice core, reveals an maximal error of 5 years at a depth of 86 m w.e., corresponding to an ice age of about 60 years (see section 2.4). Annual layer counting was possible until a depth of 91 m w.e.. Applying this method further down, the time period spanning the 1917 to 1906 years is found to be located between 91 m w.e. and 95 m w.e depth. However, as seen in Figure 2.1a, the ammonium variations in this part of the core are not regular anymore, suggesting a large inter-annual variability of the annual snow deposition at that time. That renders questionable the dating of this part of the core derived from such a stratigraphical method. On the other hand, using the mean annual snow accumulation rate of 0.2 m w.e. per year suggested in section 2.4 (see *Figure 9*) at the depth of 90 m w.e., these 4 m w.e. would cover about 20 years. Finally, comparing the SO_4^{2-}, NH_4^+ and NO_3^- levels observed in this part of the CDD ice core with the respective temporal trends related to growing man-made activities observed in Colle Gnifetti ice cores, a deposition date of about 1890 ± 10 years is suggested for the CDD ice located between 90 and

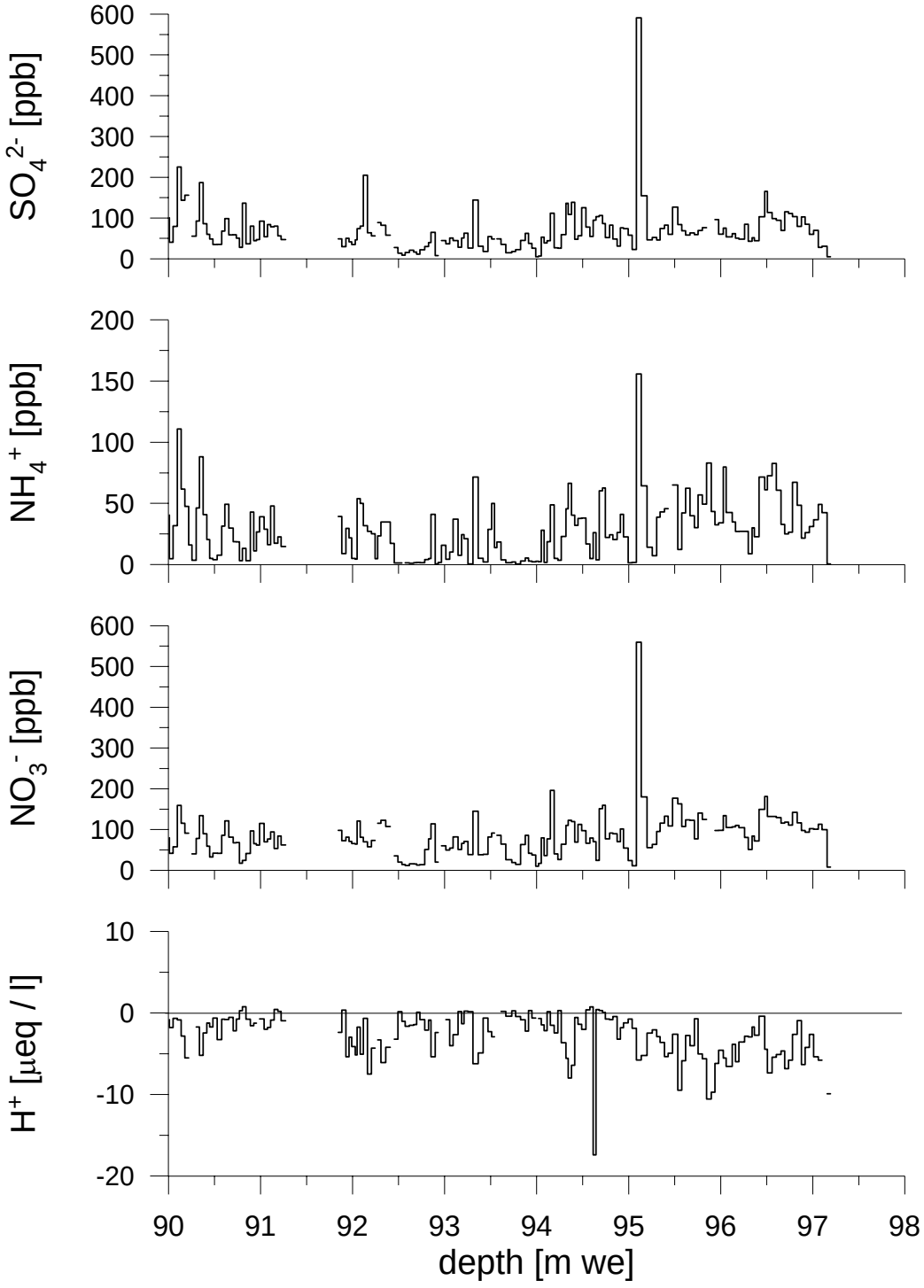

Figure 2.1a: Raw data profiles of SO_4^{2-}, NH_4^+, NO_3^-, and H^+ versus depth along the bottom part of the C10 core.

95 m w.e. depth in C10 (see section 4.1.4 (*3.3*)). Below the depth of 95.3 m w.e., the dating of the core remains essentially unknown and further studies of methane levels in air bubbles would certainly help here.

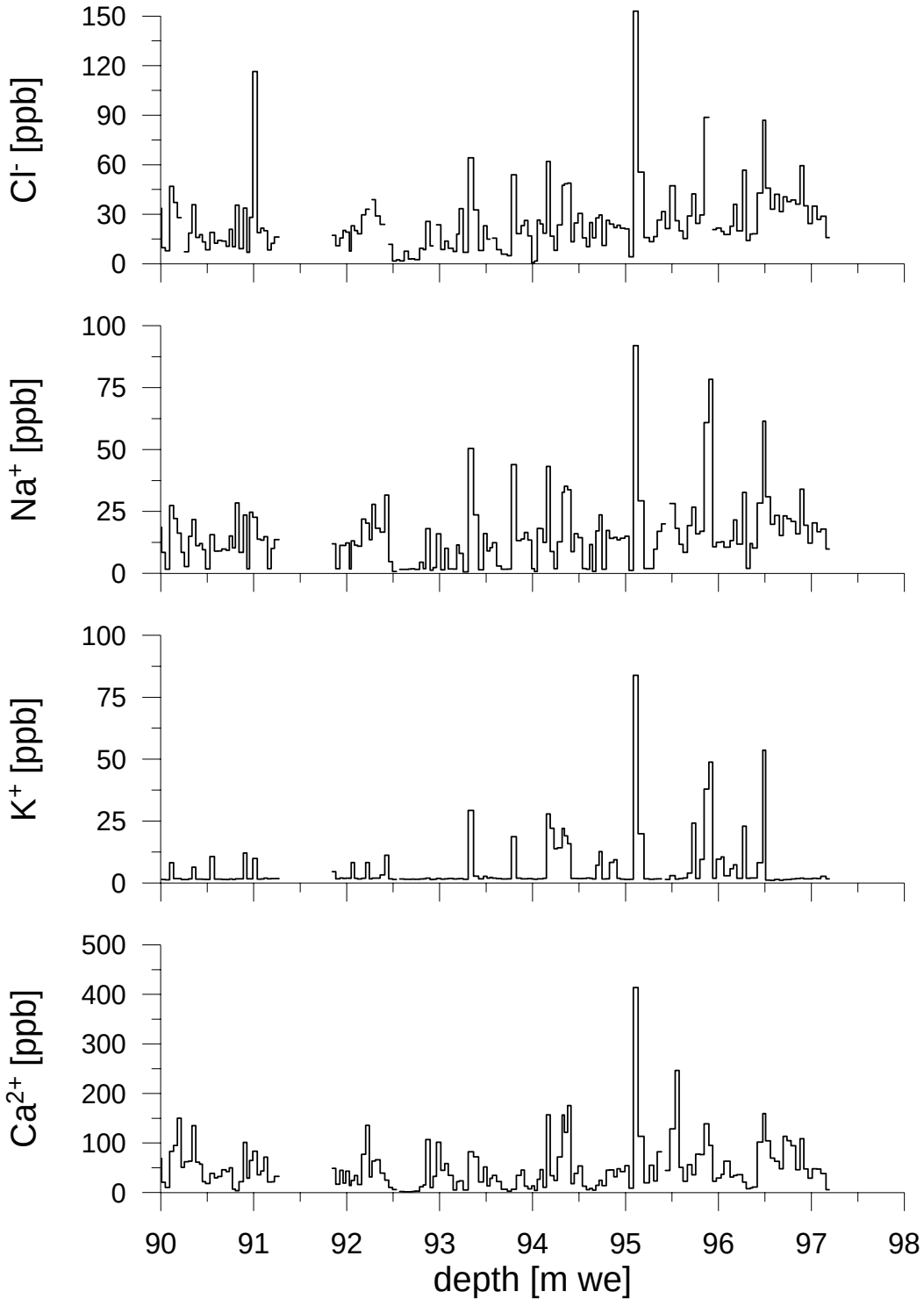

Figure 2.1b: Raw data profiles of Cl^-, Na^+, K^+, and Ca^{2+} versus depth along the bottom part of the C10 core.

2.2 Seasonal variations of the net snow accumulation versus depth along the C10 core

A specific problem related to such small area glacier has to be carefully addressed when dealing with Alpine ice core depth profiles. Figure 2.2 illustrates the mechanism of the glaciological forcing which systematically affects the impurity levels as a function of depth.

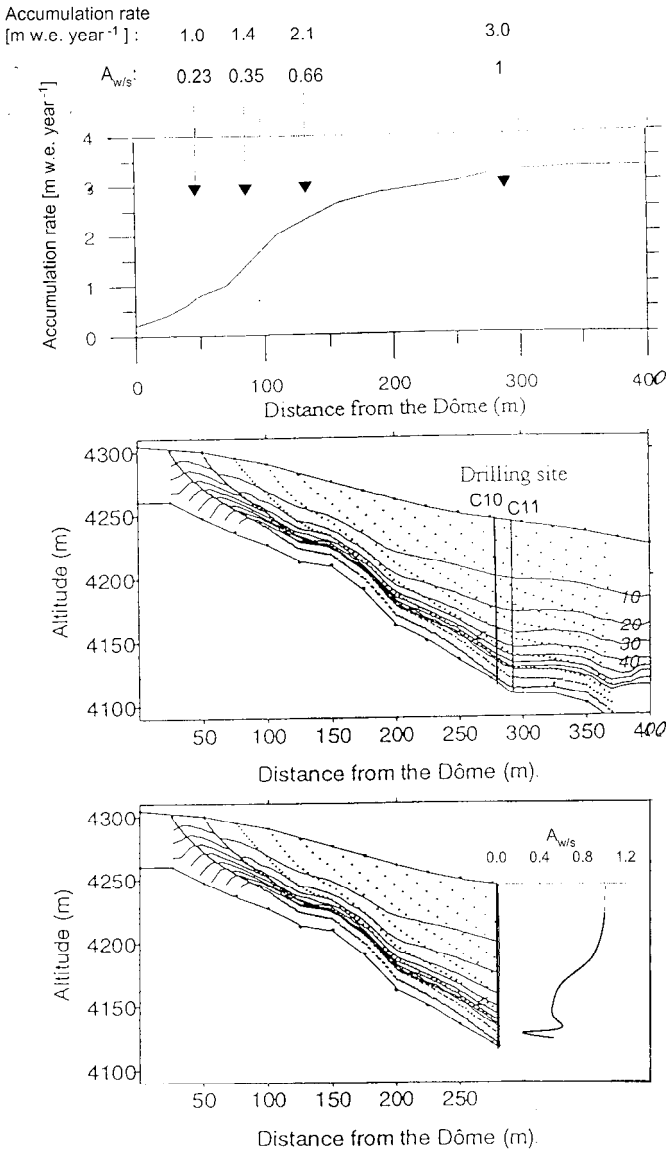

Figure 2.2: Scheme of the "glaciological forcing" effect due to ice flow between the Dôme du Gouter and the C10 CDD drill site. (Top) Accumulation rate along the flow line of the C10 core (Vincent et al., 1998). Arrows indicate accumulation and $A_{w/s}$ rates (see below) as determined from shallow ice cores (about 15 m depth) drilled upstream the C10 drill site. (Middle) Glacier flow properties with flow lines (dashed lines) and isochrones (solid lines) (adopted from Vincent et al., 1998). (Bottom) Same as middle (for upstream the C10 drill site) along with the mean evolution of the annual winter to summer net snow accumulation rate ($A_{w/s}$) versus depth of C10.

Mass balance measurements (Vincent et al., 1998) and glacio-chemical investigations of shallow ice cores revealed that the annual snow accumulation rate and the ratio of winter to summer net snow accumulation decreases upstream the borehole of the C10 site. Induced by the ice flow, this spatial variability would be mirrored along the depth of the C10 ice core. Based on the ammonium stratigraphy this effect was quantified along the C10 ice core indicating a decrease of the annual layer thickness from 3 w.e. at the surface to 0.2 m w.e. at 90 m w.e. depth as well as a decrease of the winter to summer net snow accumulation ratio ($A_{W/S}$) from 1 nearby the surface to 0.5 at 74 m w.e. depth (see *Figure 9* in section 2.4).

Therefore, because of the existence of a strong seasonal cycle of the ice impurity content (maxima in summer), the decrease of the fraction of winter (with respect to summer) snow deposition with depth may lead to an increase of the mean annual impurity levels, and that independently of any atmospheric changes over the past. This glaciological forcing is not specific to the Col du Dôme glacier site, but principally affects all ice core time series (of components underlying a seasonal variation) extracted at such small scale glacier sites. For the C10 ice core the net effect of this glaciological forcing, estimated in section 2.4 on the base of a simple model, can account for 20 and 30% for the observed changes of sulfate and ammonium, respectively. We will also evaluate this effect in section 3.5 when quantifying the NH_4^+ and SO_4^{2-} long term changes extracted from the C10 ice core.

2.3 Seasonal variation of impurity levels in the CDD snow cover

As discussed in section 2.1, the dating of snow layers is based on a stratigraphical method since no year by year absolute dating is possible. Since snow pit studies has been regularly carried out at the CDD site with the aim to derive the FAR values (see Chapter 1), we here report the seasonally dated chemical composition of the Col du Dôme snow pack from October 1997 to July 2000, as reconstructed from 6 individual snow pit studies (Figure 2.3 a-d). The seasonal resoluted dating is based on the respective sampling dates, stake measurements and Saharan dust events having occurred at known dates. Individual snow pit studies had not always been performed at the same location but at positions for which a similar snow accumulation rate (≈1 m w.e. per year) is expected (Vincent et al., 1997).

Year round (summer and winter) snow deposition was observed during the three years of snow pit investigations, with the exception of mid winter 1999/2000. The lack of winter deposition at the site during the latter winter is likely related to heavy storms with high wind speeds (e.g. 26.12.1999) having prevailed at that time. This study of snowpits indicates that low winter ammonium levels (less than 10 ng g^{-1}) used as criteria to locate winter snow layers in the C10 core (section 2.4) roughly correspond to the ammonium deposition occurring between October and March (Figure 2.4).

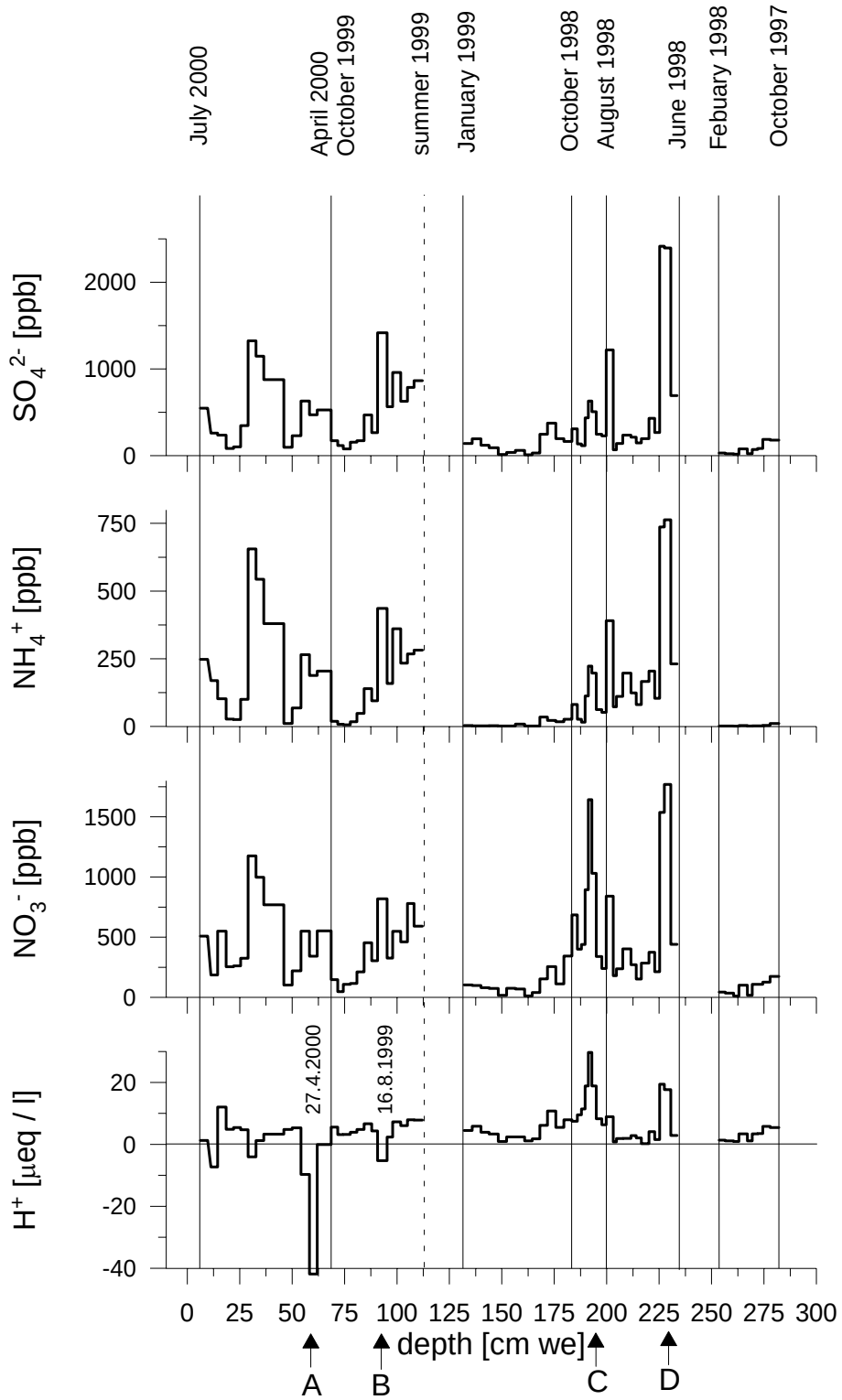

Figure 2.3a: SO_4^{2-}, NH_4^+, NO_3^-, and H^+ content of the Col du Dôme snow pack from October 1997 to July 2000, as reconstructed from successive snowpit studies. Marked snow layers are influenced by Saharan dust (A,B) and long range pollution events (B,C)

.

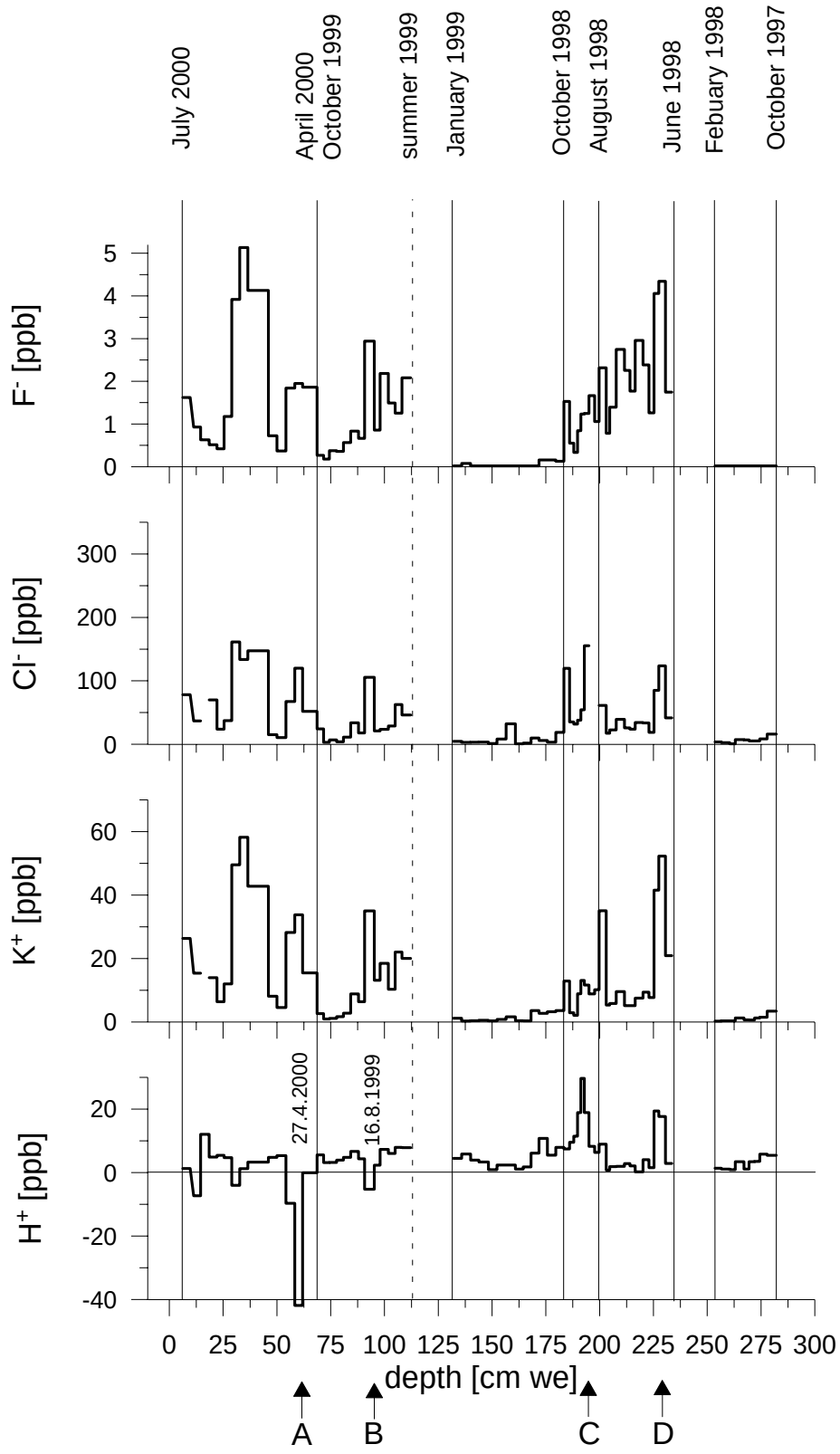

Figure 2.3b: F^-, Cl^-, K^+, and H^+ content of the Col du Dôme snow pack from October 1997 to July 2000, as reconstructed from successive snowpit studies. Marked snow layers are influenced by Saharan dust (A,B) and long range pollution events (B,C).

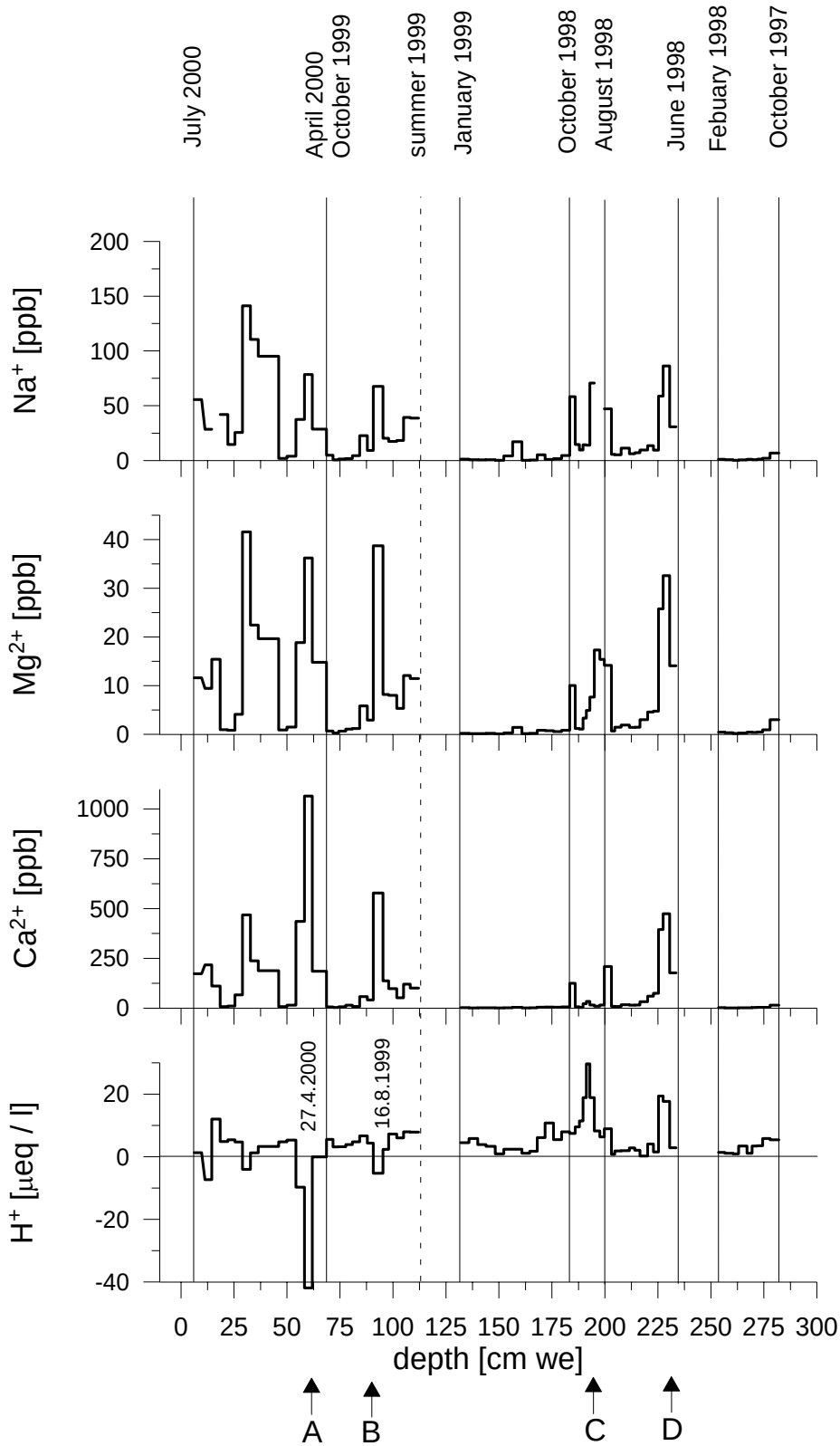

Figure 2.3c: Na^+, Mg^{2+}, Ca^{2+}, and H^+ content of the Col du Dôme snow pack from October 1997 to July 2000, as reconstructed from successive snowpit studies. Marked snow layers are influenced by Saharan dust (A,B) and long range pollution events (B,C).

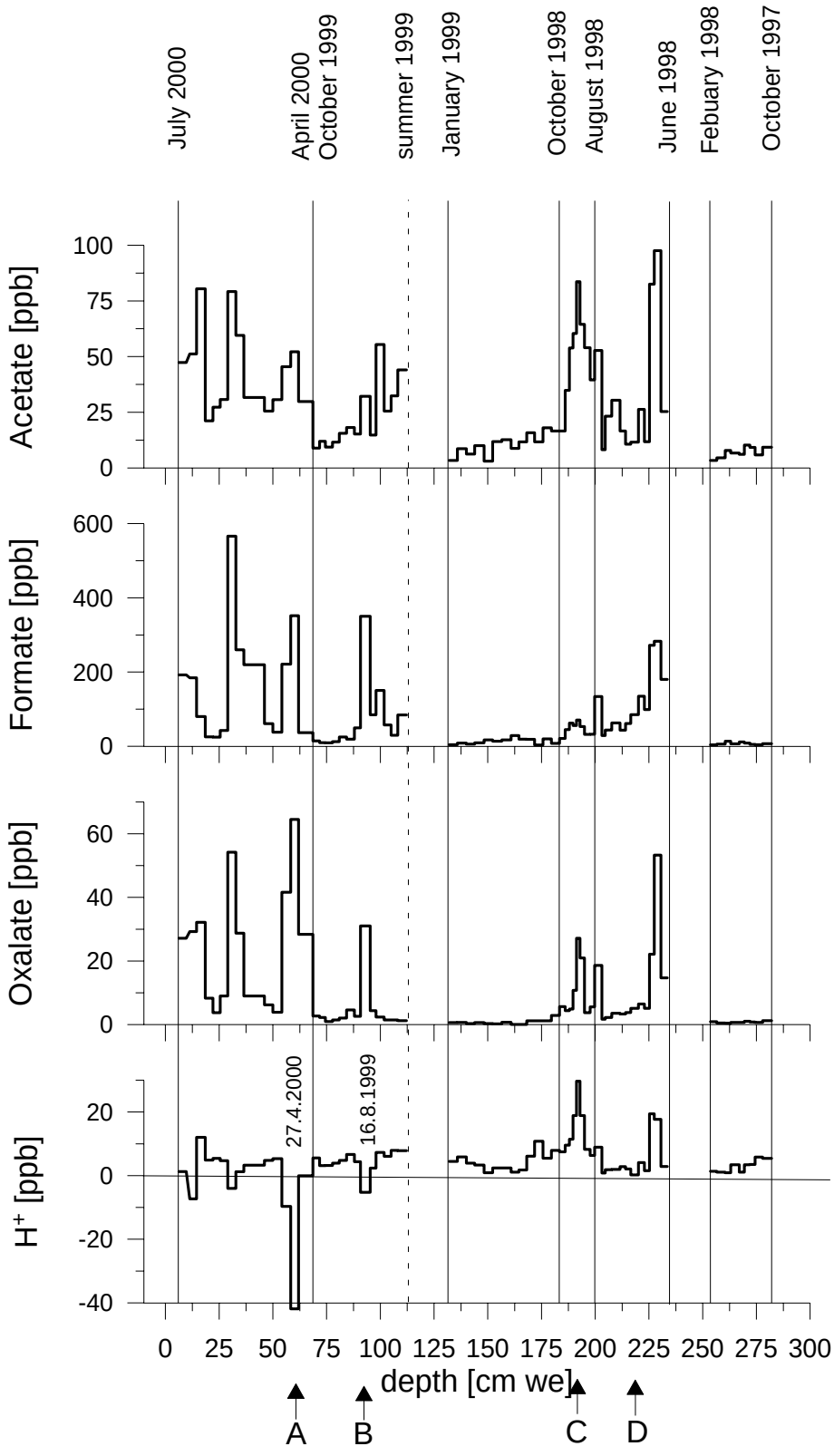

Figure 2.3d: Acetate, Formate, Oxalate, and H^+ content of the Col du Dôme snow pack from October 1997 to July 2000, as reconstructed from successive snowpit studies. Marked snow layers are influenced by Saharan dust (A,B) and long range pollution events (B,C).

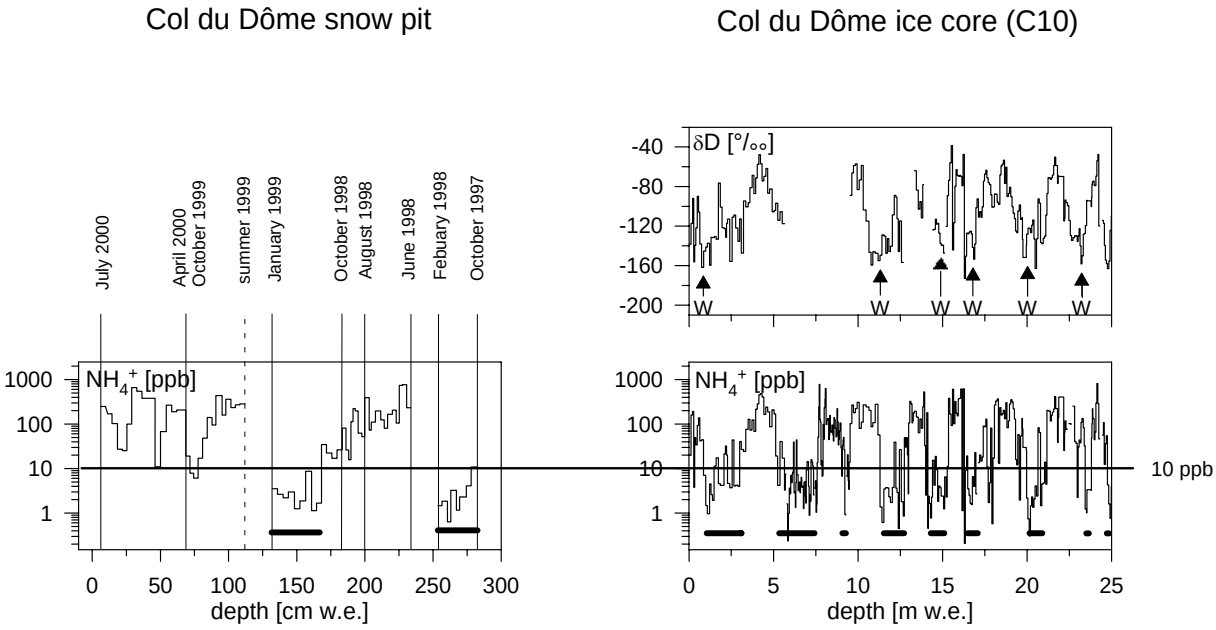

Figure 2.4: NH_4 depth profile (from 1997 to 2000) in the snow pack at Col du Dôme together with the NH_4^+ and δD depth profile of the upper part of the C10 ice core (see also Figure 3 in section 2.4)). Vertical arrows denoted W indicate the regular occurrence of minima in the δD profile. Horizontal lines reported in the two NH_4^+ profiles denote annual winter snow layers (see text).

In Table 2.1 mean summer and winter concentrations derived from snow pit samplings (from 1997 – 2000) are compared with half year (summer and winter) mean concentrations observed in the C10 core over the 1978-1994 time period which is made up by firn (snow/ice density of less than 0.83 g m^{-3}). Snow pit samples were sampled within a few months after the initial snow deposition, while the C10 firn layers were stored up to 16 years in the CDD snow cover before sampling was done. Taking into account the large inter annual variability of half year C10 means, for summer and winter snow deposits no significant differences were observed (for all investigated species) between the concentrations obtained within the snow pit study and the respective ones found within the C10 core. Such a good agreement is expected for species related to the aerosol phase (i.e., ammonium, sulfate, and oxalate for instance) for which no diffusion during firnification takes place. In contrast, such a good seasonal preservation of the seasonal cycle was not obvious for atmospheric species mainly present in the gas phase such as nitric acid, HF, HCl and monocarboxylates. For instance, at Summit, a central Greenland site characterized by a low snow accumulation rate (0.23 m w.e.) diffusive processes in firn layers of gaseous species like HF and HNO_3 (De Angelis and Legrand, 1994; De Angelis and Legrand, 1995, Fischer et al., 1998a) lead to strong distortions of the initially deposited seasonal signals of these species. These observations suggest that

Table 2.1: Mean summer and winter concentrations derived from snow pit investigations at CDD (with standard deviation of individual samples), and averaged half year (summer and winter) means derived from the C10 core (with standard deviation and ranges).

		F^- [ppb]	Acetate [ppb]	Formate [ppb]	Cl^- [ppb]	NO_3^- [ppb]	SO_4^{2-} [ppb]	Oxalate [ppb]
Snow pits (1997 – 2000)	summer	1.5 ± 1.3	35 ± 23	89 ± 102	57 ± 64	501 ± 401	496 ± 516	11 ± 13
	winter	0.05 ± 0.08	8.0 ± 2.9	10 ± 6.3	6.3 ± 7.0	72 ± 44	79 ± 59	0.7 ± 0.5
C10 core (1978 – 1994)	summer	1.3 ± 0.3 (0.7 – 1.7)	28 ± 17 (11 – 79)	78 ± 43 (28 – 203)	46 ± 15 (19 – 84)	385 ± 105 (259 – 622)	758 ± 224 (343 –1125)	20 ± 8.5 (5.7 – 41)
	winter	0.25 ± 0.16 (0.06 – 0.6)	8.5 ± 6.0 (3.6 – 23)	14 ± 6.7 (2.2 – 26)	20 ± 17 (5 – 64)	69 ± 16 (38 – 94)	85 ± 19 (44 – 110)	2.6 ± 1.2 (0.6 – 4.4)
		Na^+ [ppb]	NH_4^+ [ppb]	K^+ [ppb]	Mg^{2+} [ppb]	Ca^{2+} [ppb]		
Snow pits (1997 – 2000)	summer	33 ± 41	178 ± 185	14 ± 14	8.0 ± 9.0	88 ± 119		
	winter	2.2 ± 3.8	3.4 ± 2.8	0.9 ± 0.7	0.5 ± 0.7	2.8 ± 3		
C10 core (1978 – 1994)	summer	24 ± 10 (5.5 – 51)	180 ± 53 (102 - 296)	17 ± 6 (5.4 – 33)	15 ± 6 (3.0 – 30)	167 ± 122 (26 – 600)		
	winter	10 ± 10 (1.7 – 37)	5.8 ± 1.7 (3.3 - 9.5)	2.7 ± 1.4 (1.0 – 5.0)	1.7 ± 0.9 (0.4 – 4)	11 ± 8 (2.8 – 25)		

diffusive displacements are small at CDD due to the relative high accumulation rate prevailing at the drill site in the upper part of the core. Furthermore, for all investigated species (except formate and acetate, see section 6.3.1) seasonal cycles are preserved over the last 80 years in C10 (see section 2.4 (*Figure 7*), 4.1.4 (*Figure 2*), 5.4 (*Figure 2*), 5.5 (*Figure 2*)), what suggests that if exists the mean diffusive displacement is less than 0.1 m w.e. during firnification (see section 5.4 (*3.1*)).

2.4 Col du Dôme (Mt Blanc Massif, French Alps) suitability for ice core studies in relation with past atmospheric chemistry over Europe

Tellus (2000), 52B, 993–1012
Printed in UK. All rights reserved

TELLUS
ISSN 0280–6509

Col du Dôme (Mt Blanc Massif, French Alps) suitability for ice-core studies in relation with past atmospheric chemistry over Europe

By SUSANNE PREUNKERT[1,2]*, DIETMAR WAGENBACH[2], MICHEL LEGRAND[1] and CHRISTIAN VINCENT[1], [1]*Laboratoire de Glaciologie et Géophysique de l'Environnement, CNRS, BP96, 38402 St. Martin d'Hères, France;* [2]*Institut fur Umweltphysik, Universität Heidelberg, INF 229, 69120 Heidelberg, Germany*

(Manuscript received 12 April 1999; in final form 17 September 1999)

ABSTRACT

The site of Col du Dôme glacier, located at 4250 m a.s.l. nearby the Mont Blanc summit (French Alps), was investigated for its suitability for reconstructing the anthropogenic perturbation of the atmosphere chemistry over Europe via glacio-chemical ice core studies. For this purpose, a 126 m long ice core drilled close to bedrock has been dedicated for glacio-chemical studies. Major ions (Na^+, NH_4^+, K^+, Mg^{2+}, Ca^{2+}, Cl^-, NO_3^-, and SO_4^{2-}) and D/H isotope ratios have been measured with high seasonal resolution along the upper 60 m of this core (covering 13 years). For dating by annual layer counting, a highly resolved ammonium profile was obtained for the entire core. To assess the spatial representativity of the chemical signals obtained from this core, additional chemical profiles were obtained from two shallow firn cores (13 and 20 m long) drilled at about 100 m from the deep ice core. All ice core parameters show regular seasonal variations with low winter and high summer values. Mean summer to winter ratios (averaged over the period 1981 to 1994) are close to 4 for NO_3^-, SO_4^{2-} and Ca^{2+}, but reach 14 for NH_4^+. While the shape of the mean seasonal cycles of NH_4^+, NO_3^-, and SO_4^{2-} show a flat winter minimum followed by persistently high summer concentrations, more flickered variations are observed in the case of Ca^{2+}. In contrast to the chemical species, δD shows a smoothed seasonal cycle. The chemical impurity levels and the δD content in snow deposits from Col du Dôme have been compared with those from Colle Gnifetti (4450 m a.s.l., located in the Swiss Alps, 80 km east of Col du Dôme) over a time period of 10 years. This comparison suggests that the two sites may experience similar atmospheric pollution conditions throughout the whole year, at least for NH_4^+, NO_3^-, and SO_4^{2-}. Precise dating of the ice core drilled in 1994 was achieved by annual layer counting using the NH_4^+ stratigraphy. The latter reveals that the glacier of Col du Dôme records well preserved snow deposits, arising from summer as well as from winter precipitation, over, at least, the last 75 years. However, the seasonal signal of the δD content appears to be disturbed at increasing depth, in particular below of 115 m. A systematic decrease in the ratio of the winter to summer net snow accumulation found with increasing depth is shown to exert an important influence on mean temporal ice core trends for parameters underlying a strong seasonal variation. The comparison of chemical impurities between Col du Dôme and Colle Gnifetti indicates that glacio-chemical ice core records from Col du Dôme will provide seasonally resolved records over the 20th century which are at least representative on a regional scale.

* Corresponding author.
e-mail: ps@glaciog.ujf-grenoble.fr.

1. Introduction

Polar ice cores represent a unique opportunity to reconstruct some key aspects of the chemical composition of our past atmosphere. However, large ambiguities exist in the source region apportionment of short lived species trapped in ice deposits, making the extraction of such records at various sites over the globe mandatory. Experiencing 10 m firn temperatures below the water freezing point, some mountain glaciers in addition to the polar ice sheets, Greenland and Antarctica, open the possibility to reconstruct several aspects of the past atmospheric chemistry over various regions of the world. This includes glaciers located in tropical regions such as the Huascaran ice cap in the Peruvian Andes (Thompson et al., 1995b), the Guliya (Thompson et al., 1995a) and Dunde (Thompson et al., 1988) ice caps located in Tibet, as well as Devon Island ice cap in the Canadian Arctic (Koerner, 1977), Mount Logan (Holdsworth and Peak, 1985) in western Canada, and Alpine sites (Wagenbach, 1993).

More specifically, long term ice core records from cold Alpine glaciers may help to infer the impact of human activities on climate variability and long term climatic changes at the European scale. Present information obtained on Alpine ice cores are mainly available from the Monte Rosa region (Colle Gnifetti) (Haeberli et al., 1983; Wagenbach, 1989). Due to the relatively low annual net snow accumulation of 0.2–0.4 m of water equivalent (w.e.) at this site, the ice records span more than several centuries. These Colle Gnifetti ice core studies have already revealed an enhancement of sulphate and nitrate concentrations over the 20th century as a result of increasing anthropogenic SO_2 and NO emissions (Wagenbach and Preunkert, 1996). However a straightforward interpretation of these records in term of past environment and climate remains limited by our present poor knowledge of their spatial and seasonal representativity (Wagenbach, 1993). A pilot study (Maupetit et al., 1995) achieved in snow deposited from 1988 to 1991 at the Col du Dôme (Mont Blanc Massif) showed a rather high snow accumulation rate ($\sim$1.5 m w.e. yr^{-1}), and well-preserved winter layers. In contrast to Colle Gnifetti, this site was expected therefore to permit the examination of past changes of atmospheric chemistry at a seasonal (winter/summer) resolution at least over the last few decades or so.

Here, we examine the usefulness of the Col du Dôme site ice core records with respect to their local and regional spatial variability, their accessible time resolution, as well as with respect to their potential extending into the pre-industrial era. For these purposes basic glaciological properties of the Col du Dôme site are discussed, along with highly temporal resoluted records of major ions, obtained from a 126 m long ice core and a 20 m long ice core recently extracted at that site.

2. Present knowledge of glaciological characteristics of the Col du Dôme glacier

Scientific work carried out in the vicinity of the Mont Blanc summit has been initiated by Joseph Vallot some hundred years ago. These pioneer meteorological and glaciological observations have been published at the turn of the last century in the *Annales de l'Observatoire Météorologique du Mont Blanc (1893 to 1905)*. In the 1970s, pioneer ice core studies have been carried out by the Laboratoire de Glaciologie et Géophysique de l'Environnement, Grenoble (LGGE) on several shallow firn cores (Lliboutry et al., 1976; Jouzel et al., 1977; Briat, 1978), followed by numerous investigations of glacio-chemical parameters at various drill sites (Fig. 1, Table 1) in this area. These previous studies gave information on some key glaciological properties of the Col du Dôme glacier site.

2.1. Firn temperature

The study of the firn temperature profile permits to evaluate one of the key characteristic of a high-elevation mid-latitude glacier site: its location with respect to the recrystallization and cold infiltration zone (i.e. absence of regelated layers and melt water percolation over more than one annual snow layer (Shumsky, 1964), respectively). Vallot (1893) reported a 15 m firn temperature at Mont Blanc Summit of -16.7°C (4807 m a.s.l., Fig. 1) at the beginning of this century. Lliboutry et al. (1976) concluded that the "firn cap" regime encountered at the Mont Blanc summit belongs to recrystallization zone. On the other hand, the

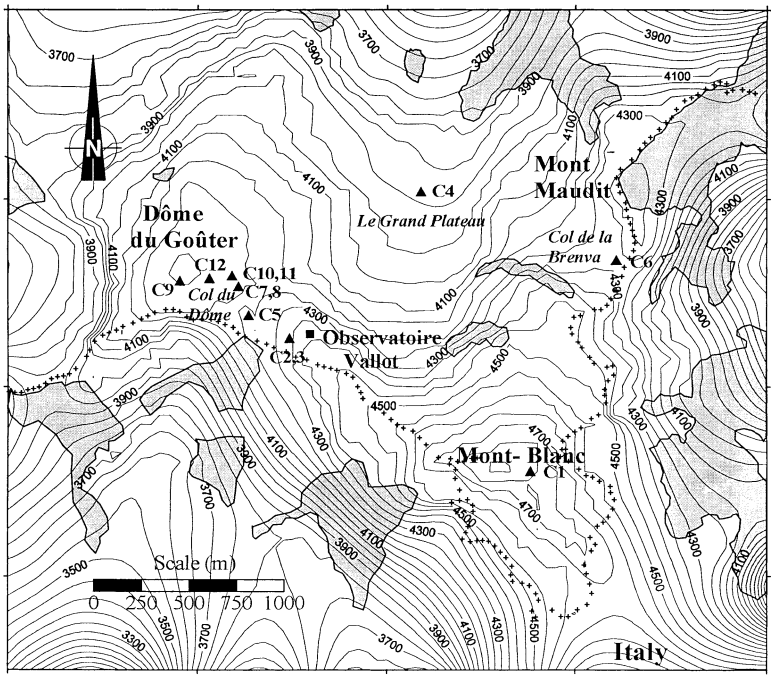

Fig. 1. Map of the Mont Blanc summit area showing the drill sites listed in Table 1. Glaciers are entered with elevation lines, rock regimes are marked in grey.

temperature close to −7.3°C observed at the Grand Plateau (3950 m a.s.l., Fig. 1) suggests that this area settles into the cold infiltration zone. More unclear is the case of the Col du Dôme (4250 m a.s.l.), where a firn temperature of −12.8°C was observed at 15 m depth in 1911 (Vallot, 1913) and no regelated layers were detected in the snow cover at that time. However, more recently, Lliboutry et al. (1976) found a firn temperature of −10.5°C and noticed the presence of a thick regelation layer. From these observations, the authors concluded that the Col du Dôme area has been located in the recristallisation-regelation zone (i.e. restriction of melt water percolation over less than one annual snow layer (Shumsky, 1964)) at the beginning of this century, but revealed characteristics of the cold infiltration zone in 1973. Based on the study of another ice core drilled at the Col du Dôme in 1980, Jouzel et al. (1984) reported a firn temperature of −12.4°C, close to the one observed by Vallot in 1911. These different pictures may be related to an unusually strong percolation having occurred in 1973, as suggested from Lliboutry et al. (1976). They may also reflect a large spatial variability of firn temperatures even at the small spatial scale of the Col du Dôme area, as it has been observed at the Colle Gnifetti (4450 m a.s.l., Mont Rosa massif, Switzerland). On this glacier, near surface firn temperatures show a systematic difference of 2°C between the southerly and northerly exposed slopes of the saddle, located in the cold infiltration zone and the recrystallization-regelation zone, respectively (Alean et al., 1983; Haeberli and Funk, 1991).

2.2. *Snow accumulation rate*

Other key information to assess the suitability of Col du Dôme for glacio-chemical studies are the spatial and seasonal variations of the snow accumulation. Although having been established for time periods limited to a few years, data reported in Table 1 suggest snow accumulation rates at the Col du Dôme ranging from 0.5 to 2.4 m w.e. yr^{-1}. Thus, a large variability of up to a factor of 5 exists within the area of about 0.4 km^2. A more detailed snow accumulation rate

Table 1. *Key parameters recorded in various firn and ice cores of the Mont Blanc Massif, for drill site positions see Fig. 1*

Drillsite	Year of drilling	Core length (m)	Mean accumulation rate of the core (m w.e. yr^{-1}) (covered time period (yr))	Analysed parameters	Ref.	No. in Fig. 1
Mont Blanc Summit	1973	16.7	2.8 (3)	firn temperature, ^3H, δD, gross β activity	Lliboutry et al. (1976) Jouzel et al. (1977)	C1
Col du Dôme	1973	24.5	—	firn temperature	Lliboutry et al. (1976)	C2
Col du Dôme	1974	21	~ 0.5[a] (26)	Na, Al, Cl, K, Ca, V, Mn, Fe, Cu, Zn, Cd and Pb	Briat et al. (1978)	C3
Grand Plateau	1974	—	—	firn temperature	Lliboutry et al. (1976)	C4
Col du Dôme	1976	30.6	~ 0.5[a] (36 ± 5)	acidity	Delmas and Aristarain (1978)	C2
Col du Dôme	1980	20	1.1 (11)	firn temperature, δD, ^3H, gross β activity	Jouzel et al. (1984)	C5
Col de Brenva	1984	10	~ 2[a] (2.5)	major ions, acidity	Ronseaux and Delmas (1988)	C6
Col du Dôme	1986	70	~ 1.5[a] (30)	Al, Ca, Na and K	De Angelis and Gaudichet (1991)	C7
Col du Dôme	1991	15	~ 1.5 (3.5)	major ions, acidity, δD	Maupetit et al. (1995)	C8
Col du Dôme	1991	—	0.61 (8)	^{137}Cs	Vincent et al. (1997)	C9
Col du Dôme	1994	126	2.22[b] (>75)	^{137}Cs, ^{210}Pb partly major ions	Vincent et al. (1997) This study	C10
Col du Dôme	1994	139	2.44[b] (>150)	^{137}Cs, ^{210}Pb CH_4	Vincent et al. (1997) Blanchard (1998)	C11
Col du Dôme	1997	20.5	2.25 (5.5)	major ions	This study	C12

[a] Estimate based on the density profile (C10 core).
[b] Mean accumulation rates from 1986 to 1994.

and surface flow study has been carried out by stake surveys from 1993 to 1995 at Col du Dôme (Vincent et al., 1997). This study reveals that: (1) the net snow accumulation rates are in good agreement with the measured vertical velocities during the investigated time period, leading the authors to conclude that the glacier is near to the steady state; (2) the vertical velocity varies from 0.2 m w.e. yr^{-1} at the Dôme du Goûter to 3.5 m w.e. yr^{-1} in the north east part of the saddle (Fig. 2b); (3) referring to the mean annual precipitation rate at Chamonix (1.25 m w.e. yr^{-1} from 1959 to 1994; data from Meteo France), part of the snow initially deposited in the vicinity of the Dôme du Goûter or in the southern part of the saddle is removed by strong winds, transported northward, and eventually deposited in the relatively wind protected north (or north east) part of the saddle. Note that at Colle Gnifetti, the net snow accumulation rate is only about 0.2–0.4 m w.e. yr^{-1} over the main part of the glacier saddle (Oeschger et al., 1977; Haeberli et al., 1983; Alean et al., 1983). This is at least three times lower than the amount of precipitation observed in surrounding valleys (Kromp-Kolb et al., 1993) suggesting that a dramatic net loss of deposited snow by wind erosion occurs at this site (Wagenbach et al., 1988). Furthermore, Vincent et al. (1997) found a regular year round snow deposition during their three year investigation by stake surveys at the Col du Dôme, while at Colle Gnifetti net the snow accumulation mainly takes place in summer (Haeberli et al., 1983; Wagenbach et al., 1988). Snow accumulation rates of ~ 2 and 2.8 m w.e. yr^{-1} are reported for Col de Brenva (Fig. 1) and Mont Blanc summit, respectively, but

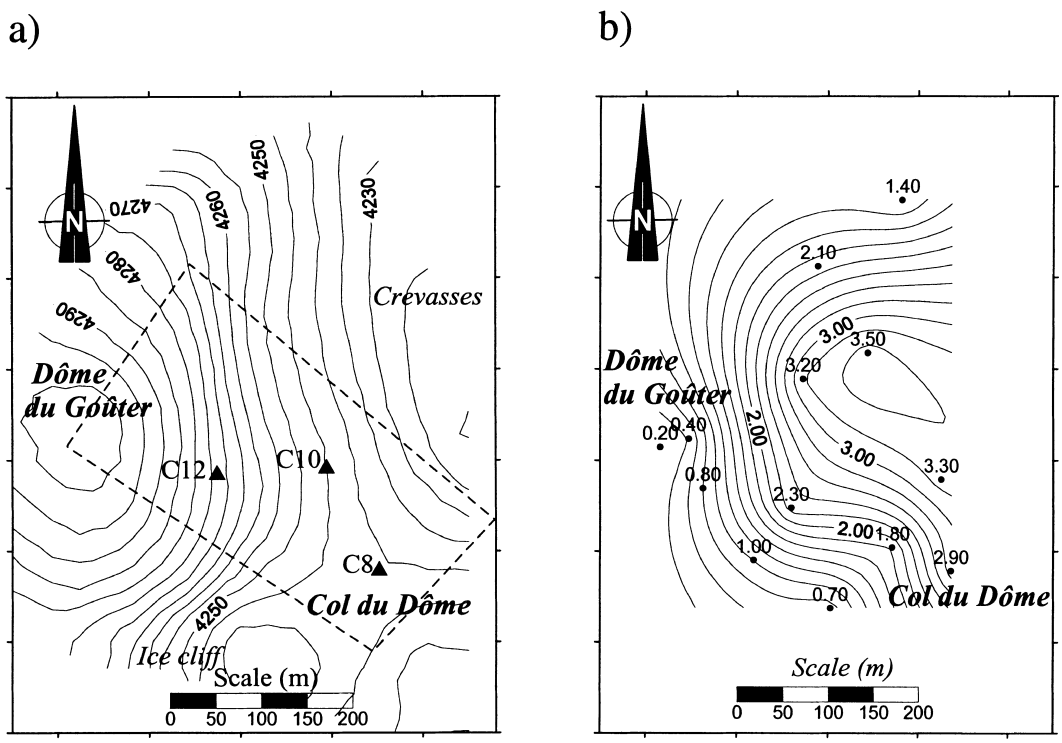

Fig. 2. (a) Map of the Col du Dôme area with positions of investigated ice cores. The dashed line refers to the area where radio echo soundings are available. (b) Vertical velocities observed at Col du Dôme (in m w.e. yr^{-1}) by Vincent et al. (1997) (reprinted from the Journal of Glaciology with permission of the International Glaciological Society).

no information on their spatial variability are presently available.

2.3. *Ice flow at Col du Dôme*

In collaboration with the ETH-Zürich, radio-echo soundings have been carried out by the LGGE in 1993 and 1994 at the Col du Dôme (Vincent et al., 1997). Within an area of 400 m by 200 m (Fig. 2a) the glacier thickness increases from about 40 m at the Dôme du Goûter to 150 m at the saddle area. The glacier bed topography appears to be very rugged, showing relatively deep (~15–30 m) and narrow (~30–60 m) canyons. Assuming that the glacier is at steady state, two models have been developed to depict the glacier flow in the Col du Dôme area, including cores C10 and C11 drilled in 1994 (Fig. 1). Using a rheological model for porous ice which is constrained by in situ measured density profiles and firn mechanical properties, a numerical simulation has been performed by Gagliardini and Meyssonnier (1997). A two-dimensional flow model was developed by Vincent et al. (1997), considering the mean mass balance derived from measured vertical surface velocities, using mass continuity and the depth profile of horizontal velocity from the analytical model proposed by Lliboutry (1981). The numerical simulations provided by the two models (Gagliardini and Meyssonnier, 1997; Vincent et al., 1997) are very consistent down to 90 m depth. They are also in agreement with the location of the ice layers corresponding to the radioactive horizons of 1986 (Chernobyl) and 1963 (nuclear bomb tests) detected in the C11 ice core at 39 and 90 m depth, respectively (Vincent et al., 1997). The radioactive horizon of 1954, appearing at 105 m depth in C11 (Vincent et al., 1997) indicates however that at this depth the two models already overestimate the age of the ice by some 20 years (Gagliardini and Meyssonnier, 1997) and 7 years (Vincent

et al., 1997), respectively. Based on the model study by Vincent et al. (1997), the ice located at ~20 to 30 m above bedrock may be 55 to 60 years old. Further down, the extensive deformation of ice layers leads to large uncertainties in the simulation. Flow model calculations applied to the low accumulation Colle Gnifetti site (Haeberli et al., 1988; Wagner, 1994) predict ice ages up to several hundred years for ice 20 m above bedrock.

2.4. *Glacio-chemical studies*

Investigations of various chemical species deposited at the Col du Dôme site over the last decades have revealed a rather well-marked seasonal signal. Jouzel et al. (1984) reported well-marked seasonal variations of the tritium content and of the total β radioactivity over the years 1970–1980. Although a clear summer maximum of δD (~ -67‰) is generally observed, a few perturbations (i.e. occurrence of a double annual peak, or a lack of well identified summer maximum) have been noticed by Jouzel et al. (1984). Maupetit et al. (1995) showed that all major ions (Na^+, K^+, NH_4^+, Mg^{2+}, Ca^{2+}, Cl^-, NO_3^-, and SO_4^{2-}) exhibit a seasonal signal in the snow deposited between 1988 and 1991, with very low concentrations in winter, enhanced levels in spring and well-marked maxima in summer. Such seasonal patterns are in agreement with atmospheric observations made on the high Alpine sites of Colle Gnifetti, Jungfraujoch (3450 m a.s.l., Bernese Alps, Switzerland) and Hoher Sonnblick (3106 m a.s.l., Hohe Tauern, Austria) (Preunkert and Wagenbach, 1998; Baltensperger et al., 1997; Kasper and Puxbaum, 1998). The low impurity content in winter at the high Alpine sites is due to the very limited contamination of these high altitude regions by polluted boundary layer air masses during that season. Conversely, in spring and summer, upward advection by convective transport significantly affects Alpine sites located well above 4000 m elevation. In addition, disturbances arise within the snow chemistry by the episodic deposition of saharan dust, as reported by Wagenbach et al. (1996), Wagenbach and Geis (1989), Wagenbach (1989) for Colle Gnifetti, and by Ronseaux and Delmas (1988), De Angelis and Gaudichet (1991) for Col du Dôme. The use of alpine ice cores as recorder of such short-term deposition events remains difficult, however. For instance, the Alpine wide strong saharan dust event of 1977 (Haeberli, 1983; Wagenbach and Geis, 1989) is not seen as a major event in the Col du Dôme snow layers (De Angelis and Gaudichet, 1991). Similarly, at the Col du Dôme the Chernobyl radioactivity horizon exhibits inventories varying up to a factor of 120 (Vincent et al., 1997).

3. Sampling and analyses

In 1994 two ice cores were drilled close to bedrock at Col Du Dôme. The core lengths are 126 m for core C10, and 139 m for core C11 (Fig. 1). The C11 core was dedicated to the measurement of trace gases in air bubbles whereas the C10 core was reserved for the snow chemistry. Major ions (Na^+, NH_4^+, K^+, Mg^{2+}, Ca^{2+}, Cl^-, NO_3^-, and SO_4^{2-}), and the stable water isotope Deuterium have been measured with high-resolution (i.e., ~30 samples per year) along the upper 60 m of the C10 core. Extended NH_4^+ measurements have been carried out over the entire C10 core for dating purpose (see Section 6). Additionally, major ions records were obtained along a 20 m long core extracted in 1997 (C12, Fig. 2a) to evaluate the spatial representativity of chemical records in this area.

In addition to ice core decontamination and chemical measurements, which have been carried out at the Institut für Umweltphysik, Heidelberg (IUP) and the Laboratoire de Glaciologie et Géophysique de l'Environnement, Grenoble (LGGE), Deuterium (D) analyses were performed at the Laboratoire des Sciences du Climat et l'Environnement, Saclay (LSCE). As usual, D/H ratios are reported here in δD units denoting the relative deviation from V-SMOW standard (Vienna-Standard Mean Ocean Water) in permille. The core decontamination at Heidelberg was done by using an electric plane device (Fischer et al., 1998), while a lathe was used at Grenoble (Legrand et al., 1993). In both laboratories ion chromatography (IC) procedure currently used for polar and alpine snow samples (Legrand et al., 1993; Maupetit, 1992; Minikin, 1994; Fischer, 1997; Preunkert, 1994) were applied here to determine major ions concentrations. Intercalibrations have shown a quite good agreement between the IC analytical procedures employed in both laboratories (Maupetit et al., 1995). The accuracy of IC determinations are typically of 5 to 10% for winter and summer samples, respectively. The only

one noticeable difference in the methods employed at the two laboratories concerns the use of an autosampler device at the IUP lab which slightly increases the ammonium blank value to 2.1 ± 3.7 ppb (averaged over 152 samples), instead of far less than 1 ppb generally obtained when using standard procedure (including individual sample load) at LGGE.

4. Seasonal variations of major ions and the δD content in the snow cover of Col du Dôme

4.1. Seasonal variations along the upper 60 m of the C10 ice core

The density of the core from close to the surface is about $0.35\ g\ cm^{-3}$. The critical density ($0.55\ g\ cm^{-3}$) is reached at 5 m depth and the close-off depth (i.e. density of 0.80–$0.83\ g\ cm^{-3}$) lies between 60 and 70 m depth. Below 100 m, density values remain quasi constant ranging between 0.90 to $0.92\ g\ cm^{-3}$. As previously argued by Jouzel et al. (1984), De Angelis and Gaudichet (1991), and Maupetit et al. (1995), the visual inspection of grain size variation and the occurrence of recristallisation ice layers, as well as the seasonal change of the δD content can be used to identify annual layers and thus help to establish the dating of the Col du Dôme ice cores. Based on the regular occurrence of δD minima (winter layers) and on the occurrence of ice layers (summer layers) (Fig. 3), we found the annual accumulation rate varying from 1.25 to 4.50 m w.e. yr^{-1} (mean value of 2.45 m w.e. yr^{-1}) along the upper 60 m of the C10 core, which cover the 1981–1994 time period (i.e. 13 years). Compared to the mean precipitation rate at Chamonix (1.25 m w.e. yr^{-1} from 1959 to 1995, Meteo France data), this high net snow accumulation rate of 2.45 m w.e. yr^{-1} within the C10 core suggests an accumulation surplus by drifting snow there. However, the regu-

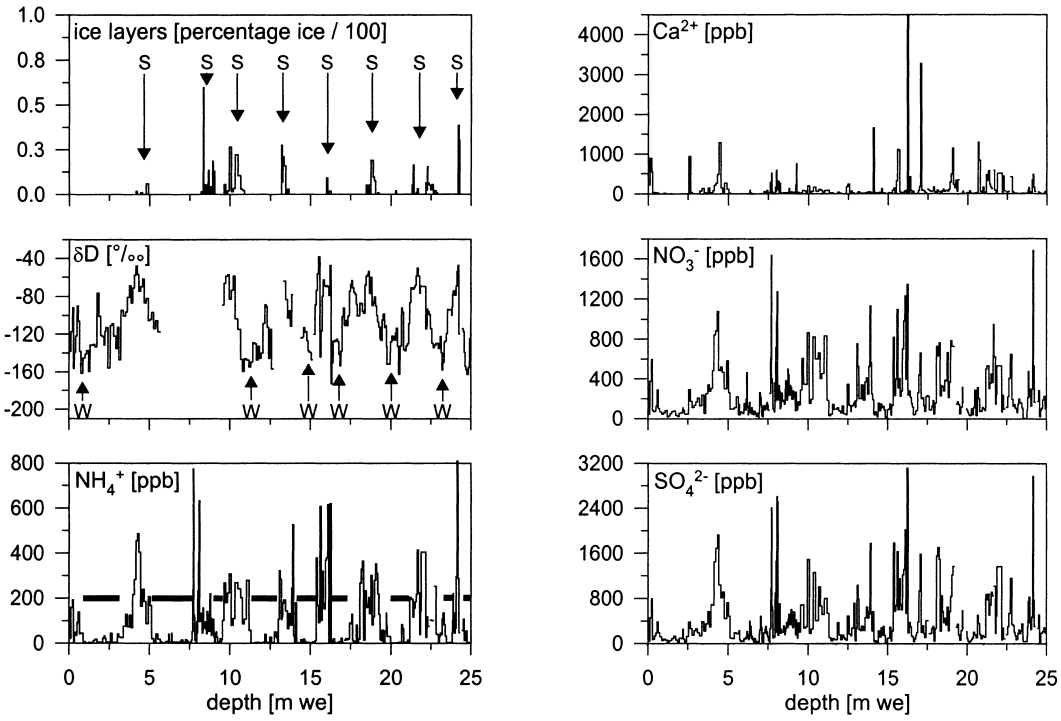

Fig. 3. Stratigraphy and chemical depth profiles of the upper part of the C10 ice core. The regular occurrence of δD minima (vertical arrows denoted *W*) and ice layers (vertical arrows denoted *S*) indicate winter and summer snow layers. Horizontal lines reported in the ammonium profile denote the annual winter snow layers (see text).

lar formation of ice layers in summer very likely prevents the perturbation of the stratigraphy by wind redistribution of snow over more than one year. In addition to summer ice layers which are up to 5 cm thick, vertical ice veins resulting from percolation had been detected four times over the 13 years of the record. Their maximum vertical extend reaches 0.20 m w.e., which remains small compared to the annual firn layer thickness of 1.25 to 4.50 m w.e..

As seen in Fig. 3, depth profiles show seasonal variations for all ions and δD, with very low winter and high summer values. Summer to winter mass ratios for individual samples may reach up to 800 for NH_4^+, 120 for SO_4^{2-}, 60 for NO_3^-, and 500 for Ca^{2+}. Given the quite large interannual variability of the annual snow accumulation, we divided each annual layer into two parts corresponding to winter and summer snow accumulation. Note that summer and winter means summer halfyear and winter halfyear, defined by the distinct atmospheric conditions prevailing at high Alpine sites, the presence and absence of upward advection of air masses from the boundary layer, respectively. The dissection cutting has been based on the NH_4^+ profile which exhibits the strongest seasonal signal as seen in Fig. 3. The frequency distribution of NH_4^+ concentrations (not shown) indicates a bimodal distribution with a low concentration mode below 10 ppb and a second mode centred on $\sim$200–300 ppb. The boundaries of the winter half year snow pack have been identified by requiring at least 3 consecutive samples to significantly exceed the 10 ppb NH_4^+ (background) level. Indeed, in more than 90% of samples assumed to be winter snow, NH_4^+ concentrations are lower than 10 ppb. Using this criterion, we found that 46 % of the net snow deposition may be attributed to winter snow precipitation in the upper 60 m of C10.

Each summer and winter layer was divided into 6 equally spaced (in w.e.) parts. A weighted interpolation was applied to years containing more or less than 12 samples. These calculations were performed for NH_4^+, Ca^{2+}, NO_3^-, SO_4^{2-}, and δD. Finally, a 13-year mean was calculated for each 1/12 annual accumulation (Fig. 4) in order to derive mean seasonal cycles. In Fig. 4, we also report the mean seasonal temperature cycle observed at 2472 m a.s.l. in the Alps (Grosser St. Bernhard, Switzerland, (Aschwanden et al., 1996)), indicating an approximate monthly time scale of the mean seasonal cycles in C10 by matching the temperature and the δD seasonality.

The seasonal cycles of major ions show a flat winter minimum from September to February followed by persistent high concentrations from March to August, in particular for NH_4^+, NO_3^-, and SO_4^{2-}. For Ca^{2+}, a more flickered seasonal cycle is observed (Fig. 4), likely due to the sporadic inputs of Saharan dust, which mainly occur from spring to fall. The mean summer to winter ratio remains close to 4 for SO_4^{2-}, NO_3^- and Ca^{2+}, and reaches 14 for NH_4^+ (Table 3). The relatively huge summer to winter mass ratio for ammonium suggests that, in addition to the atmospheric dynamics, a strong seasonal cycle of ammonia emissions may also contribute to the observed variations. Indeed, the seasonality of NH_3 emissions exhibits a strong maximum in summer in the pre-alpine areas (Puxbaum, 1993), in relation to agricultural activities and NH_3 soil emissions by bacterial activity. In contrast to ammonium, Cl^- and Na^+ reveal a low summer to winter ratio (close to a factor of two, Table 3) likely mirroring a quite complex picture. In addition to the transport, various changes in sources may modulate the Na^+ deposition in precipitation at high elevation European sites throughout the year. For instance, we can speculate that the sea salt content of the free troposphere at mid latitudes is higher in winter than in summer because of the more intense cyclogenesis over the Atlantic Ocean at that time. Conversely, the higher dust input from spring to fall over alpine sites depicted by the calcium profile may be bring Na^+ inputs because of the presence of Na^+ in airborne continental aerosols.

As a consequence of matching with the seasonal air temperature cycle, the mean seasonal δD cycle of C10 shows minimum in late winter (February) and maximum in summer (July). In contrast to chemical species, the δD profile exhibits a smoothed seasonal variation, similarly to the seasonal changes of air temperatures (Fig. 4). Since the shape and the summer/winter amplitude of the δD depth profile do not change significantly with increasing depth (Fig. 3), we can exclude that water vapour diffusion in firn contributes to the smoothed pattern of δD ice signal. This is also consistent with laboratory experiments on diffusion of deutered water vapour which suggest

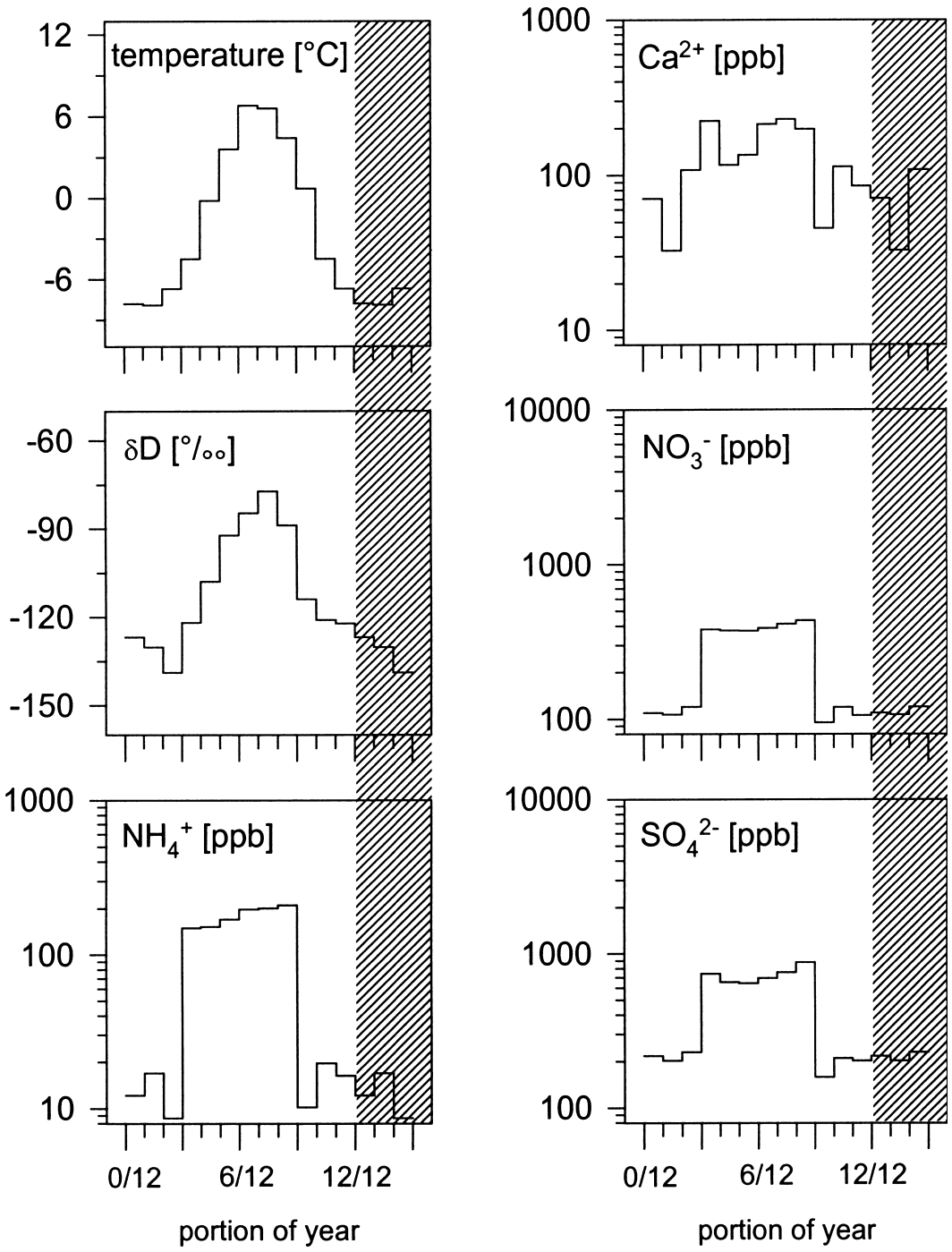

Fig. 4. Seasonal cycles of δD, NH_4^+, Ca^{2+}, NO_3^- and SO_4^{2-} from the C10 core averaged over 13 years. Monthly time scale is indicated by matching the δD annual cycle with the 30-year mean annual cycle of air temperatures (top left panel) observed at Grosser St. Bernhard (2427 m a.s.l., Switzerland) (data from Aschwanden et al., 1996).

that this phenomenon remains limited to less than 15 cm long in firn over one to two years (Jean-Baptiste et al., 1998), while within C10 the transition section summer to winter is about 1 m.

4.2. *Spatial variability of seasonal variations within the glacier site of Col du Dôme*

The seasonal pattern seen in the snow chemistry at the C10 Col du Dôme site is compared with that obtained at two neighbouring sites. Two shallow cores (C12) and (C8) were drilled 100 m away from the C10 site in 1997 and 1991 (Maupetit, 1992), respectively (Fig. 2a). With ~11.5 and 6.5 m w.e. length, the C12 and C8 cores span around 6 and 3 years, respectively. They were dated by using the same procedure as applied for the C10 core. Winter snow layers represent 40% and 44% of the annual net snow accumulation in C12 and C8 cores, respectively, what is in excellent agreement with the C10 core (46%). Considering the strong wind scouring at such exposed glacier sites, the chemical stratigraphies of the 3 cores are in good agreement, as illustrated by the ammonium profiles (Fig. 5).

In order to achieve an accurate comparison of winter and summer concentrations of chemical species present in ice from different sites, we have to account for the high spatial variability of sporadic events like episodic saharan dust inputs in our ice records (see Subsection 2.4). For instance, among five layers marked by huge calcium contents in core C10, four are clearly seen in cores C8 and C12, but their Ca^{2+} inventory differs up to a factor of 4. These sporadic calcium events are caused by deposition of large amount of alkaline dust over the Alps. As acidic species are readily scavenged by mineral dust particles, those events may add considerably to the snow inventory of sulphate and, to a lesser extend, of nitrate (Maupetit and Delmas, 1994). Following Wagenbach et al. (1996), such events can be identified in alpine ice as calcium-rich layers exhibiting a negative acidity (i.e. alkaline samples).

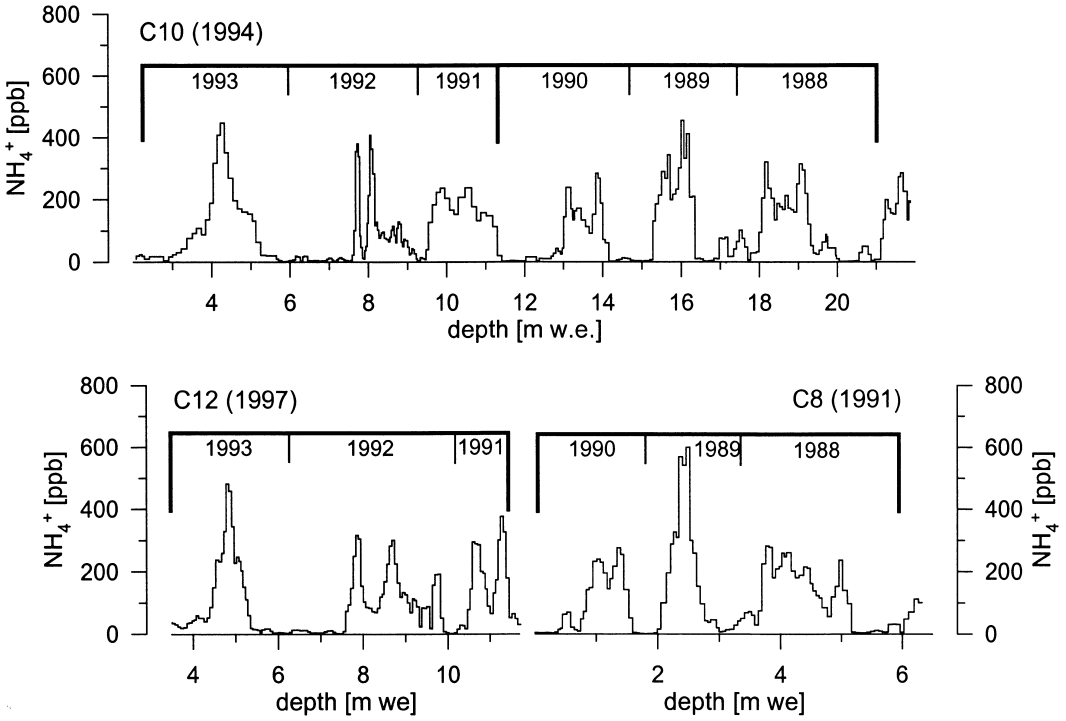

Fig. 5. Smoothed (3 sample running average) NH_4^+ profiles of the C10 core (top) and two shallow firn cores: C12 (left bottom), C8 (right bottom, adapted from Maupetit (1992)). The two latter cores have been extracted at a distance of about 100 m to C10 (Fig. 2a).

Table 2. *Seasonal snow chemistry variation over the 1988–1993 time period of the C10 core as compared to shallow firn cores C8 and C12*

		Na^+	NH_4^+	Ca^{2+}	Cl^-	NO_3^-	SO_4^{2-}
Summer	C10 mean concentration (ppb)	25 ± 14	180 ± 58	62 ± 28	43 ± 17	440 ± 101	620 ± 131
	mean square deviation (ppb)	15 ± 16	45 ± 53	48 ± 51	16 ± 17	99 ± 95	155 ± 173
	relative mean square deviation (%)	61 ± 63	25 ± 29	77 ± 83	38 ± 41	22 ± 22	25 ± 28
Winter	C10 mean concentration (ppb)	11 ± 8	13 ± 9	29 ± 17	17 ± 10	120 ± 35	180 ± 54
	mean square deviation (ppb)	3.4 ± 2.5	2.3 ± 2.0	21 ± 26	4.8 ± 2.7	29 ± 26	75 ± 62
	relative mean square deviation (%)	31 ± 22	17 ± 16	72 ± 86	28 ± 28	23 ± 21	42 ± 35

Alkaline samples were identified by calculating the ionic balance between anions and cations, acidic samples corresponding to an excess of anions, alkaline samples showing a deficit of anions. Using this method, we conclude that 13% of C10 samples, 8% of C12 and 19% of C8 have been affected by such sporadic, excess alkaline dust events. These data have been discarded from our calcium records. For sulphate, the observed concentrations were corrected for the terrigenous contribution according to $[SO_{4\,corr}^{2-}] = [SO_4^{2-}] - 0.59[Ca^{2+}]$, where the factor 0.59 represents the mean SO_4^{2-} to Ca^{2+} mass ratio observed by Wagenbach et al. (1996) in pre-industrial mineral dust horizons at Colle Gnifetti.

To compare the mean summer and winter concentrations among the three cores, we calculated water weighted mean concentrations for each summer and winter half year. To give a proportion for the spatial variability within Col du Dôme, square deviations for summer and winter layers were calculated between C10 and the shallow cores (C12, C8) for each year. Overall means have been then calculated by averaging the annual deviation values over the concurrent period from 1988 to 1993. Relative deviations given in Table 2 are normalised to the corresponding C10 mean concentrations.

In summer, annual mean square deviations range from 22% to 25% for NH_4^+, NO_3^-, and SO_4^{2-}, while Ca^{2+} shows a larger square deviation of 77%. Such a difference might be due to an enhanced variability of the non Saharan dust influenced Ca^{2+} background, or due to low level Saharan dust events being still included in the background population. The mean winter square deviations for NH_4^+, Ca^{2+} and NO_3^- are similar to their respective summer values. For SO_4^{2-}, the higher square deviation in winter compared to summer (Table 2) cannot be attributed to an incomplete correction of concentrations from the saharan dust contribution, since quite similar values are obtained when only acidic samples are considered. The variability of Na^+ and Cl^- are relatively high in summer (61% and 38%, respectively) when compared to other non crustal species. Although the source apportionment of these species is not yet established, the higher square deviation observed for sodium in summer may support the assumption of a significant dust contribution for this species.

5. Spatial variability of seasonal variations on a regional scale

An attempt was made to compare summer and winter means of chemical species and δD between Col du Dôme and Colle Gnifetti. At the low accumulation site Colle Gnifetti which is located $\sim$80 km east to Col du Dôme only a small fraction of winter snow is preserved (see Subsection 2.2). Here seasonal means have been examined along a 5.6 m w.e. long firn core (further-on denoted HK) showing relatively regular seasonal cycles and covering the time period 1982–1991. Given the annual accumulation rate of $\sim$0.37 m w.e. yr^{-1}, the identification of summer and winter

layers was still possible, and the winter snow contribution was found to account for 18% of the annual net snow accumulation (Preunkert, 1994). Seasonal subdivision, as well as the correction from saharan dust impact and the calculation of mean summer and winter values have been done by using same procedures as employed for the C10 core. Taking the overall summer and winter means (from 1982 to 1991) for each species, we calculated averaged deviations between C10 and HK normalised to the C10 means (Table 3). In spite of the more difficult subdivision between summer and winter layers in the HK core, a good overall agreement can be observed for both mean summer and winter concentrations between the two glacier sites. In summer, the δD content is lower at Colle Gnifetti with respect to Col du Dôme by 5.5‰. This is expected, given the 200 m higher elevation and the more easterly position of Colle Gnifetti. In winter, however, the δD values are higher by 10‰ in HK than the C10 core, likely reflecting the incomplete deposition of winter precipitation at Colle Gnifetti due to its lost through wind scouring.

The significance of slight differences detected for the mean summer and winter ion concentrations between the two glacier sites has been assessed by a Students test (t-test). For each species, the t-test was applied to the difference record (R), which was built up by subtracting individual seasonal means of HK from the corresponding ones of C10 over the 1982–1991 time period. The R-values (10 samples) were expected to be trend free and should be t-distributed around zero (i.e., the expected value (ξ_0) is equal to zero) under the assumption that the concentration record of C10 and HK is identical. The level of significance (α) has been chosen equal to 0.05 which leads to a critical t-value of 2.26. Calculated values of t, as well as the values of σ (standard deviation) and ξ (mean value) are reported in Fig. 6a (summer) and 6b (winter) for each species.

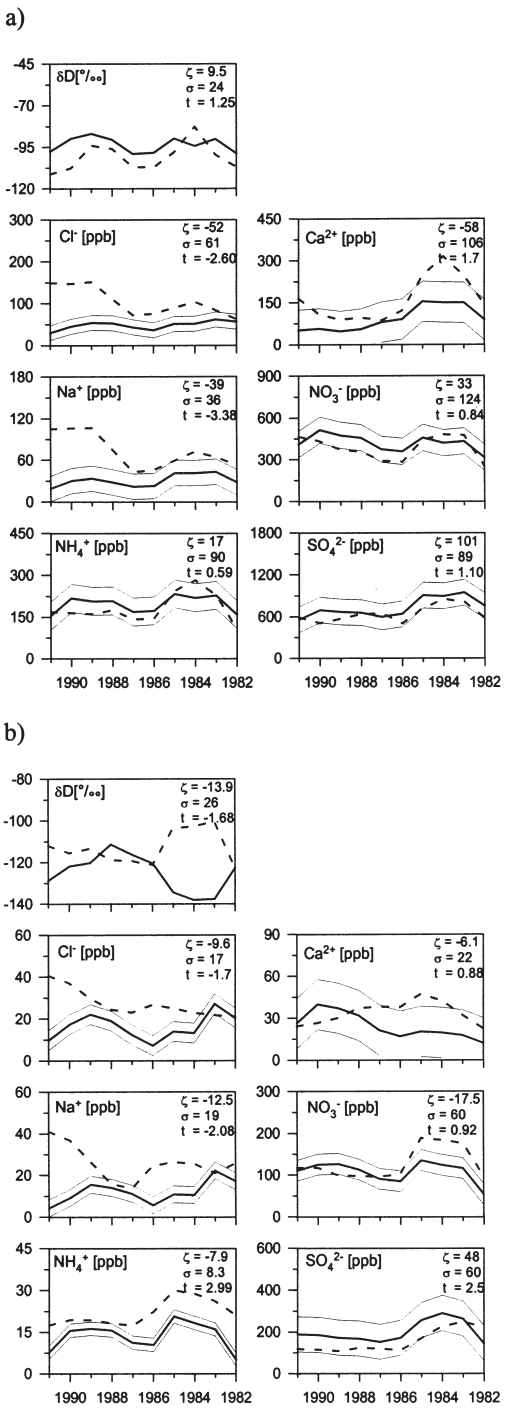

Fig. 6. Three point running averages of annual summer (6a) and winter (6b) contents of chemical species and δD at Col du Dôme (C10, solid lines) and Colle Gnifetti (HK, dashed lines). Together with the C10 curves, the respective relative mean square deviations reported Table 2 have been here applied (thin solid lines enveloping the thick solid lines). For each species, the t-test values of ξ, σ and t (see text) are included.

Table 3. *Mean 10-year (1982–1991) summer and winter concentrations of chemical species and δD at Col du Dôme (C10) and Colle Gnifetti (HK); in addition to the summer to winter concentration ratios, the differences between HK and C10 relative to C10 are given*

			Na^+	NH_4^+	Ca^{2+}	Cl^-	NO_3^-	SO_4^{2-}	δD[a)]
Col du Dôme (C10)	mean concentration (ppb)	summer	30 ± 19	200 ± 67	94 ± 60	47 ± 18	430 ± 120	740 ± 230	−93.5 ± 13
		winter	13 ± 12	14 ± 10	25 ± 16	17 ± 14	110 ± 57	200 ± 80	−126 ± 13
	ratio	summer/ winter	2.3 ± 2.6	14 ± 11.3	3.8 ± 3.4	2.6 ± 2.5	3.9 ± 2.3	3.7 ± 1.9	32.7 ± 18.4[b)]
Colle Gnifetti (HK)	mean concentation (ppb)	summer	70 ± 42	180 ± 110	186 ± 145	100 ± 60	380 ± 190	660 ± 290	−99 ± 18
		winter	25 ± 13	20 ± 9	37 ± 13	27 ± 8	134 ± 91	145 ± 85	−116 ± 23
	ratio	summer/ winter	2.8 ± 2.3	9.3 ± 7.0	4.7 ± 4.3	3.7 ± 2.5	2.8 ± 2.4	4.5 ± 3.3	17 ± 29.2[b)]
$\frac{HK-C10}{C10}$ (%)		summer	133	−7	87	112	−12	−11	5.8
		winter	92	42	48	59	23	−28	8

[a)] (‰).
[b)] Summer–winter difference.

For relative small values of $|t|$ (<1.10), for which the level of significance could be chosen higher than 0.3, the test is not sensitive enough. These small t-values could be due to a dating error of the HK core, leading to enhanced σ values. Therefore, in addition to the t-test values, we also report in Fig. 6 smoothed time records from both cores.

In summer, both the t-test and smoothed records show that Cl^- and Na^+ signals are significantly different in the two cores. Conversely, for NH_4^+, NO_3^-, SO_4^{2-} and Ca^{2+}, no significant differences are assessed by the t-test, and a good agreement of the temporal trends can be observed. Again, note the very large square deviation for Ca^{2+} at Col du Dôme. The δD signal at HK shows generally lower levels with respect to the C10 ones in summer. However, the t-test suggests that these differences are not significant.

In winter, for NH_4^+, NO_3^- and SO_4^{2-} similar temporal trends are observed in both cores. For SO_4^{2-} and NH_4^+, the t-test suggests a significant difference between C10 and HK. However, due to the high spatial variability at Col du Dôme (Fig. 6b), the lower SO_4^{2-} concentrations, with respect to the C10 ones, at HK are not necessarily caused by a systematic spatial difference between Col du Dôme and Colle Gnifetti. The higher winter NH_4^+ values for HK, compared to C10, may be explained with a regular lack of mid-winter snow preservation at Colle Gnifetti. In spite of this lack of winter snow deposition at the HK site, the good agreement on temporal trends seen for NH_4^+, NO_3^- and SO_4^{2-} (Fig. 6b) suggests that the chemical signals recorded in snow at the two sites correspond to similar air chemical situations. For Na^+, Cl^-, Ca^{2+} and δD the t-test results suggest that the records of both cores are not significantly different in winter.

This suggests that Colle Gnifetti and Col du Dôme likely experience similar atmospheric conditions throughout the whole year, at least for species such as NH_4^+, NO_3^- and SO_4^{2-}. Based on the comparison of two shallow firn cores, Maupetit et al. (1995) suggested that during summer, the Col du Dôme is more influenced by polluted air masses than the Colle Gnifetti. Such a conclusion is not supported by this study, which shows no significant difference between Colle Gnifetti and Col du Dôme for NH_4^+, NO_3^- and SO_4^{2-} in the snow deposited during the summer season. This apparent discrepancy likely comes from an underestimation of the true summer levels at Colle Gnifetti made in the study by Maupetit et al. (1995), where summer means from Col du Dôme have been compared with overall mean concentrations from Colle Gnifetti (assumed to be dominated by summer precipitation).

6. Stratigraphy and dating of the C10 core

With the aim to establish a chronology of the C10 core, the upper 119 m were subdivided in summer and winter sections based on the ammonium profile, as detailed in Subsection 4.1. In the lower part of the core, the winter snow layers are very thin (Fig. 7) and are sometimes made up by one single sample (i.e., 4 cm w.e.) below the 10 ppb NH_4^+ criterion. We identified winter layers between 103 and 119 m (77–91 m w.e.) depth via the relative NH_4^+ minima, though sometimes exceeding 10 ppb. Possibly, winter sections are smaller here than our depth resolution of 5 cm. For the very last 7 m of the core, annual layer counting was not possible by this method, since the NH_4^+ record shows no regular variations. Note

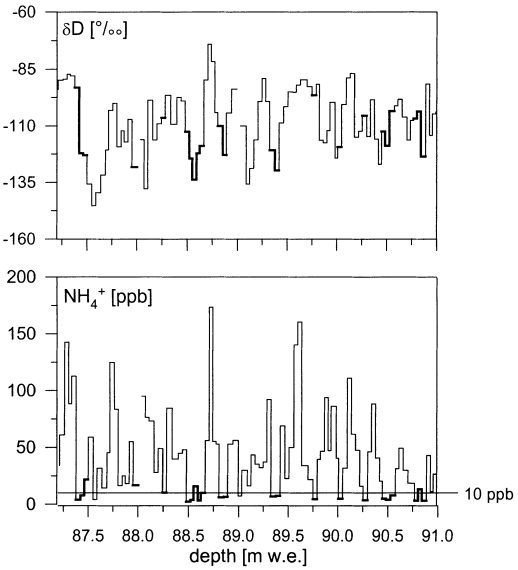

Fig. 7. δD and NH_4^+ raw data of the C10 core between 87 and 91 m w.e. depth. Winter snow layers, as identified from the ammonium stratigraphy (see text), are indicated as thick lines.

that this absence of the observance of regular NH_4^+ variations is not due to our depth resolution of 5 cm, since continuous, high resoluted NH_4^+ measurements performed over the last 20 m of C10 (depth resolution $\sim$7 mm w.e., (Fuhrer et al., 1993)) yield similar results (S. Sommer, 1995, personal communication).

6.1. *Dating of the C10 core*

The dating established by counting annual layers along the NH_4^+ profile (Fig. 8) has been compared with various time horizons and a chronology derived from an ice flow model. Time horizons are gained from ^{137}Cs measurements (Vincent et al., 1997), as well as from the calcium record of dust horizons. The dust horizons of 1977, 1947 and 1936/37 had also been detected in snow deposits at Colle Gnifetti (Haeberli et al., 1983; Jung, 1993). The theoretical time scale reported as a solid line in Fig. 8 refers to the 2D flow model from Vincent et al. (1997) applied to the C10 core. The annual layer counting is in good agreement with the three ^{137}Cs horizons (1986, 1963, and 1954). Assuming that the dust horizons of 1947 and 1936/37 are correct, a systematic overestimation of $\sim$5 years arises from the NH_4^+ dating at 114 m depth (i.e., 86 m w.e.), corresponding to an age of $\sim$60 years. The core chronology derived from the flow model still agrees within $\pm$5 years with the NH_4^+ stratigraphy down to 90 m depth (i.e., 65 m w.e. corresponding to the last 30 years). However, at 100 m depth (i.e., 74 m w.e., Fig. 8), the model overestimates the age by some 18 years, while the NH_4^+ stratigraphy is still in agreement with the ^{137}Cs horizon of 1954. This systematic error of the model may be related to an underestimation of the glacier thickness at the drill site. Radio echo soundings suggested an ice thickness of about 122 m (core length of 126 m) but this thickness determination has a quite large uncertainty of $\pm$20 m (S. Suter, 1999, personal communication). The model (dashed line in Fig. 8) and the stratigraphical time scale are in better agreement when a glacier thickness of 140 m is assumed, which remains within the range of the ice thickness determination (from 102 to 142 m).

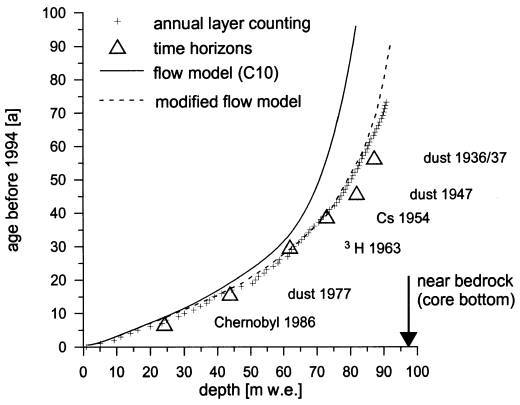

Fig. 8. Comparison of different depth-age relation in the upper 119 m of the C10 core (see text).

Given the good agreement between mean NH_4^+ summer concentrations at Col du Dôme and Colle Gnifetti (Section 5), we compared the mean NH_4^+ summer concentrations observed between 116 and 119 m depth within the C10 core (i.e., 88–91 m w.e.) with concentrations of the monotonic increasing NH_4^+ time trend during this century, gained from a Colle Gnifetti ice core (dominated by summer snow) (Jung, 1993; Wagenbach and Preunkert, 1996). The well established chronology of this core suggests that the C10 ice located at around 116–119 m depth (i.e., 88–91 m w.e.) is 75 ± 10 years old. This is again in agreement with our dating obtained by annual layer counting along the NH_4^+ profile.

6.2. *The seasonal δD signal in deep C10 ice layers*

While ammonium minima coincide rather well with δD minima from the surface down to 60 m depth (Fig. 3), a more complex picture is observed further down from 115 to 119 m depth (Fig. 7). Here, the ammonium minima do not always correspond to layers low in δD (Fig. 7). In addition, while the seasonal δD amplitude within the upper 60 m ranges from -60 to -160‰ (Fig. 3), -90 to -130‰ (i.e., a decrease by more than a factor of 2) are seen between 115 and 119 m depth (i.e., 87–91 m w.e.). This may be due to water vapour diffusion occurring during firnification. The model of Johnsen (1977) gives the ratio R of the final (post firnification) to the initial (near the surface) amplitude of an annual water isotope cycle as a function of its wavelength (A).

$$R = \exp\left(\frac{-2\pi^2 L_f^2}{A^2}\right) \quad (1)$$

Hereby L_f (the average displacement due to vapour water diffusion) was roughly estimated for the firn temperature (~ -12.5°C) and the accumulation rates prevailing at the Col du Dôme, by extrapolating the theoretical L_f values given by Cuffey and Steig (1998).

For the upper most 60 m of the C10 site, with a mean accumulation rate of 2.45 m w.e. yr^{-1}, an average displacement (L_f) of less than 13 cm (in w.e.) is obtained, leaving the R value higher than 0.95. This confirms our conclusion made in Subsection 4.1 that smoothing by diffusive water vapour transport is relatively unimportant in this part of the core. On the other hand, further down in the core, the ice has been originally deposited upstream the borehole of the C10 site. Based on the ice flow model by Vincent et al. (1997), the ice located at $\sim$115–120 m depth (i.e., 87 to 90 m w.e.) comes from sites where surface accumulation rates range from 0.5 to 0.3 m w.e. only. From such surface snow accumulation conditions, an average displacement (L_f) of $\sim$11 to $\sim$14 cm w.e. is expected, which, according to eq. (1), would correspond to R values of 0.5 to 0.01, respectively. Thus, the decreasing amplitude of the δD variations between upper layers and 115–119 m depth may be attributed to smoothing by diffusive mass transport in connection with the decrease of the net snow accumulation upstream the C10 site. Furthermore, Johnsen (1977) pointed out, that for R lower than 0.05, the seasonal δD cycle is obliterated after the firnification. Hence, the seasonal δD cycle of C10 starts to become obliterated at a core depth of 115 to 119 m, and δD fluctuations seen around 119 m depth and in deeper ice layers may be likely not connected anymore to seasonal variations.

6.3. *The seasonal variations of the net snow accumulation versus depth*

Based on the ammonium profile, a decrease of the annual layer thickness with depth is observed along the C10 core (Fig. 9). The 10-year means of the snow accumulation rate show an almost linear decrease from 3.3 m w.e. yr^{-1} at the surface to 0.2 m w.e. yr^{-1} at 118 m depth (i.e., 90 m w.e.). The change of the annual thickness with depth, as calculated by the ice flow model (Vincent et al., 1997), is also shown in Fig. 9. Based on the NH_4^+ stratigraphy, the ratio of winter to summer net snow accumulation (denoted as $A_{W/S}$) was calculated for each individual year. As is seen in Fig. 9, $A_{W/S}$ is decreasing from $\sim$1 near the surface to 0.5 at 100 m depth (i.e., 74 m w.e.). This change suggests that spatial variations in the relative amount of summer and winter snow deposition taking place upstream to the C10 borehole.

With regard to the strong seasonal cycle, exhibited by the ice impurity content (maxima in summer), the decrease in the fraction of winter snow deposition with depth may lead to a down-

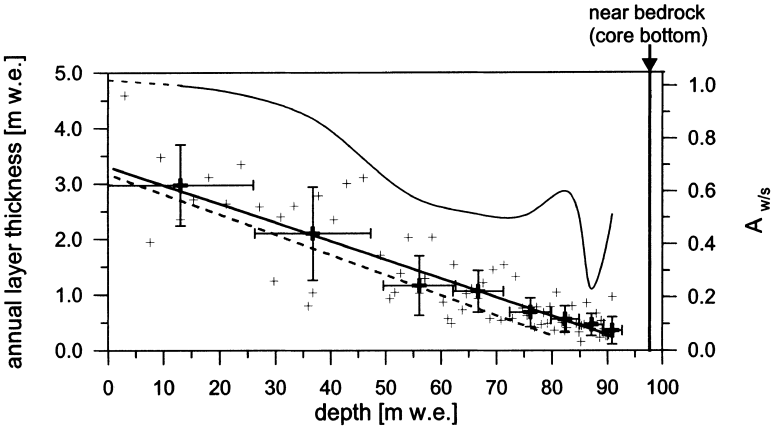

Fig. 9. Change of annual layer thickness along the C10 core: estimates via NH_4^+ stratigraphy are marked with thin crosses, corresponding 10 year means with thick crosses, and their regression with thick line. Results from the flow model of Vincent et al. (1997) are given as dashed line. Smoothed change of winter to summer snow deposition ratio $A_{w/s}$ is indicated by solid curve.

core increase of the mean annual impurity levels which is independent of temporal atmospheric changes. Using the summer (c_s) and winter (c_w) mean concentrations in recent snow of Table 3, the concentration enhancement $\Delta C(z)$ at a depth z with respect to the surface concentration $\overline{C(0)}$ can be estimated as:

$$\Delta C(z) = \overline{C(z)} - \overline{C(0)}, \quad (2)$$

$$\overline{C(z)} = f_w(z) \times c_w + f_s(z) \times c_s, \quad (3)$$

where $f_s(z)$ and $f_w(z)$ represent the summer and winter fractions of the annual layer at depth z, determined via the NH_4^+ stratigraphy, respectively.

Using eqs. (2) and (3), we estimated that (due to the increase of $f_s(z)$ and the decrease of $f_w(z)$ with depth) mean concentrations at a depth of 74 m w.e. would be enhanced by about 20% for NO_3^-, SO_4^{2-} and Ca^{2+} and by 30% for NH_4^+. Thus, such changes of the summer to winter amount of snow accumulation will systematically affect the general trends at the C10 site. Detailed investigations of the spatial variation of seasonal signals in the uppermost snow layers at Colle Gnifetti suggest, that this phenomena may introduce an artificial concentration increase in deep ice cores by up to 100% at this glacier site (Preunkert, 1994).

As seen in Fig. 9, the $A_{W/S}$ values decrease monotonically between the surface and 115 m depth (i.e., 87 m w.e.) apart from a partly recover between 101 and 110 m (i.e., 75 an 83 m w.e.). However, at a core depth of 115 m an abrupt increase of the $A_{w/s}$ values is observed. Provided that this pattern is not caused by an artefact related to a misinterpretation of the NH_4^+ stratigraphy, two possible explanations can be invoked. Such changes may be due to an abrupt increase of the winter snow contribution at approximately 200 m upstream the C10 borehole, or to a discontinuity of the ice flow trajectory starting points in this area, located $\sim$200 m upstream of the C10 borehole. The latter explanation is supported by unexpectedly high ^{210}Pb levels, found between 90 and 110 m depth in C10. The sudden increase of ^{210}Pb concentrations at these depths has been attributed to crevasses in the catchment area (Vincent et al., 1997), which may lead to this discontinuities in the ice flow. If correct, this phenomenon may have disturbed the C10 core chronology. Nevertheless, CH_4 measurements performed in the C11 core (drilled 30 m apart from the C10 site) give no evidence for a discontinuity in the core chronology at this glacier depth (Blanchard, 1998), although the ^{210}Pb profile is disturbed in this core as well. Finally, the comparison of the mean NH_4^+ summer level from 116–119 m deep ice layers from the Col du Dôme core C10 with the NH_4^+ signal incorporated in the glacier of Colle Gnifetti (see Subsection 6.2.) does not support the assumption of a discontinuity in the core chronology of C10.

7. Conclusions

Seasonally resolved measurements of major ions and δD have been performed along three ice cores extracted at the Col du Dôme glacier site. The hereby gained chemical depth records have been combined with the glaciological and glacio-meteorological properties of the glacier site, in view to exploit this glacier site for ice core investigations related to paleo-climatic and environmental issues.

Given the relative high net snow accumulation rate and the nearly complete winter snow contribution in the snow cover of Col du Dôme (as compared to corresponding values from the Colle Gnifetti glacier site), a detailed reconstruction of the mean seasonal cycle of chemical impurities and the δD content could be carried out. Mean seasonal cycles with flat winter minima and persistent high concentrations in summer are revealed for all chemical species and are particularly well-marked for NH_4^+, NO_3^-, and SO_4^{2-} (mean summer to winter concentration ratios ranging from about 4 for NO_3^- and SO_4^{2-} to 14 for NH_4^+). Although clearly visible, the Ca^{2+} seasonal cycle is more flickering due to sporadic Sahara dust inputs. In contrast to chemical species, the δD record shows more smoothed seasonal variations, exhibiting a similar pattern as the seasonal changes of air temperatures adopted from Grosser St. Bernhard (2472 m a.s.l., Switzerland).

Recent mean summer concentrations of the Col du Dôme site are in good agreement with the ones found at Colle Gnifetti 80 km apart, particularly for NH_4^+, NO_3^-, SO_4^{2-} and Ca^{2+}. In winter, a good agreement is again observed for NO_3^- and SO_4^{2-}, while NH_4^+ levels are higher at Colle Gnifetti than at Col du Dôme, probably due to a lack of winter snow deposition at Colle Gnifetti.

This comparison suggests that these two Alpine sites underlie similar atmospheric conditions year-round, at least for NH_4^+, NO_3^-, and SO_4^{2-}. This implies that for these species the two high alpine drilling sites are representative at least on a regional scale in the range of 100 km. Based on well-marked seasonal NH_4^+ cycles, in a 126 m deep Col du Dôme ice core is shown that a relative precise chronology (compared to the existing theoretical chronologies) can be established over the last 75 years (accuracy ± 5 years at an ice age of 75 years), and that snow deposits, made up by summer as well as by winter precipitation, are well preserved in the glacier over this time period.

In reconstructing long-term concentration records special attention has to be paid however to systematic changes in the snow deposition characteristics upstream to the drill site. This concerns the systematic spatial changes of the annual net snow accumulation (as linked to changing contributions by seasons) which may be mirrored in various ice core profiles. Such a glaciological forcing exerts a non-atmospheric influence on the shape of the seasonal cycle, and the mean annual levels of all species underlying a distinct seasonal variation. As a consequence, following findings have to be carefully considered in using the deep ice cores drilled at Col du Dôme in 1994: (1) the seasonal cycle of δD starts to become obliterated at a core depth of 115 m; (2) relative to the near surface regime, annual mean concentration levels of NH_4^+ are about 30% increased at a core depth of 100 m (the respective values for NO_3^-, SO_4^{2-} and Ca^{2+} are close to 20%).

In summary, the ice core drilled at Col du Dôme in 1994 will provide seasonally resolved glacio-chemical and isotopic records covering about the last 75 years. They are expected to contain information of past atmospheric conditions which are representative at least on a regional Alpine scale. This will especially help to fill the information lack, concerning long term Alpine ice core records, representative for atmospheric conditions prevailing during the winter season.

It is not clear yet, whether the Col du Dôme area provides the possibility to extend such seasonally resolved ice core records into the pre-industrial era. Current glaciological investigations include the search for an appropriate drill site to retrieve well preserved pre-industrial ice layers from Col du Dôme.

8. Acknowledgements

This paper is a contribution to the European Environment and Climate Programme ALPCLIM. Funding was provided by the European Community via contract ENV4-CT97–0639 (ALPCLIM) and ENV4-CT96–5051 (Environment and Climate Research Training Grant), the French Ministry for Environment and the German Ministry for Education and Research via the EUROTRAC subproject ALPTRAC, the Ministry for Science and Research of Baden-Württemberg within the collaboration programme between Region Rhône Alpes and Baden Württemberg and the Centre National de la Recherche Scientifique (CNRS). We thank, O. Cattani, M. Stievenard and J. Jouzel from the Laboratoire des Sciences du Climat et l'Environnement (Saclay) for performing the δD analyses. We are grateful to S. Sommer and K. Fuhrer from the Physical Institute of the University of Bern for performing some continuous flow NH_4^+ measurements. We thank R. Delmas for supporting the drilling activities in 1994, C. Rado, A. Manouvrier and P. Journé for performing the ice core drillings in 1994 and 1997. We are grateful to numerous colleagues for their commitment in the field and to Chamonix Mont Blanc Helicopter for their invaluable logistical support.

REFERENCES

Alean, J., Haeberli, W. and Schaedler, B. 1983. Snow accumulation, firn temperature and solar radiation in the area of the Colle Gnifetti core drilling site (Monte Rosa, Swiss Alps): distribution patterns and interrelationships. *Z. Gletscherkd. Glazialgeol.* **19**, 131–147.

Aschwanden, A., Beck, M., Häberli, Ch., Haller, G., Kiene, M., Roesch, A., Sie, R. and Stutz, M. 1996. Klimatologie der Schweiz: Klimatologie 1961–1990, Heft 2, Band 1, Bereinigte Zeitreihen. In: *Die Ergebnisse des Projekts KLIMA90, Band 1: Auswertungen*, Schweizerische Meteorologische Anstalt, Zürich, 137 p.

Baltensperger, U., Gaeggeler, H. W., Jost, D. T., Emenegger, M. and Naegeli, W. 1991. Continuous back-

ground aerosol monitoring with the Epiphaniometer. *Atmos. Environ.* **25A**, 629–634.

Baltensperger, U., Gaeggeler, H. W., Jost, D. T., Lugauer, M., Schwikowski, M., Weingartner, E. and Seibert, P. 1997. Aerosol climatology at the high-alpine site Jungfraujoch, Switzerland. *J. Geophys. Res.* **102,** D16, 19707–19715.

Blanchard, R. 1998. *Evolution de la teneur en methane et en monoxyde de carbon de la glace du Col du Dôme (Mont Blanc) au cours de la periode industrielle*. MS thesis, Laboratoire de Glaciologie et Géophysique de l'Environnement, University Joseph Fourier, Grenoble 1, 40 p.

Briat, M. 1978. Evaluation of levels of Pb, V, Cd, Zn and Cu in the snow of Mt Blanc during the last 25 years. In: *Studies in the environmental science*, vol. 1 (ed. M. M. Benarie). Elsevier, Amsterdam, pp. 225–228.

Cuffey, M. and Steig, E. J. 1998. Isotopic diffusion in polar firn: implications for interpretation of seasonal climate parameters in ice-core records, with emphasis on central Greenland. *J. Glaciol.* **44**, 273–384.

De Angelis, M. and Gaudichet, A. 1991. Saharan dust deposition over Mont Blanc (French Alps) during the last 30 years. *Tellus* **43B**, 61–75.

Fischer, H. 1997. *Räumliche Variabilität in Eiskernzeitreihen Nordostgrönlands — Rekonstruktion klimatischer und luftchemischer Langzeittrends seit 1500 AD*. PhD thesis. Institut für Umweltphysik der Universität Heidelberg, 135 p.

Fischer, H., Wagenbach, D. and Kipfstuhl, J. 1998. Sulfate and nitrate firn concentrations on the Greenland ice sheet 1. Large-scale geographical deposition changes. *J. Geophys. Res.* **103**, D17, 21927–21934.

Fuhrer, K., Neftel, A., Anklin, M. and Maggi, V. 1993. Continuous measurements of hydrogen peroxide, formaldehyde, calcium and ammonium concentrations along the new GRIP ice core from Summit, central Greenland. *Atmos. Environ.* **27A**, 1873–1880.

Gagliardini, O. and Meyssonnier, J. 1997. Flow simulation of a firn-covered cold glacier. *Annals of Glaciology* **24**, 242–248.

Haeberli, W., Schotterer, U., Wagenbach, D., Haeberli-Schwitter, H. and Bortenschlager, S. 1983. Accumulation characteristics on a cold, high-alpine firn saddle from a snow-pit study on Colle Gnifetti, Monte Rosa, Swiss Alps. *J. Glaciol.* **29**, 260–271.

Haeberli, W., Schmid, W. and Wagenbach, D. 1988. On the geometry, flow and age of firn and ice at the Colle Gnifetti core drilling site (Monte Rosa, Swiss Alps). *Z. Gletscherkd. Glazialgeol.* **24**, 1–19.

Haeberli, W. and Funk, M. 1991. Borehole temperatures at the Colle Gnifetti core-drilling site (Monte Rosa, Swiss Alps). *J. Glaciol.* **37**, 37–46.

Holdsworth, G. and Peak, E. 1985. Acid content of snow from a mid-troposphere sampling site on Mount Logan, Yukon Territory. *Annals of Glaciology* **7**, 153–160.

Jean-Baptiste, P., Jouzel, J., Stievenard, M. and Ciais, P. 1998. Experimental determination of the diffusion rate of deuterated water vapor in ice and application to the stable isotopes smoothing of ice cores. *Earth Planet. Sci. Lett.* **158**, 81–90.

Johnsen, S. J. 1977. Stable isotope homogenization of polar firn and ice, Isotopes and Impurities in snow and ice. *IAHS Publ.* **118**, 210–219.

Jouzel, J., Merlivat, L. and Pourchet, M. 1977. Deuterium, tritium, and β activity in a snow core taken on the summit of Mont Blanc (French Alps) : determination of the accumulation rate. *J. Glaciol.* **18** (80), 465–470.

Jouzel, J., Legrand, M. R., Pinglot, J. F., Pourchet, M. and Reynaud, L. 1984. Chronologie d'un carottage de 20 m au Col du Dôme (Massif du Mont-Blanc). *Houille Blanche* **1984**, 491–497.

Jung, W. 1993. *Hundertjährige Zeitreihen der Aerosoldeposition auf einem hochalpinen Gletscher*. MS thesis. Institut für Umweltphysik der Universität Heidelberg, 71 p.

Kasper, A. and Puxbaum, H. 1998. Seasonal variation of SO_2, HNO_3, NH_3 and selected aerosol components at Sonnblick (3106 m a.s.l.). *Atmos. Environ.* **32**, 3925–3939.

Koerner, R. M. 1977. Devon Island Ice Cap: Core stratigraphy and paleoclimate. *Science* **196,** 4285, 15–18.

Kromp-Kolb, H., Schoener, W. and Seibert, P. 1993. *ALPTRAC Data Catalogue*, EUROTRAC International Scientific Secretariat, Garmisch- Partenkirchen, 137 p.

Legrand, M., De Angelis, M. and Maupetit, F. 1993. Field investigation of major and minor ions along Summit (central Greenland) ice cores by ion chromatography. *J. Chromatogr.* **640**, 251–258.

Lliboutry, L., Briat, M., Creseveur, M. and Pourchet, M. 1976. 15 m deep temperatures in the glaciers of Mont Blanc (French Alps). *J. Glaciol.* **16**, 197–203.

Lliboutry, L. 1981. A critical review of analytical approximate solutions for steady state velocities and temperatures in cold ice-sheets. *Z. Gletscherkd. Glazialgeol.* **15**, 135–148.

Maupetit, F. 1992. *Chimie de la neige de très haute altitude dans les Alpes Francaises.* PhD thesis. Paris 7 University, publication no. 745 of the Laboratoire de Glaciologie et Géophysique de l'Environnement, 246 p.

Maupetit, F. and Delmas, R. 1994. Snow chemistry of high altitude glaciers in the French Alps. *Tellus* **46B**, 304–324.

Maupetit F., Wagenbach D., Weddeling P. and Delmas R. 1995. Recent chemical and isotopic properties of high altitude cold Alpine glaciers. *Atmos. Environ.* **29**, 1–9.

Minikin, A. 1994. *Spurenstoff-glaziologische Untersuchung von Eisbohrkernen des Filchner-Ronne-Schelfeises, Antarktis: Bestimmung der Tiefenverteilung und der Kontinentaleffekte ionischer Aerosolkomponenten.* PhD thesis. Institut für Umweltphysik der Universität Heidelberg, 219 p.

Oeschger, H., Schotterer, U., Stauffer, B., Haeberli, W. und Roethlisberger, H. 1977. First results from Alpine core drilling projects. *Z. Gletscherkd. Glazialgeol.* **13**, 193–208.

Preunkert, S. 1994. *Glazio-chemische Verhältnisse des Colle Gnifetti im Vergleich zu seiner regionalen Umgebung*. MS thesis. Institut für Umweltphysik der Universität Heidelberg, 88 p.

Preunkert, S. and Wagenbach, D. 1998. An automatic recorder for air/firn transfer studies of chemical aerosol species at remote glacier sites. *Atmos. Environ.* **32**, 4021–4030.

Puxbaum, H., Haumer, G., Moser, K. and Ellinger, R. 1993. Seasonal variation of HNO_3, HCl, SO_2, NH_3 and particulate matter at a rural site in northeastern Austria (Wolkersdorf, 240 m asl). *Atmos. Environ.* **27A**, 2445–2447.

Ronseaux, F. and Delmas, R. J. 1988. Chemical composition of bulk atmospheric deposition to snow at Col de la Brenva (Mt. Blanc area). In: *Acid deposition at high evaluation sites* (ed. M. H. Unsworth and D. Fowler). Kluwer Academic Publishers, Dordrecht, pp. 491–510.

Shumsky, P. A. 1964. *Principles of structural glaciology* (transl. D. Kraus). Dover Publications, New York, 497 p.

Thompson, L. G., Xiaoling, W., Mosley-Thompson, E. and Zichu, X. 1988. Climatic records from the Dunde Ice Cap, China. *Annals of Glaciology* **10**, 178–182.

Thompson, L. G., Mosley-Thompson, E., Davis, M. E., Lin, P. N., Mikhalenko, V. and Dai, J. 1995a. A 1000 year ice core climate record from the Guliya Ice Cap, China and its relationship to global climate variability. *Annals of Glaciology* **21**, 175–181.

Thompson, L. G., Mosley-Thompson, E., Davis, M. E., Lin, P. N., Henderson, K. A., Cole-Dai, J., Bolzan, J. F. and Liu, K. B. 1995b. Late glacial stage and holocene tropical ice core records from Huascaran, Peru. *Science* **269**, 46–50.

Vallot, J. 1893. Recherches scientifiques dans le tunnel du Mont Blanc. *Annales de l'Observatoire Météorologique, Physique et Glaciaire du Mont-Blanc* **1**, 131–134.

Vallot, J. 1913. Valeur et variation de la température profonde du glacier, au Mont Blanc. *Comptes Rendus Hebdomadaires des Séances de l'Académie des Sciences* **156**, 1575–1578.

Vincent, C., Vallon, M., Pinglot, F., Funk, M. and Reynaud, L. 1997. Snow accumulation and ice flow at Dôme du Goûter (4300 m), Mont Blanc, French Alps. *J. Glaciol.* **43**, 513–521.

Wagenbach, D., Muennich, K. O., Schotterer, U. and Oeschger, H. 1988. The anthropogenic impact on snow chemistry at Colle Gnifetti, Swiss Alps. *Annals of Glaciology* **10**, 183–187.

Wagenbach, D. 1989. Environmental records in alpine glaciers. In: *The environmental record in glaciers and ice sheets* (ed. H. Oeschger and C. C. Langway). Dahlem Konferenzen, John Wiley and Sons, Chichester, 69–83.

Wagenbach, D. and Geis, K. 1989. The mineral dust record in a high alpine glacier (Colle Gnifetti, Swiss Alps). In: *Paleoclimatology and paleometeorology : modern and past patterns of global atmospheric transport* (ed. M. Leinen and M. Sarnthein). Kluwer Academic publishers. NATO ASI Series, Serie C 282, pp. 543–564.

Wagenbach, D. 1993. Special problems of mid latitude glacier ice core research. In: *Proceedings of the ESF/EPC Workshop: Greenhouse gases, isotopes and trace elements in glaciers as climatic evidence for Holocene time* (ed. W. Haeberli and B. Stauffer). Report of the ESF/EPC Workshop, Zürich 27.-28.10.1992, Arbeitsheft Nr. 14, VAW-ETH-Zürich, pp. 10–14.

Wagenbach, D., Preunkert, S., Schaefer, J., Jung, W. and Tomadin, L. 1996. Northward transport of Saharan dust recorded in a deep Alpine ice core. In: *The impact of African dust across the Mediterranean* (ed. S. Guerzoni and R. Chester). Kluwer Academic Publishers, The Neetherlands, pp. 291–300.

Wagenbach, D. and Preunkert, S. 1996. The History of European Pollution Recorded in Alpine Ice Cores. In: *Proceedings of the EUROTRAC Symposium 1996*. G.-Partenkirchen (ed. P. M. Borell et al.). Computational Mechanics Publications, Southampton, pp. 273–281.

Wagner, S. 1994. *Dreidimensionale Modellierung zweier Gletscher und Deformationsanalyse von eisfreiem Permafrost*. PhD thesis, ETH-Zürich, 91 p.

Chapter III

Analysis of the C10 ice core: Data presentation and evaluation

In this Chapter, we first summarize analytical protocols employed to analyze organic and inorganic ions trapped in the C10 ice core. Then we discuss the procedure applied to derive from these chemical depth profiles, summer, winter and annual long term changes in view to infer relevant atmospheric information. Here we examine the impact on these long term records of sporadic Saharan dust inputs which can strongly disturb the chemistry of Alpine snow layers, particularly in summer.

3.1 Analyses

The 126 m long CDD ice core was analyzed in high seasonal resolution by using ion chromatography (IC) working conditions established in both LGGE and IUP laboratories for polar and Alpine snow samples (including the use of an autosampler at IUP) (Minikin, 1994; Preunkert, 1994; Legrand et al., 1993; Maupetit, 1992). Intercalibrations have shown a quite good agreement between the IC analytical procedures deployed in two laboratories (Maupetit et al., 1995). The evaluation of blank values obtained in the two laboratories for the investigated ionic species are summarized in Table 3.1.

Table 3.1: Mean laboratory blank values (and their standard deviation) achieved at IUP Heidelberg and LGGE Grenoble.

		F^- [ppb]	Acetate [ppb]	Formate [ppb]	Cl^- [ppb]	NO_3^- [ppb]	SO_4^{2-} [ppb]	Oxalate [ppb]
IUP-Heidelberg	mean	n.a.	n.a.	n.a.	1.7 ± 1.5	3.8 ± 1.5	2.7 ± 1.9	n.a.
	number	-	-	-	38	38	38	-
LGGE-Grenoble	mean	0.04 ± 0.05	2.5 ± 1.6	1.1 ± 0.6	0.4 ± 0.3	0.1 ± 0.2	0.9 ± 0.7	0.06 ± 0.13
	number	11	11	11	11	11	11	11
		Na^+ [ppb]	NH_4^+ [ppb]	K^+ [ppb]	Mg^{2+} [ppb]	Ca^{2+} [ppb]		
IUP-Heidelberg	mean	1.26 ± 1.0	1.7 ± 1.5	2.1 ± 1.8	1.0 ± 2.1	3.2 ± 3.4		
	number	38	38	38	38	38		
LGGE-Grenoble	mean	0.6 ± 0.3	0.2 ± 0.2	0.1 ± 0.2	0.1 ± 0.1	4.3 ± 2.1		
	number	11	11	11	11	11		

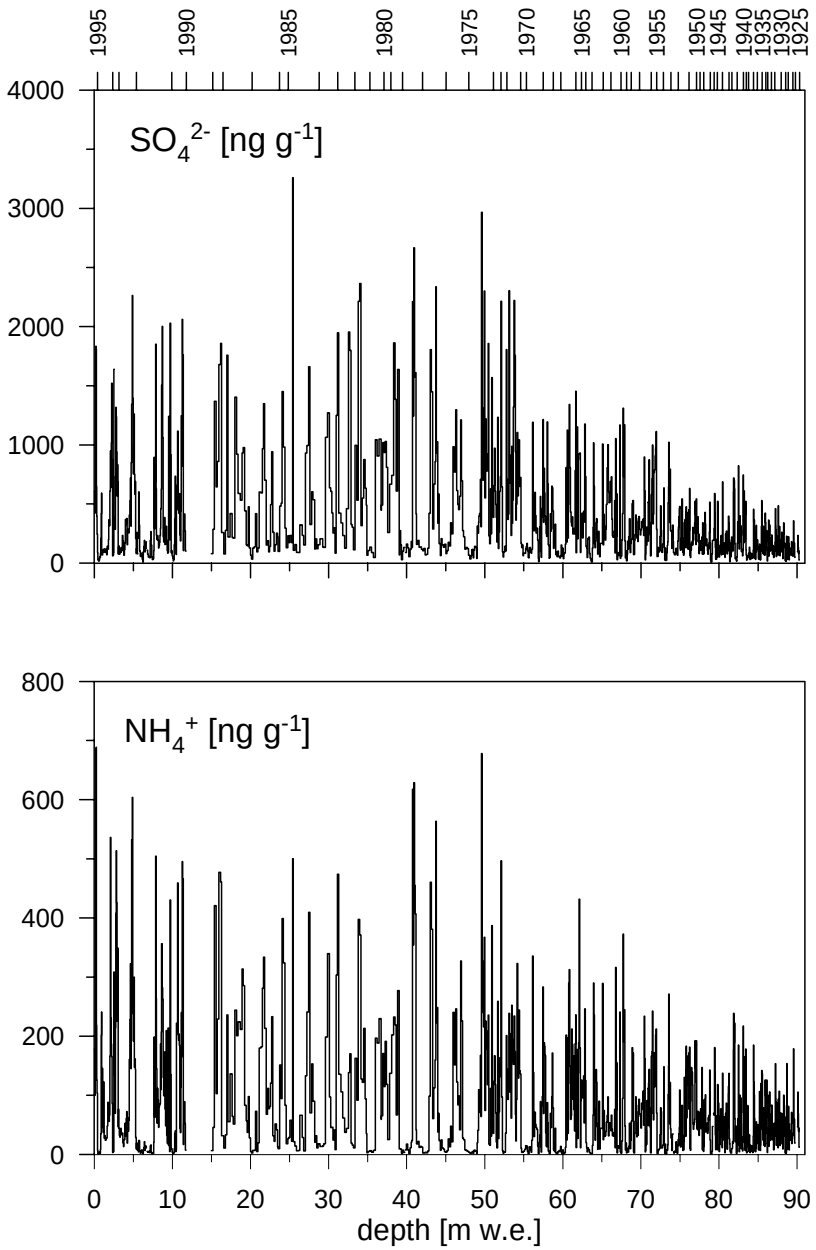

Figure 3.1. Depth profiles of SO_4^{2-} and NH_4^+ raw data along the upper 90 m w.e. of the C10 CDD ice core. The annual layer dating reported on the top is discussed in Chapter 2.

The blank samples consist in pieces of frozen ultrapure water (18 MΩ, Millipore system) which were decontaminated and analysed in the same way than the firn and ice samples collected at the CDD site. At IUP major ions were analysed in 1550 samples for dating purpose (see Chapter 2). At LGGE ≈1050 samples were analysed, for major ions (see Chapter 4), as well as fluoride (see Chapter 5) and light carboxylates (see Chapter 6) along the upper 117 m of the C10 core, which corresponds to the well-dated (1923-1994 time period) of the C10 ice core. An example of the obtained raw data set is reported in Figure 3.1 (ammonium and sulfate).

3.2 Data presentation

Figure 3.2 summarizes the protocol applied to the C10 raw data set to derive relevant information on atmospheric changes from the long term CCD ice core records. Referring to the distinct air conditions prevailing during summer and winter at high elevated Alpine sites (see section 1.2) and in order to avoid misleading interpretation induced by the local glaciological bias detailed in Chapter 2, the C10 data set was separately examined for both winter and summer snow composition. The seasonal dissection was done following the NH_4^+ dissection criteria detailed in section 2.4.

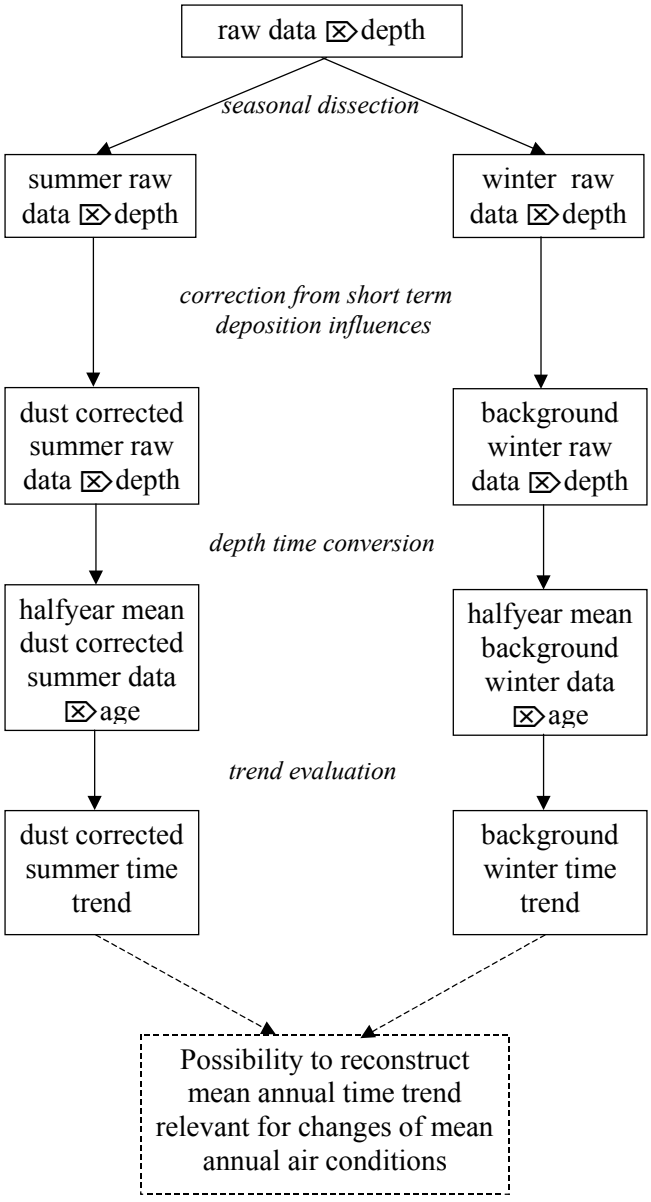

Figure 3.2. Scheme of the procedure applied on the raw data of the C10 ice core to deliver relevant information to discuss past atmospheric chemistry changes (see text).

3.2.1 Short term perturbations influencing the chemical composition of summer snow deposits.

Saharan dust events sporadically disturb the chemical composition of high Alpine snow layers (De Angelis and Gaudichet, 1991; Wagenbach et al., 1996). Since the occurrence of these Saharan dust inputs reaching the Alps can change over time, it is needed to correct the long term chemical trend from their contribution. Samples containing a Saharan dust input were identified as calcium-rich layers exhibiting a relative high alkalinity (Wagenbach et al., 1996). The acidity (or alkalinity) of samples has been evaluated by checking the ionic balance between anions and cations:

$$[H^+] = [F^-] + [Cl^-] + [NO_3^-] + [SO_4^{2-}] + [CH_3COO^-] + [HCOO^-] + [C_2O_4^{2-}] - [Na^+] - [K^+] - [Mg^{2+}] - [Ca^{2+}] - [NH_4^+] \quad (3.1)$$

Since the mean acidity level has been itself modified from the beginning of 20th century to present, a non constant selection criterion was applied to identify snow layers suspected to contain Saharan dust: samples lying below the 25% percentile of a robust spline (Bloomfield and Steiger, 1983) through the raw acidity profile, are considered as significantly affected by Saharan dust input. Since the value of the acidity in meltwater samples represents a "budget value", which is rather independent of the absolute impurity levels, an additional criterion was applied (Ca^{2+} concentration > 100 ppb) to be sure that a relevant dust input is given. Following that, 85 samples on a total of 762 summer samples were identified as contaminated by Saharan dust. Note that 17% of the whole sample population exhibit Ca^{2+} concentrations higher than 100 ppb and that they contribute up to 77% of the total Ca^{2+} deposition over the last 80 years.

In recent time, however, samples influenced by Saharan dust input can remain acidic (Maupetit and Delmas, 1994). Such samples were characterized by Maupetit and Delmas (1994) as having typical sulfate to calcium and nitrate to calcium weight ratios up to about 2.6 and 1.2, respectively. Thirteen CDD snow layers deposited after 1960, containing more than 100 ppb of calcium and having not be identified as contaminated by Saharan dust inputs by using the alkalinity criteria, show a mean sulfate to calcium and nitrate to calcium weight ratio of 2.8 and 1.1, respectively (see Figure 3.3). We have also considered these samples as contaminated by Saharan dust input.

In the following we discuss how samples regarded as contaminated by Saharan dust have been corrected from this contribution. Since an important part of the Ca^{2+} level in these samples is relative to the presence of dust, with the aim to extract the long-term changes of calcium not related to the changing frequency of these events, we assigned these samples the calcium level obtained as half year mean summer level in the corresponding year of the event, instead of considering their originally measured Ca^{2+} level (see Figure 3.4). For other ion

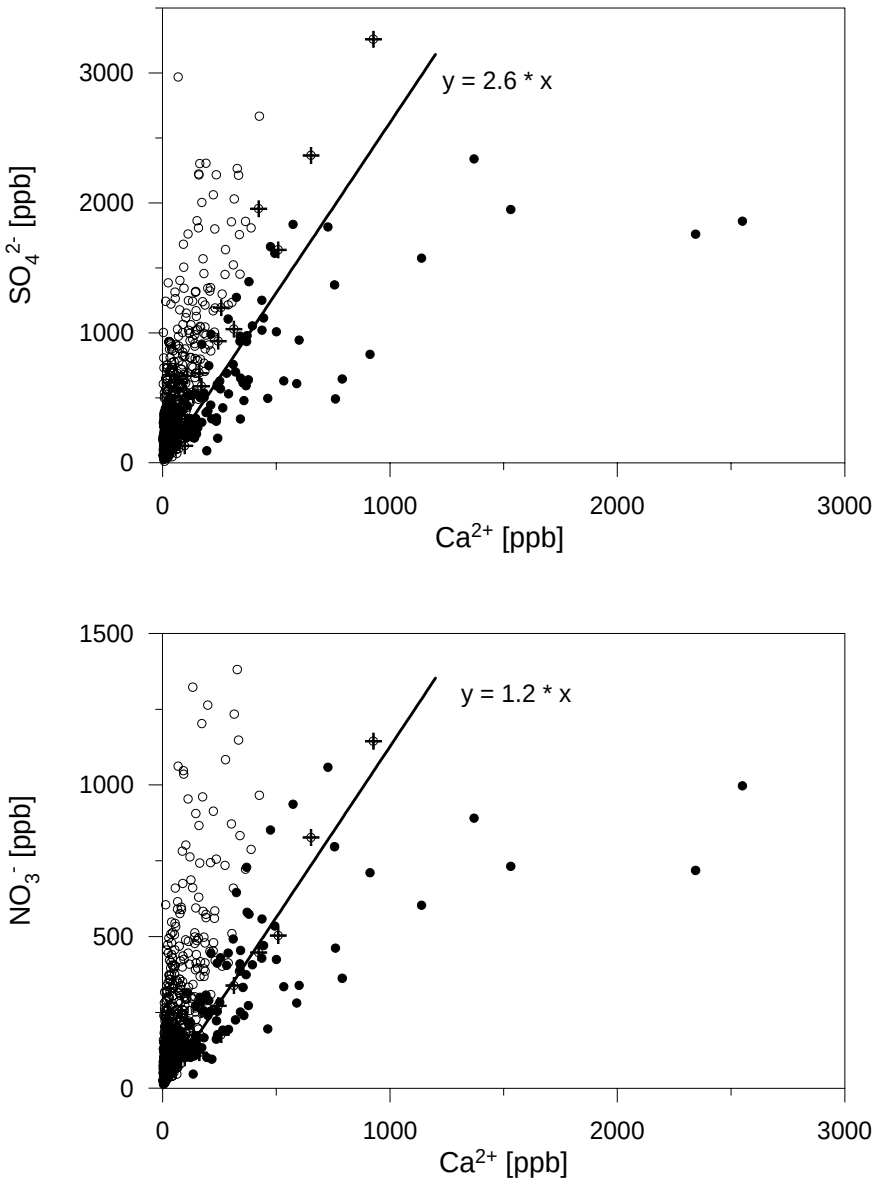

Figure 3.3. Sulfate (top) and nitrate (bottom) versus Ca^{2+} levels in the C10 summer samples. Samples regarded as free of Saharan dust input are denoted with open circles. Samples suspected to contain Saharan dust (using the alkaline criteria) are marked with black circles. Saharan dust samples identified via their SO_4^{2-} to Ca^{2+} and NO_3^- to Ca^{2+} mass ratio (see text) are marked with crosses in open circles.

species (C) an attempt was made to correct their levels ([C]) from their dust contribution following: $[C]_{cor.} = [C] - \alpha\,[Ca^{2+}]$

where C is the observed concentration, and α is the C to Ca ratio in Saharan dust.

Since SO_4^{2-} is present in Saharan dust aerosol as gypsum, the occurrence of Saharan dust events reaching the Alps may influence the C10 sulfate data set. To correct the sulfate profile from this effect, samples regarded as contaminated by such inputs were corrected by

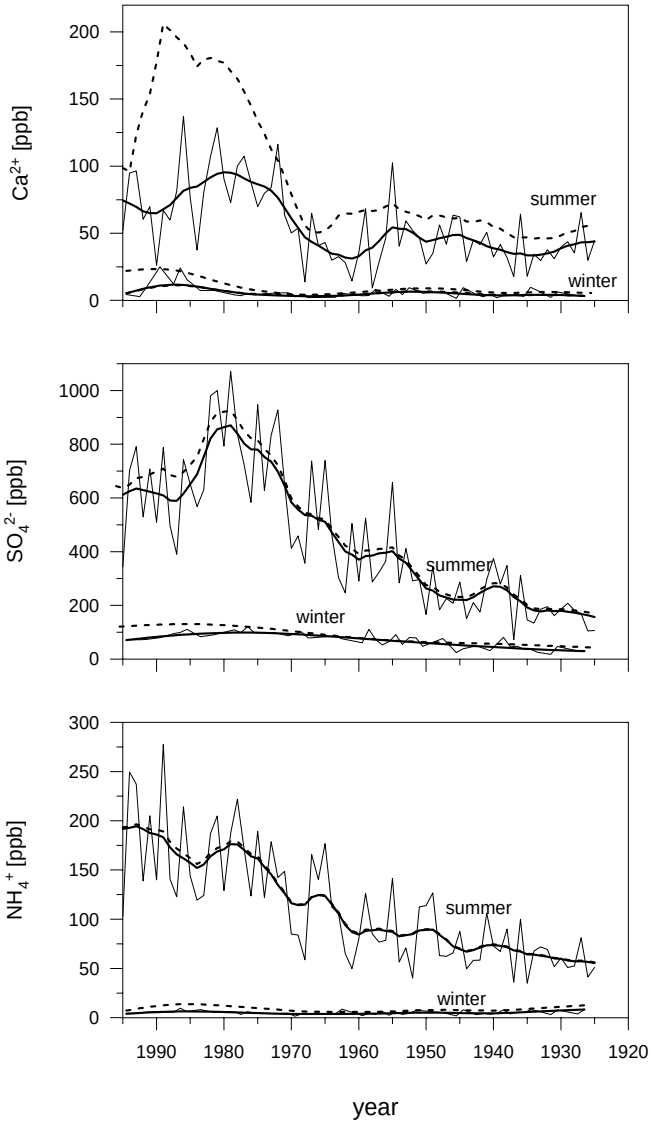

Figure 3.4. Smoothed summer and winter time trends of Ca^{2+}, SO_4^{2-} and NH_4^+ derived from C10 with (thick solid lines) and without (thick dashed lines) corrections from short term sporadic events (Saharan dust and unusual high winter levels) (see text). Smoothed summer trends are derived by Single Spectrum Analyses (SSA) winter ones by applying a robust spline (see section 3.2.4) on the respective half year means of individual years. In addition to the smoothed trends the summer and winter means of individual years are reported (thin solid lines).

using an α value of 0.59. This value represents the mean weighted sulfate to calcium ratio observed by Wagenbach et al. (1996) in dust horizons of the pre-industrial era at CG and is consistent with the one observed in dust events located in the bottom part (i.e. deposited at the turn of the last century, $\approx 1890 \pm 10$) of the C10 core (see section 5.4 (*3.2*)). Following that, we found that these dust events account for up to 17% of the sulfate summer snow deposition at CDD (see Figure 3.4).

In addition to calcium and sulfate, Saharan dust likely contains other cations (sodium, potassium, and magnesium) and anions (chloride, fluoride, and possibly carboxylates), but in a lower amount. Since fluoride and light carboxylates have not been determined in the bottom part of the CDD core as well as in the pre-industrial Colle Gnifetti ice cores, we here have used two different approaches to estimate their mean content in Saharan dust and the corresponding α values (Table 3.2). First the mean composition of dust was examined by checking the linear relationship between C species and Ca^{2+} in CDD ice samples regarded as containing dust events. This procedure is certainly correct to evaluate the α values for sodium, potassium, and magnesium. In contrast, for species having an acidic property (fluoride, chloride, nitrate, and carboxylates), the slope of the corresponding linear correlation with calcium may represent an overestimate of the α values due to the possible uptake of these species during the transport of this alkaline dust material in the acidic atmosphere. This effect

Table 3.2: Mean ion concentrations in Saharan dust plumes (Talbot et al., 1986) and their estimated relative contribution (mass ratio) versus Ca^{2+} (see text). Also given are estimated mean mass ratios of ion species versus Ca^{2+} in dust influenced C10 summer samples (see text).

	Saharan dust plume (Talbot et al., 1986)			Col du Dôme ice core C10			dust contri-bution (α) used in this study
Species	Concentration [μg/g] ± s.d.	contribution with respect to reference Ca^{2+} value ± s.d. (see text)	n	Linear relationship versus Ca^{2+} in C10	R^2	n	
Na^+	3704 ± 2370	0.071 ± 0.045	6	0.071 [Ca^{2+}] + 20.8	0.66	98	0.071
NH_4^+	1796 ± 1204	0.034 ± 0.023	6	0.185 [Ca^{2+}] + 112.8	0.31	98	0.034
K^+	1663 ± 829	0.032 ± 0.016	6	0.035 [Ca^{2+}] + 12.5	0.56	98	0.035
Mg^{2+}				0.045 [Ca^{2+}] + 9.2	0.77	98	0.045
Ca^{2+}							
F^-	65 ± 18	(1.25 ± 0.3) 10^{-3}	6	2.1 10^{-3} [Ca^{2+}] + 1.55	0.3	89	2.1 10^{-3}
Cl^-	3158 ± 1186	0.06 ± 0.023	6	0.113 [Ca^{2+}] + 35	0.68	98	0.06
NO_3^-	5132 ± 4641	0.098 ± 0.088	6	0.405 [Ca^{2+}] + 188	0.5	98	0.098
SO_4^{2-}	12887 ± 8902	0.25 ± 0.17	6	0.9 [Ca^{2+}] + 398	0.45	98	0.59
Formate	681 ± 610	0.013 ± 0.012	6	0.26 [Ca^{2+}] + 118	0.47	98	0.013
Acetate	843 ± 882	0.016 ± 0.017	6	0.084 [Ca^{2+}] + 11	0.72	98	0.016
Oxalate	658 ± 399	0.013 ± 0.008	6	0.03 [Ca^{2+}] + 27	0.23	98	0.013

can be identified by comparing the obtained α values with the ones derived from the study of the ionic composition of aerosol samples collected in Saharan dust plumes located over the tropical North Atlantic by Talbot et al. (1986) (see Table 3.2) for which post emission phenomena would be far more limited (less contact of the plume with polluted air masses of the continental boundary layer). Reversely, since the dust composition can vary from one to another event, the composition reported in the study of Talbot (only based on 6 dust plumes) can only be used to extract an order of magnitude of the dust composition. Because of that, as detailed below, the α values applied in this work (see Table 3.2) were chosen by considering the different nature of species.

Since calcium was not determined by Talbot et al. (1986), we normalized their data on a reference Ca^{2+} value deduced from the relationship found between sodium and calcium in the dust samples of C10. Note that soluble sodium is twice more abundant than soluble potassium in the Saharan dust inputs of C10 and in the dust composition reported by Talbot et al. (1986) (Table 3.2). For cations, since no uptake is expected during the atmospheric transport of plumes we adopted α values derived from the examination of the CDD samples except for ammonium which exhibit a larger α value (0.185) in CDD samples than in the study from Talbot, but with a rather poor correlation coefficient ($R^2 = 0.3$, Table 3.2).

In general for anions, Table 3.2 indicates higher α values derived from the CDD samples than those reported in the study of Talbot. For fluoride, a weak additional input seems to take place during the transport as suggested by the difference by less than a factor of two between the slope of $2.1\ 10^{-3}$ of the linear regression of the C10 data set and the fluor to calcium ratio in dust plumes. For chloride, nitrate, and carboxylates an even larger difference appears and we applied therefore for these species the α values observed by Talbot et al. (1986) in dust plumes.

3.2.2. Short term perturbations influencing the chemical composition of winter snow deposits

Using the ammonium dissection criterion, 337 samples were identified as deposited under background winter conditions. Within several winter half year sections, however, some samples exhibit concentrations (up to 70 ppb and to 600 ppb for ammonium and sulfate, respectively) significantly higher than their respective typical winter levels. These unusual sporadic winter snow layers are found to be not uniformly deposited over the CDD glacier site (i.e. on a distance of about 100 meters), suggesting that they result from short-term deposition events (due to long range transport of pollution or sporadic occurrence of convective weather conditions during winter). However, we cannot exclude that these sporadic unusual events are created by wind re-distribution of snow deposited during the preceding summer or fall. Note that two thirds of winter samples exhibiting ammonium concentrations higher than 10 ppb are randomly located in all individual winter half years sections, while the remaining third of samples is located in the winter half year section of

1980. To examine the temporal change of pure « background » winter conditions (further denoted as winter), only samples exhibiting ammonium levels lower than 10 ppb (217 samples) were considered in the following (Figure 3.4).

Among 217 winter background samples, four exhibit an alkalinity below the 25% percentile of the alkalinity robust spline smoothing (see section 3.2.1) and a calcium content higher than 20 ppb. They were therefore regarded as contaminated by Saharan dust input. For these samples measured ion concentrations were corrected accordingly to what is described in section 3.2.1 for Saharan dust containing summer samples.

3.2.3 Summer and winter long-term trends

Individual summer and winter means have been calculated for each year. Following Fischer (1997), Singular Spectrum Analyses (SSA) (Vautard et al., 1992) was applied on the equidistant summer data sets, to separate in the whole profile the temporal trend from periodic contributions and noise. In order to suppress annual variabilities, the time window of the SSA was chosen to be 5 years, and the first reconstructed component was contained. This component is identified as trend, explaining for example (see Figure 3.4) 57%, 64% and 77% of the total variance in the Ca^{2+}, SO_4^{2-} and NH_4^+ data sets, respectively.

Since the background winter data set lacks some individual years, a robust cubic spline smoothing was applied (Fischer, 1997) to evaluate the temporal trend of the individual annual winter means. In contrary to the commonly used cubic spline approximation, in which the squared deviations from the mean are minimized, here the absolute deviations from the median, or any other pre-selected percentile, are minimized (Bloomfield and Steiger, 1983).

3.2.4 Reconstruction of representative annual mean time trends

The availability of separate winter and summer time trends permit to reconstruct a mean annual time trend, which is free of the glaciological forcing described in section 2.2 and is therefore relevant for examination of the temporal change of mean annual atmospheric conditions over the last 70 years. To do so, mean half year concentrations of the (background) winter and summer data set were averaged, assuming that winter and summer conditions prevail each for 6 months per year (see section 2.3 and 2.4 (*Figure 4*)). Note that no significant differences occur for the mean annual trend, when background-winter levels (only winter samples with NH_4^+ of less than 10 ppb) or the total winter data set (including winter samples with NH_4^+ higher than 10 ppb) are considered. Since no significant difference is seen between the amount of recent summer and winter precipitation at the CDD site (Auer, personal communication) the reconstructed mean air condition trends are assumed to be also representative for the change of the mean annual precipitation conditions over the last 70 years.

Commonly (Van de Velde, 1999; Döscher et al., 1996, Schwikowski et al., 1999a) temporal trends inferred from these small area glacier sites were built on the base of the total annual snow deposition, and interpreted without taking into account the glaciological forcing effect. To evaluate the importance of this bias, we compared the strongly smoothed (SSA time window:10 years) reconstructed mean annual trend, to the respective one achieved from C10 if annual concentration means, built on the base of the total annual C10 snow deposition, are considered (see Figure 3.5).

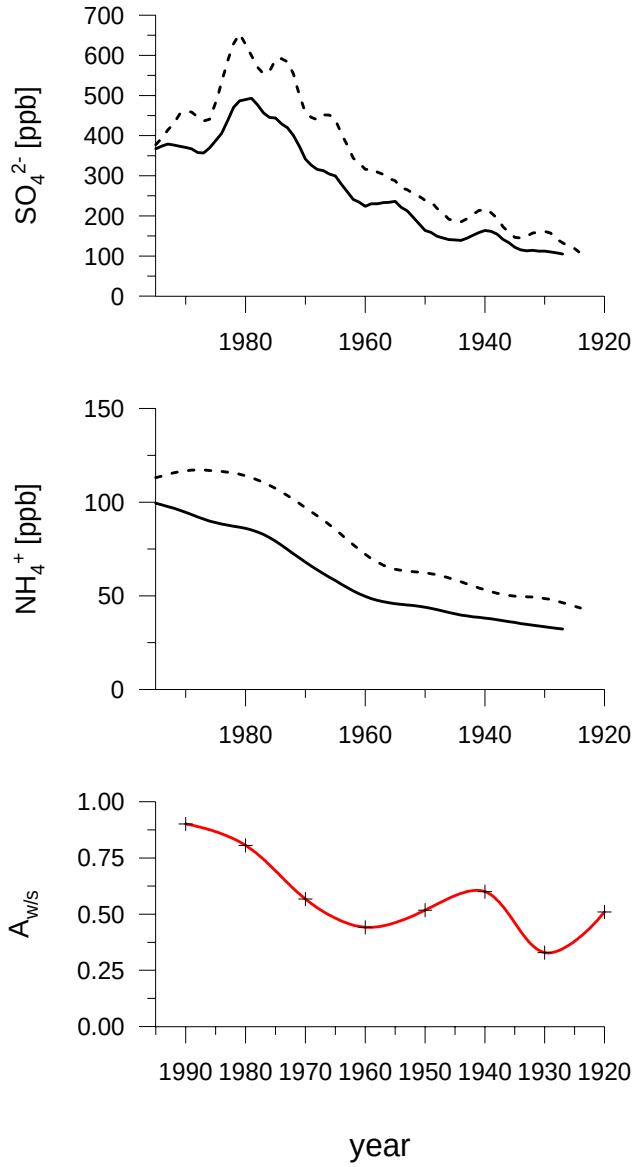

Figure 3.5. (Top and middle) Reconstructed mean annual SO_4^{2-} and NH_4^+ trends (solid lines) together with annual mean SO_4^{2-} and NH_4^+ trends derived by considering annual means averaged over the total annual snow deposition (dashed lines) (see text). (Bottom) Annual winter to summer net snow accumulation ratio ($A_{w/s}$) of C10 versus time.

The annual mean deposition time trend shows systematic higher levels, 28% in 1980 and 35% in 1930 for sulfate, 37% in 1980 and 45% in 1930 for ammonium if compared to the reconstructed annual trend. This is due to the systematic increase of summer snow accumulation (with respect to winter) down the length of the core. In addition to this offset effect, Figure 3.5 shows that also the trend evolution could be significantly modified by the glaciological forcing effect. While the reconstructed time trend indicates enhanced concentration between 1930 and 1980 by a factor 4.2 for sulfate (2.6 for ammonium), the annual mean deposition record indicates a factor of 3.7 (2.4 for ammonium) only. Note also that after 1980 the rate of increasing concentrations is significant lower for sulfate and ammonium within the annual means deposition trend, if compared to the respective changes revealed by the reconstructed annual trends. This difference is likely due to the fact that the amplitude of the seasonal cycle of sulfate and ammonium is higher after 1980 than before. We cannot exclude however that this difference is also due to potential existing uncertainties of the smoothed time trends at the boundaries of the data sets.

Based on this example of the CDD C10 ice core, it becomes obvious that glaciological forcing can exert a non negligible effect on the long term changes extracted from small area glacier sites. This work would recommend for future studies dealing with such Alpine ice core records to inspect more carefully the seasonality of ice records before interpreting them in terms of atmospheric changes. Note that, this problem renders difficult a direct comparison of the long term trends obtained in this work with other already obtained records at other high Alpine glacier sites.

Chapter IV

SO_4^{2-}, NO_3^-, and NH_4^+ changes revealed in CDD snow and ice layers: Implications for atmospheric chemistry changes at the scale of Europe over the last 80 years

Based on the seasonally resolved trends of impurities trapped in snow deposited since 1925 at CDD presented in Chapter 3, we here discuss the atmospheric meaning of their long-term changes. We will start with sulfate, a species derived from the S cycle which is thought to be now dominated by anthropogenic emissions, at least over continental regions of the northern hemisphere. Furthermore, the spatial and temporal variations of anthropogenic SO_2 emissions are quite well documented at the scale of Europe. Then we will discuss the trend of the major nitrogen species derived from the N cycle (ammonium and nitrate) which come from ammonia and nitrogen oxides for which emissions (natural and anthropogenic) are still not so well quantified with respect to the sulfur ones.

4.1 CDD sulfate trends

4.1.1 The temporal evolution of CDD summer and winter snow deposits and their relation to European SO_2 emissions

The C10 winter and summer sulfate records derived from raw data using the procedure detailed in Chapter 3 are here discussed in terms of past atmospheric changes. We first compare the long term ice record of the anthropogenic sulfate fraction with the changes of SO_2 emissions from European countries located at various distances from the Alps. The anthropogenic sulfate fraction is calculated by subtracting the pre-industrial level from the total sulfate concentrations. Since the reliable dated part of the C10 ice core only extends back to 1925, the natural (pre-industrial) summer and winter sulfate levels were estimated by

Table 4.1: Chemical composition of summer and winter layers located on the bottom part of the 1994 CDD core (between 90.3 and 95.3 m w.e.) which were estimated to span the 1880-1900 time period (see section 2.1). Values refer to means after correction of samples (16 on a total of 111) suspected to contain Saharan dust (see section 3.2.1).

Species	Winter (in ppb)	Summer (in ppb)
NH_4^+	1.7 ± 2	36 ± 17
NO_3^-	35 ± 15	102 ± 45
SO_4^{2-}	20 ± 18	70 ± 40

considering levels revealed in the summer Colle Gnifetti pre-industrial ice as well as the mean summer and winter levels observed in the C10 ice (see Table 4.1) located between 90.3 and 95.3 m w.e. depth (i.e., likely corresponding to 1890 ± 10 years, see section 2.1). Following that, we have assumed a pre-industrial sulfate level of 80 and 20 ppb in summer and winter, respectively (see also section 4.1.4 (*3.3*)).

The comparison of the long term changes of anthropogenic SO_4^{2-} summer (see also section 4.1.4 (*4.1*)) and winter (see also section 4.1.4 (*4.2*)) CDD levels with past anthropogenic SO_2 emissions from Europe was performed considering different European regions (western Europe and total Europe). These comparisons suggest the following anthropogenic source region apportionment :

In summer, the sulfate CDD levels were increased by a factor of 10 from the pre-industrial time to 1980 with a marked increase between 1960 and 1980, and closely follow the course of growing SO_2 emissions from France, Italy, Spain, Switzerland, and to a lesser extend West Germany (Figure 4.1). Note that the agreement becomes poorer if other

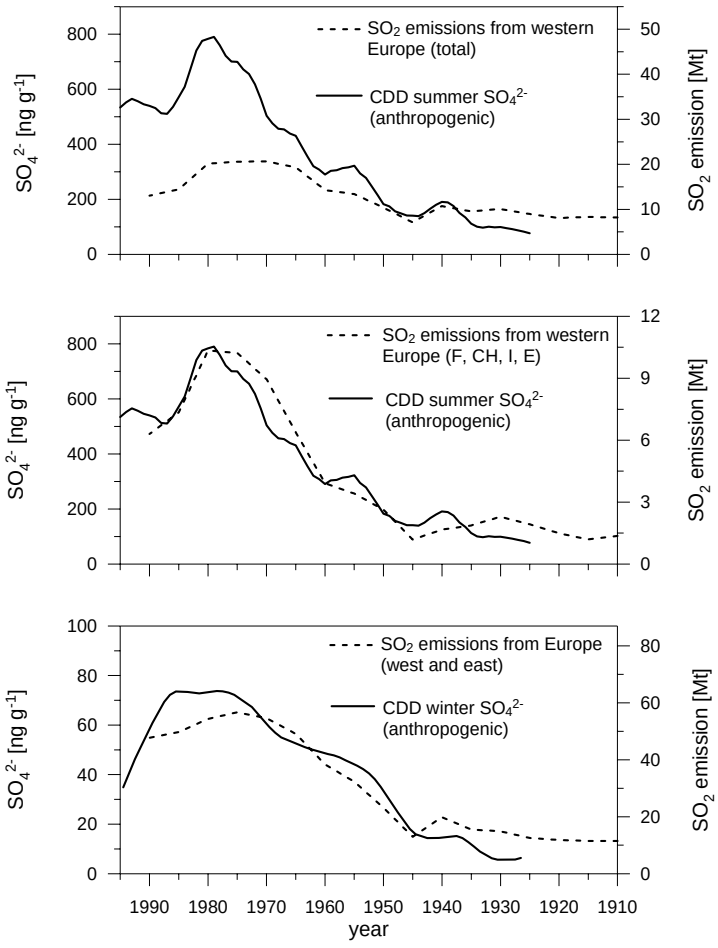

Figure 4.1: Comparison of anthropogenic summer and winter CDD SO_4^{2-} trends with European SO_2 inventories (Mylona, 1996) (see text).

important contributors of the northern part of western Europe such as United Kingdom, whose emissions were already very large in 1925 (4 Mt of SO_2) and only enhanced by 50% from 1925 to the 1980's, are considered. These comparisons suggest that countries having an impact on the high-elevated Alpine sites in summer include regions located within 700-1000 km from the Alps with a major influence of emissions from France, Spain, and Italy. The fact that SO_2 emissions from northern countries (such UK, Belgium, and partly western Germany) have there a weaker impact than those from southern countries is likely due to a dominant transport of air masses from south-west rather than from north or north-west towards the Alps in summer (I. Auer, personal communication).

For winter, Figure 4.1 indicates that anthropogenic sulfate levels only exhibit an increase by a factor of 4 from the pre industrial era to 1980, with a rather constant increasing rate through the 1925-1980 time period. That contrasts with the summer trend and would suggest a limited contamination of the free troposphere by SO_2 emissions at the scale of total Europe (including former USSR) (Figure 4.1) at that season.

4.1.2 Comparison with Greenland sulfate trends

For comparison, we performed a similar attempt to estimate the source apportionment for anthropogenic sulfate reaching the Greenland ice cap by comparing long term seasonally resolved anthropogenic sulfate record gained by Legrand and De Angelis (1996) at Summit (central Greenland) with available world wide documented SO_2 anthropogenic emissions from Lefohn et al. (1999). One first major difference between Greenland and Alpine ice sulfate records merges from the relatively high contribution of the natural background level in Greenland (see also section 4.1.4 (*4.3.1*)) which accounts for a quarter (in winter and summer) to a third (in summer) of the total sulfate deposition at the time of the anthropogenic maximum input (1960–1980). This differs clearly to the situation in the Alps, where natural sulfate sources contribute only in the range of 10% in summer to 20% in winter to the total SO_4^{2-} budget between 1970 and 1990. Comparing the seasonal resolved anthropogenic sulfate trends of the Greenland ice core with SO_2 emissions from different source areas of the northern hemisphere it appears that whatever is the considered season, the Greenland ice core sulfate trend mimics the course of SO_2 emissions originating from both United States and Eurasia (see section 4.1.4 (*4.3.2*)). That is in agreement with the study of 10-days back air trajectories at 500 hPa (Kahl et al., 1997) which indicates air masses reaching the Greenland ice cap coming from these two source regions. With respect to the Greenland records which certainly contain valuable information to constrain the complex interplay between long-range transport and removal process acting between source regions and high northern latitudes, Alpine ice core records are more connected to Europe emissions containing information that can be directly used in evaluating the climatic effect of changing sulfate atmospheric load over continental mid-latitude northern hemisphere regions. Since we found that Alpine sulfate

records are essentially driven by past SO_2 emissions from the European continent for which anthropogenic emissions are quite well-known and natural sulfur emissions weakly influence the sulfur budget, it is here more powerful than in Greenland to compare past atmospheric changes with current global and regional model simulations.

4.1.3 Atmospheric implications of the CDD sulfate trend

Using the relationship between present day concentrations in air and in the snow pack at the CDD site (see Chapter 1), the CDD ice core records permit to reconstruct present and past atmospheric SO_4^{2-} concentrations at 4300 m asl over Europe during summer and winter. Following that, the annual atmospheric sulfate mixing ratio of 106 pptv derived at 4300 m asl in 1985 from CDD ice record suggests an overestimation by a factor of two to three of levels simulated by current models for this elevation. Furthermore, atmospheric sulfate levels derived from ice cores at the CDD site together with sulfate levels observed at lower elevated Alpine sites correspond for 1991-1993 to an equivalent column sulfate between the ground and 4300 m elevation of 7 and 11 mg SO_4^{2-} m^{-2} in winter and summer, respectively (see also section 4.1.4 (*5.2*)). Since the column sulfate is an important parameter for the radiative balance, such information on the total column (and its seasonality) are invaluable to estimate accurately the present and past radiative aerosol forcing over Europe.

4.1.4 Sulfate Trends in a Col du Dôme (French Alps) ice core: A record of anthropogenic sulfate levels in the European mid-troposphere over the 20^{th} century.

Sulfate Trends in a Col du Dôme (French Alps) Ice Core: A Record of Anthropogenic Sulfate Levels in the European Mid-Troposphere over the 20th Century

Susanne Preunkert[1], Michel Legrand[1,*], and Dietmar Wagenbach[2]

[1] *Laboratoire de Glaciologie et Géophysique de l'Environnement du Centre National de la Recherche Scientifique, BP 96, 38402, St Martin d'Hères, France*

[2] *Institut für Umweltphysik, Universität Heidelberg, INF 229, 69120 Heidelberg, Germany*

* Corresponding author. Phone: +33/(0)476824243; Fax: +33/(0)476824201; e-mail: mimi@glaciog.ujf-grenoble.fr

In press at "Journal of Geophysical Research"

Abstract

A high-resoluted sulfate record from a Col du Dôme (CDD, 4250 m above sea level, French Alps) ice core was used to investigate the impact of growing SO_2 emissions on the mid-troposphere sulfate levels over Europe since 1925. The large annual snow accumulation rate at the CDD site permits examination of the summer and winter sulfate trends separately. Being close to 80 ± 10 ng g^{-1} in pre-industrial summer ice, sulfate CDD summer levels then increase at a mean rate of 6 ng g^{-1} per year from 1925 to 1960. From 1960 to 1980 the increase continued at a rate of 24 ng g^{-1} per year. Concentrations reach a maximum of 860 ng g^{-1} in 1980 and subsequently decrease to 600 ng g^{-1} in the 90s. These summer sulfate changes closely follow the course of growing SO_2 emissions from source regions located within 700-1000 km around the Alps (France, Italy, Spain, and to a lesser extent West Germany). In winter, the CDD sulfate levels are three to eight times lower than in summer, due to more limited upward transport of air masses from the boundary layer at that season. Being close to 20 ng g^{-1} in the pre-industrial ice, winter levels were regularly enhanced at a mean annual rate of 1.2 ng g^{-1} from 1925 to 1980. The weak winter change from the pre-industrial era to 1980 (a factor of 4 instead of 10 in summer) reflects a limited contamination of the free troposphere which, in contrast to summer, occurs at a larger scale (total Europe/former USSR). Intimately connected to Europe, these long term changes in the Alps clearly differ in time and amplitude with the ones revealed by Greenland ice cores which indicate an increase by a factor of three between 1880 and 1970 in relation with long-range transport of pollutants from Eurasia as well as from North America. Furthermore, due a lower natural contribution to the total sulfate level, the anthropogenic changes can be more accurately derived in the Alps than in Greenland. Using the observed relationship between present-day concentrations in air and snowpack, the CDD ice core record permits to reconstruct present and past atmospheric sulfate concentrations at 4300 m above sea level over Europe in summer and winter. These data are compared with the sulfate levels simulated by current global sulfur models at 600 hPa for which uncertainties are still ranging within a factor of two. Together with observations made at lower elevation in the early 90s, the atmospheric levels derived for the CDD site (~ 20 and 400 ng m^{-3} STP in winter and summer, respectively) document the vertical sulfate distribution between the ground and 4300 m elevation over western Europe at that time. In this way, data gained at high elevated Alpine sites are powerful in evaluating the recent role of sulfate aerosol in forcing the climate over Europe.

1. Introduction

The most direct evidence for the change in the aerosol load from the pre-industrial era to present has been depicted so far from chemical studies of Greenland ice cores. For instance, it was shown that Greenland sulfate ice core records qualitatively depict the expected changes of growing anthropogenic SO_2 emissions in the northern hemisphere [*Neftel et al.*, 1985;

Mayewski et al., 1986]. However, in these remote regions, large uncertainties exist in the source region apportionment of short lived sulfur species due to complex interplay between long-range transport from different source regions (Eurasia and North America, *Fischer et al.* [1998]), gas/particles conversion, and removal processes, which are seasonally dependant. The evaluation of the impact of sulfate aerosol on climate is based on the sulfate aerosol distribution for which estimates are only available from atmospheric chemistry models. In view to quantify the climatic impact of changing aerosol load over industrialized regions, there is thus a strong need to gain ice core records at mid-latitudes. Together with eastern USA, western and central Europe are regions where the direct radiative effect of anthropogenic sulfate aerosol is believed to be largest [*Charlson et al.*, 1991]. Due to their intimate connection to European source regions, ice cores extracted from high-elevated Alpine glaciers may be here useful to reconstruct past sulfate atmospheric load and its climatic effect over Europe. It has to be noted that the atmosphere at these continental sites is far less influenced than Greenland by natural biogenic marine sulfur emissions for which past fluctuations are not well known. Finally, as shown for HF [*Preunkert et al.*, 2001], advantages of Alpine ice records with respect to the Greenland ones also include less contamination by volcanic emissions (SO_2, HCl, and HF) at mid-latitudes compared to the situation at high-northern latitudes.

At the scale of Europe, present information extracted from Alpine ice cores are mainly available from Colle Gnifetti (CG) [*Wagenbach et al*., 1988; *Wagenbach et al.*, 1997, *Schwikowski et al.*, 1999a], showing an increase of annual mean sulfate content by a factor of 10 (i.e. three to five times larger than in Greenland) between the pre-industrial era and 1980. Atmospheric studies achieved at high-elevated Alpine sites indicated a strong seasonal cycle of short-lived species with summer maxima [*Baltensperger et al.*, 1997]. A straightforward interpretation of the CG ice records in terms of past environment remains therefore limited by the poor knowledge of their seasonal representativity [*Wagenbach and Preunkert*, 1996], since a preferential loss of deposited winter snow occurs at that site by wind erosion. In contrast, it was shown that the Col du Dôme (CDD) Alpine drill site, is characterized by large annual snow accumulation rate (~1.5 m water equivalent (w.e.) instead of 0.2 to 0.4 m w.e. at CG) and well preserved winter snow which would permit to gain records of past changes of atmospheric chemistry at seasonal resolution [*Preunkert et al.*, 2000]. This opens the possibility to examine in detail a seasonally resolved source region apportionment of anthropogenic species for the past free troposphere over Europe by comparing these summer and winter long term trends with estimates of past pollutant emissions.

In this paper, we present temporal variations of sulfate levels recorded in a CDD ice core covering the essential part of the 20th century. For the first time, the temporal trend is

seasonally resolved, permitting to discuss in detail the source region apportionment for the mid-troposphere over Europe under winter and summer conditions. Based on our present knowledge of the relationship between air and snowpack composition in winter and summer there, these seasonally resolved trends are translated into changes of summer and winter atmospheric sulfate levels since 1925. These inverted data are compared to current model simulations of the impact of SO_2 anthropogenic emissions from Europe on the present and past atmospheric sulfate distributions. Finally we investigate to what extent such mid-latitude ice core records are more useful than the Greenland ones in assessing the climatic impact of the growing SO_2 emissions over the very sensitive continental regions of the northern hemisphere.

2. Sampling, and Dating

A 126-m long ice core extracted in 1994 at Col du Dôme (4250 m asl, located near the Mont Blanc summit), was first analyzed for major ions at the Institut fur Umweltphysik (IUP) laboratory using ion chromatographs equipped with an autosampler (1393 samples down to 90 m water equivalent (w.e.) depth, and 111 samples between 90.3 and 95.3 m w.e.) for dating purpose. Based on this first set of data, a more complete chemical study including major ions (Na^+, NH_4^+, Ca^{2+}, Mg^{2+}, Cl^-, NO_3^-, and SO_4^{2-}) as well as fluoride [*Preunkert et al.,* 2001] and light carboxylates (not discussed here) was achieved with a seasonal resolution at Laboratoire de Glaciologie et Géophysique de l'Environnement (LGGE) laboratory using working conditions detailed in *Legrand et al.* [1993]. This was done (1050 samples) along the upper 117 meters of the core (i.e., 90 m w.e.) which correspond to the well-dated part of the core covering the 1923-1994 time period (Figure 1). For major ions determinations, the accuracy is typically of 5 %. Ice samples were cleaned at LGGE by using an electric plane device previously developed at IUP [*Fischer et al.*, 1998]. The validity of the decontamination procedure was tested by checking blank values obtained on pieces of frozen ultrapure water (Millipore system). Mean blank values (11 samples) obtained at LGGE were 1 ± 0.7 ng g^{-1} for sulfate. Mean blank values (~40 samples) obtained at IUP using the autosampler were slightly higher, 2.7 ± 1.9 ng g^{-1} for sulfate. Hence, data obtained on the bottom part of the core were corrected from this blank value.

The glaciological characteristics of this CDD ice core indicate an annual layer thickness ranging from 3 to 0.2 m water equivalent (w.e.) from the surface to a depth of 90 m w.e. and a relative amount of winter to summer snow deposition close to 1 nearby the surface and ~ 0.5 at 74 m w.e. depth [*Preunkert et al.,* 2000]. The precise dating of the CDD ice core based on the well-preserved seasonality of ammonium indicates an ice age of 75 ± 5 years at the depth of 90 m w.e. From 90.3 to 95.3 m w.e., the counting of years becomes difficult and *Preunkert*

et al. [2000] suggested that this bottom part of the core may cover some 17 years (1906-1922).

3. Data Reduction and Data Presentation

3.1. Seasonal Cycle

In evaluating long-term chemical records extracted from a small-scale glacier as the Col du Dôme one, special caution has to be paid to systematic changes in the snow deposition characteristics upstream to the drill site. As shown by *Preunkert et al.* [2000], along the CDD ice core, the ratio of winter to summer net snow accumulation is decreasing from 1 near the surface to 0.5 at 100 m depth (i.e. 74 m w.e.). This effect is due to the systematic change of the surface topography upstream to the borehole. Thus, depending on the summer to winter contrast of the ice impurities content, such a glaciological forcing would induce a non-atmospheric effect in ice core records there.

Given the quite large interannual variability of the snow accumulation, and with the aim to examine the mean seasonal cycle over periods covering several years, each winter and summer snow layer has been divided into six equally spaced parts (in w.e.). The dissection cutting was based on the profile of ammonium which is the ion exhibiting the strongest seasonal cycle. As detailed by *Preunkert et al.* [2000], the boundaries of the winter half year snow pack have been identified by requiring at least 3 consecutive samples to significantly exceed the 10 ng g^{-1} (background) level of ammonium. A weighted interpolation was applied to years containing more (or less) than 12 samples. Finally, multi-annual means were calculated for each 1/12 annual accumulation fraction for different key time periods. As seen in Figure 2, ammonium levels exhibit a well-marked seasonal cycle characterized by summer maxima, with a mean summer to winter ratio ranging from 5 between 1925 and 1935 to 15 between 1975 and 1985. As already pointed out by *Preunkert et al.* [2000], that shows the good preservation of the seasonal cycle of impurities trapped in snow deposited at this site since at least 1925. The sulfate levels also exhibit clear summer maxima, with a mean summer to winter ratio ranging from 3 to 6 over the 1925-1935 and 1975-1985 time periods, respectively (Figure 2). These well-marked summer maxima are consistent with atmospheric observations made at high-elevated Alpine sites, reflecting distinct seasonal atmospheric conditions prevailing there due to the presence or absence of upward advection of air masses from the boundary layer in summer and winter, respectively [*Preunkert and Wagenbach*, 1998; *Kasper and Puxbaum*, 1998].

To examine winter and summer trends of sulfate, we first calculated the individual means of summer and winter half years from all samples along the well dated part of the core (1925-1995). Summer means were smoothed using single spectra analysis (SSA) with a time

window of five years. We here examine the first SSA component which depicts the general trend (Figure 3). From the 337 samples regarded as deposited during the winter half year, we considered here only those having ammonium concentrations lower than 10 ng g^{-1} (i.e., 217 samples). Because of the lack of some individual winter means we here applied a robust spline smoothing [*Bloomfield and Steiger*, 1983] (Figure 3). Note that, only background values have been considered in examining the trend, and the mean winter level may here some 50% higher.

In order to illustrate the effect of the downcore decrease in the winter to summer snow ratio ($A_{W/S}$) we compare in Figure 3 smoothed trends of annual mean sulfate values which were calculated differently from the raw data set: (1) as arithmetic means of data attributed to individual years, (2) as arithmetic means of the respective winter and summer level in each year. Annual mean values derived by method (1) are thus implicitly weighted by a winter to summer contrast of the net snow accumulation ($A_{W/S}$). This is not the case for those based on method (2) which are in this way more representative of annual mean atmospheric levels. While the trend lines of the two data sets do not differ much in the top ice core section (since winter and summer accumulation are similar there), significant higher levels are obtained further down for the $A_{W/S}$ weighted annual mean trend. This is due to the now marked decrease of the winter to summer snow ratio (see Figure 3) and the strong sulfate surplus in summer relative to winter snow layers. The annual mean differences account up to 150 ng g^{-1} between 1965 and 1980 leading, for instance, to $A_{W/S}$ weighted annual means around 1965 which are higher by 45%. This effect is also seen (Figure 3) to modify the overall pattern of the long term trend. These observations clearly indicate that direct evaluation of long term changes along this Alpine ice core by examining the commonly employed yearly averaged levels without the scrutination of seasonal trends leads to significant errors. Due to the complexity of ice flow dynamic of such small scale glaciers, it would be therefore important to investigate systematically the summer to winter snow accumulation change with depth along Alpine ice cores.

3.2. Impact of Saharan Dust in Alpine Records

Previous studies have shown that deposition of saharan dust can sporadically affect high-elevated Alpine sites and disturb the chemical composition of snow deposits. Following *Wagenbach et al.* [1996], such events can be identified as calcium-rich layers exhibiting a negative acidity (i.e. alkaline samples). The acidity (or alkalinity) of samples has been here evaluated by checking the ionic balance between following anions and cations (denoted [Δ]):

$$[\Delta] = [F^-] + [Cl^-] + [NO_3^-] + [SO_4^{2-}] + [CH_3COO^-] + [HCOO^-] + [C_2O_4^{2-}] - [Na^+] - [K^+] - [Mg^{2+}] - [Ca^{2+}] - [NH_4^+] \quad (1)$$

with concentrations expressed in microequivalents per litre (μEq L^{-1}). Significantly positive values of [Δ] correspond to the acidity, negative values to the alkalinity of the samples.

Preunkert et al. [2001] identified 98 summer and 4 winter samples as significantly contaminated by saharan dust along this CDD core. Since sulfate is present in saharan dust aerosols (gypsum), sulfate concentrations of these 102 samples were corrected for the terrigeneous contribution following: $[SO_4^{2-}]_{cor.} = [SO_4^{2-}] - \alpha\,[Ca^{2+}]$ with α representing the mean sulfate to calcium ratio in saharan dust inputs reaching the Alps. *Wagenbach et al.* [1996] derived a α value of 0.59 from dust horizons of the pre-industrial era at CG. *Schwikowski et al.* [1999a] found a slightly lower value (0.42) in pre-industrial ice from another CG ice core. Finally, a α value of 0.47 is observed in dust events located in the bottom part (from 90.3 to 95.3 m w.e.) of the CDD core [*Preunkert et al.*, 2001]. Using the highest α value of 0.59, we found that on average the effect of saharan dust on sulfate levels remains moderate, except in summer layers deposited at the end of the 80s where a mean enhancement of 100 ng g^{-1} is seen (i.e., amounting to 17 % approximately) (Figure 3).

3.3. The Pre-Industrial Sulfate Level at CDD

Anthropogenic sulfate fraction is evaluated by subtracting the natural background sulfate level from the total sulfate concentrations. The well-dated part of the CDD core extends back to 1925 only. To evaluate the pre-industrial level, we report in Table 1 the mean major ion chemistry of summer and winter CDD layers located between 90.3 and 95.3 m (w.e.) depth for which the dating remains uncertain. The counting of annual layers based on the ammonium record suggests that this part of the core spans the 1906-1922 time period [*Preunkert et al.*, 2000]. On the other hand, using the mean annual layer thickness of 0.2 m w.e. derived by *Preunkert et al.* [2000] at the depth of 90 m w.e., these five meters (w.e.) of ice would cover some 25 years.

The mean summer CDD sulfate level was close to 160 ng g^{-1} in 1925 (Figure 3) instead of 70 ng g^{-1} in the bottom part of the core (Table 1). A similar decrease is also observed for ammonium whose the mean summer level (not shown) is close to 60 ng g^{-1} in 1925 instead of 36 ng g^{-1} in the bottom part of the core (Table 1). The summer levels of sulfate, ammonium and nitrate are very similar to the ones observed in summer layers in CG ice cores over the 1980-1990 decade [*Preunkert et al.*, 2000] as well as over the last 80 years [*Wagenbach et al.*, unpublished data]. Comparison of the mean chemistry of summer layers at CDD (Table 1) with concentrations of the monotonic increasing ammonium, and sulfate trends from 1880 to 1980 gained from a deep CG ice core dominated by summer snow [*Jung,* 1993; *Wagenbach et al.*, 1988] suggests that the CDD ice located between 90.3 and 95.3 m w.e. would correspond

to about 1890 ± 10 years. The study of this CG core suggested a pre-industrial sulfate level of 89 ng g^{-1}, a value which remains consistent with the mean 70 ng g^{-1} seen in the bottom part of the CDD core (Table 1). In the following we have therefore assumed a typical pre-industrial summer sulfate level of 80 ± 10 ng g^{-1} for CDD layers. The winter pre-industrial sulfate level can only be deduced by examining the bottom part of the CDD ice core which indicate (Table 1) a natural winter level of 20 ng g^{-1}.

4. CDD Sulfate Trends Versus SO_2 Emissions and Comparison With Greenland

With the aim to investigate the source region apportionment for anthropogenic sulfate present over the Alps (and Greenland) we compare long term changes of anthropogenic sulfate levels with past SO_2 anthropogenic emissions from various regions. Depending on source regions, SO_2 emissions vary throughout the year, rather constant over the eastern part of United States they are significantly higher in winter than in summer in Europe. In the following, we have neglected these seasonal changes of emissions. The comparison between long term sulfate trends and SO_2 emissions was done by focusing on both the amplitude and the time phase of changes.

4.1. CDD Summer Trend

The sulfate summer CCD trend is characterized by an increase from 160 ng g^{-1} in 1925 to 375 ng g^{-1} in 1960 (i.e., a mean increasing rate of 6 ng g^{-1} per year), with a slight, transient decrease during the second World War (Figure 4). The level is then enhanced at a stronger rate of 24 ng g^{-1} per year between 1960 and 1980, leading to a 1980 maximum of the anthropogenic sulfate input at that site. Afterwards, the sulfate decreased significantly, probably as a result of improvement in the quality of fuel and emission abatements [*Mylona*, 1993].

With the aim to investigate the source region apportionment for anthropogenic sulfate present at high Alpine site in summer we compare long term changes of anthropogenic sulfate summer CDD levels (assuming a pre-industrial value of 80 ± 10 ng g^{-1}) with past SO_2 anthropogenic emissions in western Europe. We first consider the following nine countries of western Europe (hereafter denoted WE9): Belgium, France, West Germany, Switzerland, Italy, Netherlands, Spain, Portugal, and United Kingdom. Alternatively we also selected the six countries: France, West Germany, Belgium, Spain, Italy, and Switzerland located within 700-1000 km around the Alps (hereafter denoted WE6). From 1925 to 1960, the anthropogenic sulfate level was enhanced at CDD from 80 to 300 ng g^{-1}. Over this time period, *Mylona* [1996] estimated that SO_2 emissions were enhanced from 9 to 14 Mt, and from 5 to 8 Mt when considering WE9 and WE6, respectively. The increase of SO_2 emissions

from WE9 were then enhanced from 14 to 20 Mt of SO_2 between 1960 and 1980 (i.e. a similar increase than the 1925-1960 one). Conversely, a further increase from 8 to 14 Mt is calculated by *Mylona* [1996] (i.e. twice the 1925-1960 increase) for WE6, which is in better agreement with the enhancement of sulfate seen in CDD ice from 1960 to 1980 (Figure 4). Note that the weaker change of SO_2 emissions from WE 9 between 1925 and 1980 with respect to WE6 one is mainly due to the fact that emissions from United Kingdom, a main contributor of WE9, were already very large in 1925 (4 Mt of SO_2) and were enhanced by 50% in the 80s only [*Mylona,* 1993]. Although the strong sulfate increase after 1960 is in good agreement with changes of SO_2 emissions from WE6, we note that emissions remained rather constant between 1970 and 1980, in contrast to the sulfate which peaked in 1980 (Figure 4). Since the course of growing SO_2 emissions was different in the six WE6 countries, we scrutinized in Figure 5 which of them show the best fit with the sulfate record, focusing on the 1960-1980 time period. This examination shows that emissions in the northern WE6 part (Belgium and a part of West Germany) systematically reached their maximum values in 1960-1970 in contrast to emissions from the southern part of WE6 which peaked later (from 1970 to 1990 in Italy and Spain, respectively) [*Mylona*, 1993]. Figure 5 indicates a better agreement (amplitude and time phase) between the sulfate trend and SO_2 emission changes when Belgium and a part (or total) of West Germany are not considered.

Whatever are the considered countries, Figure 4 indicates a difference of some 5 millions tons (Mt) of SO_2 between the estimates of *Lefohn et al.* [1999] and *Mylona* [1996] after 1960. That is caused by a larger estimation of liquid fuel contributions by *Mylona* [1996] compared to *Lefohn et al.* [1999], whereas both estimates are in good agreement for solid fuel (hard coal and brown coal) contribution. In spite of these differences in the two inventories, as seen in Table 2, the changes of anthropogenic sulfate summer levels are also in better agreement with estimated SO_2 emission changes from *Lefohn et al.* [1999] when WE6 instead of WE9 is considered, and when Belgium and West Germany are not considered.

This discussion suggests that countries having an impact on the high-elevated Alpine sites in summer include regions located within 700-1000 km from the Alps with a major influence of emissions from France, Spain, and Italy. The fact that SO_2 emissions from northern countries (such UK, Belgium, and partly West Germany) have there a weaker impact than those from southern countries is likely due to a dominant transport of air masses from south-west rather than from north or north-west towards the Alps in summer (I. Auer, personal communication).

4.2. Winter Trend

Sulfate in winter snow layers were gradually enhanced from 30 ng g^{-1} in 1925 to 98 ng g^{-1} in 1980 (Figure 6). Assuming a pre-industrial background ranging between 15 and 25 ng g^{-1} (Table 1), the here calculated anthropogenic sulfate winter fraction enhanced from 6 to 47 ng g^{-1} over 1925-1960 and up to 73 ng g^{-1} in 1980. Such a regular trend of 1.2 ng g^{-1} per year over the whole 1925-1980 time period, clearly differs from the summer increase rate which was four times larger after 1960 than before. In order to determine possible source regions influencing the winter sulfate record at the CDD site, we compare in Figure 6 the anthropogenic sulfate trend with estimates of past SO_2 emissions by *Lefohn et al.* [1999] and *Mylona* [1996] from the nine countries of western Europe (WE9) as well as from total western plus eastern Europe (denoted WEE). For WEE, following *Mylona* [1996], we considered WE9 plus Austria, Bulgaria, Czech Republic, Denmark, Finland, former East Germany, Greece, Hungary, Ireland, Norway, Poland, Romania, Sweden, Turkey, and the western part of former USSR. SO_2 emissions from WE9 are close to 9 Mt in 1925 and remained quasi-constant until 1950 (~10 Mt). They were then enhanced to 19 Mt in 1965 and remained quasi-constant until 1980 [*Mylona*, 1996]. As seen in Figure 6, this course of SO_2 emissions from WE9 since 1925 contrasts with the trend of winter sulfate levels at CDD characterized by a regular increase from 1925 to 1980. A better agreement between the winter sulfate CDD trend and SO_2 emissions is found when total Europe (WEE) whose emissions were enhanced from 12 to 38 Mt between 1925 and 1960 and from 38 to 54 Mt from 1960 to 1980 is considered. The agreement remains good when we add emissions from United States divided by a factor of four (amounting for ~10% of European emissions) but becomes poorer if an enhanced fraction of these transatlantic emissions is considered (not shown). Such a limited contribution of North America emissions to the sulfate deposition over Europe has already been pointed out by *Barrett et al.* [1995].

4.3. Comparison Between Greenland and Alpine Ice core Records

Previous Greenland ice records (see *Legrand and Mayewski* [1997] for a review) have shown an increase of annual sulfate levels by a factor of 2 to 4 since the pre-industrial era. This increase factor is similar to the one revealed by winter Alpine snow layers but remains far less important than what is seen in Alpine summer snow layers. This difference suggests a stronger impact of anthropogenic emissions relative to natural sources in summer in the Alps compared to the situation in Greenland. With the objective to examine in more detail the effect of the natural background on the evaluation of the anthropogenic trend as well as the seasonal anthropogenic source region apportionment for sulfate in Greenland, we here have examined a high-resolution chemical record (470 samples) extracted from a Summit (central Greenland) ice core covering the 1870-1992 time period [*Legrand and De Angelis*, 1996]. Trends of MSA and sulfate have been discussed by *Legrand et al.* [1997] but only based on annual means. We here performed a seasonal dissection along this Summit ice core. Based on

the examination of the seasonal variations of sodium, ammonium and calcium contents and following previous works [*Whitlow et al.*, 1992; *Legrand and Mayewski*, 1997; *Fischer et al.*, 1998], we assigned three seasons: spring characterized by calcium maximum, summer by sodium and calcium minima, and winter by sodium maximum and ammonium minimum.

4.3.1. Natural Sources Influencing the Greenland Sulfate Budget

Numerous short-term (~one year) peaks have disturbed the baseline sulfate level of the Summit ice core (Figure 7). These events can be easily identified as likely of volcanic origin between 1870 and 1945, a period over which the anthropogenic sulfate input remained still limited. In previous Greenland ice core studies, only the major event has been considered and clearly attributed to the 1912 Katmai eruption. In Figure 7, we associate historical volcanic events with volcanic explosivity index (VEI) [*Newhall and Self,* 1982] higher than 4 with Summit layers exhibiting a sudden sulfate increase. The nineteenth century ended with three years marked by major volcanic events between 1872/73 and 1883 followed by a quiet period of almost 20 years. Given the dating uncertainty in this part of the Summit ice core (± 2 years, *Legrand and De Angelis* [1996]), the three peaks seen between 1873 and 1886 in the Summit profile (Figure 7) can be attributed to the three above mentioned eruptions. The first decade of the twentieth century was again characterized by several important eruptions events (from 1904 to 1908). The 1910-1926 time period was marked by three volcanic events (among them the Katmai one in 1912) and then again the volcanic activity remained weak during almost 20 years. Such a flickering from quiet periods to periods marked by several successive major events is clearly seen in the Summit sulfate record (Figure 7). In order to evaluate the impact of these volcanic inputs on the anthropogenic sulfate profile at Summit, we compare in Figure 8 the spring trends obtained when discarding either only the major volcanic 1912 Katmai event or all layers suspected to reflect volcanic inputs. When only the 1912/1913 event is discarded, the first increase at the turn of the 20^{th} century represents 40% of the increase seen between 1880 and 1970. Conversely, when discarding all volcanic layers the first increase at the turn of the 20^{th} century is still detected but represents a quarter of the increase between 1880 and 1970 only. Such a difference is of importance when examining the major anthropogenic source regions influencing the Greenland ice sheet since, already at the turn of the 20^{th} century SO_2 anthropogenic emissions from US were strongly enhanced whereas those from Europe remained still limited. In the following, all snow layers suspected to have been impacted by volcanic inputs (denoted with stars in Figure 7) were discarded therefore.

As seen in Table 3, the natural background sulfate level at Summit is close to 30 ng g^{-1} in good agreement with those obtained by *Fischer et al.* [1998] in northern (30 ng g^{-1}) and southern (50 ng g^{-1}) regions of the Greenland ice sheet. The natural sulfate fraction at Summit still represented a quarter (in winter and spring) to a third (in summer) of the total sulfate

deposited during the anthropogenic input maximum (1960-1980) (Table 3). As discussed by *Legrand et al.* [1997], two major natural sources contribute to the natural sulfate budget in Greenland, namely the passive quasi-permanent volcanic emissions from the high northern latitude belt and the marine biogenic emissions. Both sources may have changed over the 20th century. For example, *Legrand et al.* [1997] reported a decrease of MSA by a factor of 2 over the 20th century possibly as a result of a decrease in the marine sulfur biota emissions. We can therefore expect also a change of the natural biogenic sulfate source over the 20th century. We conclude that the significant contribution of natural sulfate sources in Greenland renders more inaccurate the examination of past sulfate trends versus anthropogenic SO_2 emissions compared with the situation in the Alps. Here natural sulfur sources contribute only in the range of 10% in summer and 20% in winter to the total budget between 1970 and 1990.

4.3.2. Anthropogenic Source Apportionment in Greenland

As seen in Table 3, the anthropogenic sulfate input in Greenland is maximum in spring and winter. Assuming a pre-industrial value of 38 ng g^{-1} (i.e., the mean value seen between 1870 and 1895), the anthropogenic sulfate fraction in spring is found insignificant (6 ng g^{-1}) until the end of 19th century and was then rapidly enhanced at the beginning of the 20th century (36 ng g^{-1} in 1915) (Figure 8). A second well-marked increase occurred between 1950 and 1970. North America SO_2 emissions were enhanced from 6 to 20 Mt between 1895 and 1915 whereas European plus Asian emissions remaining below 4 Mt until 1895. The first sulfate increase seen at the turn of the 19th century therefore suggests a contribution of North America to the sulfate Greenland level in spring. On the other hand, the large increase of sulfate levels in spring snow deposited after the second World War is not caused by North America SO_2 emissions which remained quite stable (around 20 Mt) at that time with respect to the 1940 ones. That suggests that European and Asian sources whose SO_2 emissions have been mainly enhanced between 1950 (15 Mt) and 1980 (50 Mt) are also contributing to the sulfate budget of Greenland ice in spring. As seen in Figure 8 the trend of Greenland sulfate in spring follows rather well the course of growing SO_2 emissions from Eurasia (eastern Europe, former USSR, Japan, and Korea) and North America. Such a wide geographical contribution of source regions is supported by analysis of a 44-year record of isobaric back trajectories at 500-hPa level made by *Kahl et al.* [1997] who suggested that air masses arriving at Summit in winter and spring correspond to a fast transport from various source regions including North America and extended upwind (westward) as far as Asia/Europe. Thus the enhancement of 100 ng g^{-1} of spring sulfate levels in Summit ice, which largely governed annual changes, reflects long-range transported pollutants from various regions including North America and Europe/Asia. A similar conclusion is drawn for winter trends not shown here.

These investigations of anthropogenic source region apportionment at Summit in spring, a season during which the anthropogenic input is maximum, are in agreement with the conclusion drawn for several other Greenland sites on an annual basis by *Fischer et al.* [1998]. In contrast to the CCD Alpine record, the anthropogenic trend recorded in Greenland ice cores mainly correspond to the SO_2 emissions from different continents (Eurasia and North America).

5. Atmospheric Implications of CDD Data

In this section we compare sulfate data gained at CDD with (1) current atmospheric model simulations, (2) data gained at sites located around the Alps at lower elevation. Aerosol measurements were carried out in 1999 at the Vallot Observatory (4361 m asl), located at the CDD drill site indicating a mean summer and winter level of 530 and 100 ng m^{-3} STP, respectively [*Preunkert et al.,* in press]. Comparing these atmospheric concentrations with the mean seasonal concentration in the snowpack, *Preunkert et al.* [in press] derived for the Vallot area volume based Firn/Air ratios (denoted FAR) of ~2.6 and 1.3 10^6 in winter and summer, respectively. Although covering only one year, these preliminary values are nevertheless very consistent with those derived for 1993/94 at Colle Gnifetti (4450 m asl) (1.8 and 1.5 10^6 in winter and summer, respectively, *Preunkert et al.* [in press]*, Preunkert and Wagenbach* [1998]). Using data gained at Sonnblick (3106 m asl) by *Kasper-Giebl et al.* [1999], *Preunkert et al.* [in press] calculated FAR values of 2.5 and 0.9 10^6 in winter and summer, respectively. Note however that, as discussed in *Preunkert et al.* [in press], these values derived from comparison between composition of fresh snow and air are not pure FAR values. Finally, *Schwikowski et al.* [1999b] calculated an annual FAR value of 0.2 by comparing composition of firn at 3880 m elevation (Fiescherhorn glacier) with air concentrations at Sonnblick located at 3450 m elevation. Due to the complexity of scavenging process and its changes with elevation and season, in the following we only used seasonal FAR values derived for CDD and CG sites to invert our CDD ice core data.

5.1. Comparison of Present-day 600 hPa Sulfate Levels With Simulations

Various recent global sulfur models have simulated the sulfate distribution over Europe. The simulations are available with 1980 and 1985 emissions only and due to the change of emissions between 1980 and 1999, the atmospheric sulfate level observed in 1999 at CDD is not immediately useful. We therefore reported in Figure 9 the mean annual sulfate concentrations observed at 4300 m asl over the Alps calculated as the mean arithmetic summer and winter atmospheric levels derived from corresponding CDD ice core concentrations and local FAR values (assuming that they have not changed over the past). That leads to annual atmospheric sulfate concentration of 340 ng m^{-3} (i.e., 580 ng m^{-3} STP or 136 pptv) and 265 ng m^{-3} (i.e., 440 ng m^{-3} STP or 106 pptv) for 1980 and 1985, respectively.

Note that similar levels are obtained when the FAR values derived at CG are applied (525 and 390 ng m^{-3} STP or 120 and 90 pptv for 1980 and 1985, respectively). The zonal mean annual mixing ratios simulated by models at 45°N and 600 hPa are generally ranging between 100 and 200 pptv (~170 pptv for 1980 [*Langner and Rodhe*, 1991], 100 pptv for 1985 [*Chin et al.,* 1996], and slightly more than 100 pptv for 1980 [*Feichter et al,* 1996]). Some other simulations suggested mixing ratio slightly higher than 250 pptv [*Pham et al.*, 1995] for 1980 or close to 200 pptv for 1985 [*Barth et al.*, 2000]. All these simulated mixing ratios are zonally averaged and, as predicted by models, we can expect higher values over regions located close to major emissions (North America and Europe) by some 50%. Thus, as a mean, it appears that simulated mixing ratios at this elevation over Europe exceed observations made at the CDD site by up to a factor of two. Note however that since GCMs don't resolve the Alpine topography, more accurate comparison between observation and simulation would require the use of mesoscale models.

5.2. Comparison with sulfate levels at lower elevation sites located around the Alps

In evaluating the sulfate radiative effect, the dominant sources of uncertainties result from the sulfate aerosol load and its vertical distribution for which estimates are available only from atmospheric chemistry models [*Boucher et al.*, 1998]. Data gained at the CDD site are here compared to those collected at somewhat lower Alpine elevation and at the pre-alpine surface level in winter and summer in the Alpine region. In Figure 10, we reported winter and summer concentrations observed in the early 90s at sites located around the Alps including Payerne (Swiss Plateau, 500 m asl) [*Filliger et al.*, 1994], Schauinsland (Black Forest, Germany, 1205 m asl), the Sonnblick Observatory (Austrian Alps, 3106 m asl) [*Kasper and Puxbaum*, 1998], the Jungfraujoch (Swiss Alps, 3450 m asl) [*Gehrig*, 1996] and the values derived for the Vallot Observatory at CDD (based on the CDD ice record and FAR values). The large enhancement of atmospheric sulfate levels at 4300 m asl in summer with respect to winter contrasts with the situation at the surface where almost no summer to winter change is observed (Figure 10). Such a quasi-absence of seasonal variations in surface sulfate levels has also observed over a large part of western and central Europe (see the compilation of data from EMEP in *Kasibhatla et al.* [1997]). It is thought to be due to a slower conversion of SO_2 into sulfate partly resulting from lower OH and H_2O_2 concentrations in winter, in spite of two times higher SO_2 emissions in January than in July [*Schaug et al.*, 1991]. The systematic enhancement of the summer to winter sulfate ratio seen above 1 km elevation (Figure 10) reflects the more efficient upward motion of air masses from the polluted boundary layer in summer with respect to winter. This picture suggests that the amount of sulfate present between the surface and 1250 m elevation is similar the amount above in winter whereas in summer 66 % of sulfate is present between 1250 and 4300 m elevation. This seasonal change in the vertical sulfate distribution is due to the stronger decrease of concentrations with

increasing elevation seen in winter than in summer which likely reflects the enhancement of the convective activity in summer. Note that this vertical sulfate distribution corresponds for the early 90s to an equivalent column sulfate between the ground and 4300 m asl of 7 and 11 mg SO_4 m^{-2} in winter and summer, respectively. These values and their seasonal changes are quite consistent with the total column sulfate simulated for the region located near the Alps: 9 and 15 mg SO_4 m^{-2} in 1985 winter and summer, respectively [*Kasibhatla et al.,* 1997], 5 and 17 mg SO_4 m^{-2} in 1980 for January and July, respectively [*Feichter et al.,* 1996].

6. Conclusions

From the study of sulfate concentrations in snow layers deposited since 1925 at the CDD site, long term summer and winter trends have been separately extracted for the first time in the Alps. That permitted to discuss in detail the anthropogenic source apportionment of sulfate at a high-elevated continental site. The comparison between the summer and winter trends of sulfate levels in CDD ice with SO_2 emissions from various source regions suggests that the pre-industrial summer level of 80 $\forall$ 10 ng g^{-1} has been enhanced by a factor of ten in relation with upward transport of air from the boundary layer of western Europe regions located within 700-1000 km around the Alps. In contrast, the pre-industrial winter level close to 20 ng g^{-1} was only enhanced by a factor of four due to a diffuse contamination of the free troposphere taking place at a large scale (total Europe with a possibly weakened contribution from the United States). With respect to Greenland records which certainly contain valuable information to constrain the complex interplay between long-range transport and removal process acting between source regions and high northern latitudes, Alpine ice core records are more connected to Europe emissions and contain information that can be directly used in evaluating the climatic effect of changing sulfate atmospheric load over continental mid-latitude northern hemisphere regions. Due to difficulties to accurately identify the natural contribution (explosive volcanic activity, quasi-permanent passive volcanic emissions, marine biogenic emissions) which represents a significant contribution of the present day sulfate budget, the anthropogenic trend derived in Greenland is less accurate than the one extracted in the Alps where the anthropogenic source largely dominates the present day budget.

Since we found that Alpine sulfate records are essentially driven by past SO_2 emissions from the European continent for which anthropogenic emissions are quite well-known and natural sulfur emissions weakly influence the sulfur budget, it is here more powerful than in Greenland to compare past atmospheric changes with current global regional model simulations. The annual sulfate level of 90-106 pptv derived at 4300 m asl in 1985 suggests an overestimation of levels simulated by current GCM models at this elevation. More accurate comparison between observations and simulations will here require the use of mesoscale models. Atmospheric sulfate levels derived at the CDD ice core site together with

sulfate levels observed at lower elevation sites permit to highlight the vertical distribution and its seasonal variation between the ground and 4300 m elevation over western/central Europe in winter and summer, respectively. Since the vertical distribution is an important parameter for the radiative balance, such information are invaluable to estimate accurately the present and past radiative forcing over Europe.

Acknowledgements

This work has been supported by the European Environment and Climate program ALPCLIM. Funding was provided by the European Community via contract ENV4-CT97 (ALPCLIM) and ENV4-CT96-5051 (Environment and Climate Research Training), the Centre National de la Recherche Scientifique (programme PNCA), and the Ministery for Science and Research of Baden-Württemberg within the collaboration programme between Region Rhône-Alpes and Baden-Württemberg. We would like to thank the two anonymous reviewers for their valuable comments.

References

Baltensperger, U., H.W. Gaeggeler, D.T. Jost, M. Lugauer, M. Schwikowski, E. Weingartner, and P. Seibert, Aerosol climatology at the high-alpine site Jungfrauchjoch, Switzerland, *J. Geophys. Res.*, *102*, 19,707-19,715, 1997.

Barrett, K., O. Seland, A. Foss, S. Mylona, H. Sandnes, H. Styve, and L. Tarrasen, European transboundary acidifying air pollution, EMEP/MSC-W Rep. 1/95, Meteorol. Syn. Cent.-West, Norw. Meteorol. Inst., Oslo, 1995.

Barth, M.C., P.J. Rasch, J.T. Kiehl, C.M. Benkovitz, and S.E. Schwartz, Sulfur chemistry in the national center for atmospheric research community climate model: Description, evaluation, features, and sensitivity to aqueous chemistry, *J. Geophys. Res.*, *105*, 1387-1415, 2000.

Bloomfield, P., W.L. Steiger, In *Last absolute deviations: Theory, Applications and Algoritms*, Birkhauser, Boston, 1983.

Boucher, O., and 29 others, Intercomparaison of models representing direct shortwave radiative forcing by sulfate aerosols, *J. Geophys. Res.*, *103*, 16,979-16,998, 1998.

Charlson, R., J. Langner, H. Rodhe, C.B. Leroy, and S.G. Warren, Perturbation of the northern hemisphere radiative balance by back-scattering from anthropogenic aerosols, *Tellus*, *43*, 152-163, 1991.

Chin, M., D.J. Jacob, G. Gardner, M.S. Foreman-Fowler, and P.A. Spiro, A global three-dimensional model of tropospheric sulfate, *J. Geophys. Res.*, *101*, 18,667-18,690, 1996.

Feichter, J., E. Kjellström, H. Rodhe, F. Dentener, J. Lelieveld, and G-J. Roelofs, Simulation of the tropospheric sulfur cycle in a global model, *Atmos. Environ.*, *30*, 1693-1707, 1996.

Filiger, P., B. Buchmann, and B. Schwarzenbach, Air pollution measurements at the high Alpine station Jungfraujoch (3580 m a.s.l.), Switzerland, 1973-1993., In *The Proceedings of EUROTRAC Symposium >94*, edited by P.M. Borrell et al., pp. 259-262, 1994.

Fischer, H., D. Wagenbach, and J. Kipfstuhl, Sulfate and nitrate firn concentrations on the Greenland ice sheet 1. Large-scale geographical deposition changes, *J. Geophys. Res.*, *103*, 21927-21934, 1998.

Gehrig, R., Swiss EMPA data, annual reports, Eur. Monit. And Eval. Programme, Chemical Coord. Cent., Norw. Inst. For Air Res., Kjeller, 1996.

Jung, W., Hundertjährige Zeitreihen der Aerosoldeposition auf einem hochalpinen Gletscher, MS thesis, Institut für Umweltphysik der Universität Heidelberg, 71pp., 1993.

Kahl, J.D., D.A. Martinez, H. Kuhns, C.I. Davidson, J.L. Jaffrezo, and J.M. Harris, Air mass trajectories to Summit: A 44-year climatology and some episodic events, *J. Geophys. Res.*, *102*, 26,861-26,875, 1997.

Kasibhatla, P., W.L. Chameides, and J. St. John, A three-dimensional global model investigation of seasonal variations in the atmospheric burden of anthropogenic sulfate aerosols, *J. Geophys. Res.*, *102*, 3737-3759, 1997.

Kasper, A., and H. Puxbaum, Seasonal variation of SO_2, HNO_3, NH_3 and selected aerosol components at Sonnblick (3106 m a.s.l.), *Atmos. Environ.*, *32*, 3925-3939, 1998.

Kasper-Giebl, A., M. F. Kalina, and H. Puxbaum, Scavenging ratios for sulfate, ammonium and nitrate at Mt. Sonnblick (3106 m a.s.l.), *Atmos. Environ.*, *33*, 895-906, 1999.

Langner, J., and H. Rodhe, A global three-dimensional model of the tropospheric sulfur cycle, *J. Atmos. Chem.*, *13*, 225-263, 1991.

Lefohn A.S., J.D. Husar, and R.B. Husar R.B., Estimating Historical Anthropogenic Global Sulfur Emission Patterns for the Period 1850-1990, *Atmos. Environ.*, *33*, 3435-3444, 1999.

Legrand, M., M. De Angelis, and F. Maupetit, Field investigation of major and minor ions along Summit (central Greenland) ice cores by ion chromatography, *J. Chromatogr.*, *640*, 251-258, 1993.

Legrand, M., and De Angelis, M., Light carboxylic acids in Greenland ice: A record of past forest fires and vegetation emissions from the boreal zone, *J. Geophys. Res*., *101*, 4129-4145, 1996.

Legrand, M., and P. Mayewski, Glaciochemistry of polar ice cores: A review, *Rev. of Geophys.*, *35*, 219-243, 1997.

Legrand, M., C. Hammer, M. De Angelis, J. Savarino, R. Delmas, H. Clausen, and S.J. Johnsen, Sulfur-containing species (methanesulfonate and SO_4) over the last climatic cycle in the Greenland Ice Core Project (central Greenland) ice core, *J. Geophys. Res.*, *102*, 26,663-26,679, 1997.

Mayewski, P., and 7 others, Sulphate and nitrate concentrations from the south Greenland ice core, *Science*, *232*, 975-977, 1986.

Mylona, S., Trends of sulfur dioxide emissions, air concentrations, and deposition of sulfur in Europe since 1880, EMEP/MSC-W Rep. 2/93, Meteorol. Syn. Cent.-West, Norw. Meteorol. Inst., Oslo, 1993.

Mylona, S., Sulphur dioxide emissions in Europe 1880-1991 and their effect on sulphur concentrations and deposition, *Tellus*, *48*, 662-689, 1996.

Neftel, A., J. Beer, H. Oeschger, H. Zurcher, and F. Finkel, Sulphate and nitrate concentrations in snow from south Greenland, 1895-1978, *Nature*, *314*, 611-613, 1985.

Newhall, C.G., and S. Self, The volcanic explosivity index (VEI): An estimate of explosive magnitude for historical volcanism, *J. Geophys. Res.*, *87*, 1231-1238, 1982.

M. Pham, J.F. Müller, G.P. Brasseur, C. Granier, and G. Mégie, A three-dimensional study of the tropospheric sulfur cycle, *J. Geophys. Res.*, *100*, 26,061-26,092, 1995.

Preunkert, S., and D. Wagenbach, An automatic recorder for air/firn transfer studies of chemical aerosol species at remote glacier sites, *Atmos. Environ.*, *32*, 4021-4030, 1998.

Preunkert, S., D. Wagenbach, M. Legrand, and C. Vincent, Col du Dôme (Mt Blanc Massif, French Alps) suitability for ice core studies in relation with past atmospheric chemistry over Europe, *Tellus*, *52*, 993-1012, 2000.

Preunkert, S., M. Legrand, and D. Wagenbach, Causes of enhanced fluoride levels in Alpine ice cores over the last 75 years: Implications for the atmosphere fluoride budget, *J. Geophys. Res.*, *106*, 12,619-12,632, 2001.

Preunkert, S., D. Wagenbach, and M. Legrand, Improvement and characterization of an automatic aerosol sampler for remote (glacier sites), *Atmos. Environ.*, in press.

Schaug, J., U. Pedersen, J.E. Skjelmoen, and I. Kvalvaagnes, Data report 1991. Part 2: Seasonal summaries. EMEP/CCC-Report 4/93. Norwegian Institute for Air Research, Lillestrom, Norway.

Schwikowski, M., A. Döscher, H..W. Gäggeler, and U. Schotterer, Anthropogenic versus natural sources of atmospheric sulphate from an alpine ice core, *Tellus*, *51*, 938-951, 1999a.

Schwikowski, M., A. Döscher, H..W. Gäggeler, and U. Schotterer, A high-resolution air chemistry record from an Alpine ice core: Fiescherhorn glacier, Swiss Alps, *J. Geophys. Res.*, *104*, 13,709-13,719, 1999b.

Simkin, T., and L. Siebert, In *Volcanoes of the world*, 349 pp., Geoscience Press, Tucson, Arizona, 1994.

Wagenbach, D., K.O. Münnich, U. Schotterer, and H. Oeschger, The anthropogenic impact on snow chemistry at Colle Gnifetti, Swiss Alps, *Ann. of Glaciol.*, *10*, 183-187, 1988.

Wagenbach, D., S. Preunkert, J. Schaefer, W. Jung, and L. Tomadin, Northward transport of saharan dust recorded in a deep Alpine ice core. In *The impact of African dust across the Mediterranean*, S. Guerzoni and R. Chester eds., Kluwer Academic Publishers, The Netherland, 291-300, 1996.

Wagenbach, D., and S. Preunkert, The history of European pollution recorded in Alpine ice cores, In *Proceedings of EUROTRAC Symposium=96*, P.M. Borell et al. eds., 273-281, Computational Mechanics Publications, Southampton, 1996.

Wagenbach, D., and 8 others, Retrospective and present state of anthropogenic aerosol deposition at a high Alpine glacier (Colle Gnifetti, 4450 m a.s.l.), In *Cloud multi-phase processes and high Alpine air and snow chemistry*, S. Fuzzi and D. Wagenbach eds., 223-233, Springer-Verlag, Berlin, 1997.

Whitlow, S., P. Mayewski, and J. Dibb, A comparison of major chemical species input timing and accumulation at South Pole and Summit, Greenland, *Atmos. Environ.*, *26*, 2045-2054, 1992.

Tables

Table 1: Chemical composition of summer and winter layers located on the bottom part of the 1994 CDD core (between 90.3 and 95.3 m w.e.) which were estimated to span the 1906-1922 time period (see section 2). All data have been blank corrected. Values refer to means after correction of samples (16 on a total of 111) suspected to contain saharan dust. For winter the median value is given with the 25^{th} and 75^{th} quantiles.

Species	Winter (in ng g^{-1})	Summer (in ng g^{-1})
NH_4^+	mean: 1.7 ± 2 median: 1.7 (0.2 - 3.0)	mean: 36 ± 17
SO_4^{2-}	mean: 20 ± 18 median: 20 (15 - 25)	mean: 70 ± 40

Table 2: Comparison of anthropogenic sulfate CDD summer changes and past SO_2 emissions from different regions in western Europe (WE9, WE6, and France, Italy, Spain, and Switzerland, see text) from Lefohn et al. [1999].

SO_2 emissions, Mt	1925	1960	1980
WE9	11.7	14.6	15.7
WE6	5.3	8.0	11.2
F + I +CH + E	2.3	3.2	5.8
Anthropogenic CDD sulfat levels, ng g^{-1}	80	300	780

Table 3: Sulfate levels observed in spring, summer, and winter in Summit (central Greenland) snow layers deposited during the preindustrial era and over the recent period (1960-1980)

Time periods	Spring (in ng g^{-1})	Summer (in ng g^{-1})	Winter (in ng g^{-1})
1873-1881	38 ± 10	21 ± 6	24 ± 9
1960-1980	146 ± 13	65 ± 6	99 ± 14

Figures

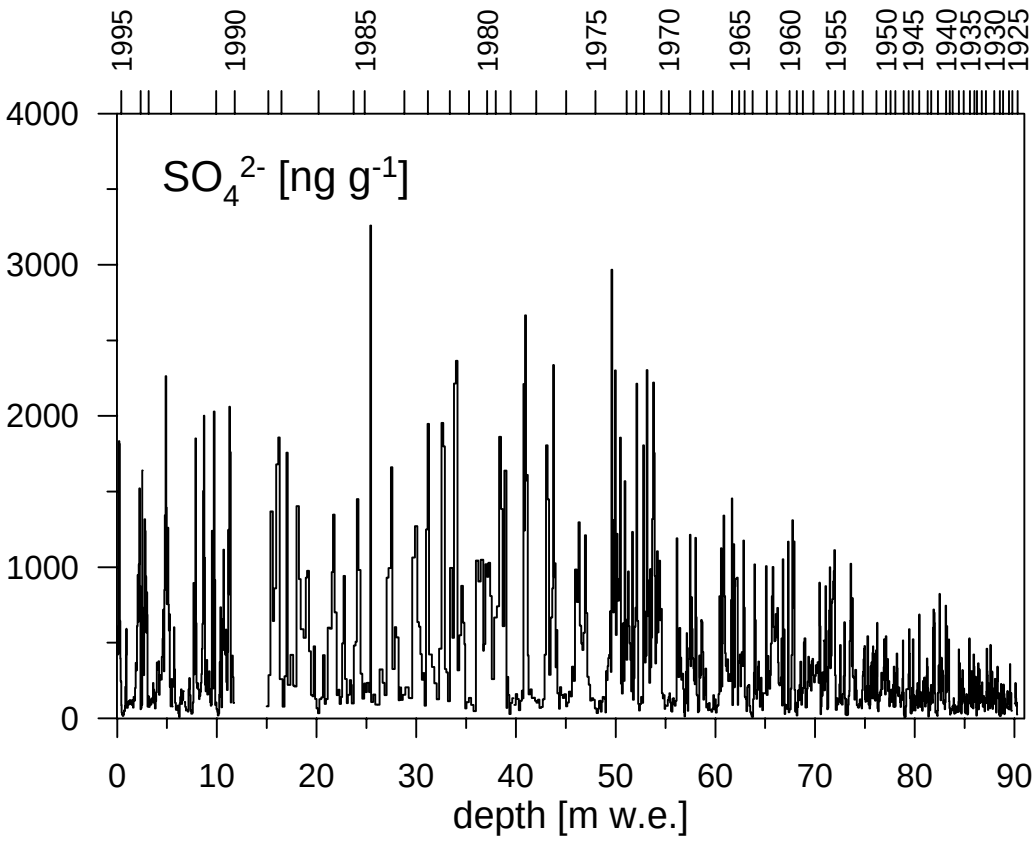

Figure 1: High-resolution depth profile (in meters water equivalent) of sulfate along the upper 90 m w.e. of the 1994 CDD core. The annual layer dating reported on the top is discussed in section 2.

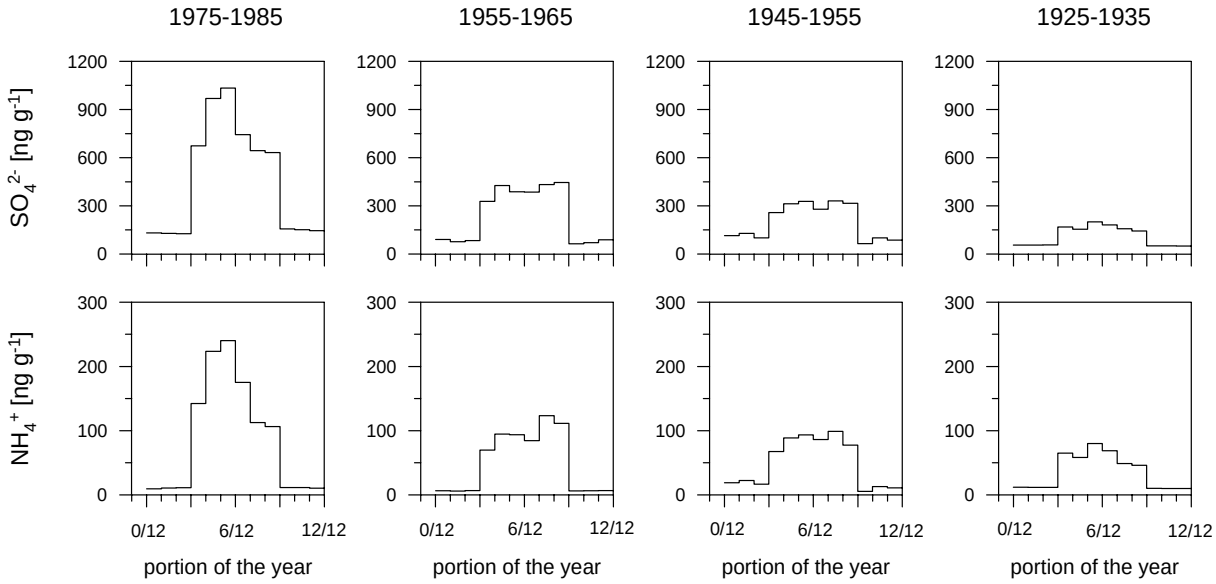

Figure 2: Seasonal cycle of sulfate in the 1994 CDD ice core averaged over four time periods: 1925-1935 (low anthropogenic sulfate input), 1945-1955, 1955-1965, and 1975-1985 (maximum of the anthropogenic sulfate input) (see text). Sulfate levels have been corrected from saharan dust inputs. Changes of ammonium used for the seasonal dissection are also shown.

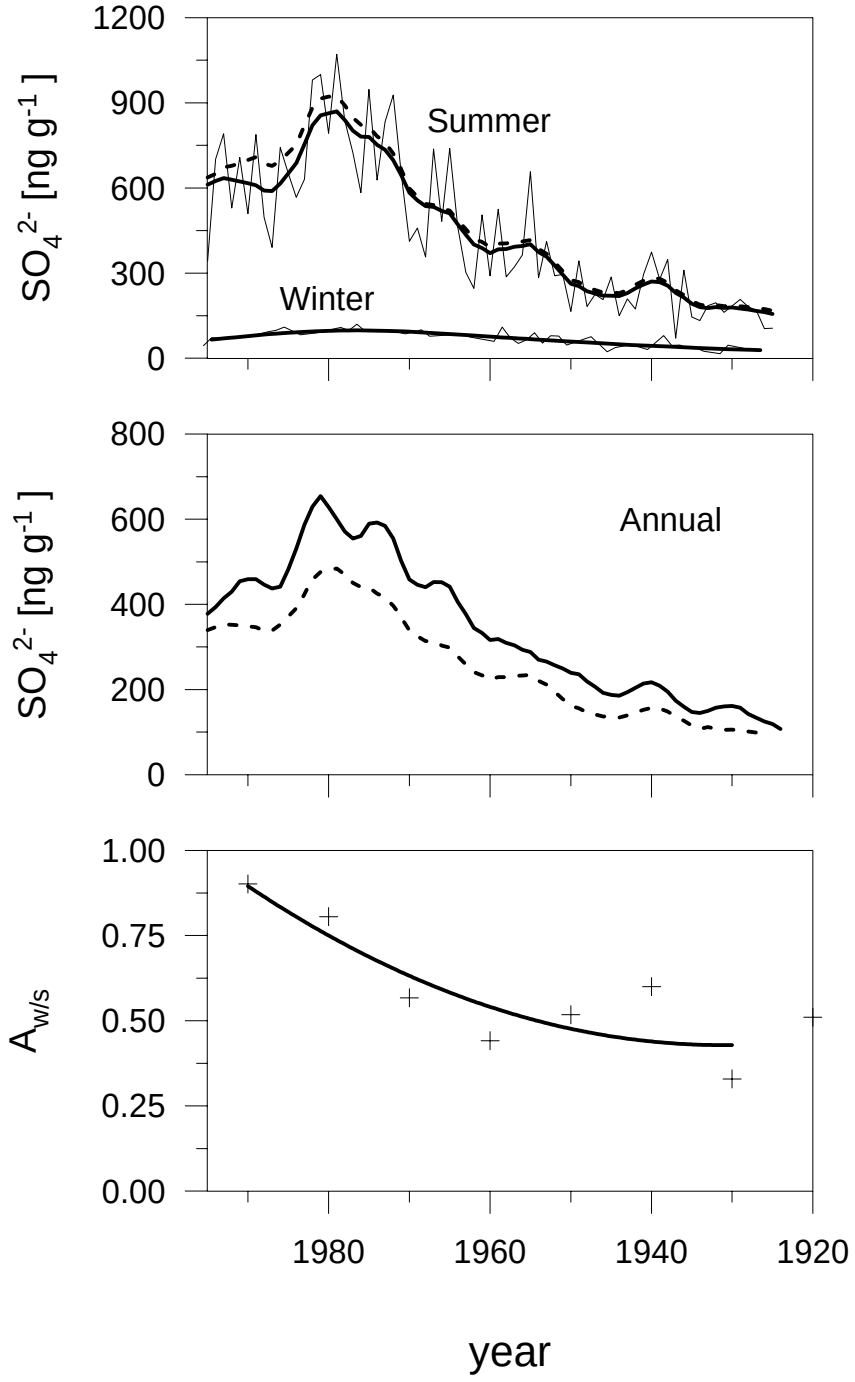

Figure 3: Sulfate CDD trend (summer, winter, and annual) since 1925. (Top) Summer and winter trends of sulfate levels in the 1994 CDD core. The thin lines refer to the individual summer and winter means. The solid thick lines are the smoothed profiles (first component of SSA with a 5-year time window for summer, and robust splines for winter) (see section 3.1). The dashed lines refer to summer and winter trends when no correction has been applied to samples suspected to contain saharan dust (see section 3.2). (Middle) Trends of annual mean sulfate concentrations calculated as arithmetic mean of winter and summer levels (dashed line) and as arithmetic mean of annual data (solid line) (see section 3.1). (Bottom) Winter to summer ratio of net snow accumulation ($A_{W/S}$) along the upper 90 m w.e. of the CDD core.

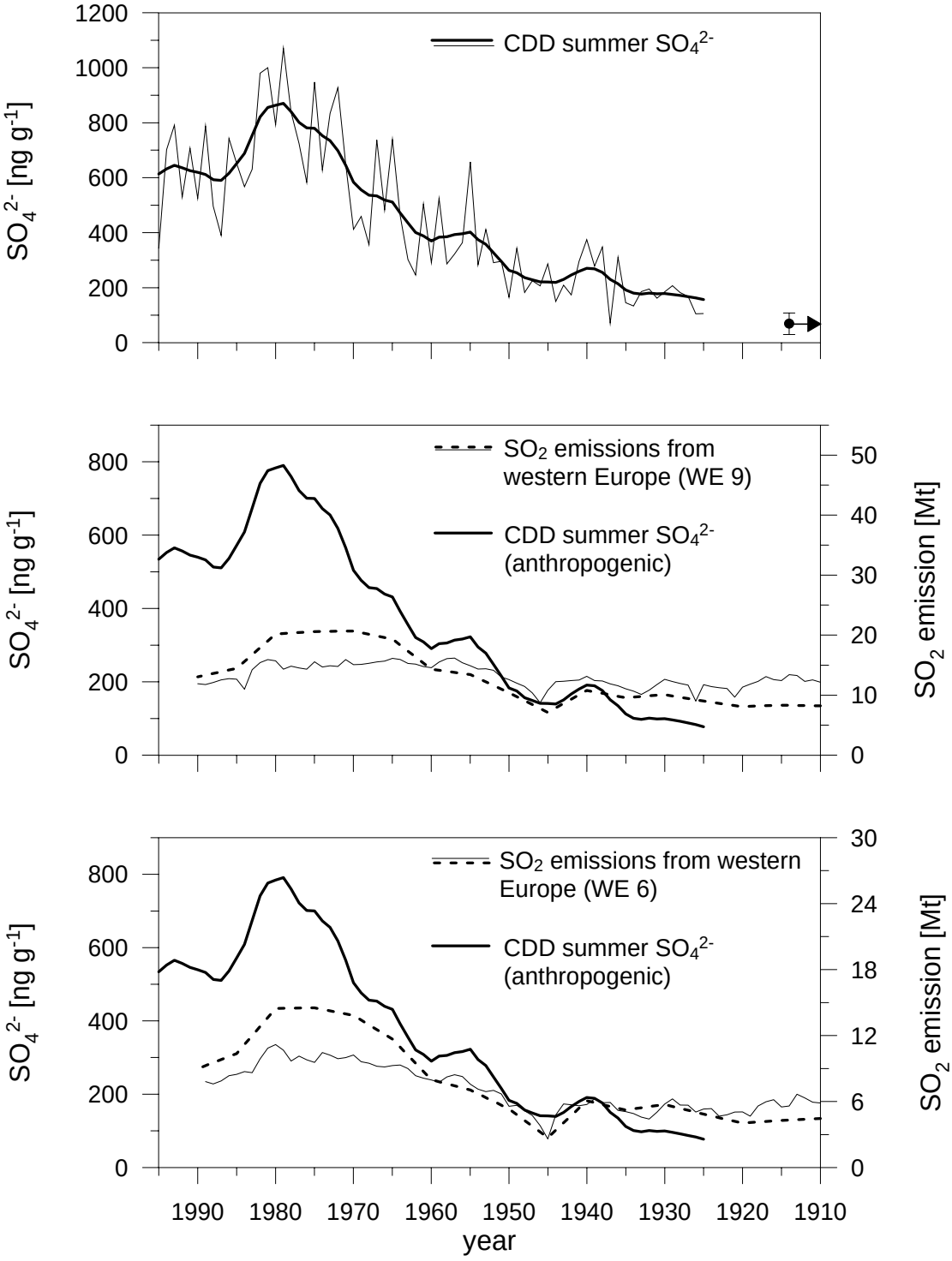

Figure 4: The summer CDD sulfate trend and past SO_2 emission inventories. (Top) Summer trend of sulfate levels in the 1994 CDD core. The solid line is the smoothed profile (first component of SSA with a 5-year time window), the thin line refers to individual summer means. The arrow on the right side refers to the mean pre-industrial level. (Middle and bottom) Comparison of the SSA summer anthropogenic sulfate trend (thick solid line) with SO_2 inventories from Lefohn et al. [1999] (thin solid lines) and Mylona [1996] (dashed lines) considering the WE9 countries of western Europe (see text) (middle) and countries located within 700 km around the Alps (WE6, see text) (bottom).

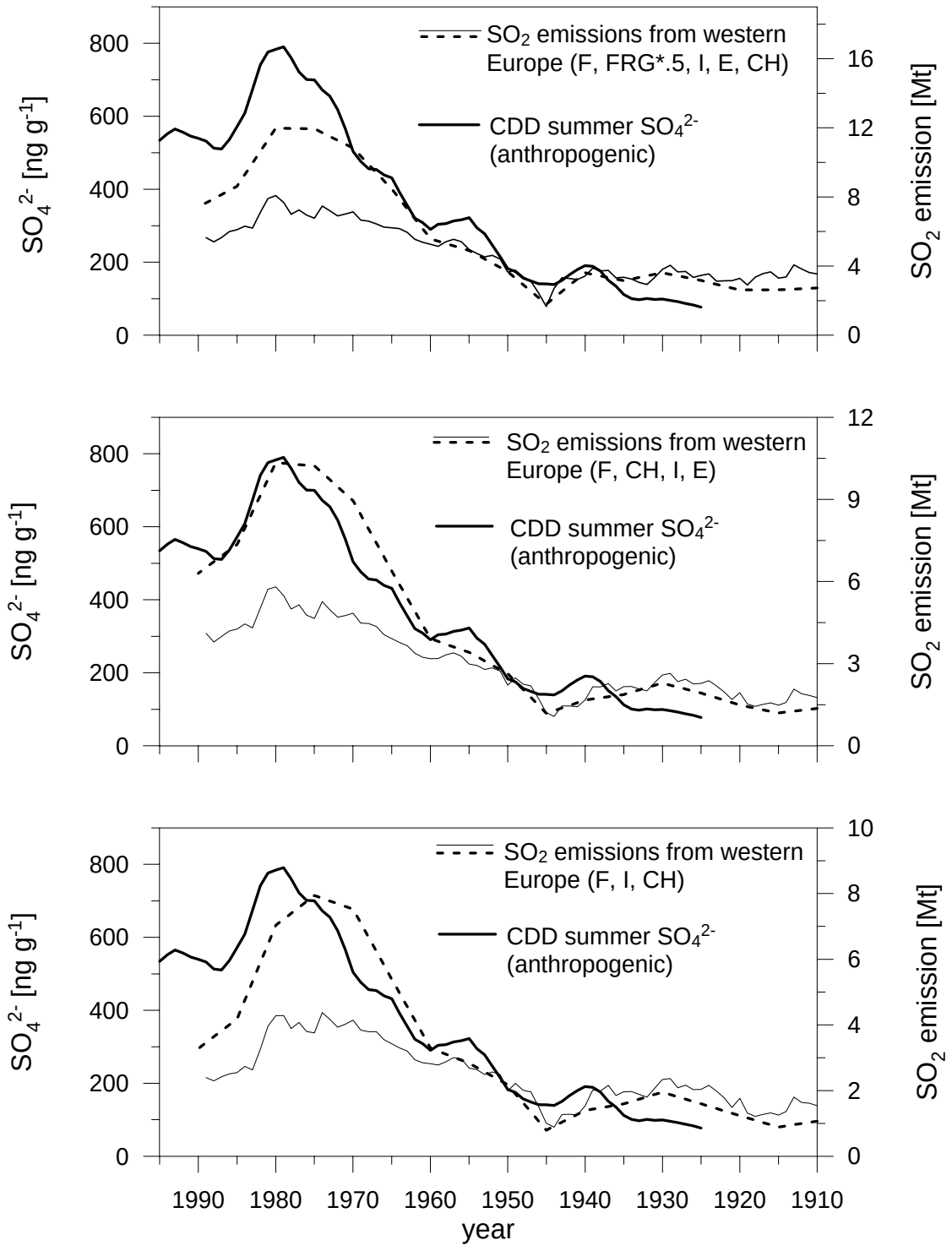

Figure 5: Same as Figure 4 (middle and bottom) but considering different countries located within 700 km around the Alps: (Top) France, Switzerland, Spain, Italy, and half of emissions from West Germany, (Middle) France, Switzerland, Spain, and Italy, (Bottom) France, Switzerland, and Italy.

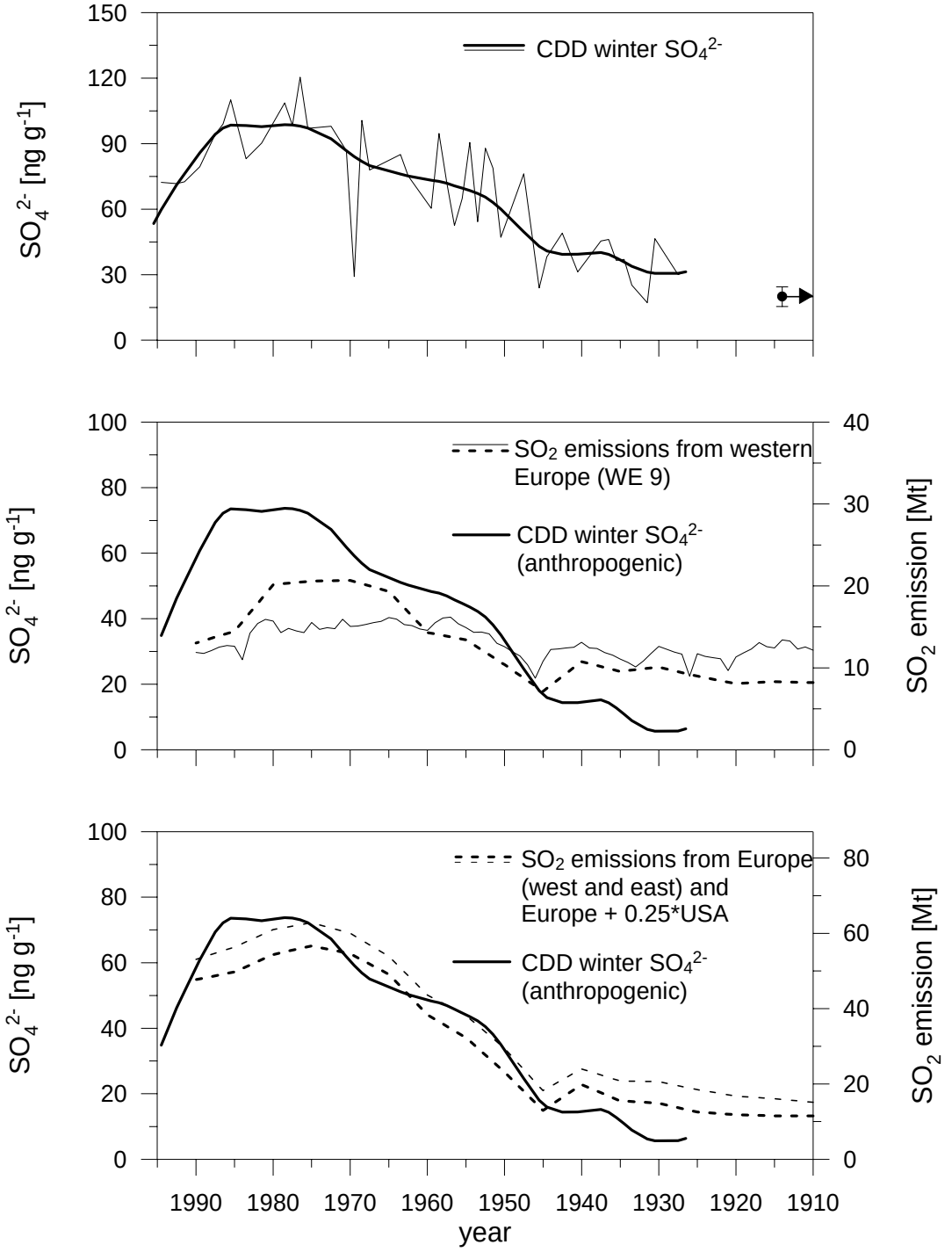

Figure 6: The winter CDD sulfate trend and past SO_2 emission inventories. (Top) Winter trend of sulfate levels in the 1994 CDD core. The thick solid line is the smoothed profile (robust spline). (Middle) Comparison of the sulfate robust spline with SO_2 inventories from Lefohn et al. [1999] (thin solid lines) and Mylona [1996] (dashed lines) considering the nine countries of western Europe (WE9). Sulfate data have been corrected from a pre-industrial winter level of 20 ng g^{-1} (see section 3.3). (Bottom) Same as middle but compared to SO_2 inventories from total Europe including Turkey and the western part of USSR as reported by Mylona [1996] (dashed thick line). The thin dashed line corresponds to SO_2 emissions from United States from total Europe plus 25% emissions from US from Lefohn et al. [1999].

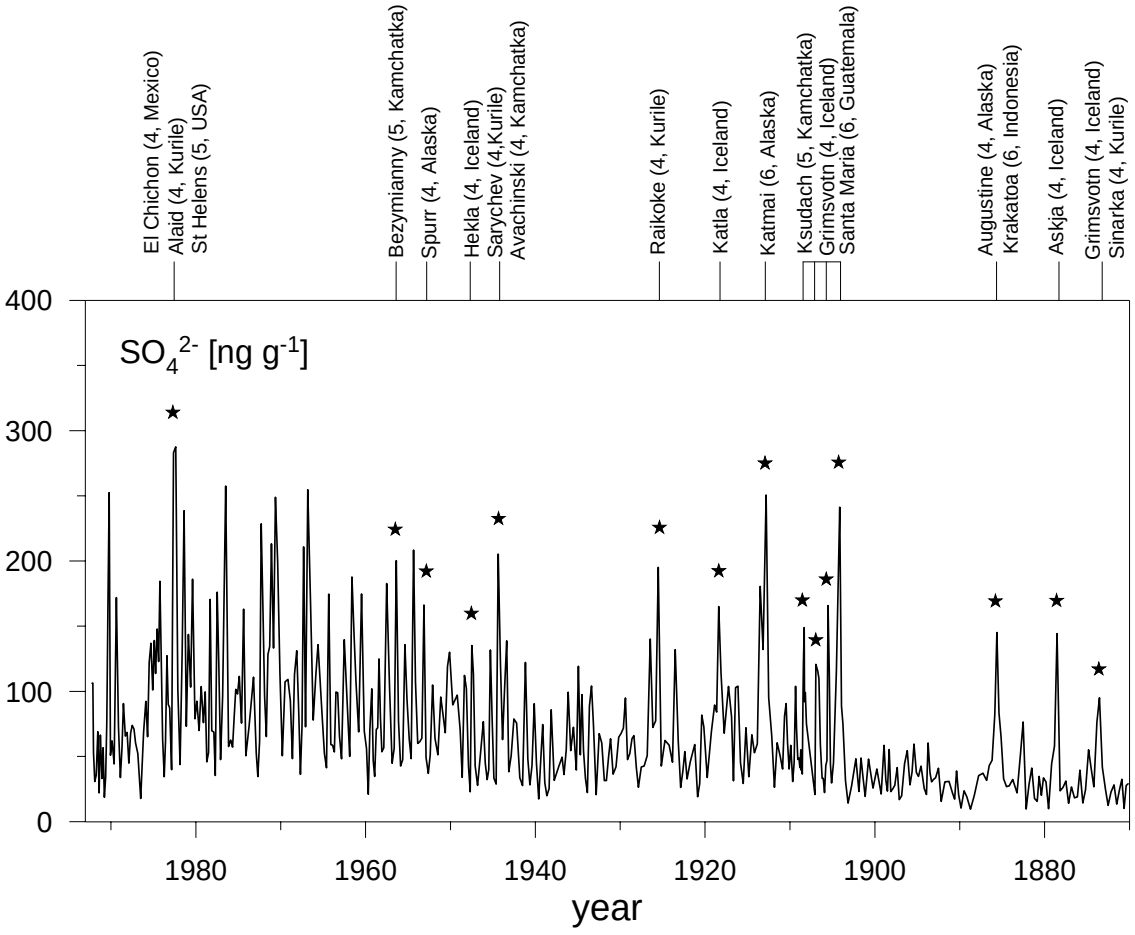

Figure 7: High-resolution profile of sulfate along a Summit (central Greenland) ice core spanning the 1870-1993 time period. The dating of this core reported on the bottom is from Legrand and De Angelis [1996]. Stars reported on the sulfate profile refer to layers which are suspected to be contaminated by volcanic input. All major volcanic events (VEI equal or higher than 4 [Simkin and Siebert, 1994]) having occurred since 1783 are reported on the top.

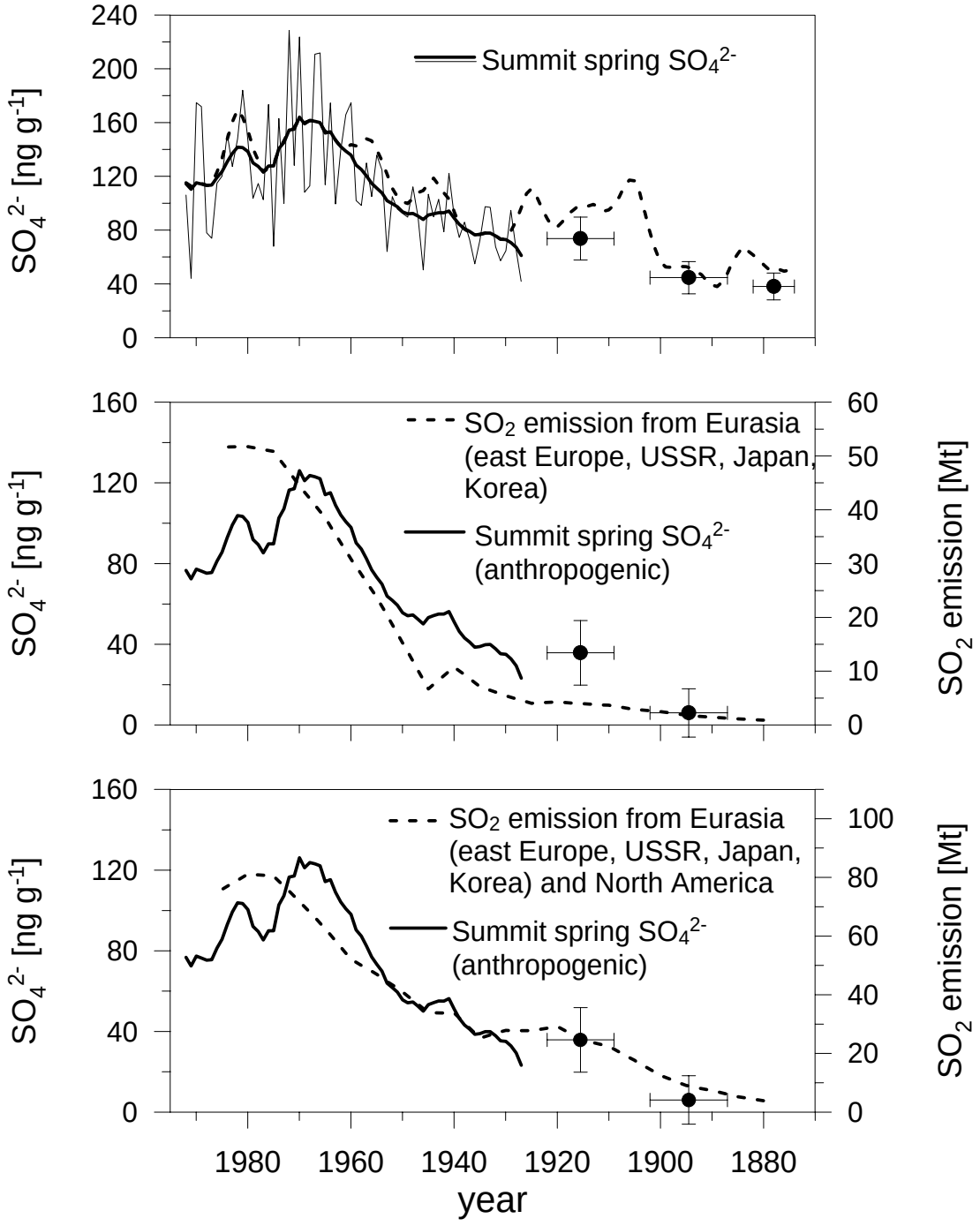

Figure 8: Summit (central Greenland) spring snow records over the 1870-1993 time period. (top) sulfate trend (first component of SSA with a time window of five years): the solid thick line corresponds to the smoothed profile when all layers suspected to be contaminated by volcanic events are discarded (see stars in Figure 7), the thin solid line to rough data, and the three filled dots to multiple-year means (1873-1881, 1886-1901, and 1908-1922) (horizontal bars are covered time periods, vertical bars refer to standard deviation). The dashed line refers to the trend obtained when only the 1912/1913 event (see text) has been discarded. (middle) comparison between anthropogenic sulfate trend (calculated assuming a 1880 natural level of 38 ng g^{-1}) and SO_2 emissions from eastern Europe, former USSR, Japan, and Korea. (Bottom): same as middle when SO_2 inventories also include those from North America.

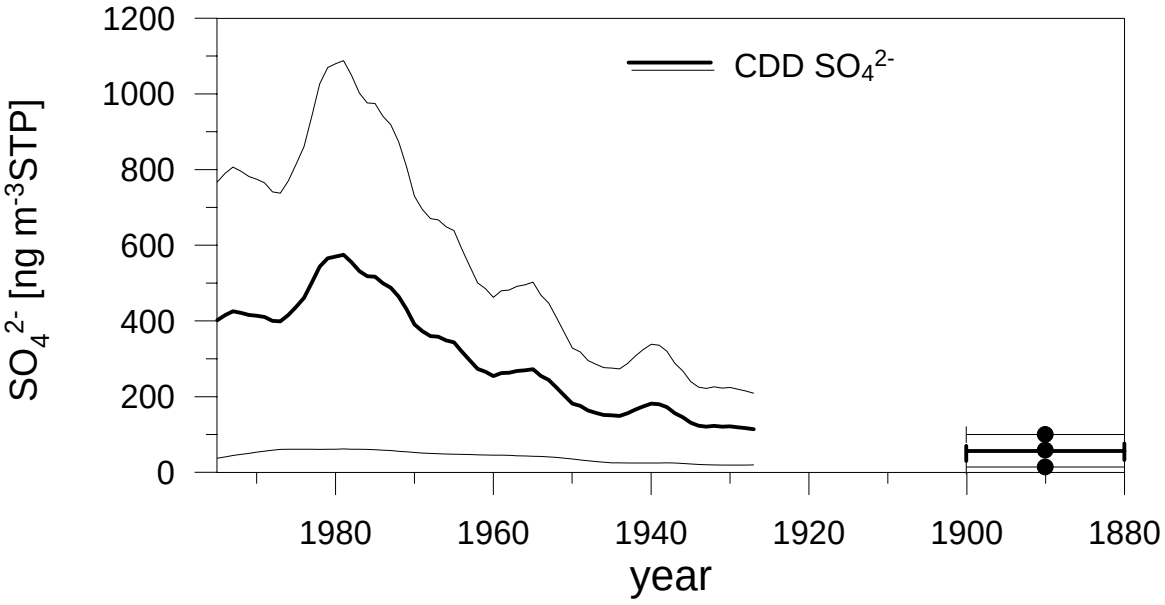

Figure 9: Long term atmospheric sulfate concentrations at the CDD site since 1925. The two thin lines refer to the summer and winter trends, the solid line to the annual mean.

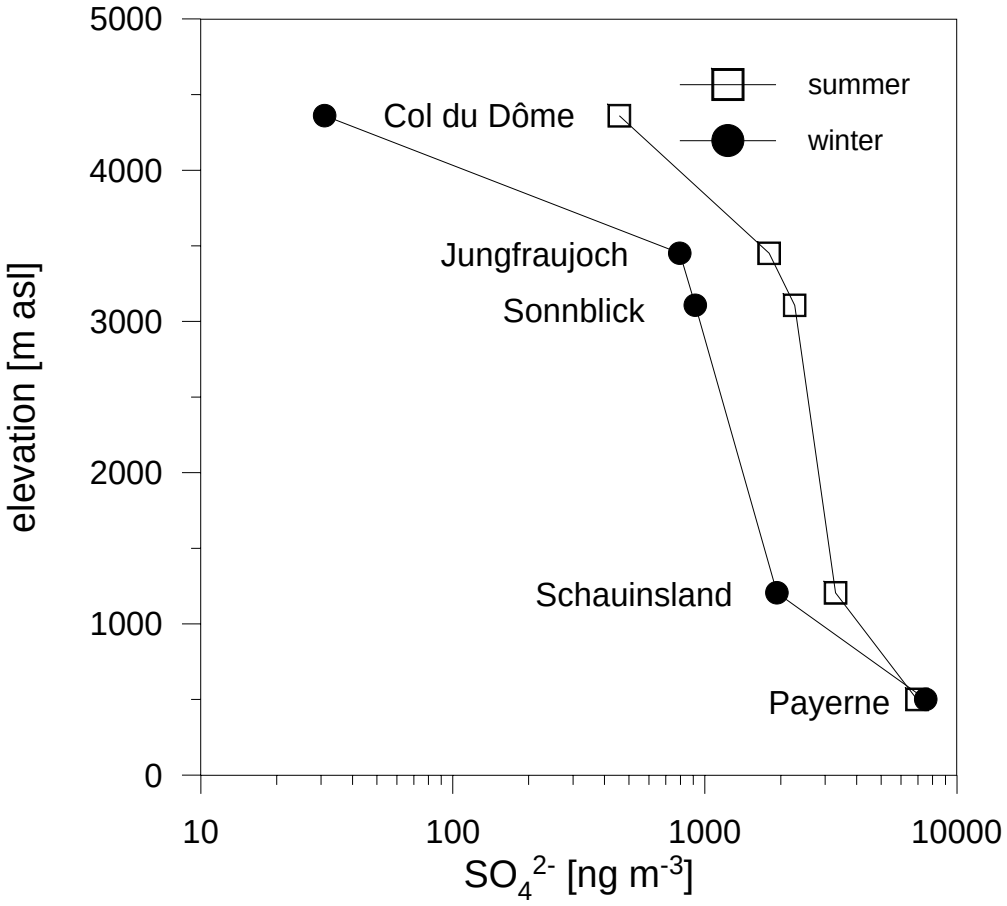

Figure 10: Sulfate atmospheric concentrations in winter and summer versus elevation using observations made in 1991-1993 at various European sites located around the Alps (Payerne, Swiss Plateau, Schauinsland in Germany, Sonnblick in Austrian Alps, and Jungfraujoch in Swiss Alps) and inverted data from the CDD ice core.

4.2 CDD nitrate trends

4.2.1 The natural NO_3^- level in CDD summer and winter snow deposits: Implications for natural NO_x emissions at the European scale

In Figure 4.2 we report the CDD long-term nitrate winter trend achieved by robust spline smoothing (see section 3.2.3). Remaining rather close to 20 ppb from 1925 to 1945, winter nitrate levels were then enhanced up to 65 ppb in the 1990's. The mean winter nitrate level seen in the bottom part of the C10 ice core (from 90.3 to 95.3 m w.e.) corresponding to snow deposited in the very beginning of the 20th century is close to 30 ppb (± 8 ppb) (Table 4.1) and is significantly higher than the 20 ppb seen between 1925 and 1950 (Figure 4.2). These values are rather surprising with regard to the expected impact of growing NO emissions from the very beginning of the 20th century to 1925 (Dignon and Hameed, 1989). The only atmospheric relevant cause for this discrepancy would be an enhancement of natural nitrate level at the beginning of the century with respect to the 1925-1950 one. Another possibility may be that the nitrate level in the CDD winter ice of this bottom part of the deep ice core has been enhanced as a result of diffusion of nitrate (nitric acid) from summer to winter layers after deposition due to the strongly reduced thickness of annual snow layers at these depths (0.2 m w.e., see section 2.1), as it is also observed for Deuterium at around 90 m w.e. (see section 2.4 (*6.2*)). Note that the examination of pre-industrial nitrate levels in CG ice will not help here for the same reason. Therefore, in contrast to the case of sulfate, the pre-industrial winter nitrate level cannot be directly estimated from the examination of pre-industrial ice layers. Nevertheless, the natural winter nitrate level could be indirectly estimated by assuming that the CDD nitrate winter trend follows the course of NOx emissions from total Europe between 1925 and 1980. Such an assumption is legitimate since a similar source apportionment for anthropogenic SO_2 emissions was concluded for the CDD site in winter (see section 4.1.4 (*4.2*)). Following that, since the increase in NO_x emissions of total Europe from the 1925-1950 time period (~5 Mt per year) to 1980 (~15 Mt per year) (see Figure 4.2) is proportional to the respective increase of nitrate winter levels (~20 ppb from 1925 to 1945, ~60 ppb in the 90s), we conclude that the natural nitrate winter level would be close to zero.

The pre-industrial summer level was estimated by considering the mean nitrate summer level observed in the bottom part of the C10 core (90.3 to 95.3 m w.e.) which is close to 100 ppb (Table 4.1), and the preindustrial nitrate levels found in Colle Gnifetti summer snow deposition (see section 4.2.3) which ranges from about 60 to 85 ppb (Wagenbach et al., 1988; Jung, 1993). As a rough estimate we have therefore assumed that the natural summer nitrate level at CDD ranges between 60 and 100 ppb.

In the following we discuss this estimate of the natural nitrate level at CDD with our present knowledge of the natural source emission over Europe. On a global scale, about 8-20% of the total annual NO_x emissions come from lightning activities, 4-16% from microbial

activity in soils, and 16-24% from biomass burning, whereas the anthropogenic contribution of fossil fuel combustion amounts for 28-56% in recent times (Logan, 1983). A quite different picture appears for Europe where anthropogenic emissions, which mainly result from fuel combustion, dominate the NO_x emission budget in recent times with a contribution from 80% to 98%. Soil emission from agricultural lands are thought to built up the main natural/biogenic source of total NO_x emissions in Europe, their estimations varying however by more than a factor of 10 (2 to 20%). Recently, Skiba et al., 1997 and Davidson and Kingerlee et al., 1997 estimated that this source represents from ≈2% to ≈20% of the total NO_x emissions. Emission contributions from lightning (at ground level) and fires are assumed to account to ≈0.06% and ≈0.15% to the total NO_x emission budget of Europe (Simpson et al., 1999). That contrasts with what is reported by Logan (1983) for USA where lightning activities as well as soil emissions are found to dominate the natural NO_x sources.

An estimation of the annual mean natural NO_x source contribution to the recent total NO_x budget based on the recent and pre-industrial CDD nitrate levels may here help to constrain the contribution of natural sources to the present-day atmospheric nitrate budget over Europe. Using an annual natural level of 40 ppb, obtained as the arithmetic average of the summer and winter levels (0 ppb in winter and 80 ± 20 ppb in summer), and comparing it to the mean annual level in 1990 of 230 ppb (60 ppb in winter, 400 ppb in summer), we found that at present natural sources contribute between 13% and 22% to the total NO_x budget in western Europe. Such a comparison between high elevation CDD nitrate levels with European NO_x emission may be however biased, since the contribution of natural source to the present-day NO_x emission above reported are calculated for ground level conditions. For instance, an enhanced contribution from lightning activities is expected (0.3% in 7 km asl instead of 0.06% at ground level, Simpson et al., 1999), while soil contributions may be decreased between the ground level and the elevation of 4000 m. In spite of that, our estimation of a contribution of natural source for the present-day nitrate atmospheric budget is more consistent with the order of magnitude of NO_x soil emissions made by Davidson and Kingerlee (1997) and suggests that the estimate from Skiba et al. (1997) underestimates natural sources. Finally, note that our estimate of the natural winter nitrate level (close to zero) is also consistent with the nature of natural NO_x emissions since soil emissions underlie a strong seasonal variation with minima (i.e. almost no NO_x release) during the winter season and lightning activities are very rare during that season.

4.2.2 The nitrate winter CDD trend.

As already discussed in Figure 4.2, the long-term nitrate winter CDD trend shows temporal changes which are qualitatively in agreement with European anthropogenic emissions of NO_x. The robust spline trend of the Col du Dôme winter data set, suggests no significant further nitrate increase between 1985 and 1995. Since this time period is situated

however at the border of our data set, we can not decide yet, whether this is just an artificial

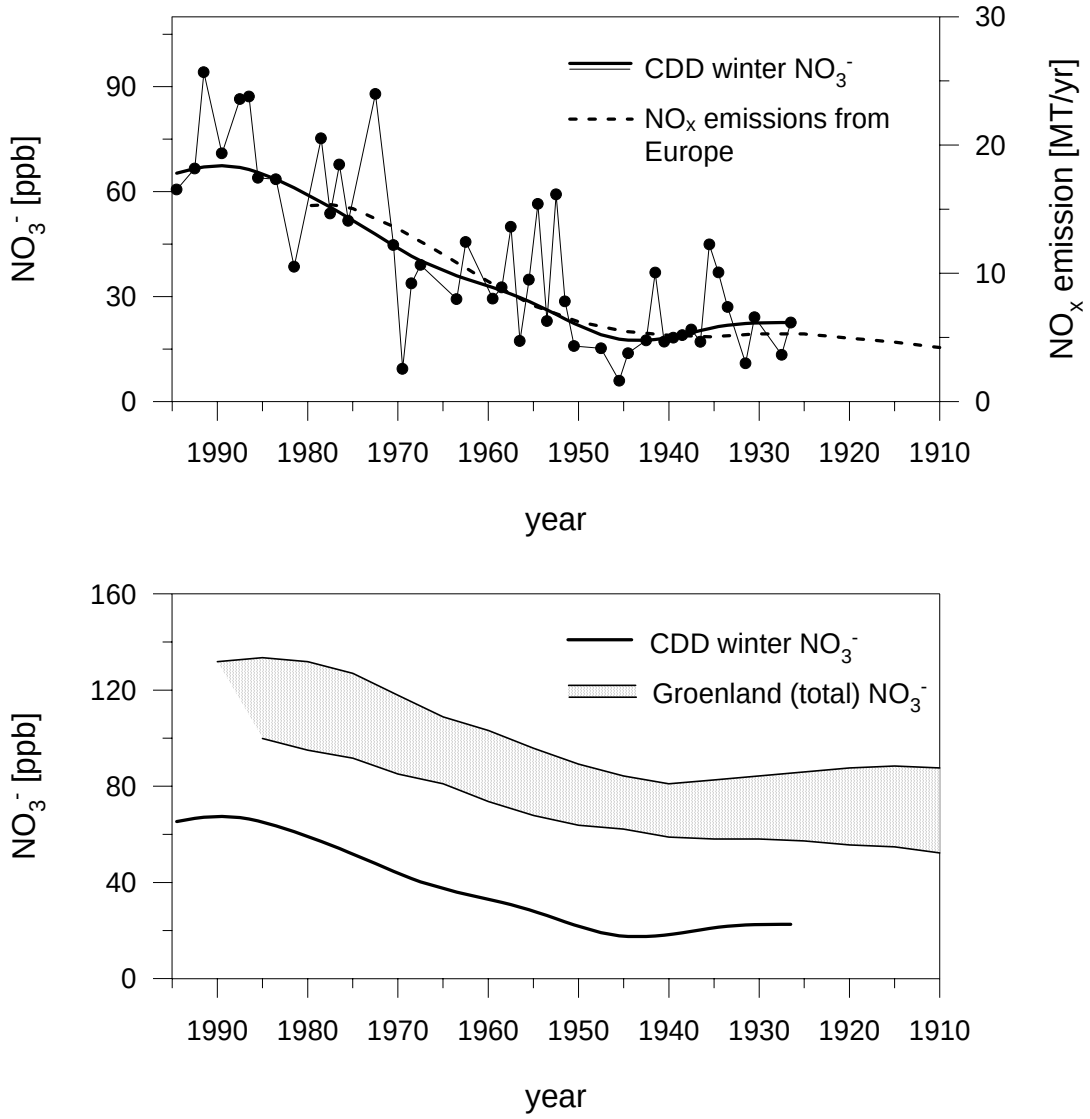

Figure 4.2:The CDD nitrate winter trend over the 20th century. (Top) NO_x emissions from Europe (Hov et al., 1987) and nitrate winter trend (background conditions) derived from the CDD C10 core. The thin line with dots refers to the winter means of individual years. The solid line is the smoothed trend profile (robust spline smoothing). (Bottom) Smoothed nitrate winter trend from CDD (same as top) together with the envelop of nitrate annual trends observed at different Greenland drill sites (Fischer et al., 1998b and references there).

phenomena resulting from the applied smoothening protocol (what cannot be excluded when examining the recent temporal evolution of individual annual means (see Figure 4.2)), or in fact relevant for atmospheric conditions (e.g. caused by restricted NO_x emissions).

In contrary to what is observed in CDD deep ice core (at least back to 1925), in Greenland the initially seasonal nitrate signal is not well preserved in firn layers due to the

occurrence of significant evaporation of gaseous nitrate species like nitric acid (De Angelis and Legrand, 1995) and diffusion process in firn layers (Fischer et al., 1998a). Therefore only annual long term trends are here of atmospheric relevance. Since the annual long term trends of nitrate in Greenland ice are related to long range transport of NO_x emitted from a wide region of the northern hemisphere (Fischer et al., 1998b), we here tentatively compare the Greenland annual long term trends with the CDD winter trend which is also related to changes having occurred at a large geographical scale. As seen in Figure 4.2 the nitrate winter CCD record differs from the one obtained at different Greenland ice core sites (data from Fischer et al., 1998b and references therein) located on a south-north transect over the Greenland ice cap. Systematic higher nitrate levels are revealed by the annual mean Greenland trend with respect to the winter CDD levels. Such a difference does not necessarily reflect different atmospheric conditions but may rather be due to the different precipitation rates prevailing at the Greenland and the Alpine site. Fischer et al. (1998b) showed that the nitrate level in Greenland snow deposits depends strongly on the snow accumulation rate of the respective site. Using the relationship between the nitrate level and the snow accumulation rate obtained by Fischer et al. (1998b) for Greenland ice, we found for the precipitation rate expected during winter at CDD (about 1.5 m w.e., I. Auer, personal communication) a corresponding nitrate level of 55, 45, and 30 ppb, in 1970, 1950, and 1930, respectively. These values are more comparable to the one we found in the winter CDD layers.

4.2.3 The nitrate summer CDD trend

The temporal evolution of nitrate CDD levels is reported in Figure 4.3 as reconstructed with the first SSA component (time window 5 years) representing 79% of the total variance of the data set. We also report in Figure 4.3 the nitrate trend achieved by applying SSA with a 10 year time window (first component, representing 72% of the total variance of the data set). Subtracting the pre-industrial nitrate summer level of 80 ± 20 ppb (see Figure 4.3) from the total nitrate summer concentrations, the obtained anthropogenic nitrate trend exhibits an increase by a factor of 3 to 4 between 1955 and 1980. Anthropogenic NO_x emission scenarios (data from Barret et al., 1995 and Simpson et al., 1997) suggest for total Europe (not shown), Italy, France, western Germany, Belgium, Swiss, Spain (WE6 countries), and Italy, France, Spain and Switzerland (WE4 countries) by a factor 2, 4.5 and 6 increased NO_x emissions in 1980 when compared to 1955. The increase seen from 1955 to 1980 for NO_x emissions of the WE4 countries is higher than the nitrate increase seen in CDD summer nitrate trend, whereas a better agreement is obtained if NO_x emissions from west Germany and Belgium are also considered (WE6 countries). On the other hand, the increasing trend of nitrate in CDD snow layers deposited between 1980 and 1990 fits better with NO_x emissions from the WE4 countries than with the ones from the WE6 countries. Finally, as

done for the source region apportionment of sulfate in summer CDD snow layers (see section 4.1.4 (*4.1*)), NO_x emissions

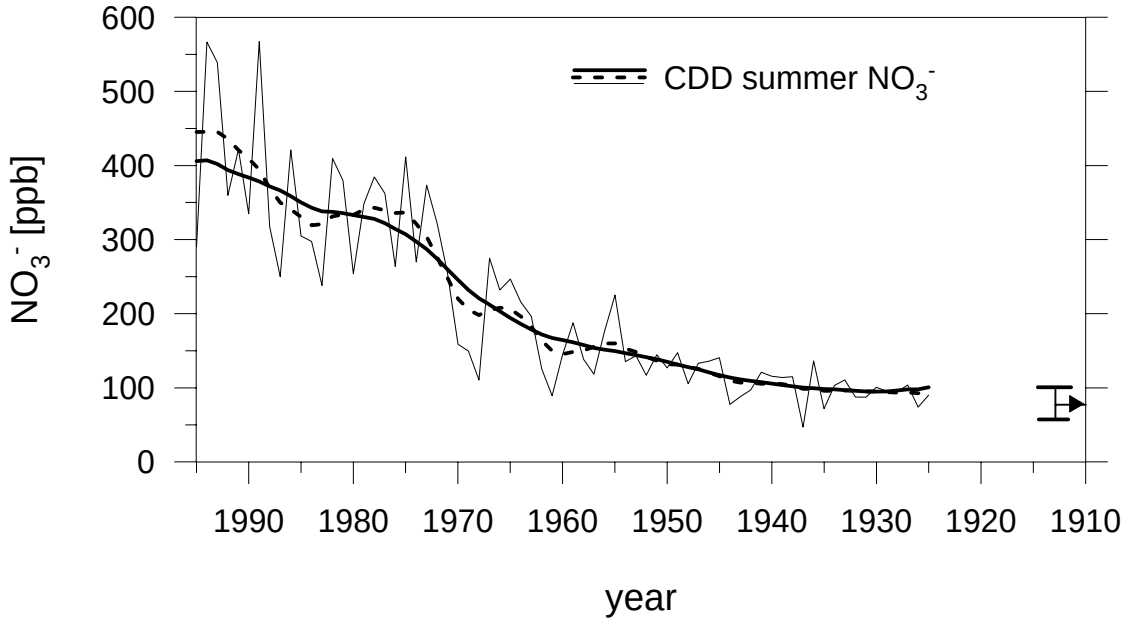

Figure 4.3a: Summer trend of nitrate levels in the CDD C10 core. The thin line refers to summer means of individual years. Thick lines are smoothed profiles (first SSA components with time window of 5 years (dashed) and 10 years (solid). The arrow at the right side refers to the range of the preindustrial summer level.

from west Germany were taken into account for 50% in addition to the WE4 countries. With that an increase of a factor 5 is found from 1955 to 1980, which is not far away from what was estimated for the nitrate CDD long term trend. In addition the shape of the emission trend fits rather well with the one observed for CDD deposits. Thus, we may consider the source regions of NO_x and SO_2 emissions relevant for the nitrate and sulfate summer depositions at CDD as rather similar.

In this study the observed nitrate trends of summer and winter (at least until 1990) snow deposition show a steady increase over the last four decades until recent times. This is in agreement with the temporal evolution observed in a Colle Gnifetti ice core which contains almost only summer snow deposits (Jung, 1993; Wagenbach and Preunkert, 1996), and in agreement with the European NO_x emission scenarios (at least until 1990). On the other hand the CDD trends differ from observations previously made at other high Alpine ice core sites by Döscher et al, 1995, and Schwikowski et al., 1999b. In the latter ice core studies, nitrate levels were found to remain approximately constant over the 1965-1980 time period, to exhibit a maxima in 1975, respectively. Since glaciological forcing effects (see section 2.2) were however not investigated in these studies, we assume that the derived snow deposition

trends are not necessarily driven by changes of atmospheric conditions but may be biased by local deposition artefacts (see section 3.2.4).

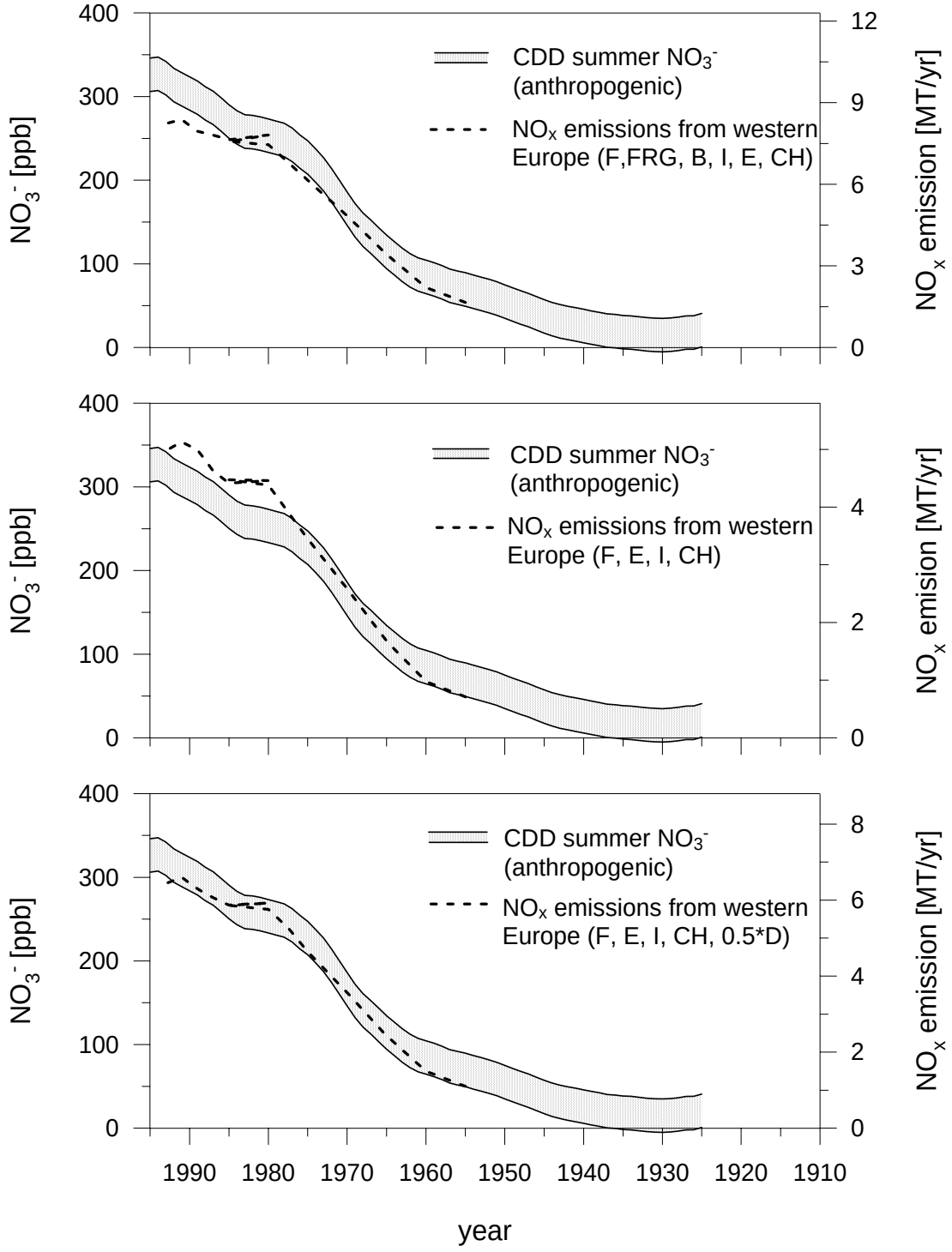

Figure 4.3b: Comparison of the long term trend of anthropogenic summer nitrate levels (grey area) with NO_x emission inventories from Barrett et al., 1995 and Simpson et al., 1997 (dashed lines) considering different source regions in Europe (see text).

4.3 CDD ammonium trends

4.3.1 The ammonium summer CDD trend

The long term summer trend of ammonium levels in the CDD ice is reported in Figure 4.4 (SSA smoothing curves considering a time window of 5 and 10 years). As for sulfate we can estimate the ammonium level at the beginning of the century from the examination of the bottom part of the CDD ice core (Table 4.1) and the summer levels seen in the CG pre-industrial ice. Based on that, we found a summer ammonium level of about 40 ppb at the beginning of the century. As seen in Figure 4.4, ammonium summer levels were enhanced from 1925 to 1950 with a mean increasing rate of 0.9 ppb per year. From 1950 to 1980, a more stronger increase is seen (mean increasing rate of 2.7 ppb per year). Ammonium summer CDD levels were thus enhanced by a factor of 4.5 since the beginning of the 20th century. Such changes are qualitatively in agreement with the expected impact of growing NH_3 emissions related to historical livestock statistics and fertiliser application (Asman et al., 1988).

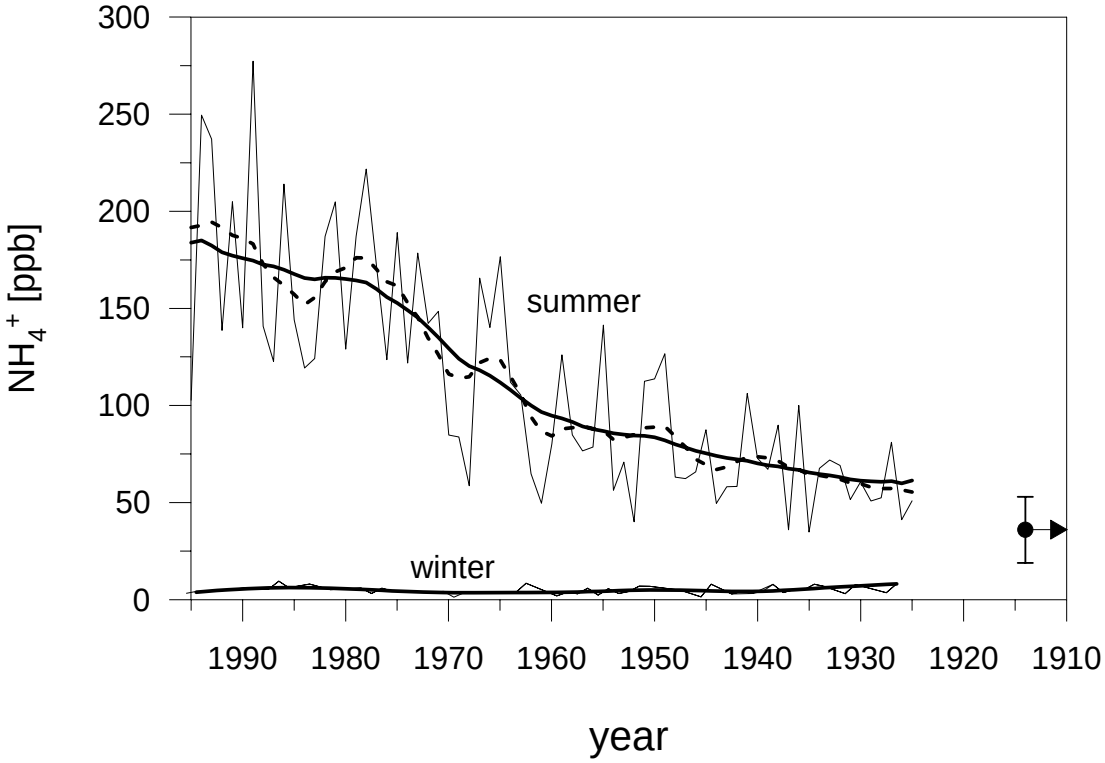

Figure 4.4: Ammonium summer trend of the CDD C10 ice core. The thin line refers to the summer means of individual years. The thick lines are smoothed trend profiles (first SSA components with a time window of 5 years (dashed) and ten years (solid). The arrow at the right side refers to the estimated pre-industrial summer level. To illustrate the strong seasonal difference observed for NH_4^+ within CDD snow deposits we also report the ammonium winter trend (as shown in Figure 4.6).

With main inputs from fires, mammals, birds, and humans, natural ammonia emissions amount in recent time to a little bit more than 1% to the total ammonia emission in Europe (Simpson et al., 1999). Important anthropogenic sources of ammonia are (Buijsman et al., 1987, and references given there) animal wastes, fertilisers and some industrial activities as fertiliser and ammonia production plants, whereas emissions from vehicles, coal combustion and sewage sludge remain insignificant. The total ammonia emission from Europe in the early 1980's was estimated to be of about 6.4 Mt NH_3 per year, with source contributions of 1.5% from industry, 17% from fertiliser and 81.5% from livestock wastes (Buijsman et al., 1987). Detailed estimates of agricultural emission factors (Van der Hoeck 1998, Pain et al., 1998) revealed that cattle production is the major source of atmospheric ammonia in recent times.

A more detailed examination of the summer ammonium long-term changes with ammonia emissions reveals however some discrepancies. For instance, from 1920 to 1980 ammonia emissions from total Europe as well as those from WE4 countries (Asman et al., 1988) were enhanced by a factor of about two whereas the long term ammonium summer CDD trend exhibits an enhancement of levels by almost a factor of 3 over this time period (Figure 4.5). Furthermore, while ammonia emissions indicate no significant change from 1900 to 1920, the ammonium CDD summer trend shows again an increase by a factor of 1.5 over this time period. Similar discrepancies between the estimates of European ammonia emissions and high Alpine ammonium snow deposits were already pointed out by the study of Colle Gnifetti ice cores (Jung, 1993; Döscher et al., 1996). These differences between ammonia emission and ammonium deposition trends could be either due to a more efficient atmospheric transport between the boundary layer and 4000 m elevation in the 1980's than at the beginning of the 20th century, or to an overestimation of the historical ammonia emissions, or to a more efficient present-day production of ammonium aerosol from ammonia due to the increasing presence of anthropogenic acidic aerosols since the beginning of the 20th century (Jung, 1993). Since, as discussed in sections 4.1.1 and 4.2.3, the sulfate and nitrate CDD summer trends mimic quite well the historical emission estimates of SO_2 and NO_x, we can exclude that the discrepancy between ammonia emissions and long-term ammonium trend is due to an enhanced atmospheric upward transport from the boundary layer over the course of the 20th century. Since the atmospheric lifetime of ammonia is shorter than the one of ammonium aerosol (ammonium nitrate, ammonium sulfate or bisulfate), the increase of SO_2 and NO_x emissions since the beginning of the 20th century may have enhanced the impact of ammonia emissions on ammonium levels at 4000 m elevation. For their modelled historical ammonium concentrations, Asman et al. (1988) have assumed that in 1900 the amount of potentially emitted anthropogenic acid was still larger than the amount of what could be neutralized by ammonia. As seen in Figure 4.5 over the entire 1925-1995 time period the amount of acidic species (sulfate and nitrate) exceeded the amount of ammonium in CDD summer snow deposits suggesting that neutralization of ammonia was in the same order in

1925 than in

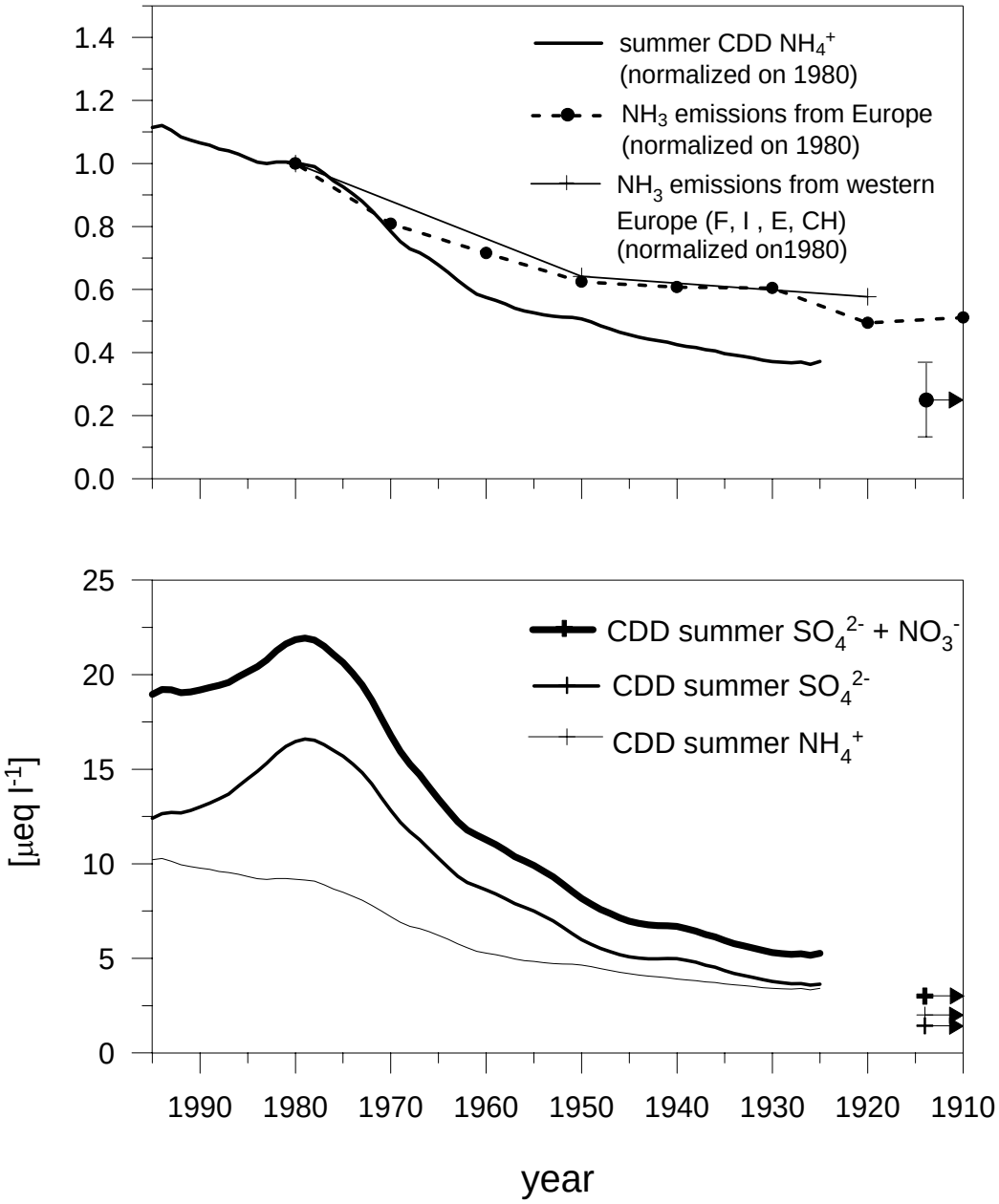

Figure 4.5: (Top) Comparison of the summer CDD ammonium trend with past ammonia emission inventories from Asman et al. (1988). The CDD summer trend as well as the emission scenarios (total Europe and the WE4 countries) are normalized to the 1980 year. (Bottom) The long term CDD summer trend of ammonium compared with the trends of sulfate and sulfate plus nitrate (expressed in microequivalent per litre) (with a time window of 10 years).

1995. Although such a scenario would require model simulations to assess if this observation remains true at all elevations, our discussion tends to suggest that past ammonia emission estimates made by Asman et al. (1988) are somewhat overestimated. These past ammonia

emission are estimated from the knowledge of historical live stock numbers by using recent ammonia emission factors. As alluded (but not considered in their study) by Asman et al. (1988) lower emission factors in the past (e.g. due to changed fodder etc.) may have biased past ammonia emission data.

Finally, applying the ammonium firn/air relations derived for recent summer conditions at CDD (section 1.2), we found ammonium air concentrations of 97, 49, 36 and 24 ng m^{-3} for 1980, 1950, 1925, and 1900 for summer conditions at 4300 m asl, respectively. The recent value of 97 ng m^{-3} fits very well with an extrapolation of the airborne ammonium data measured by Lenhard (1977) and Lenhard and Georgii (1978) (references given in Warneck, 1988) up to an altitude of 3000 m asl during the summer season.

4.3.2 The ammonium winter CDD trend

The winter (background as well as total winter) long term trends of ammonium in CDD snow layers are reported in Figure 4.6. A first examination reveals no obvious anthropogenic trend between 1925 and 1995 but note the large scattering of individual values (±2 ppb). In the following we examine if such an absence of detectable winter trend is due to the scattering of individual values or not. Over the 1985-1995 period, mean ammonium levels are of 180 and 5.6 ppb in summer and winter, respectively. Applying the corresponding summer to winter ratio of 32 to the summer ammonium level of 57 ppb seen in the middle of the 1920's, we may expect an ammonium winter level close to 2 ppb. Thus the expected winter trend between 1925 and 1995 is in the order of 3 to 4 ppb which remains close to the standard deviation of individual winter values. From that we conclude that given the strong seasonality of ammonium levels, the strong summer trend may be mirrored by a change of a few ppb in winter which is not easily detectable. Note that this is not true for other species like nitrate and sulfate. For instance the de-trended standard deviation of sulfate winter levels is close to ±15 ppb whereas the change of winter levels between 1925 and 1985-1995 is close to 50 ppb (see section 4.1.4). That is due to a weaker summer to winter ratio for sulfate than for ammonium.

Compared to other ions like sulfate, the ammonium seasonal cycle recorded in CDD snow layers is some three times stronger with respect to the sulfate one. For instance, over the 1975-1985 period, we found a summer to winter ratio of ≈15 for ammonium compared to ≈5 for sulfate (see section 4.1.4 (*Figure 2)*). Although needed to be confirmed, a part of the difference between the seasonal amplitude of signals for ammonium and sulfate seems to be due to the lower FAR values in summer with respect to winter for sulfate and a reverse change for ammonium (see section 1.2). Although weaker than what is seen in snow layers such a difference in the summer to winter ratio between ammonium and sulfate is also observed for the atmospheric conditions at the Vallot Observatory (see section 1.3 (*6.1*)). Indeed the atmospheric summer to winter ratio is close to 5.6 and 9 for sulfate and

ammonium, respectively. Anthropogenic SO_2 emissions are clearly two times higher in winter than in

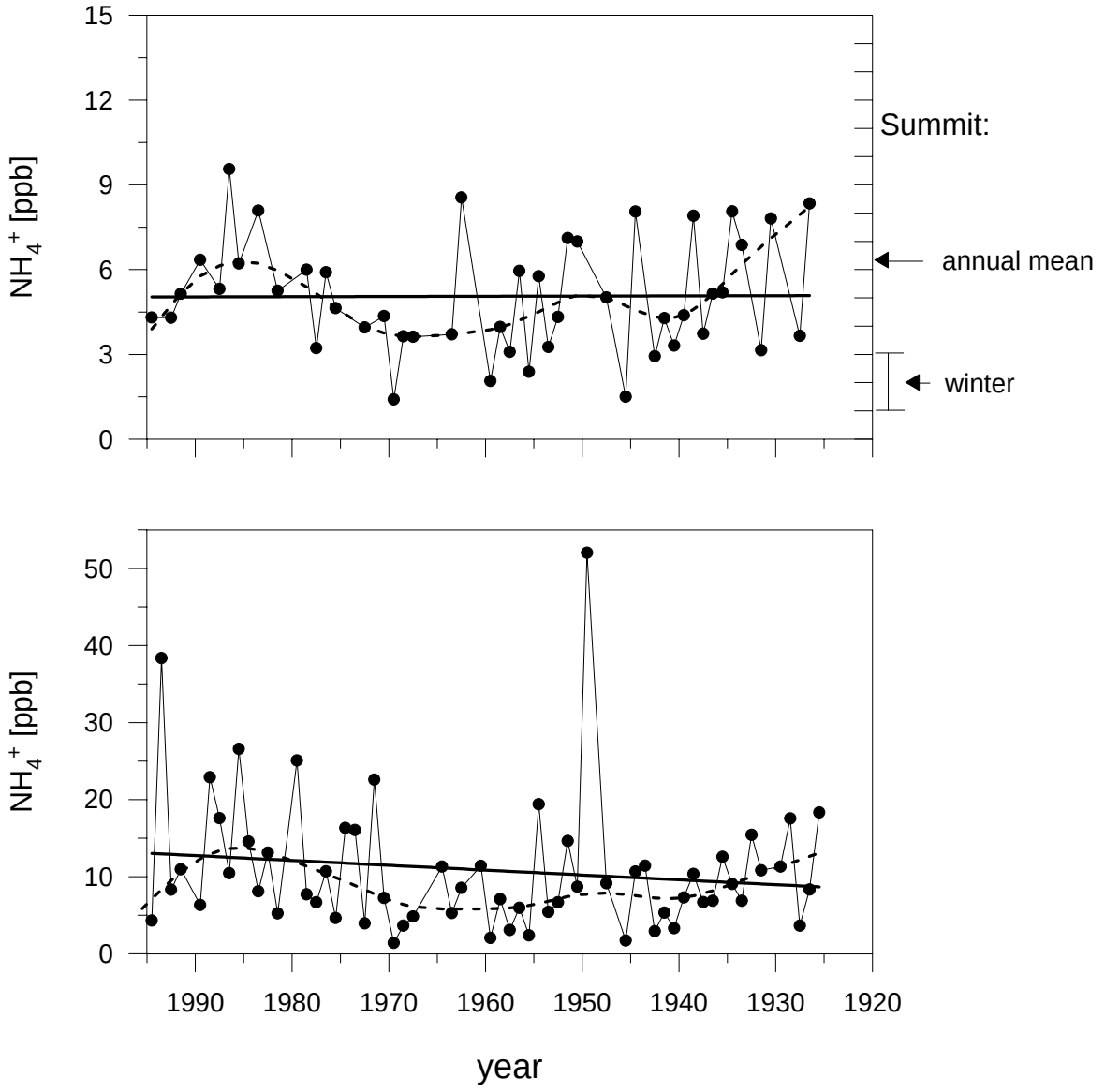

Figure 4.6: The winter CDD ammonium trend derived from the C10 ice core. (Top) CDD winter background conditions: The thin line (with dots) refers to the winter means of individual years. The thick lines are smoothed trend profiles as retrieved by robust spline smoothing (dashed) and linear regression (solid). The arrows on the right side refer to the mean ammonium levels observed in Greenland snow layers from 1983 to 1990 (Fuhrer et al., 1996). (b) (Bottom) Same as top for overall CDD winter conditions (see definition of "total winter" in section 3.2.2).

summer at the ground level in Europe as reflected in measurements of SO_2 and sulfate (see Puxbaum et al., 1993 for pre-Alpine valleys, and EMEP stations in numerous other ground level European sites). For ammonium and ammonia, the situation is less clear. Ammonia air

concentrations at ground level in Europe were found to underlie a strong seasonal variation with higher values in summer and lower ones in winter (Puxbaum et al., 1993; Horvath and Sutton, 1998), likely due to the temperature dependence of ammonia emissions itself, but also due to the more efficient formation of ammonium nitrate and ammonium chloride aerosols at lower temperatures (e.g. Seinfeld, 1986). With that, ammonium air concentrations are enhanced during winter if compared to summer (e.g. Horvath and Sutton, 1998) and lead to a quasi absence of seasonal variations in air concentrations of total reduced N species (ammonium plus ammonia) as also observed for ground level air masses in a pre-alpine valley (Puxbaum et al., 1993). Other studies (Warneck, 1988) suggested an increase of ammonia plus ammonium in summer with respect to winter. Assuming a similar change of the lifetime of ammonium plus ammonia and SO_2 plus sulfate in winter and summer, the observed atmospheric levels of sulfate and ammonium at the Vallot Observatory suggests that ammonium plus ammonia at the emission stage are in the same order of magnitude in summer and winter.

As previously discussed, the anthropogenic trend of sulfate and nitrate are also recorded in Greenland snow layers. For ammonium, no significant long term change of ammonium levels in snow layers was detected at Summit (central Greenland) during summer and winter seasons (Fuhrer et al., 1996). For the summer season, air back trajectories indicate that most of the air masses arriving at Summit come from northern America (Kahl et al., 1997). Thus, the fact that this region is rather dominated by wooden areas than agricultural can explain such an absence of an ammonium trend in Greenland snow deposits during this season. Conversely, Fuhrer et al. (1996) pointed out an increase by a factor of two of spring ammonium levels between 1950 and 1990. During this season emissions from Eurasia and Northern America are expected to influence the Arctic snow deposition (Kahl et al., 1997). Eurasian ammonia air concentrations at ground level peak very strong in relation with agricultural activities at the beginning of the spring season. That may be the cause of the observed anthropogenic increase of ammonium in spring Greenland snow layers.

4.4 Comparison of the CDD trends with other Alpine ice core records

As discussed in Chapter 2, at present the CDD ice cores cover the 20th century at the best, whereas Colle Gnifetti (CG) ice cores potentially offer the possibility to explore the natural variability of atmospheric chemistry (under summer conditions) at the scale of Europe. However drill site related shortcomings (e.g. a seasonally distortion of snow deposition and very low accumulation rate, glacier flow effects) limits a straightforward interpretations in terms of past atmospheric changes (Wagenbach, 1993a).

Atmospheric measurements (see section 1.3 (*6.1*)) and a detailed comparison of the recent snow cover at CDD and CG within a 10-year temporal high resoluted (half year) comparison of summer and winter snow deposition at both sites (section 2.4 (*5*)) revealed: (1)

an excellent agreement (in air and snow) at least for sulfate, nitrate, and ammonium between the both glacier sites; (2) that atmospheric short term changes on the scale of a few years are preserved and are detectable in the snow deposition high Alpine glacier sites. Assuming that these conditions were not significantly different in the past, we compare here the sulfate and nitrate trends seen in the CDD (C10) summer snow deposition with the temporal changes observed within a deep ice core from CG (Jung, 1993) (which spans roughly the last 400 years (Schäfer, 1995) and in which snow depositions are almost exclusively made up by summer precipitation (Wagenbach and Preunkert, 1996)), to estimate the atmospheric relevance of this latter ice core record. The CG data set has been corrected from Saharan dust inputs and was processed similarly as the C10 summer deposition data set (see section 3.2.1). Since the accumulation rate of the Colle Gnifetti ice core is however very low (surface accumulation rate: ≈20 cm w.e./year; Jung, 1993) but highly variable from year to year, it is likely that even the summer precipitation is not completely stored each summer within this ice core. Note that also negative annual snow accumulation rates were observed at Colle Gnifetti (Alean et al., 1983). As a consequence, short term trend variations of non- atmospheric origin, related to the presence or absence of singular precipitation events can take place in this core. To minimize such potential short term effects, we have applied a SSA smoothing with a time window of 30 years to annual means of the CG data set and to summer means of the CDD (C10) data set. To extend the comparison to the longest time period available we also consider the part of the C10 core which corresponds to precipitation deposited before 1922, but for which however the dating is not accurately established (see section 2.1).

Figure 4.7 reports the resulting long term trends as reconstructed by the respective first SSA components. For nitrate as well as for sulfate the overall temporal trend as well as the absolute levels are in very good agreement at the two high Alpine sites over the whole 20th century. This suggests that, at least for major anthropogenic derived species (nitrate, sulfate, and ammonium (not shown)), long term variations of snow impurity levels observed within the low accumulation CG ice core are determined rather by the prevailing summer air conditions which are similar at these two (CG and CDD) high Alpine glacier sites than by local (glacier specific) deposition effects.

Recently an ice core was recovered at CG (surface accumulation rate: ≈55 cm w.e./year) in which summer conditions seem to be archived more representative than within the CG ice core discussed here, and in which traces of winter snow deposits are present at least over the last 140 years (Armbruster, 2000). A long term intersite comparison (performed in seasonal resolution) between the CDD (C10) and this CG ice core would permit to assess in how far representative and reliable information about pre-industrial winter conditions and their natural variability could be extracted from this CG ice core.

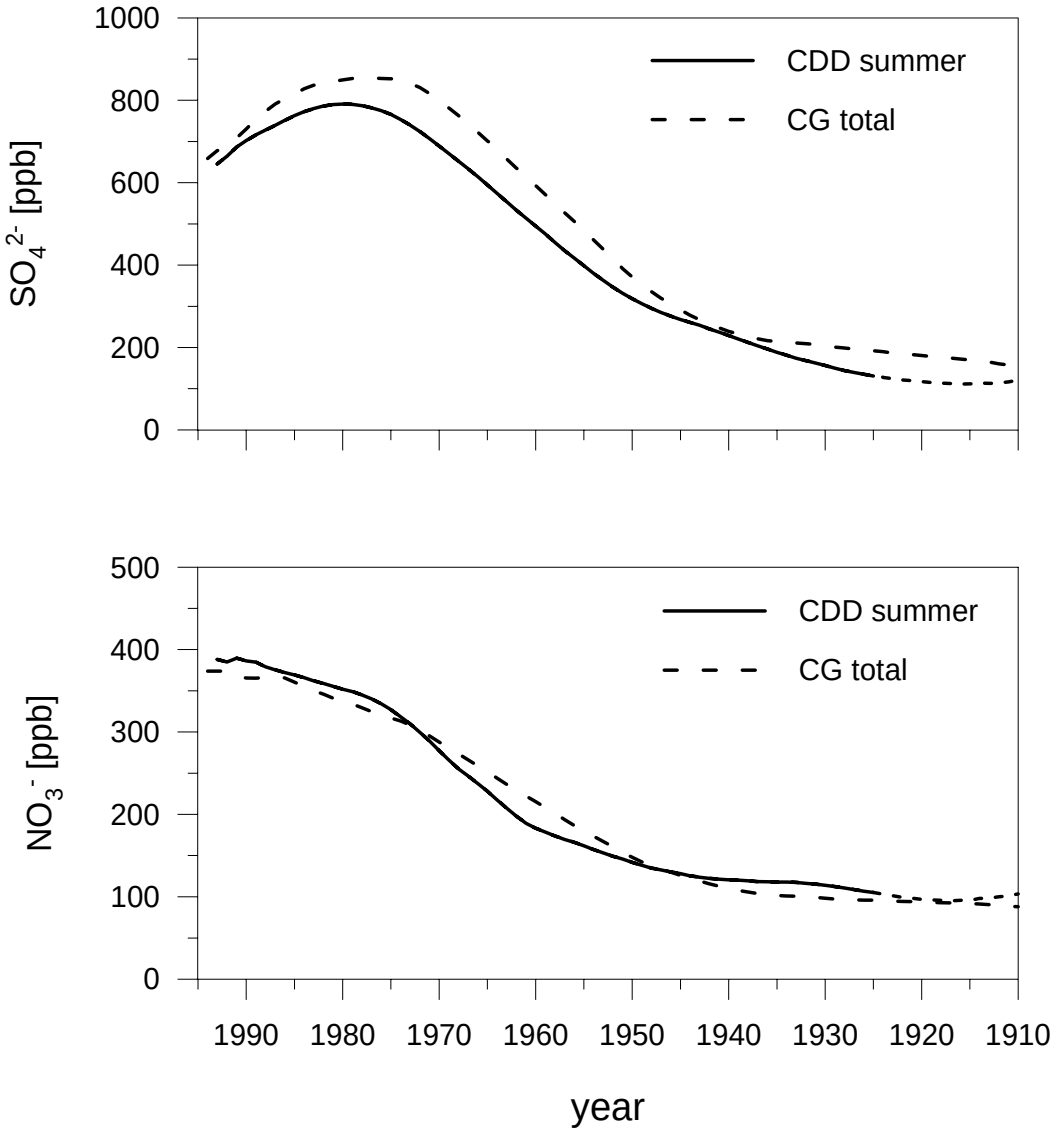

Figure 4.7: Long term temporal trend of sulfate and nitrate summer levels in CDD (C10) and CG (Jung, 1993) ice as reconstructed using the first SSA components (time window: 30 years).

Chapter V

Temporal changes of the halogens (F^- and Cl^-) in CCD snow and ice deposited over the last 80 years

5.1 Introduction and data presentation

The temporal change of the halogenated species F^- (see section 5.4) and HC^- (see section 5.5) was investigated over the last 75 years in summer and winter snow deposition at Col du Dôme. Until now, within only one other ice core study (Eichler et al., 2000) temporal HF and HCl changes were investigated (between 1937 and present) at a high Alpine site. The major findings of this study, namely a decrease of F^- levels in the 1970's and an enhancement of HCl levels after 1965, were interpreted as resulting from the decreasing releases of fluoride by aluminium smelters at the Swiss department Wallis in the 1970's, and the deployment of waste incinerators in the late 1960's at the Swiss plateau, respectively. However, in this study HCl concentrations were calculated as total chloride minus the amount of particulate chloride assumed to be there related to sea salt ($HCl = Cl^- - 1.8\ Na^+$). Furthermore annual mean ice core trends were interpreted without any examination of the potential glaciological effect (changes of the relative amount of summer to winter snow accumulation with depth, see section 2.2).

Chloride is incorporated in precipitation as hydrochloric acid as well as various chloride containing aerosols. Apart from the sea spray chloride contribution, chloride aerosols appearing in continental precipitation also include contributions from soil weathering and halide evaporite, but may also come from manure fertilized fields as proposed for Austria (Simeonov et al., 1999). With that, the aerosol derived chloride fraction in continental precipitation would depend on the respective sodium and calcium levels, since sodium is mainly present in halide components (sea spray, evaporites and manure fertilized field emission) and calcium in soils. Since sources of chloride aerosol are mainly of natural origin, the dependence of chloride to sodium and calcium can be expressed as follows:

$$[Cl^-] = k_{Na}\,[Na^+] + k_{Ca}\,[Ca^{2+}] + a \qquad (5.1)$$

This was examined in C10 snow layers deposited before 1955 a period over which the anthropogenic chloride input remained moderate. The hereby obtained correlation coefficients for summer and winter snow deposits are given in Table 5.1. The knowledge of k_{Na} and k_{Ca} values permits then to evaluate the HCl level as follows:

$$[HCl] = [Cl^-] - (k_{Na}\,[Na^+] + k_{Ca}\,[Ca^{2+}]) \qquad (5.2)$$

Table 5.1: Correlation coefficients as derived from equation 5.1, representing the linear relationship between sodium and calcium versus chloride in C10 summer and winter snow deposits from the 1925 – 1955 time period (n denotes the number of samples).

	k_{Na}	k_{Ca}	a	R^2	n
summer	1.46 ± 0.054	0.025 ± 0.013	3.4	0.8	240
winter	1.74 ± 0.056	0.14 ± 0.87	-0.5	0.9	69

With mean HCl and HF concentrations ranging from less than 3 to 18 ppb, and from 0.3 to 2.4 ppb in summer (from 0 to 2 ppb, and 0.1 to 0.4 ppb in winter) within this century, total HCl and HF contribute only for less than 2.2% and less than 0.4% to the free acidity of the high Alpine snow deposition, respectively. Since gaseous species like HF and HNO_3 were observed to diffusive within Greenland snow layers (De Angelis and Legrand, 1994; Fischer et al., 1998a) we examined here in what extend seasonal variations of these two species are preserved in snow layers at the CDD site. The seasonality of HCl and HF versus depth along the deep CDD ice core reveals no sign of smoothing with depth but is well preserved over the last 80 years (see section 5.4 (*3.1*) and 5.5 (*2*)). Such an absence of HF diffusion in CDD snow layers is likely due to the relative high snow accumulation appearing over the last 30 years when the acidity of snow layers was high and exhibited a rather strong summer/winter contrast (due to anthropogenic sulfate and nitrate), and the relative low acidity with a moderate summer/winter contrast of old snow layers (before 1960), respectively (see also Figure 6.3). This contrasts with what was observed at Summit (Greenland), where diffusion of HF from acid snow layers corresponding to volcanic inputs occurs during firnification, leading to an average displacement of the initial signal by at least one year (De Angelis and Legrand, 1994). For HCl, such effects were not observed in Greenland snow and therefore we don't expect that they take place at CDD.

5.2 Source contribution of the high Alpine F^- and Cl^- snow deposition

5.2.1 Natural contributions to the high Alpine deposition of F^- and Cl^-

The main part of the fluoride present in Alpine snow deposited during the pre-industrial era is assumed to be soil dust derived, what follows the previously made observation of a major soil dust contribution to the natural fluoride budget in Greenland (De Angelis and Legrand, 1994). A quantification of this natural contribution in snow deposits of Col du Dôme was made, considering the relationship between fluoride and calcium in snow layers which could be regarded as almost free of coal burning and aluminium smelter inputs

(see section 5.2.2 and 5.4 (*4*)). Applying this relationship ($[F^-]/[Ca^{2+}] \approx 3.5\ 10^{-3}$) to the fluoride data set of C10 with respect to the observed calcium levels, soil dust was found to contribute in 1930 and 1970 for 38% and 8% to the total summer fluoride levels and for 37% and 5% to the total winter fluoride levels, respectively (see Figure 5.1). Thus, due to enhanced anthropogenic inputs in Alpine snow (see section 5.2.2 and 5.4 (*5*)), the natural source contribution to the total fluoride input became significantly decreased from 1930 to 1980. A significant marine fluoride source from sea salt aerosol is unlikely at high Alpine sites and has been estimated to be at the best about 1.6% and 1.8% of the total F^- input in summer and winter snow deposition. In spite of its relatively large continuous HF emissions, it is assumed that the Mount Etna volcano does not contribute to the modern Alpine fluoride budget either because the volcanic plume is not efficiently transported towards the Alps or due to a too short lifetime of HF in the atmosphere (see section 5.4 (*5*)). This is different to what was observed in Greenland snow layers, which are very often impacted by fluoride emissions from the numerous volcanoes located in the high-northern latitude belt (Iceland, Aleutians, Kamchatka) (De Angelis and Legrand, 1994).

Chloride present in the CDD ice core corresponds to chloride trapped as HCl as well as chloride bearing particles as sea spray from ocean, evaporites and weathered soil particles from continents and possibly particles emitted from manure fertilized fields. As detailed in

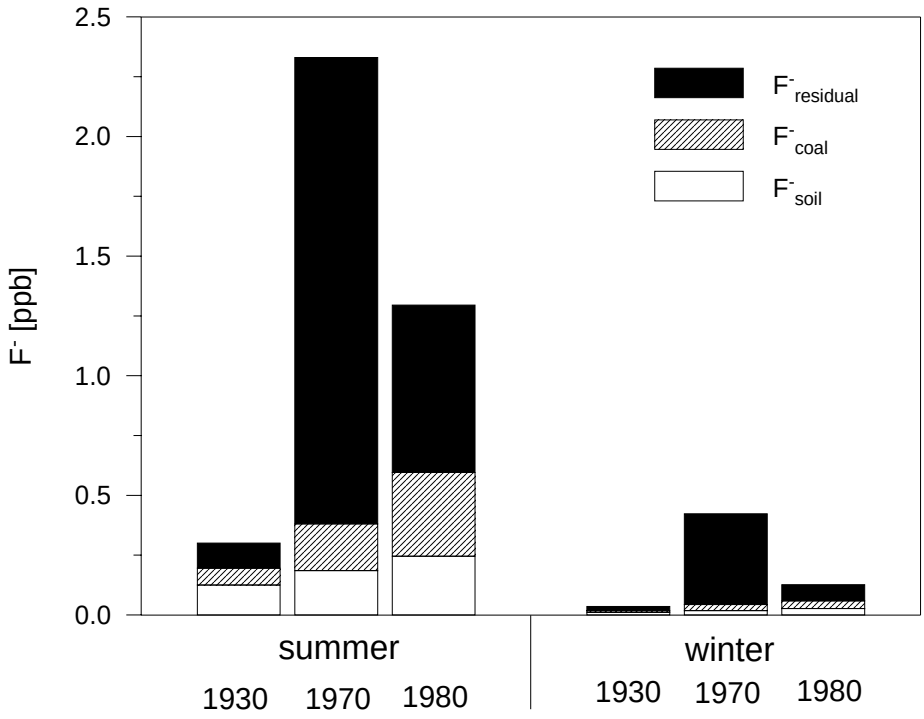

Figure 5.1. Estimated contributions of soil (F^-_{soil}), coal burning (F^-_{coal}), and residual (mainly related to release from Aluminium smelting) ($F^-_{residual}$) to the fluoride summer and winter snow deposition at CDD.

section 5.5 (*3.2*), this latter contribution can be neglected at high elevated Alpine sites. To quantify the contribution of halides (evaporites and sea spray) and soil weathering, the relation of chloride to non soil derived sodium and calcium was considered (see equation 4 in section 5.5 (*3.2*)). Following that (Figure 5.2) we found that in 1930 ≈65% of the total summer Cl^- deposition is related to halide, ≈24% to crustal origin, and the remaining part to HCl. The HCl contribution is mainly of anthropogenic origin (see section 5.2.2 and 5.5 (*4.1*)) except the contribution related to biomass burning in summer. In 1930, at a time when the anthropogenic input was still weak, the biomass burning contribution accounts on average for not more than 12% to the total chloride level in summer CDD snow layers. Due to enhanced anthropogenic inputs (see section 5.2.2 and 5.5 (*4.1*)), the sum of the relative contributions of halide and crustal sources to the total chloride input became however less important in recent times with respect to the situation in 1930. In 1980 the soil input accounted for ≈36% and the halide one for ≈25% to the total Cl^- input in the summer snow deposition at Col du Dôme.

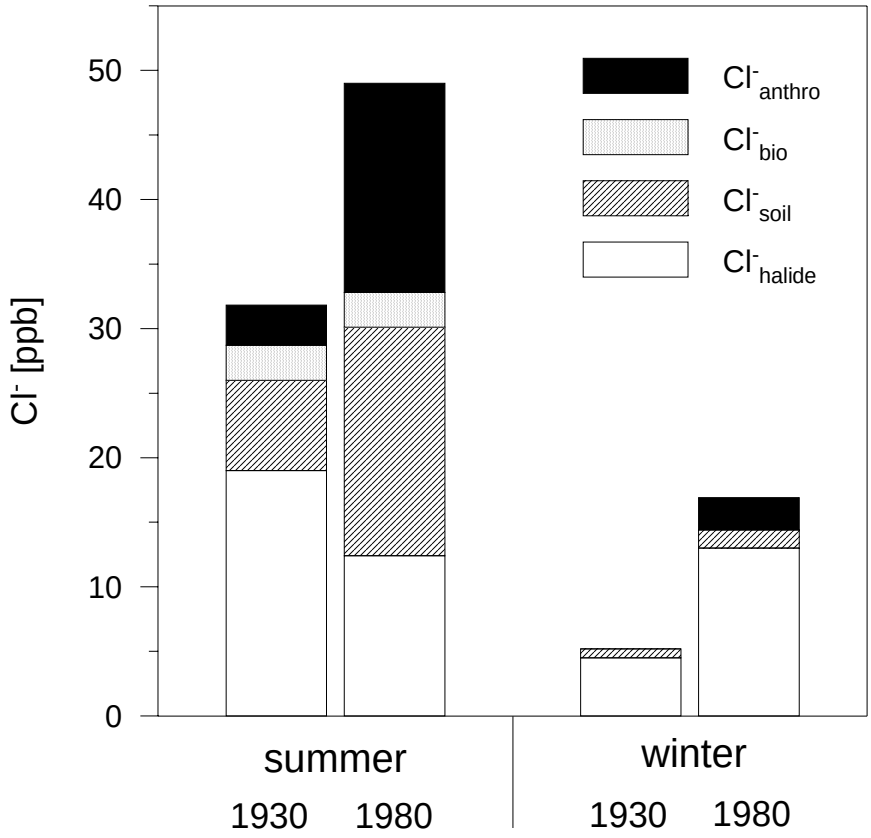

Figure 5.2. Estimated contributions of anthropogenic (Cl^-_{anth}) and biogenic (Cl^-_{bio}) chloride emissions as well as contributions from soils (Cl^-_{soil}) and halides (Cl^-_{halide}) to the Cl^- deposition at CDD. Although the contribution of HCl biomass burning (biogenic) is highly variable with time, we have assumed in this picture that the mean contribution of this source seen over the years 1925 to 1955 is the same over the 1955-1995 time period.

Compared to summer snow layers, the chloride deposition in winter is driven by a larger halide contribution, accounting for more than 75% (Figure 5.2). Note that while in summer the halide fraction is assumed to be mainly made up by evaporites (as a result of an efficient upward transport from the continental boundary layer), during winter sea spray likely dominates this fraction (due to a more active cyclogenis over the Atlantic ocean) (see section 5.5 (*3.2*)).

5.2.2 Anthropogenic contributions to the high Alpine deposition of F^- and Cl^-

Fluor, chlor as well as sulfur are present at significant levels in coal, and during combustion all three species are emitted more or less efficiently to the atmosphere in the form of HF, HCl, and SO_2, respectively. An attempt was made to quantify in CDD snow layers the fluoride and chloride inputs due to coal combustion (see also section 5.4 (*5.1*) and 5.5 (*4.1.1*)). To estimate HF and HCl releases from coal combustion, we have used the fluoride, chloride and sulfur contents of coal ($C_{halogen}$ and C_S) and annual S coal burning emissions (E_S) following:

$$E_{halogen} = (C_{halogen}/C_S)\, E_S \qquad (5.3)$$

Concerning HF, Cadle (1980) proposed a mean HF to SO_2 weight ratio of $2\ 10^{-3}$ (from 1.7 to 5.9) giving a corresponding fluoride to sulfur ratio of 3.4 to $12\ 10^{-3}$. This ratio is however dependant of the geographical origin of the employed coal. At present the coal used in western Europe thermal-electric stations leads to a F^- to S weight ratio of $7.2\ 10^{-3}$ (Electricité de France, personal communication). For chloride, the amount of particulate versus HCl emissions is not well known and may depend of the combustion process (Mc Culloch et al., 1999). In addition, also a fraction of chloride can be retained in ash. We here have assumed that a similar fraction of chloride and sulfur is retained in ash during the combustion and that chloride released into the atmosphere is mainly in the form of HCl. With that, the emission rate of HCl versus sulfur is estimated via the mean chlorine to sulfur content in hard (0.12- 0.24) and brown coal (0.01 – 0.06) employed in western Europe (data from Mc Culloch et al., 1999 and Lefohn et al., 1999). The contribution of coal combustion to the levels of the halogen species Cl^- and F^- in CDD ice was then estimated from the level of anthropogenic sulfate observed in summer CDD ice layers ($[SO_4^{2-}] - SO_4^{2-}{}_{preind}$, see section 4.1.1), the total anthropogenic annual sulfate emission including fuel contribution ($E_{sulfate}$, data from Mylona et al., 1996) and the annual HCl and HF, respectively, ($E_{halogen}$) emission calculated from equation (5.3) following:

$$[Halogen] = E_{halogen}\, ([SO_4^{2-}] - SO_4^{2-}{}_{preind})/\ \delta\, E_{sulfate} \qquad (5.4)$$

The δ factor refers to the change of the atmospheric halogen to sulfate ratio between emission and deposition at the CDD site. He was estimated to range between 2 and 2.4, and

higher than 1.6, for fluoride and chloride, respectively (see sections 5.4 (*5.1*) and 5.5 (*4.1.1*)). Based on the realistic assumption that the atmospheric lifetimes of HCl and HF are similar, calculations were carried out assuming a δ factor of 2.2 in equation (5.4) for the HCl/SO_4^{2-} ratio.

Following this latter assumption, coal burning HF emissions contributed to the total fluoride summer snow deposition at Col du Dôme for 26% in 1930, 6 to 11% in 1970, and 16-33% in 1980-1995. The residual fraction (non-soil and non-coal burning) was proposed to be related to the fluoride release from aluminium smelters mainly located nearby the Alpine massif in France and Switzerland (see section 5.4 (*5.2*)). This anthropogenic contribution which accounts for more than 80% of the total fluoride deposition in summer in 1970 largely dominates the fluoride budget between 1950 and 1970. This is in contrary to what was observed in Greenland snow layers where the main anthropogenic fluoride input is here related to coal burning (De Angelis and Legrand, 1994).

Between 1925 and 1960 HCl summer levels have been enhanced from their natural input (mainly related to biomass burning) in response to enhanced emissions from coal burning which are estimated to account for about 12% to the total chloride deposition during this time period. While particles emitted from manure fertilized fields have been found not to contribute significantly, an additional anthropogenic HCl input occurred in the late 1960's. We proposed that this contribution is related to HCl emissions from waste incineration (particularly PVC) in western Europe (see section 5.5 (*4.1.3*)). In this way, the total anthropogenic HCl contribution represented ≈ 32% of the total chloride budget in 1970, of which ≈ 16% and ≈ 84% were due to coal burning and waste incineration, respectively. As already seen for fluoride, anthropogenic sources influencing the chloride (HCl) deposition at high Alpine sites are different from those influencing Greenland snow layers. For the latter site it is assumed that sea salt dechlorination represents a major source of enhanced HCl deposition since 1960 in response to the acidification of the atmosphere (see section 5.5 (*5.2*).

Though less well documented than the summer trends (see section 2.2), the CDD winter trends of fluoride and HCl seem to reflect inputs of similar anthropogenic sources as seen in the respective mean summer trends at least until the 1980's. Due to the strong input of aluminium smelter releases between the 1940's and the 1970's, coal burning emissions in winter represented 25% in 1930 and 17-34% in 1980 but only 4 to 8% in the 1970's of the total fluoride input (see Figure 4.1 and section 5.4 (*5.1*)). HCl winter values at CDD are most of the time not significantly different from zero with respect to uncertainties. The temporal trend tends to suggest however an increase of levels after 1965, what could reflect a limited contamination of the free troposphere in winter by waste incineration emissions (see section 5.5 (*4.2*)).

After 1980 an important difference shows up between the winter and the summer fluoride trend. While residual (non soil and non coal combustion) fluoride winter levels were

significantly enhanced from 1980 to 1995 (from about 0.05 to 0.3 ppb), such a very recent change is not detected in the summer trend. Referring to the overall poorer documentation of the winter trend, this very recent change of winter fluoride level still needs to be confirmed by other ice core records (note that in contrast to C10 levels in 1995 a very low F^- winter level of about 0.05 ppb was observed from 1997 to 2000 within the snow pit study). Nevertheless, an estimation was made to quantify roughly the potential recent stratospheric HF (and HCl) input in CDD snow layers which would be expected from recent stratospheric CFC degradation inputs. To do so, the cosmogenic ^{36}Cl radioisotope which is mainly produced in the stratosphere and mixed downwards into the troposphere was used as tracer (see section 5.4 (*5.2.2*) and 5.5 (*4.2*)). With that, a maximal stratospheric derived HF level of 0.16 ppb and 0.32 ppb is estimated for 1980 and 1990, respectively. This increase remains in the order of magnitude of the fluoride winter trend observed at CDD from 1980 to 1990, but contrasts however to the low winter levels found for the years 1997 to 2000. For HCl a maximal stratospheric level of 1.8 ppb was estimated, which is not unrealistic in view of the HCl winter level observed from 1998-2000 (2.2 ± 0.6 ppb). Further, this level is only three times lower than the corresponding one observed in summer (6.2 ± 5.8 ppb) whereas a summer to winter ratio of a factor 5 is seen in older snow layers for HCl. Thus, though this needs to be confirmed with other ice core records, we cannot exclude the possibility that winter snow layers have already started to record the stratospheric changes related to the changing load of CFC in the stratosphere.

5.3 Spatial representativeness of anthropogenic halogen trends detected at Col du Dôme

Based on comparisons between long term trends of anthropogenic fluoride and sulfate observed in the deep CDD ice core and European anthropogenic HF and SO_2 emission inventories, source region apportionments were estimated for the anthropogenic sulfate and fluoride deposition at the CDD site. The residual fluoride Col du Dôme summer trend, assumed to be mainly related to HF releases from aluminium smelters, was found to reflect emissions from aluminium smelters from France and Switzerland which are mainly located at the border of the Alpine massif at a distance of 130 km or less from the Col du Dôme site (see section 5.4 (*5.2.1*)). In the case of sulfate, anthropogenic SO_2 emissions (coal and fossil fuel burning) influencing the CDD site in summer are found to be located within a distance up to ≈ 700 –1000 km (i.e. mainly arriving from France, Switzerland, Italy, Spain, and to a lesser extent from west Germany; see section 4.1.4 (*4.1*)). A direct comparison of theses differences in the source region apportionment for the two species in terms of respective atmospheric lifetimes of fluoride versus SO_2/SO_4 species is however somewhat misleading, since, as schematized in Figure 5.3, the geographical distribution of sulfur emissions with respect to the

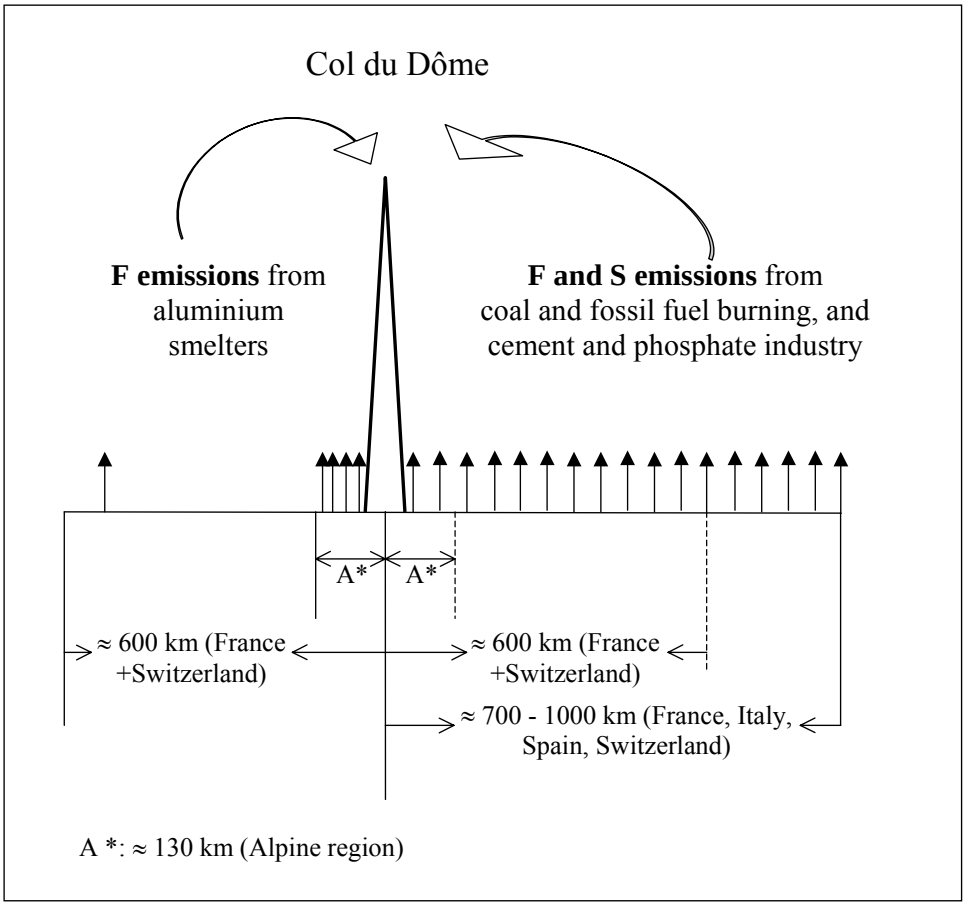

Figure 5.3. Sketch of anthropogenic fluoride and sulfur source apportionment for fluoride and sulfate in summer snow layers at CDD.

fluoride ones is totally different. While sulfur emissions are homogeneously distributed over the European countries of concern, fluoride emissions are restricted to regions located nearby mountain valleys (Alpine and Pyrenean for France). For example, in 1970 the fluoride level of the Col du Dôme summer snow layers attributed to aluminium smelters was ten times higher than the amount attributed to coal burning, whereas annual fluoride emissions from coal burning from France and Switzerland were three times higher than fluoride emissions from aluminium smelters of these two countries. This emission-deposition difference is clearly related to the proximity of the aluminium smelters to the Alpine massif, in contrary to the rather well distributed coal burning sources.

The source region apportionment for fluoride as well as the one for HCl (see section 5.5 (*4.1.1*)) that we propose in this study conflicts with what was concluded on the base of a recent ice core study derived from the Grenzgletscher glacier (4200 m asl, Monte Rosa massif, Swiss Alpes) by Eichler et al. (2000). Within the latter study, local sources were pointed out to explain the high Alpine F^- and HCl deposition trends. In particular it is

suggested that the observed fluoride trend is related to the two aluminium smelters located in Switzerland about 60 km from the drill site. Conversely at CDD, we found that the long term trend of fluoride cannot be explained only by the aluminium smelters of Saint Jean de Maurienne located 70 km away from the site though emissions from this site account for 20% to the total fluoride release from French aluminium smelters. In fact, being restricted to the 1937-1990 time period, the record from Eichler et al. (2000) is too limited in time to properly investigate the source region apportionment from aluminium smelters situated either in Switzerland or in France. Indeed, emissions from the aluminium smelters in Switzerland and France located close to the Alps (distance of less than 200 km) show similar temporal evolutions from 1935 to 1990, whereas that is not true before 1935 (aluminium production being already important in Switzerland in contrast to the situation in France in 1920-1930).

5.4 Causes of enhanced fluoride levels in Alpine ice cores over the last 75 years: Implications for the atmospheric fluoride budget

5.5 Seasonally resolved Alpine and Greenland ice core records of anthropogenic HCl emissions over the 20th century

JOURNAL OF GEOPHYSICAL RESEARCH, VOL. 106, NO. D12, PAGES 12,619–12,632, JUNE 27, 2001

Causes of enhanced fluoride levels in Alpine ice cores over the last 75 years: Implications for the atmospheric fluoride budget

Susanne Preunkert and Michel Legrand

Laboratoire de Glaciologie et Géophysique de l'Environnement du Centre National de la Recherche Scientifique, Saint Martin d'Hères, France

Dietmar Wagenbach

Institut fur Umweltphysik, Universitat Heidelberg, Heidelberg, Germany

Abstract. A continuous high-resolution record from a Col du Dôme (Mont Blanc massif, 4250 m above sea level (asl), French Alps) ice core in addition to discontinuous samples from a Colle Gnifetti (Monte Rosa massif, 4450 m asl, Swiss Alps) ice core were used to reconstruct the history of the atmospheric fluoride pollution at the scale of Europe. Such studies are mandatory by large uncertainties in our understanding of the natural fluoride cycle which have confounded assessment of the environmental impact of anthropogenic emissions. For fluoride, advantages of Alpine ice core records with respect to the Greenland ones include less efficient post-depositional effects in relation with higher snow accumulation rates, and less contamination by quasi-permanent passive volcanic HF emissions at midlatitudes compared to the situation at high northern latitudes. Hence Alpine ice records permit detailed examination of natural sources of fluoride for the free troposphere over Europe and the impact of anthropogenic sources such as aluminium smelters, coal burning, and contribution of the stratospheric reservoir built up from the chlorofluorocarbon (CFC) degradation since the beginning of the twentieth century. At Col du Dôme (CDD), fluoride concentrations in summer snow layers were close to 0.30 ng g^{-1} in 1930, started to increase in the late 1930s, reaching 1.4 ng g^{-1} in 1940 and 2.4 ng g^{-1} in the late 1960s. From 1970 to 1980 they were strongly decreased, exhibiting a plateau value close to 1.3 ng g^{-1} between 1980 and 1995. It is shown that at the scale of Europe in summer, soil dust emissions dominated the atmospheric fluoride budget prior to 1880. In the late 1960s the soil contribution decreased to 6 ± 1% due to enhanced release of fluoride by aluminium smelters and coal burning which accounted for 86 ± 3% and 8 ± 2% of the total fluoride content, respectively. From 1970 to 1980, effective precautions have been taken to minimize the release of fluoride from aluminium smelters to the atmosphere. Thus, over the 2 last decades, 26 ± 8% of the fluoride summer level of Alpine snow was due to coal combustion. The remaining part was related to the release from the less pollutant aluminium smelters as well as other anthropogenic processes (cement and phosphate industrial processings) (56 ± 11%) and to soil dust emissions (18 ± 2%). Winter levels close to 0.10 ng g^{-1} or less in 1930 were gradually increased after the late 1930s, reaching a maximum of 0.4 ng g^{-1} in 1970. Similarly to the summer level, the winter one has then strongly decreased (~0.12 ng g^{-1} in 1980). A major difference between summer and winter trends is the reincrease of winter level up to 0.4 ng g^{-1} (i.e., similar to the 1970 maximum) in 1990. Such a very recent change of fluoride background levels may be partly related to the impact via stratosphere/troposphere exchanges of the growing HF stratospheric load related to the CFC degradation.

1. Introduction

Until now, data on the distribution and the budget of HF and fluoride species present in the atmosphere and precipitation are extremely limited. Potential natural sources have been reviewed by *Cicerone* [1981], more recently by *Harnisch* [1999], and include sea salt, soil dust particles, and HF volcanic emissions. At a regional scale it is expected that the atmospheric boundary layer can be severely affected by anthropogenic sources such as cement and phosphate industrial processings, and aluminium smelters [*Low and Bloom*, 1988]. Nevertheless, because of the lack of available data, it remains still difficult to evaluate the relative contribution of natural versus anthropogenic sources on the budget of fluoride in the free troposphere. One way to fill this

Paper number 2000JD900755.
0148-0227/01/2000JD900755$09.00

gap is to check temporal variations of fluoride levels in solid precipitation stored over the past on polar ice sheets (Greenland, Antarctica) or in high-elevated cold glaciers. Such a study was first achieved by *De Angelis and Legrand* [1994] on an ice core extracted from Summit (central Greenland). It was shown that the atmospheric budget of natural fluoride is dominated there by long-range transported soil dust aerosols. In addition, the natural budget of fluoride in the Greenland atmosphere has been frequently disturbed by volcanic emissions in the high-northern latitude belt (Iceland, Aleutians, Kamchatka). Furthermore, the study of recent Greenland snow deposits revealed that the fluoride budget has been significantly disturbed by man-made activities (mainly coal burning) from 1960 to the present day. Finally, this unique study of fluoride in Greenland snow pointed out some difficulties in translating ice core data into atmospheric signals because of the high mobility of fluoride in both firn (exchange of HF inside the porous firn material) and ice (diffusion of fluoride in the ice lattice) layers. That stimulated studies of ice cores from other sites characterized by larger snow accumulation rates which, at least, would limit the modification of initial signals during firnification. The second motivation was mandatory by the fact that large uncertainties exist in the source region apportionment of short live species trapped in Greenland ice deposits.

In this paper, we present variations of fluoride summer and winter levels in Alpine ice cores spanning the twentieth century. That permits us to examine the natural sources contributing to the fluoride budget. The nonnatural contribution is discussed with respect to various anthropogenic sources, in particular coal burning, release of fluoride from aluminium smelters, cement and phosphate industrial processings, the photochemical degradation of recently emitted hydrofluorocarbons (HCFCs) within the troposphere, and the stratospheric HF reservoir built up from the CFC degradation.

2. Sampling, Dating, and Methods

A deep ice core (126-m long) drilled close to bedrock in 1994 at the Col du Dôme, a site located at 4250 m above sea level (asl) nearby the Mont Blanc summit (French Alps), was analyzed at Laboratoire de Glaciologie et Géophysique de l'Environnement (LGGE) and Institut fur Umweltphysik (IUP) laboratories for major ions including Na^+, NH_4^+, Ca^{2+}, Cl^-, NO_3^-, and SO_4^{2-} in seasonal resolution. In addition, fluoride and light carboxylates (formate, acetate, and oxalate; not discussed in this paper) measurements (~1050 samples) were achieved at LGGE laboratory along the upper 117 m of the core which correspond to the well-dated part of the core covering the 1923-1994 time period (Figure 1). The glaciological characteristics of this CDD ice core indicate an annual snow accumulation ranging from 3 to 0.5 m water equivalent (w.e.) from the surface to a depth of 90 m w.e. and a relative amount of winter to summer snow deposition close to 1 nearby the surface and ~ 0.5 at 74 m w.e. depth (see details in the work of *Preunkert et al.* [2000]). Hence seasonally resolved chemical records covering about the last 75 years can be obtained. The precise dating of the 1994 CDD core has been obtained based on well preserved seasonality of ammonium with an accuracy of ±5 years at an ice age of 75 years [*Preunkert et al.*, 2000].

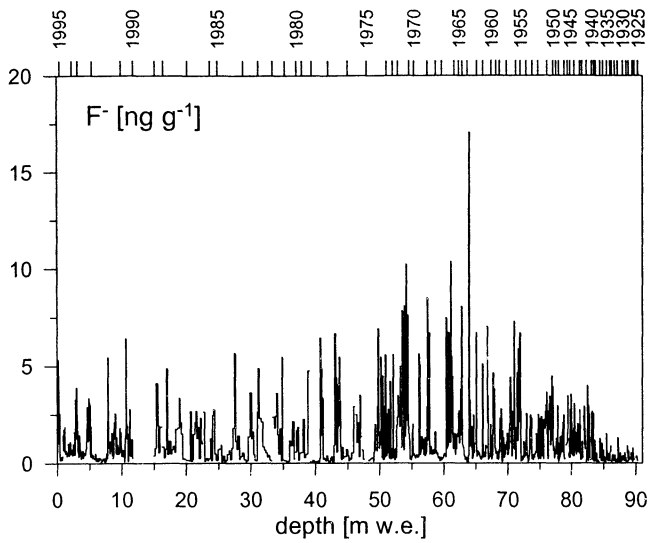

Figure 1. High-resolution depth profile (in meters water equivalent) of fluoride along the upper 90 m w.e. of the 1994 CDD core. The dating reported on the top is discussed in section 2.

Fluoride measurements were achieved by using ion chromatography (IC) procedures commonly used at LGGE [*Legrand et al.*, 1993]. For fluoride a sensitivity of 0.02 ng g^{-1} and an accuracy of 0.05 ng g^{-1} are obtained in the 0.05-50 ng g^{-1} range, when 1 mL sample is used. For other ions the accuracy is typically of 5%. Ice samples were cleaned at LGGE by using an electric plane device previously developed at IUP [*Fischer et al.*, 1998]. The validity of the decontamination procedure for fluoride determinations was tested by checking blank values of pieces of pure ice obtained by freezing ultrapure water from a Millipore system. Blank values were close to the detection limit (0.02 ng g^{-1}), remaining well below the mean fluoride levels observed in Alpine ice (means of 0.35 ± 0.3 ng g^{-1} and 1.5 ± 1.7 ng g^{-1} in winter and summer layers, respectively).

3. Data Presentation

In evaluating long-term chemical records extracted from a small-scale glacier as the Col du Dôme one, special caution has to be paid to systematic changes in the snow deposition characteristics upstream to the drill site. As shown by *Preunkert et al.* [2000], the ratio of winter to summer net snow accumulation is decreasing from 1 nearby the surface to 0.5 at 100 m depth (i.e., 74 m w.e.). This is due to spatial variations in the relative amount of summer and winter snow deposition taking place upstream the borehole. Thus, given the strong seasonality of most chemical species present in CDD snow deposits whose concentrations are characterized by strong summer maxima, such a glaciological forcing induces there a nonatmospheric effect. In this paper, we will therefore discuss temporal trends for both summer and winter seasons instead of the more commonly employed examination of the mean annual trend. Furthermore, the seasonal cycles of various chemical species with summer maximum reflect distinct atmospheric conditions prevailing at high Alpine sites due to presence and absence of upward advection of air

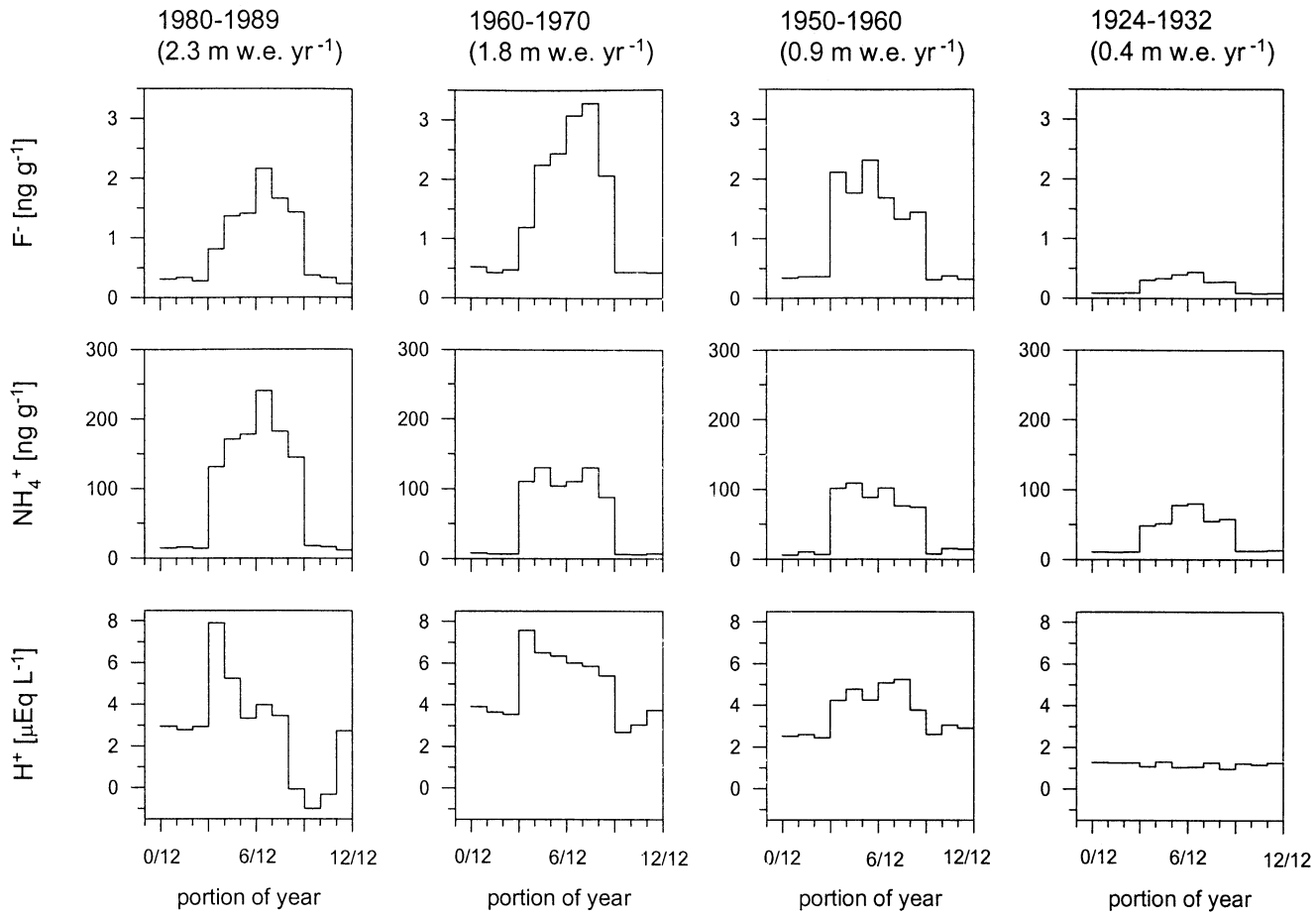

Figure 2. Seasonal cycles of fluoride, ammonium, and acidity (see text) levels in the 1994 CDD ice core averaged over four time periods: 1924-1932 (low anthropogenic input), 1950-1960 and 1960-1970 (maximum of the anthropogenic input related to aluminium smelters), and 1980-1989 (maximum of the anthropogenic input related to coal burning) (see text).

masses from the boundary layer in summer and winter, respectively [*Preunkert and Wagenbach*, 1998; *Baltensberger et al.*, 1997; *Kasper and Puxbaum*, 1998]. Thus the summer trend would depict changes having occurred in the boundary layer at mesoscale or regional scale, whereas the winter trend would reflect changing background conditions of the free troposphere at a larger geographical scale (at least of western Europe).

3.1. Seasonal Cycle

Given the quite large interannual variability of the snow accumulation, and with the aim to examine the mean seasonal cycle over periods covering several years, each winter and summer snow layer has been divided into six equally spaced parts (in w. e.). Following *Preunkert et al.* [2000], the dissection cutting was based on the profile of ammonium which, compared to other ions, exhibits the strongest seasonal cycle. A weighted interpolation was applied to years containing more (or less) than 12 samples. Finally, multiannual means were calculated for each 1/12 annual accumulation fraction for different key time periods. As depicted in Figure 2, whatever the considered time period, fluoride levels exhibit a well-marked seasonal variation characterized by a summer maximum. The mean summer to winter ratio is close to 4, 5, 7, and 4 over the 1924-1932, 1950-1960, 1960-1970, and 1980-1989 time periods, respectively. Such a good preservation of the seasonal cycle of fluoride concentrations over the whole CDD ice core contrasts from the situation at Summit (central Greenland). At that site the diffusion of HF from acidic snow layers corresponding to volcanic inputs occurs during firnification, leading to an average displacement of the initial signal of some 0.3 m w.e. [*De Angelis and Legrand*, 1994]. Given the mean annual snow accumulation rate of 0.23 m w.e. at Summit, such a process renders the identification of the seasonality of fluoride in snow deposits difficult there. As seen in Figure 2, the acidity of CDD snow and ice layers exhibits a summer maximum and has been enhanced over the recent decades. The acidity (or alkalinity) of CDD samples have been evaluated by checking the ionic balance between anions and cations:

$$[H^+] = [F^-] + [Cl^-] + [NO_3^-] + [SO_4^{2-}] + [CH_3COO^-] + [HCOO^-] + [C_2O_4^{2-}] - [Na^+] - [K^+] - [Mg^{2+}] - [Ca^{2+}] - [NH_4^+] \quad (1)$$

with concentrations expressed in microequivalents per liter (μEq L^{-1}).

For the very recent time decades (1960-1970 and 1980-1989) the high acidity of CDD summer layers (~8 μEq L^{-1}) would have permitted the diffusion of fluoride in firn layers. It is likely that the good preservation of the seasonality of fluoride in CDD snow layers over the 1980-1989 and 1960-1970 time periods is related to a sufficient annual accumulation rate of snow, which is close to 2 m w.e. there [*Preunkert et al.* [2000] (i.e., 10 times higher than the one at Summit). As emphasized by *Preunkert et al.* [2000], the seasonal cycle of water isotopes become obliterated at depths corresponding to the 1924-1932 time period in relation with corresponding snow deposits coming from upstream sites where surface accumulation rates are relatively low (from 0.3 to 0.5 m w.e.). Nevertheless, as seen in Figure 2, the fluoride seasonal cycle is still preserved in these layers. The good preservation of the seasonality of fluoride in these bottom layers of the CDD core suggests that, if it had occurred, the diffusion of HF during firnification would have produced a mean displacement of the initial summer maximum of less than some 0.1 m w.e. Such a relatively small displacement in the CDD snow layers compared to the 0.3 m w.e. average seen in Summit snow layers is likely due to an absence of the driving force for the diffusion of fluoride, as suggested by the low acidity (~1 μEq L^{-1}) and its flat seasonal cycle in these bottom CDD layers (Figure 2).

3.2. Impact of Saharan Dust

Previous studies have shown that deposition of saharan dust can sporadically affect Colle Gnifetti (CG) [*Wagenbach et al.*, 1996] and Col du Dôme [*Ronseaux and Delmas*, 1988; *De Angelis and Gaudichet*, 1991] and disturb the chemical composition of snow deposits. Following *Wagenbach et al.* [1996], such events can be identified as calcium-rich layers exhibiting a negative acidity (i.e., alkaline samples). The acidity (or alkalinity) of samples have been evaluated by checking the ionic balance between anions and cations (equation 1). Positive values of $[H^+]$ correspond to acidic samples, negative values to alkaline samples.

In this work, summer samples containing more than 100 ng g^{-1} of calcium and lying below the 25% quantile of a robust spline [*Bloomfield and Steiger*, 1983] through the raw acidity profile, are considered as significantly affected by saharan dust input (85 samples on a total of 762 summer samples). In addition, over the last 4 decades (after 1960), because of enhanced acidity, samples containing saharan dust input can remain acidic [*Maupetit and Delmas*, 1994]. Such samples were characterized by *Maupetit and Delmas* [1994] as having typical sulfate to calcium and nitrate to calcium weight ratios close to 2.6 and 1.2, respectively. Thirteen CDD snow layers deposited after 1960, containing more than 100 ng g^{-1} of calcium and having not be identified as contaminated by saharan dust inputs by using the alkalinity criterium, show a mean sulfate to calcium and nitrate to calcium weight ratios of 2.8 and 1.1, respectively. They were here also considered as contaminated by saharan dust input. With the aim to examine the winter trend of background conditions, based on examination of the ammonium profile (see section 3.1), on the 337 samples regarded as deposited during the winter half year, we here only considered those having ammonium concentrations lower than 10 ng g^{-1} (i.e., 217 samples).

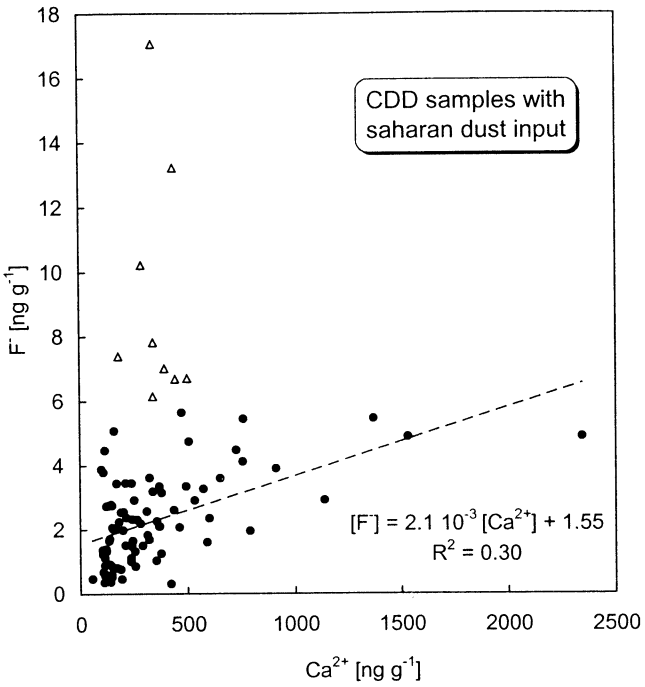

Figure 3. Fluoride versus calcium contents of CDD samples suspected to contain saharan dust inputs (see section 3.2). Open triangles and solid circles refer to samples having more and less than 6 ng g^{-1} of fluoride, respectively (see text). The dashed line refers to the linear relationship between fluoride and calcium contents when the nine samples containing more than 6 ng g^{-1} of fluoride (i.e., strongly influenced by anthropogenic inputs, see text) are discarded.

Among these winter samples, four containing a calcium content higher than 20 ng g^{-1} and having an alkalinity lying below the 25% quantile of the robust spline, were also suspected to be contaminated by saharan dust input.

For sulfate the observed concentrations of these 98 summer and 4 winter samples were corrected from the terrigeneous contribution (presence of gypsum) according to

$$[SO_4^{2-}]_{cor} = [SO_4^{2-}] - 0.59 \times [Ca^{2+}],$$

where the factor of 0.59 represents the mean weighted sulfate to calcium ratio observed by *Wagenbach et al.* [1996] in dust horizons of the preindustrial era at Colle Gnifetti.

Note that this ratio (0.59) is consistent with the one observed in dust events located in the bottom part (from 117 to 126 m depth, i.e., samples older than 1910) of the CDD core (0.47, with R^2 = 0.37 for 40 samples). Since the fluoride content has not been measured neither in preindustrial CG dust layers nor in the bottom part of the 1994 CDD core, it is not possible to gain an accurate estimation of the amount of fluoride present in such saharan dust inputs. The examination of the 98 CDD summer samples suspected to be contaminated by saharan dust inputs (Figure 3) points out the complexity of the problem. Indeed, samples regarded as contaminated by saharan dust events include the nine samples (open triangles in Figure 3) exhibiting the highest fluoride levels of the entire profile (more than 6 ng g^{-1}) in which a quite moderate amount

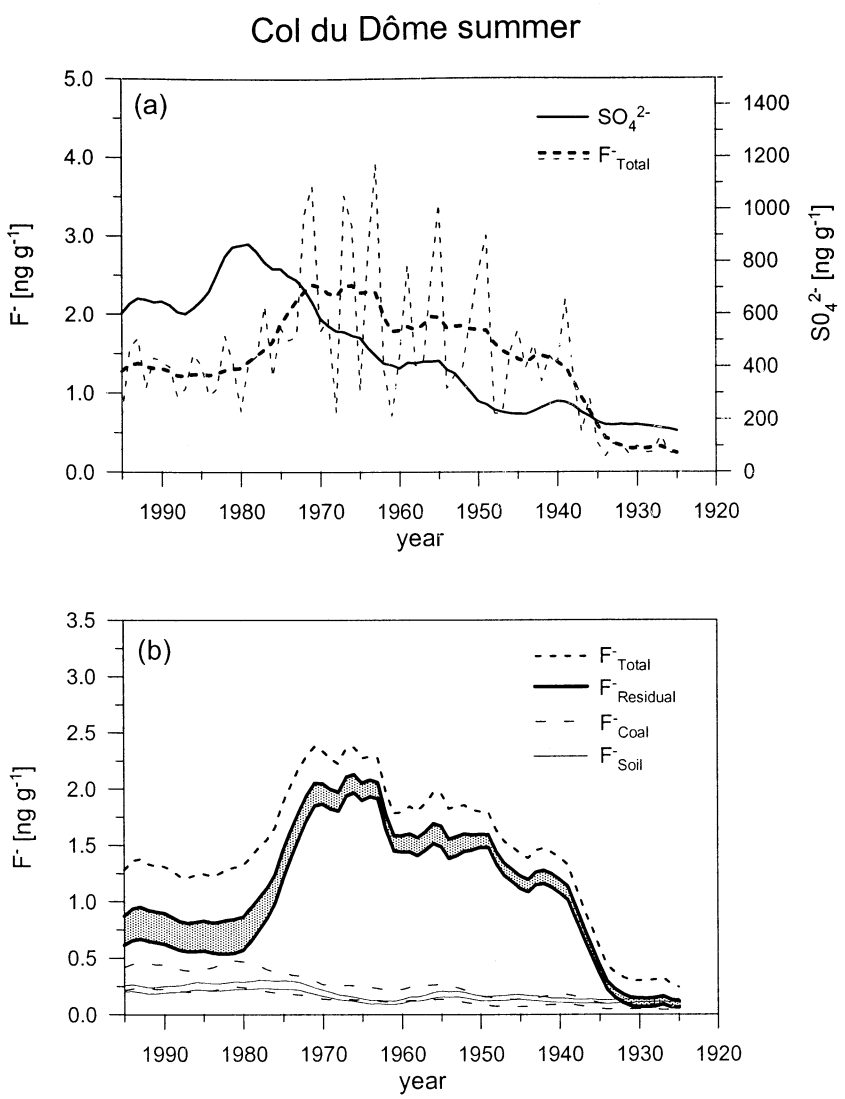

Figure 4. (a) Summer trend of sulfate (solid line) and total fluoride (dashed line) levels in the 1994 CDD core. In addition, for total fluoride, individual summer means are reported as well (thin-dashed line). (b) Contribution to the total fluoride (F^-_{Total}, dashed line) of soil dust (F^-_{Soil}, thin-dashed line), coal burning (F^-_{Coal}, thin solid line), and residual ($F^-_{Residual}$, grey area) emissions since 1925 in summer CDD layers. Calculations of residual fluoride levels have been made by considering a fluoride to sulfate ratio corresponding to coal burning ranging from 0.56 to 1.1 10^{-3} (see section 5.1) and two values of the fluoride to calcium content of soil dust (3 and 4 10^{-3}, see section 4). All curves are smoothed profiles (first component of SSA with a 5-year time window).

of calcium (less than 600 ng g^{-1}) is present. They are located at depths between 53.5 and 72 m w.e. and correspond to samples deposited at CDD between 1954-1972, a period over which a maximum of anthropogenic fluoride input related to aluminium smelters took place (see section 5.2.1). Thus the fact to discard these nine samples would bias the overall trend. On the other hand, other samples contaminated by dust inputs reveal a quite low fluoride content with respect to a high calcium content (Figure 3). Among samples contaminated by saharan dust input, only considering those containing less than 6 ng g^{-1} of fluoride (89 samples, solid circles in Figure 3), we obtained the following relationship:

$$[F^-] = 2.1\ 10^{-3} \times [Ca^{2+}] + 1.55 \text{ (with } R^2 = 0.29).$$

Although exhibiting a rather poor correlation, likely due to the variable amount of fluoride of anthropogenic origin present in ice, this relationship suggests that, with a fluoride to calcium ratio close to 2 10^{-3}, saharan dust likely contains less fluoride than soil inputs (fluoride to calcium ratio of 3 to 4 10^{-3}, see section 4). On the basis of this discussion we will examine the fluoride trend considering all samples, including those suspected to be influenced by saharan dust which have been corrected from their terrigeneous contribution using a fluoride to calcium ratio of 2 10^{-3}.

3.3. Summer and Winter Trends

With the aim to examine winter and summer trends, we first calculated individual half (summer and winter) means. For

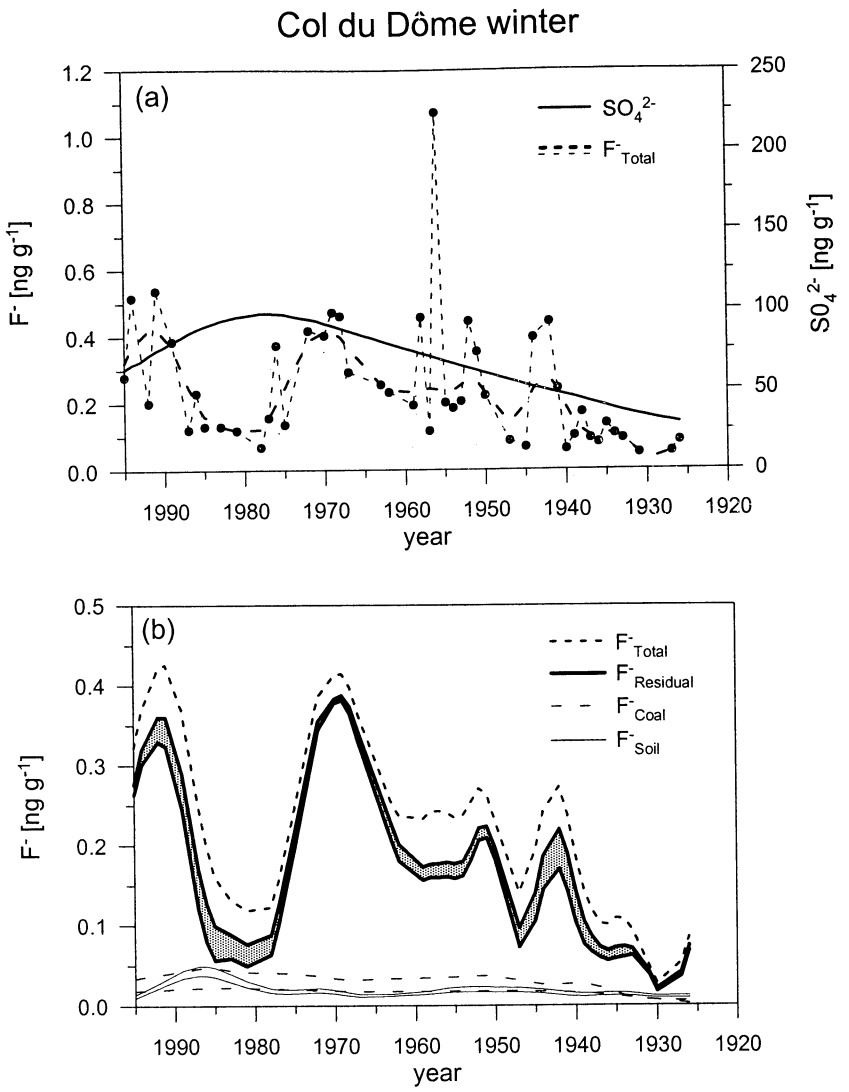

Figure 5. (a) Winter trend of sulfate (solid line), and total fluoride (dashed line) levels in the 1994 CDD core. In addition, for total fluoride, individual winter means are reported as well (thin-dashed line). Owing to difficulties sometimes encountered to identify some winter layers, for smoothing we here applied a robust spline (dots indicate the years for which a winter layer can be estimated). (b) Contribution to the total fluoride (F^-_{Total}, dashed line) of soil dust (F^-_{Soil}, thin-dashed line), coal burning (F^-_{Coal}, thin-solid line), and residual ($F^-_{Residual}$, grey area) emissions since 1925 in winter CDD layers. Calculations of residual fluoride levels have been made by considering a fluoride to sulfate ratio corresponding to coal burning ranging from 0.56 to 1.1 10^{-3} (see section 5.1) and two values of the fluoride to calcium content of soil dust (3 and 4 10^{-3}, see section 4).

summer the individual half-year means were smoothed using Single Spectra Analysis (SSA) with a time window of 5 years. We here examine the first component of SSA summer trends which depicts the overall tendency of the temporal change detected in summer CDD layers (Figure 4a). For winter, owing to the lack of some individual winter means (see section 3.2), we applied a robust spline smoothing [*Bloomfield and Steiger*, 1983] (Figure 5a).

4. Natural Fluoride Inputs

In this section we examine the sources contributing to the natural fluoride budget at high elevated Alpine sites. Natural fluoride sources include primary sea-salt and soil dust aerosol emissions as well as volcanic HF plumes. Apart from explosive volcanic eruptions, the quasi-passive emissions can contribute to the background fluoride level of the free troposphere. Given the relative short life time of HF (a few days), these passive emissions can be of importance when volcanoes are located close to the glacier site. For instance, Greenland snow layers are very often impacted by fluoride emissions from the numerous volcanoes located in the high northern latitude belt (Iceland, Aleutians, Kamchatka) [*De Angelis and Legrand*, 1994]. For the Alps the Mount Etna (Sicily), which continuously emits acidic gases at more than 3000 m asl, represents a possible fluoride source. On the basis of remote sensing of SO_2 emitted by Mount Etna in its normal state of permanent activity (0.37 10^{10} g per day

[*Haulet et al.*, 1977]) and a few HF measurements achieved in gas exhausts by *Le Guern* [1988], we calculate a mean annual fluoride flux of 8 10^{10} g. Compared to the annual fluoride emissions from aluminium smelters (~2 10^{10} g in 1970, for instance, calculated with assumptions detailed in section 5.2.1) and from coal burning (7 10^{10} g in 1970, see details in section 5.1) at the scale of Europe, these volcanic emissions are significant. Given the mean fluoride levels seen in summer and winter CDD layers deposited prior to 1930 (0.25 and 0.07 ng g^{-1}, respectively) with respect to the ones seen in layers deposited between 1940 and 1990 (1.6 and 0.25 ng g^{-1}, respectively) (Figure 2), the Mount Etna contributes, in spite of its relatively large continuous HF emissions, at the best for 16 to 28% to the mean fluoride budget in Alpine snow deposited over the last 60 years. Furthermore, no evidence of an impact of the Mount Etna during eruptive stages could be detected in CDD snow layers which reveal no unusually high concentrations of fluoride in 1983 and 1992/1993 (Figure 1), 3 years of major activity of the volcano. Probably the Mount Etna does not contribute therefore to the modern Alpine fluoride budget either because the volcanic plume is not significantly transported toward the Alps or due to a too short lifetime of HF in the atmosphere. Indeed, as emphasized by *De Angelis and Legrand* [1994] for other volcanoes, it is likely that a large fraction of volcanic HF emissions is rapidly scavenged along with ash particles from plume.

The relevance of an oceanic fluoride source from sea salt aerosol is unlikely for high Alpine sites. The sodium concentration present in high-elevated Alpine sites is thought to be related to sea salt aerosols as a well as from sodium bearing soil dust [*Maupetit and Delmas*, 1994]. As an upper limit, assuming that the sodium content of CDD snow layers is only related to the sea salt content of the atmosphere at the site and considering the fluoride to sodium weighted ratio in ocean water (1.2 10^{-4} *Mason* [1982]), we obtain a sea-salt fluoride contribution ranging from 1.2 to 4.8 10^{-3} and from 0.6 to 1.8 10^{-3} ng g^{-1} in summer and winter CDD snow layers, respectively.

Assuming that sea-salt aerosols and volcanic HF emissions do not contribute to the fluoride budget of Alpine snow, the only natural source expected to contribute to the fluoride budget is soil dust emission. With the aim to quantify the natural crustal fluoride contribution, we have measured fluoride in eight ice samples deposited at CG previous to 1880. Although based on a limited number of samples, the small amount of fluoride non related to the calcium content (0.04 ng g^{-1} derived from the linear relationship reported in Table 1) suggests that the main part of fluoride present in Alpine snow deposited during the preindustrial era is soil derived, confirming the previous finding from *De Angelis and Legrand* [1994] of a major contribution of soil dust to the natural fluoride budget in Greenland. In order to quantify the fluoride soil dust contribution, we examined the relationship between fluoride and calcium in the CDD snow layers deposited between 1923 and 1935, a period over which anthropogenic inputs related to coal burning and fluoride release from aluminium smelters remained relatively limited (see sections 5.1 and 5.2.1). When only samples containing less than 100 ng g^{-1} of sulfate are considered (i.e., samples which can be regarded as virtually free of coal burning input given the mean sulfate summer level of 80 ng g^{-1} observed at CG previous to 1880), a fluoride to calcium weighted ratio of 3.4 10^{-3} is obtained (Table1). A similar value is obtained (3.9 10^{-3}) when all samples, including those containing up to 300 ng g^{-1} of sulfate of which ~ 220 ng g^{-1} can be considered as related to coal combustion, are considered. The consistency between these two values is due to the fact that the fluoride coal burning contribution in these samples (up to 0.22 ng g^{-1}, see section 5.1) remains moderate compared to the soil dust fluoride input (~0.52 ng g^{-1}, assuming a 3.4 10^{-3} fluoride to calcium ratio). As summarized in Table 1, these values of the ionic fluoride to calcium weight ratios derived in Alpine (CG and CDD) snow deposits are in the range of the one derived from Greenland ice, and are 3 to 8 times lower than the fluor to calcium weight ratio measured in soils (1.5 10^{-2} [*Vinogradov*, 1959]). Such a difference is likely related to the fact that only the ionic fluoride content has been determined in ice cores whereas soils would contain other insoluble fluoride derived species.

The preindustrial fluoride (prior to 1880) level in CG samples, which can be regarded as of natural origin (soil emissions), is found to be close to 0.3 ng g^{-1}. For CDD we calculate the contribution of these natural soil dust emissions for summer and winter layers based on the calcium profiles and using fluoride to calcium ratios of 3 and 4 10^{-3}. In summer the soil dust contribution ranges from 0.10 to 0.26 ng g^{-1}, representing for example 42 ± 5% and 6 ± 1% of the total fluoride levels in 1930 and 1970, respectively (Figure 4b). In winter the soil dust fluoride levels range from 0.01 to 0.04 ng g^{-1}, contributing with 39 ± 9% in 1930 and 4 ± 1% in 1970 to the total fluoride levels (Figure 5b). Thus this major natural source contribution to the total fluoride decreases from a

Table 1. Estimated Values of the Fluoride to Calcium Weighted Ratio in Alpine (This Work) and Greenland Snow Layers [*De Angelis and Legrand*, 1994] and in Soils [*Vinogradov*, 1959]

	Number of Samples	R^2	Relationship Between Ca and F Contents
Pre-1880 CG snow deposits	8	0.96	$[F^-] = 2\ 10^{-3}\ [Ca^{2+}] + 0.04$
1923-1935 CDD snow deposits ($[SO_4^{2-}] < 100$ ng g^{-1})	40	0.47	$[F^-] = 3.4\ 10^{-3}\ [Ca^{2+}] + 0.07$
1923-1935 CDD snow deposits (all samples)	106	0.53	$[F^-] = 3.9\ 10^{-3}\ [Ca^{2+}] + 0.11$
1910-1962 Summit snow deposits	525	0.28	$[F^-] = 5\ 10^{-3}\ [Ca^{2+}] + 0.015$
Mean soils	-	-	$[F] = 1.5\ 10^{-2}\ [Ca]$

third in 1930 to less than a tenth over the recent decades, which is related to enhanced anthropogenic inputs in Alpine snow.

5. Causes of Anthropogenic Increases

As seen in Figures 4a and 5a, both summer and winter fluoride levels were enhanced at CDD in the late 1930s. In the following, we will examine the impact of various anthropogenic processes on the fluoride budget of CDD layers deposited between 1930 and 1995.

5.1. Coal Burning Contribution

HF and SO_2 are both primarily emitted by coal burning. Assuming an averaged mixing ratio of 100 (from 85 to 295) ppm fluoride in coal and that 60% of it is emitted during combustion as HF, *Cadle* [1980] proposed a mean HF to SO_2 weight ratio of 2 10^{-3} (from 1.7 to 5.9), giving a corresponding fluoride to sulfate weighted ratio ranging from 1.1 to 4.0 10^{-3} for coal burning emissions. The value of this ratio is dependant of the geographical origin of the employed coal. At present, the coal used in western Europe thermal-electric stations contains 180 ppm of fluoride, leading to a HF to SO_2 weight ratio of 3.6 10^{-3} (i.e., a corresponding fluoride to sulfate weighted ratio of 2.4 10^{-3}) (Electricité de France, personal communication, 2000).

The fraction of fluoride related to coal burning can be estimated from the sulfate snow content. Since the atmospheric fates of HF and SO_2 are not identical with respect to wet and dry deposition processes and considering the further conversion of SO_2 into sulfate aerosols, the fluoride to sulfate ratio is, however, not necessarily conservative after emission. In order to evaluate to what extent this ratio has been modified after the long-range transport of HF and SO_2 (or sulfate) toward the remote glacier site, we examined CDD ice layers corresponding to the 1923-1935 time period over which the anthropogenic input related to aluminium smelters can be still neglected (see section 5.2.1). For these samples the multiple regression of fluoride to calcium and anthropogenic sulfate related to coal combustion yields

$$[F^-] = 0.09 + 3.7\ 10^{-3} \times [Ca^{2+}] + \alpha\, 0.56\ 10^{-3} \times [SO_4^{2-} - SO_4^{2-}{}_P]$$
$$(R^2 = 0.69 \text{ for } 96 \text{ samples}),$$

where $SO_4^{2-}{}_P$ is the preindustrial sulfate level at CG (80 ng g^{-1}) and α the mean relative fraction of fossil fuel combustion to the total anthropogenic sulfate emission in Europe between 1923 and 1935 (0.85 [*European Monitoring and Evaluation Programme (EMEP),* 1993]).

From that we derive a mean weighted fluoride to coal burning related sulfate of 0.56 10^{-3} in snow deposited at CDD. Referring to the (1.1-4.0) 10^{-3} range proposed by *Cadle* [1980] for the F^-/SO_4^{2-} ratio in coal burning emissions, we thus may infer a depletion of this ratio during transport to and deposition at CDD by at least a factor of 2.

In order to evaluate an upper limit of such a depletion factor (mostly driven by long-range transport), we examined the ice core record from Greenland since (1) the main anthropogenic fluoride input is thought to be related to coal burning there [*De Angelis and Legrand*, 1994], and (2) for this site the transport time between the source regions and the deposition site is much more important than for Alpine sites. As previously discussed by *De Angelis and Legrand* [1994], the Summit fluoride ice core record exhibits an increase of the background level in the late 1950s (related to growing coal burning emissions) and sporadic perturbations which have been attributed to either volcanic eruptions (Hekla in 1970 and 1947, Katmai in 1912) or large forest fire (1908) (Figure 6). Owing to an efficient remobilization of fluoride in firn layers, sporadic fluoride perturbations also disturb the background fluoride level in adjacent layers corresponding to one year before and after the time of the event. Discarding these layers (1970 and 1971, 1946 to 1948, and 1907/1908), we calculated the nondust fluoride level of Summit snow layers deposited between 1886 and 1980 by using the fluoride to calcium

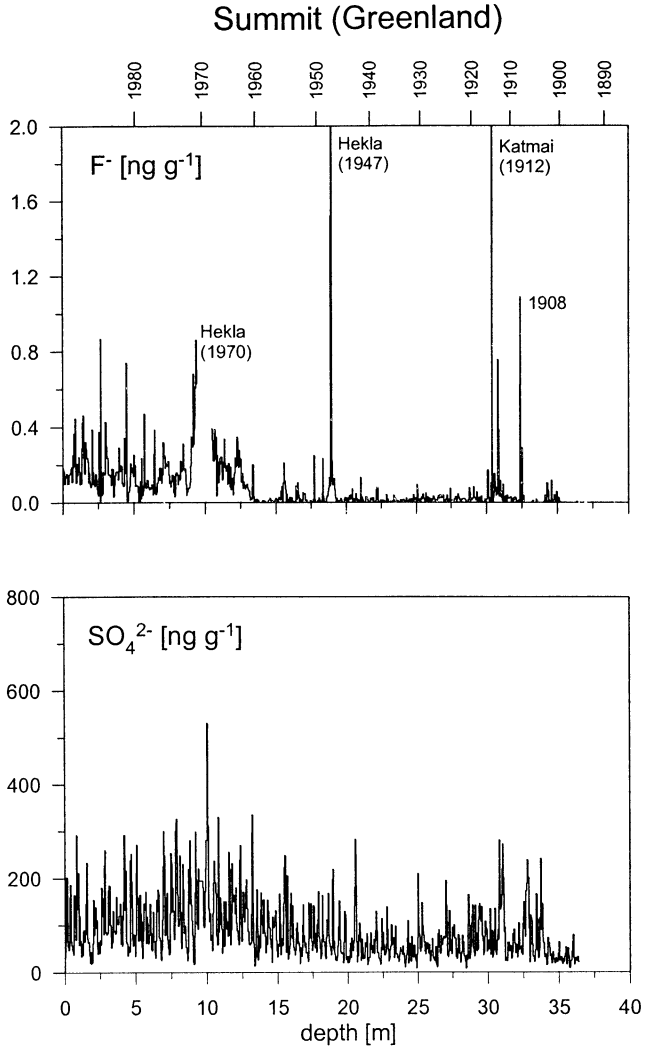

Figure 6. Fluoride and sulfate depth profiles (in meters) at Summit (central Greenland) from 1890 to 1989. Note the sporadic perturbations which correspond to the 1970 Hekla eruption, the 1947 Hekla eruption, the 1912-1913 Katmai eruption, and the 1908 fire event. Adapted from *De Angelis and Legrand* [1994].

weight ratio of 5 10^{-3} observed by *De Angelis and Legrand* [1994] in preindustrial Greenland layers following:

$$\text{Nondust } [F^-] = [F^-] - 5\ 10^{-3} \times [Ca^{2+}].$$

The linear relationship between nondust fluoride and sulfate levels yields the following: Nondust $[F^-] = 0.0011\ [SO_4^{2-}] - 0.04$ ($R^2 = 0.45$ for 77 samples), suggesting a mean ratio of 1.1 10^{-3}. Assuming that the sulfate amount related to coal burning accounted from 77% in 1960 to 60% in 1980 [*EMEP*, 1993] to the total anthropogenic sulfur emissions in Eurasia, the fluoride to sulfate ratio of 1.1 10^{-3} suggests a fluoride to sulfate ratio related to coal burning of 1.65 10^{-3}. Whatever the fluoride content of the burned coal impacting Greenland, this ratio suggests that, after long-range transport, the emission ratio is at the best reduced by a factor of 2.4.

Having no information on the fluoride content of coal used at the beginning of the twentieth century in Europe, we have used two possible values of the fluoride to sulfate weighted ratio in order to estimate the contribution of coal burning to the total fluoride content in CDD snow. As discussed above, a value of 0.56 10^{-3} derived from the bottom CDD layers (i.e., the 1924-1935 time period) can be used. Over the more recent decades it is not possible to derive this ratio directly since the CDD layers are strongly disturbed by fluoride release from aluminium smelters (see section 5.2.1). For this time period, based on the known value of the ratio (2.4 10^{-3}) at the emission and assuming a mean decrease of the ratio at the deposition stage by a factor 2.2 (see above discussions), a value of 1.1 10^{-3} is realistic.

In Figures 4b and 5b we report summer and winter trends of the level of fluoride related to coal burning in CDD layers which were obtained by multiplying sulfate levels by a factor of 0.56 and 1.1 10^{-3}, respectively (see above) and by a time-dependant factor α corresponding to the estimated fraction of the total sulfate related to solid fuel combustion in western Europe [*EMEP*, 1993].

In summer, coal burning emissions led to increased fluoride levels in CDD layers from 0.04-0.09 ng g^{-1} in 1930 to 0.22-0.44 ng g^{-1} in 1980 to 1995, which represented 23 ± 7% in 1930, 8 ± 2% in 1970, and 25 ± 8% in 1980-1995 of the total fluoride input. The coal burning emissions in winter increased fluoride levels in CDD layers from less than 0.02 ng g^{-1} in 1930 to 0.02-0.04 ng g^{-1} in 1980 to 1995, which represented 23 ±1% in 1930, 6 ± 2% in 1970, and 26 ± 9% in 1980 of the total fluoride input.

5.2. Other Anthropogenic Inputs

As discussed in sections 4 and 5.1, soil dust emissions and coal burning input only represented minor contributions (together less than a half) of the total fluoride amount seen in CDD winter and summer layers deposited after 1930. In Figures 4b and 5b we reported the summer and winter trends of the residual part of fluoride related neither to soil dust nor to coal burning. Common features of temporal changes include a strong increase between 1930 and 1940 (from 0.02 to 0.12 ng g^{-1} in winter, and from 0.1 to 1.2 ng g^{-1} in summer), reaching a maximum in 1970 (0.37 and 1.6 ng g^{-1} in winter and summer, respectively). They were then strongly decreased in 1980 to 0.06 and 0.70 ng g^{-1} in winter and summer, respectively. Note that these changes of fluoride clearly differ from those of sulfate levels which were mainly enhanced after the second world war, and reached their maximum in the early 1980s (Figures 4a and 5a). That suggests that, in addition to fossil fuel combustion, other anthropogenic sources had likely disturbed the fluoride budget of high-elevated Alpine snow deposited since 1930.

5.2.1. Impact of fluoride release from aluminium industry. Apart from coal burning emissions, among other possible anthropogenic sources of fluoride impacting the Alps, the release of fluoride from aluminium smelters might represent a very significant source. Indeed, the aluminium productions started in Europe well before the second world war and are well-known for their damages caused to nearby vegetation and animals in Alpine valleys due to the massive release of fluoride in the 1960s. The igneous electrolytic reduction of Al_2O_3 into aluminium ($2\ Al_2O_3 + 3C \rightarrow 4\ Al + 3\ CO_2$) requires the addition of fluorinated compounds (typical mixture of 80% of Na_3AlF_6, 12% AlF_3, 5% CaF_2, and 3% Al_2O_3) to reach a temperature of ~950°C. The amount of fluoride released to the atmosphere by aluminium smelters has changed over the whole twentieth century depending on the aluminium production rate, the amount of fluoride used in the bath to depress the temperature of the igneous electrolysis of alumine, and the efficiency of systems set up to limit fluoride emissions. For instance, in France, at the pioneer stage of the aluminium production in 1900, a large amount of fluoride was needed for the electrolysis: 300 to 400 kg per ton of produced aluminium [*Morel*, 1992]. The amount was then progressively reduced, from 100 to 50 kg between 1914 to 1930, and to around 30 kg in 1950. From 1952 to 1963 this amount was decreased to 25 kg per ton of aluminium. Previous to 1963, no efficient systems was available to reduce fluoride emissions and more than a half of the deployed fluor amount was released to the atmosphere. From 1963 to 1975, due to injuries which reached an apotheosis in the late 1960s, efficient precautions were gradually taken to reduce fluoride releases from aluminium smelters. In particular the use of cap systems equipped with Al_2O_3 filter (chimisorption of HF) permitting a strong reduction of fluoride release from ~20 to 6 kg per ton of produced aluminium. As an example, Figure 7 depicts the evolution of the annual amount of aluminium produced by one of the major aluminium smelter of France (St Jean de Maurienne) located in the Alps, which accounted on average for 20 to 40% of the total French aluminium production (see Table 2) and for which a detailed documentation of annual fluoride release is available since 1940. The major change occurred at St Jean between 1970 and 1975 with a strong decrease of the amount of fluoride release from 17 to 6 kg per ton of aluminium.

In order to estimate temporal changes of fluoride release from the aluminium smelters in western European countries located around the Alps, we collected data from France, Switzerland, western Germany, and Italy. Since Italy represents a rather weak contributor among western Alpine border countries, we neglected this contribution. In general, the annual aluminium production is more or less accurately documented for these countries since the beginning of the twentieth century in *Morel* [1992] and *Rauch* [1962] (additional data are also available in statistics from

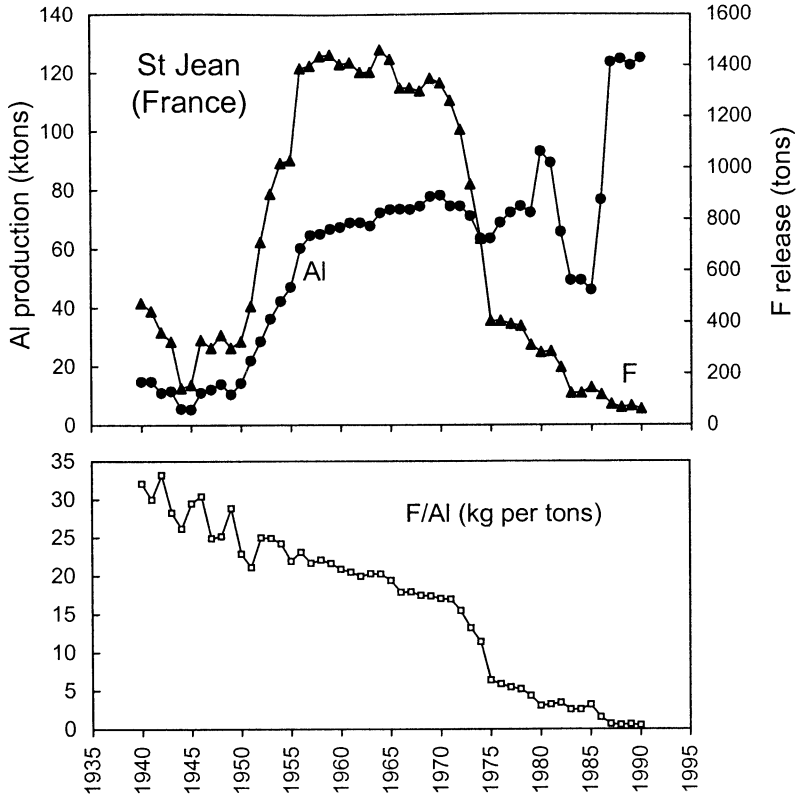

Figure 7. (Top) Aluminium production (in kilotons) and fluoride release (in tons) from the aluminium smelters at the Saint Jean station (French Alpine valley) since 1940. (Bottom) Amount of fluoride (in kg) released per ton of produced aluminium.

Organization for Economic Cooperation and Development (OECD)). The annual ratio of fluoride emissions to the aluminium production is essentially documented in Switzerland and France. Before 1970, values of this ratio clearly represent crude estimates, except for the St Jean de Maurienne station (France) for which the values are based on measurements since 1940. For Switzerland the estimated fluoride releases are available each 5 or 10 years since 1900 (see the corresponding F/Al ratios reported in Table 2), and the annual aluminium production is fairly well documented since 1900; when not available we performed a linear interpolation. For France the annual aluminium production is well documented since 1900 [*Morel,* 1992]. As shown in Table 2, an annual documentation of the fluoride release due to the aluminium production is available at St Jean, whereas information before 1970 for total France has to be considered as crude estimates. We thus have assumed a mean total ratio for France taking into account the significant St Jean production with respect to the total France. For western Germany we used available aluminium production [*Rauch,* 1962] to which we have applied the same ratio as applied for total France.

Since winter and summer residual fluoride trends show a common feature until 1980 but though the winter trend is less well documented (see section 3.3), we compared in Figure 8 the estimated fluoride release from Switzerland, Switzerland plus France, and Switzerland plus France and western Germany with the summer trend of residual fluoride levels. A good agreement between the residual fluoride trends and temporal variations of fluoride emissions from the aluminium smelters is found when total emissions from Switzerland and France or France alone are considered (Figure 8). Conversely, when the releases from western Germany are also considered, the total fluoride emissions reached a high value in 1940 and remained in this order of magnitude until 1980. That clearly differs from the changes of residual fluoride levels detected in ice which gradually increased from 1940 to 1970 and then strongly decreased from 1970 to 1980. Thus it appears that emissions from Germany accounted less than France (or France together with Switzerland) for fluoride deposition in the Alps. That is coherent with the location of smelters in Germany which are essentially located several hundreds of kilometers from the Alps. Reversely, in France, smelters are mainly located around the Mont Blanc massif (within 130 km) with only a few ones in the Pyrenees (600 km from the site). In addition, the release of fluoride from Pyrenean smelters remained insignificant until 1960 and accounted for 30% of total France emissions between 1970 and 1995.

The gradual increase of residual fluoride levels between 1940 and 1970 (Figure 8) displays with past fluoride emissions from the St Jean smelters located 70 km away from the CDD site, showing a huge increase between 1950 and 1955 and then a constant value from 1955 to 1970 (Figure 7). Thus the CDD record does not reflect fluoride emissions from sites located within a few tens of kilometers from the site. This conclusion contrasts with a very recent study of fluoride in

Table 2. Amount of Fluoride Released per Ton of Produced Aluminium[a]

Years	Switzerland	Total France	St Jean (France)	Adopted Values for France and Western Germany
1900	27.6	more than 180		200 (1900 to 1905), then 45
1914		>30		30
1920	26.4	>30		30
1930	22.7	>30		30
1933		~30		30
1940	21		32.1 (24%)	30
1943			28 (22%)	30
1950	22.6		23 (23%)	27
1953		15-25	25 (34%)	25
1955	18.3		22 (37%)	22
1960	12.2		21 (29%)	16
1963		12.5	20.3 (23%)	14
1965	12.7		19.4 (21%)	12.5
1970	8.6	9.26	17.0 (19%)	9.3
1975	7.6	7.66	6.4 (18.5%)	7.66
1979		4.2	4.3 (18%)	4.2
1980	2.56		3.05 (21%)	L.E.
1987		2.6	0.7 (37%)	2.6
1990	2.28		0.55 (38%)	2.3
1995				2

[a] Fluoride is in kilograms. Switzerland data are from the Swiss Agency for the Environment, Forests and Lanscape; total France data are from *Morel* [1992], and the St Jean Station data were provided by the manufactory environmental and research department of Pechiney at St Jean. For St Jean, numbers in parenthesis depict the relative contribution (in %) of the site to the total France aluminium production.

an ice core extracted from the Grenzgletscher glacier (Monte Rosa massif) spanning the 1937-1994 time period [*Eichler et al.*, 2000]. The authors suggested that the observed fluoride trend can be related to increasing aluminium production from two smelters located in Switzerland, 40 km from the site. However, since the Grenzgletscher record only extends back to 1937, a period over which fluoride emissions from Switzerland were almost as high as in the 1960s (see Figure 8), it remains difficult to establish a source region apportionment for this site.

Interestingly, in 1970 the level of fluoride attributed to aluminium smelters (~2 ng g^{-1}) was 10 times higher than the amount attributed to coal burning (Figure 4b), whereas annual coal burning emissions from France and Switzerland (~14 10^9 g, based on an emission of 3 10^{12} g of SO_2 [*EMEP*, 1993]) were 3 times higher than emissions from aluminium smelters. This difference between emission rates and deposition is likely due to the proximity of the aluminium smelters to the Alpine massif (more than 70% of the total France plus Switzerland emissions being located in western Alpine valleys). Finally, note that whatever is the considered history of emissions, it seems that emissions have been underestimated between 1940 and 1950 (Figure 8). That is plausible since during that time emissions of fluoride remained poorly documented.

Finally, note that the summer to winter ratio of residual fluoride concentrations in 1970, which we can mainly attribute to releases from aluminium smelters at that time, is close to a factor of 5. Since no seasonal variation is expected for this anthropogenic source, this value may represent a typical enhancement factor for short-lived chemical species deposited at high Alpine sites which is governed by the reinforced upward motion in summer.

5.2.2. Very recent anthropogenic input. The mean residual summer fluoride level which was maintained from 1980 to 1995 (0.75 ng g^{-1}) is well above the level observed in 1930, whereas release from aluminium smelters were similar (Figure 8). That suggests that over the 2 last decades other anthropogenic activities also contribute to the fluoride budget at CDD in summer. The degradation of HCFCs whose emissions strongly increased after 1985 as substitutes of CFCs may also contribute the recent summer fluoride budget. Some of the carbonyl compounds (COF_2, COFCl, HCOF, and CF_3COF) produced from the OH oxidation of HCFCs can subsequently produce HF via hydrolysis. *Harnisch* [1999] estimated that 5 10^{10} g of total fluorine are annually removed from the atmosphere, with a maximum deposition occurring in tropical regions associated with high oxidation rates of the parent compounds and high rainfall there [*Kanakidou et al.*, 1995]. Compared to the global fluoride coal burning emissions of 18 10^{10} g in 1970 [*Cadle*, 1980], and since fluoride (in the form of HF) only represents a fraction of the total fluorine (5 10^{10} g) removal from HCFCs, it is likely that the degradation of HCFCs is not the origin of the remaining level of residual fluoride present in CDD snow layers deposited from 1980 to 1990.

With a global annual fluoride emission of 15 and 20 10^{10} g [*Harnisch*, 1999], phosphate and cement industrial

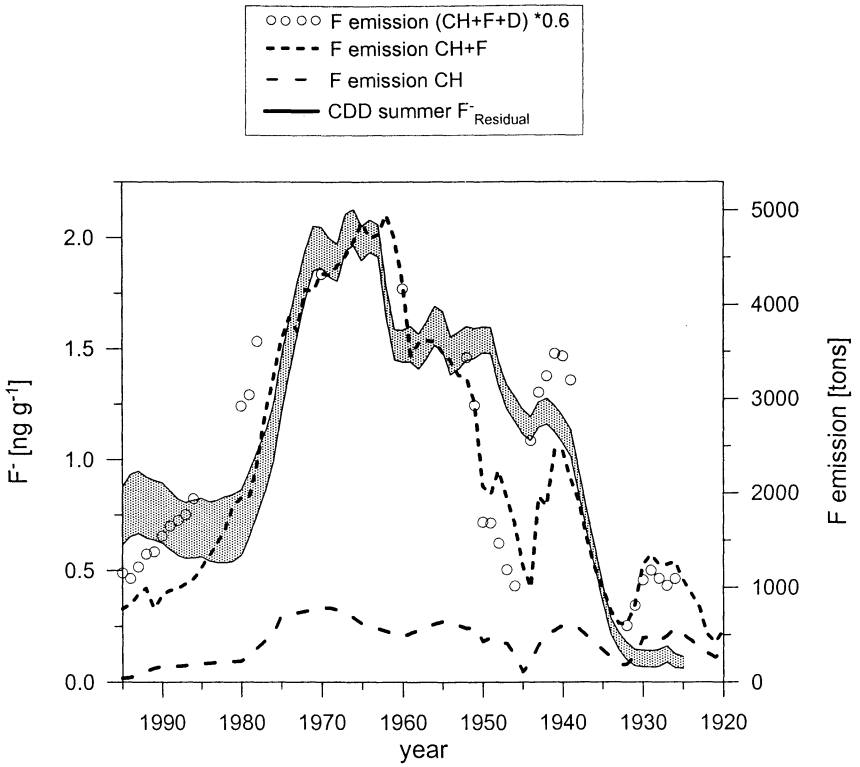

Figure 8. Temporal CDD summer trend of residual fluoride levels (see text) (grey area) along with history of fluoride release from Switzerland (CH), Switzerland plus France (CH + F), and Switzerland plus France and western Germany (CH + F + D) (multiplied by a factor of 0.6).

processings, respectively, may largely contribute to the present-day summer fluoride CDD layers. On a global scale, present-day fluoride emissions from these two industrial sources are as high as twice emissions from coal burning in 1970. Referring to our estimated contribution of coal burning at the deposition stage for 1970 (~0.2 ng g^{-1}, see Figure 4b), we estimate that ~ 0.4 ng g^{-1} of fluoride may be related to these industrial processes in snow layers deposited in the 1990s. That is a half of the residual fluoride level (0.75 ng g^{-1}) seen in 1990's snow deposits. Finally, these industrial processes may also have contributed to the fluoride budget prior 1980. However, with an expected contribution of less than 0.4 ng g^{-1} at the deposition stage, their impact were likely far less important with respect to emissions from aluminium smelters before 1980.

Because of difficulties concerning the identification of some of the winter half years, the winter fluoride trend is less documented at CDD, if compared to the summer one (section 3.3). Nevertheless, as discussed in section 5.2, both trends exhibit a common feature until 1980. An important difference shows up, however, in the 1985 to 1990 period where the winter residual fluoride fraction increases from 0.05 to 0.30 ng g^{-1} which is not detected in the summer trend due to its much higher level and variability. Although this very recent change of the winter fluoride level still needs to be confirmed by other ice core records, it suggests that a distinct enhancement of the fluoride background occurred at least on the western Europe scale since the late 1980s (note that, as emphasized in section 3, Alpine winter levels of pollutants are representative for a large spatial scale). Among others, this change may possibly be attributed to the photochemical degradation of freons to form stratospheric HF which is then transported to CDD by subsidence of stratospheric air masses. In order to verify this hypothesis we made a first-order estimate of the stratospheric HF level to be expected at high accumulation Alpine drill sites by deploying cosmogenic ^{36}Cl data. Chlorine 36 is steadily produced mainly in the stratosphere and mixed downward in the form of $H^{36}Cl$ to become eventually deposited at the Earth surface. Therefore naturally produced ^{36}Cl may mimic the tropospheric cycle of stratospheric HF quite well. The mean stratospheric fluoride level at CDD (F_{strato}) is thus estimated as follows:

$$[F_{strato}] = (P_F/P_{Cl})\,[^{36}Cl],$$

with $[^{36}Cl]$ denoting the mean cosmogenic ^{36}Cl level at CDD (neglecting any bomb-produced fraction), P_F representing the CFC-derived fluoride, and P_{Cl} indicating the cosmogenic ^{36}Cl production rate, respectively.

Since HF is the only fluoride-containing end-product of the CFC degradation [*Cicerone*, 1981], we adopted the global P_F value of 6.5 10^{10} g yr^{-1} given by *Harnisch* [1999] for the 1990s, which is consistent with P_F = 4.8 10^{10} g yr^{-1} inferred from the inventories and lifetimes of freon 11 and freon 12 [*Intergovernmental Panel on Climate Change (IPCC)*, 1996]. The global ^{36}Cl production rate is taken from latest compilations of *Masarik and Beer* [1999] as 3 10^{23} at yr^{-1}. Referring to the global instead of the stratospheric ^{36}Cl

production partly compensates for the tropospheric fraction contributing to the mean ^{36}Cl ice core level. For the latter a value of 700 at g^{-1} was obtained, using recent ^{36}Cl records reported by *Synal et al.* [1997] from Fiescherhorn (an Alpine ice core site subject to comparably high snow accumulation as at CDD) which were corrected for a small bomb-produced ^{36}Cl excess via prebomb ^{36}Cl records in the Greenland Dye-3 ice core [*Synal et al.*, 1990]. We thus arrive at a typical fluoride level at CDD from CFC degradation of the order of 0.16 ng g^{-1}. The uncertainties in the ^{36}Cl production rate alone are up to a factor of 2, and we assume an upper limit for the CFC-derived fluoride level around 0.32 ng g^{-1}. Given the lower CFC load in 1980, this calculation gives an upper limit of 0.16 ng g^{-1} at that time. Thus we can expect an increase of ice concentration of fluoride from 0.16 to 0.32 ng g^{-1} between 1980 and 1995. This increase remains of the order of the observed winter trend from 1980 to 1990 (Figure 5b). Thus we cannot exclude the possibility that winter Alpine snow layers have already started to record stratospheric changes related to the changing load of CFC in the stratosphere.

6. Conclusions

This study of fluoride concentrations present in winter and summer snow layers deposited at high-elevation Alpine sites allowed us to discuss natural and anthropogenic sources of fluoride having impacted the free troposphere over Europe since the beginning of the twentieth century. In spite of a relatively large HF emission, the permanent activity of Mount Etna does not contribute significantly to the fluoride budget over the Alps since 1940 (a time over which anthropogenic inputs were already significant). Such an observation would be useful in investigating the potential role of this volcano to the natural sulfate budget. At the beginning of the twentieth century the major natural source of fluoride is soil dust emission, whereas sea-salt emissions represent a very minor source there. Fluoride emissions from aluminium smelters mainly located nearby the Alpine massif in France and Switzerland represented a major contribution (up to 80% in 1970) of the total fluoride deposition in summer between 1950 and 1970. The contribution of coal-burning emissions was more significant in 1930 (23 ± 7%) than in 1970 (8 ± 2%). The contribution of coal burning to fluoride levels reached a maximum of 25 ± 8% over the 2 last decades. Over the last 2 decades, in spite of the strong decrease of aluminium smelter emissions, the total fluoride level remains well above its natural level likely due to a present-day strong contribution of other anthropogenic sources like cement and phosphate industrial processes. With lower values the winter fluoride trend mimics the summer trend until 1980. Although needed to be confirmed by other ice core studies, the remarkable reincrease of winter levels seen after 1985 may possibly reflect stratospheric HF changes related to CFC degradation.

Acknowledgments. This work has been supported by the European Environment and Climate program ALPCLIM. Funding was provided by the European Community via contract ENV4-CT97 (ALPCLIM) and ENV4-CT96-5051 (Environment and Climate Research Training), the Centre National de la Recherche Scientifique (programme PNCA), and the Ministery for Science and Research of Baden-Württemberg within the collaboration program between Region Rhône-Alpes and Baden-Württemberg. We thank Andreas Stanzick for his help in evaluating the stratospheric HF input. We are grateful to Elisabeth Couzinie and Michel Reverdy from Aluminium Pechiney who provided us with data on the fluoride release as well as the aluminium production of the Saint Jean de Maurienne site, and the aluminium production from Pyrenean sites, respectively. We thank H. Hinüber from German Aluminium-Zentrale e.V. and R. Flueckiger from the Aluminium Verband Schweiz for providing aluminium production data from western Germany and Switzerland.

References

Baltensberger, U., H.W. Gaeggeler, D.T. Jost, M. Lugauer, M. Schwikowski, E. Weingartner, and P. Seibert, Aerosol climatology at the high-alpine site Jungfrauchjoch, Switzerland, *J. Geophys. Res.*, *102*, 19,707-19,715, 1997.

Bloomfield, P., and W.L. Steiger, *Last Absolute Deviations: Theory, Applications and Algoritms*, Birkhauser, Boston, Mass., 1983.

Cadle, R.D., A comparison of volcanic with other fluxes of atmospheric trace gas constituents, *Rev. Geophys.*, *18*, 746-752, 1980.

Cicerone, R., Halogens in the atmosphere, *Rev. Geophys.*, *19*, 123-139, 1981.

De Angelis, M., and A. Gaudichet, Saharan dust deposition over Mont Blanc (French Alps) during the last 30 years, *Tellus*, *43*, 61-75, 1991.

De Angelis, M., and M. Legrand, Origins and variations of fluoride in Greenland precipitation, *J. Geophys. Res.*, *99*, 1157-1172, 1994.

Eichler, A., M. Schwikowski, and H.W. Gäggeler, An Alpine ice-core record of anthropogenic HF and HCl emissions, *Geophys. Res. Lett.*, *27*, 3225-3228, 2000.

European Monitoring and Evaluation Programme (EMEP), Trends of sulfur dioxide emissions, air concentrations, and deposition of sulfur in Europe since 1880, edited S. Mylona, Norw. Inst. For Air Res., Lillestrom, Norway, 1993.

Fischer, H., D. Wagenbach, and J. Kipfstuhl, Sulfate and nitrate firn concentrations on the Greenland ice sheet, 1, Large-scale geographical deposition changes, *J. Geophys. Res.*, *103*, 21,927-21,934, 1998.

Harnisch, J., Reactive fluorine compounds, in *Reactive Halogens Compounds in the Atmosphere*, edited by P. Fabian and O.N. Singh, pp. 81-111, Springer-Verlag, New York, 1999.

Haulet, R., P. Zettwoog, and J.C. Sabroux, Sulphur dioxide discharge from Mount Etna, *Nature*, *268*, 715-717, 1977.

Intergovernmental Panel on Climate Change (IPPC), *Climate Change 1995*, Cambridge Univ. Press, New York, 1996.

Kanakidou, M., F.J. Dentener, and P.J. Crutzen, A global three-dimensional study of the fate of HCFCs and HFC-134a in the troposphere, *J. Geophys. Res.*, *100*, 18,781-18,801, 1995.

Kasper, A., and H. Puxbaum, Seasonal variation of SO_2, HNO_3, NH_3 and selected aerosol components at Sonnblick (3106 m a.s.l.), *Atmos. Environ.*, *32*, 3925-3939, 1998.

Legrand, M., M. De Angelis, and F. Maupetit, Field investigation of major and minor ions along Summit (central Greenland) ice cores by ion chromatography, *J. Chromatogr.*, *640*, 251-258, 1993.

Le Guern, F., Ecoulements gazeux réactifs à hautes températures, mesures et modélisation, Thèse d'Etat, 314 pp., Univ. de Paris VII, Paris, 1988.

Low, P.S., and H. Bloom, Atmospheric deposition of fluoride in the lower Tamar valley, Tasmania, *Atmos. Environ.*, *22*, 2049-2056, 1988.

Masarik, J., and J. Beer, Simulation of particle fluxes and cosmogenic nuclides production in the Earth's atmosphere, *J. Geophys. Res.*, *104*, 12,099-13,112, 1999.

Mason, A.S., *Principles of Geochemistry*, 166 pp., John Wiley, New York, 1982.

Maupetit, F., and R. Delmas, Snow chemistry of high altitude glaciers in the French Alps, *Tellus*, *46*, 304-324, 1994.

Morel, P., *Histoire Technique de la Production d'aluminium*, 352 pp., Presses Univ. de Grenoble, Grenoble, 1992.

Preunkert, S., and D. Wagenbach, An automatic recorder for air/firn transfer studies of chemical aerosol species at remote glacier sites, *Atmos. Environ.*, *32*, 4021-4030, 1998.

Preunkert, S., D. Wagenbach, M. Legrand, and C. Vincent, Col du Dôme (Mt Blanc Massif, French Alps) suitability for ice core studies in relation with past atmospheric chemistry over Europe, *Tellus*, *52*, 993-1012, 2000.

Rauch, E., *Geschichte der Hüttenaluminiumindustrie in der westlichen Welt*, 316 pp., Aluminium-Verlag, Düsseldorf, 1962.

Ronseaux, F., and R. Delmas, Chemical composition of bulk atmospheric deposition to snow at Col de la Brenva (Mt Blanc area), in *Acid Deposition at High Elevation Sites*, edited by M.H. Unsworth and D. Fowler, pp. 491-510, Kluwer Acad., Norwell, Mass., 1988.

Synal, H.A., J. Beer, G. Bonani, M. Suter, and W. Wolfli, Atmospheric transport of bomb produced ^{36}Cl, *Nucl. Instrum. Methods Phys. Res.*, *52*, 483-488, 1990.

Synal, H.A., J. Beer, U. Schotterer, M. Suter, and L. Thompson, Bomb produced ^{36}Cl in ice core samples from mountain glaciers, in *Glaciers From the Alps: Climate and Environmental Archives*, pp. 99-102, PSI, Wengen, Switzerland, 1997.

Vinogradov, A.N., *The Geochemistry of Rare and Dispersed Chemical Elements in Soils*, 2nd ed., p. 231, Consult. Bur., New York, 1959.

Wagenbach, D., S. Preunkert, J. Schaefer, W. Jung, and L. Tomadin, Northward transport of saharan dust recorded in a deep Alpine ice core, in *The Impact of African Dust Across the Mediterranean*, edited by S. Guerzoni and R. Chester., pp. 291-300, Kluwer Acad., Norwell, Mass., 1996.

M. Legrand and S. Preunkert, LGGE, Centre National de la Recherche Scientifique, BP 96, 38402, St Martin d'Hères, France. (legrand@glaciog.ujf-grenoble.fr)

D. Wagenbach, Institut fur Umweltphysik, Universitat Heidelberg, INF 229, 69120 Heidelberg, Germany.

(Received August 30, 2000; revised November 17, 2000; accepted November 22, 2000.)

Seasonally resolved Alpine and Greenland ice core records of anthropogenic HCl Emissions over the 20th century

Michel Legrand [1,*], Susanne Preunkert[1], Dietmar Wagenbach[2], and Hubertus Fischer[2,o]

[1] *Laboratoire de Glaciologie et Géophysique de l'Environnement du Centre National de la Recherche Scientifique, BP 96, 38402, St Martin d'Hères, France*

[2] *Institut für Umweltphysik, Universität Heidelberg, INF 229, 69120 Heidelberg, Germany*

[o] *Now at Alfred-Wegener-Institut für Polar und Meeresforschung, Bremerhaven, Germany*

* Corresponding author. Phone: +33/(0)476824243; Fax: +33/(0)476824201; e-mail: mimi@glaciog.ujf-grenoble.fr

to be submitted to "Journal of Geophysical Research" in July, 2001

Abstract

The continuous high-resolved records of chloride, sodium, magnesium and calcium in ice cores from Col du Dôme (Mont Blanc Massif, 4250 m above sea level, French Alps) and Summit (3240 m above sea level, central Greenland) are used to reconstruct the history of atmospheric HCl pollution over Europe and Greenland since the early 20th century. The evaluation of the HCl amount in summer snow deposits at high-elevated Alpine site is complex since continental emissions (halide evaporites and soils) account for 80% of the chloride budget and only a fifth of chloride is related to HCl. During the pre-industrial era, the HCl content of summer Alpine snow layers fluctuated between zero and 6 ng g^{-1} likely in relation with a highly variable interannual biomass burning activity in western Europe. From 1925 to 1960, the HCl levels were slightly higher (3 to 9 ng g^{-1}) due to the growth of coal burning emissions in western Europe. It is found that, if it exists, the contribution of the chlorocarbon oxidation to the HCl concentrations of Alpine summer snow layers would not exceed 1 ng g^{-1} over the 1925-1960 time period. In the late 60s, a sharp increase of HCl levels (up to 17 ng g^{-1}) took place as a result of the set up of waste incineration in western Europe. Between 1970 and 1990, waste incineration contributed three to four times more than coal combustion to the HCl budget of summer Alpine snow layers. In winter, sea spray emissions dominate (~78%) the total chloride level of Alpine snow layers. The HCl trend in winter Alpine snow layers remained limited to ~2 ng g^{-1} over the 20th century in relation to waste incineration after 1960, and possibly more recently to the impact via stratosphere/troposphere exchange of the growing HCl stratospheric load related to the CFC degradation. In Greenland snow layers most of particulate chloride originates from sea spray, one and two thirds of chloride being present as HCl in spring and summer, respectively. The Greenland HCl ice core records indicate a pre-industrial HCl level close to 4 ng g^{-1} which is found to be mainly due to the sea salt dechlorination, while the contribution of passive volcanic HCl emissions at high northern latitudes can be neglected. The input from sea salt dechlorination has been enhanced by a factor of two to three during the second half of the 20th century, partly as a result of the increase of the atmospheric acidity in response to growing NO_x and SO_2 anthropogenic emissions.

1. Introduction

In addition to nitric and sulfuric acids, HCl represents the third mineral acid contributing to the acidity of precipitation. Furthermore HCl is one of the major constituent of reactive atmospheric chlorine. Although the spatial distribution of natural and anthropogenic sources of HCl has been recently reviewed [*Keene et al.*, 1999 and references therein], some large uncertainties still exist on the strength of these sources which include continental (passive

volcanic emissions, biomass burning, coal combustion, and waste incineration) and oceanic (dechlorination of sea salt aerosol) emissions. In addition to these primary emissions, the production of HCl from the chlorocarbons oxidation was recently proposed as a significant source of HCl for the global background atmosphere [*Sanhueza*, 2001]. Due to these uncertainties, it remains yet difficult to evaluate to what extent anthropogenic processes may dominate natural HCl emissions. Such gaps stimulate the studies of HCl in ice cores extracted from glaciers located in continental mid-latitude regions as well as from drill sites more exposed to marine influence such as at the Greenland ice cap.

The most direct evidence for changing composition of the atmosphere from the pre-industrial era to present has been depicted so far from chemical studies of Greenland ice cores. At present, most of Greenland ice core studies have been dedicated to sulfate and nitrate species and only two of them have alluded a recent trend of hydrochloric acid. First, *Mayewski et al.* [1993] pointed out a significant increasing trend of HCl levels in the 60s in a Summit (central Greenland) ice core in which the 1950-1990 level is twice as high as the pre-industrial level [*Legrand and Mayewski*, 1997]. A similar change was found in other Greenland ice cores [*Fischer*, 1997] but the cause of these HCl trends in Greenland remains unclear (growing primary HCl emissions from industrialized regions of the northern hemisphere or enhanced sea salt dechlorination by increasing acidification of the atmosphere). In these two studies, the HCl content of ice was evaluated by using either total sodium [*Fischer*, 1997] or total sodium corrected from its soil contribution (using calcium) [*Mayewski et al.*, 1993] as a tracer of sea salt and have assumed that sea salt aerosol contains chloride and sodium in similar proportion than in seawater. It remains however unclear if this last assumption is valid and if other chloride containing particles emitted from continents can be neglected in these calculations.

A recent study of the HCl (using total sodium as a tracer of sea salt and the seawater chloride to sodium ratio) in an Alpine ice core extracted in the Monte Rosa Massif revealed an increase of annual levels from 1965 to 1985 [*Eichler et al.*, 2000]. This change was attributed to the development of HCl emissions from waste incineration from the Swiss Plateau suggesting a poor spatial representativeness of Alpine ice records for this species. However other Alpine ice core studies are needed to investigate separately winter and summer trends which are representative of different air masses (tropospheric background in winter versus boundary layers in summer) and to increase the spatial representativeness of HCl Alpine ice core records.

In the present paper, based on examination of chloride and sodium as well as magnesium and calcium, we first examine in more detail the origins of particulate chloride and sodium present in snow layers deposited at high-elevated Alpine and Greenland sites. Based on a more accurate estimate of the HCl level in these snow layers, we then examine the long term change of HCl levels since the beginning of the 20th century over Europe and central Greenland. That permits us to discuss the relative contribution of natural versus anthropogenic sources to the HCl budget and to evaluate the major anthropogenic processes influencing these marine and continental remote atmospheres.

2. Drill Site Characteristics, Ice Core dating, and Analyses

A 126-m long ice core extracted in 1994 at Col du Dôme (CDD) (4250 m asl, located near the Mont Blanc summit), was analyzed for major ions (Na^+, NH_4^+, Ca^{2+}, Mg^{2+}, Cl^-, NO_3^-, and SO_4^{2-}) with a seasonal resolution at Laboratoire de Glaciologie et Géophysique de l'Environnement (LGGE) and the Institut fur Umweltphysik (IUP). This was done at LGGE along the upper 117 meters of the core (1050 samples) which correspond to the well-dated part of the core (75 ± 5 years, *Preunkert et al.* [2000]) and from 117 to 126 m depth at IUP (Figure 1). For major ion determinations, the accuracy is typically of 5%. CDD ice samples were cleaned at LGGE by using an electric plane device previously developed at IUP [*Fischer et al.*, 1998]. The validity of the decontamination procedure was tested by checking blank values obtained on pieces of frozen ultrapure water (Millipore system). Mean blank values (11 samples) obtained at LGGE were 0.4 ± 0.3 ng g^{-1} for chloride, 0.6 ± 0.3 ng g^{-1} for sodium, 0.1 ± 0.1 ng g^{-1} for magnesium, and 4.3 ± 2.1 ng g^{-1} for calcium. Mean blank values (~40 samples) obtained at IUP using an autosampler were slightly higher, 1.7 ± 1.4 ng g^{-1} for chloride, 1.3 ± 1.0 ng g^{-1} for sodium, 1.0 ± 2.1 ng g^{-1} for magnesium, and 3.2 ± 3.4 ng g^{-1} for calcium. Hence, data obtained on the bottom part of the CDD core were corrected for these blank values. The Summit core was cleaned using a lathe developed at LGGE [*Legrand et al.*, 1993]. Due to the larger ice fraction removed by this procedure from the entire core (instead of lamellae from the CDD ice core), all ions blank values corresponding to the decontamination step were found insignificant for the Summit core.

The glaciological characteristics of this CDD ice core indicate an annual layer thickness ranging from 3 to 0.2 m water equivalent (w.e.) from the surface to a depth of 90 m w.e. (i.e., 117 m depth) [*Preunkert et al.,* 2000]. The studies of seasonal variations of ammonium [*Preunkert et al.*, 2000], fluoride [*Preunkert et al.*, in press] and sulfate [*Preunkert et al.*, submitted] indicate that seasonally resolved records are here available for these species until 1925. Similarly, for chloride we found (Figure 2) summer maxima with summer to winter ratios of 2 to 3 over the 1925-1935, 1945-1955, and 1985-1995 time periods. Such well-

marked summer maxima are consistent with atmospheric observations made at high-elevated Alpine sites, reflecting distinct seasonal atmospheric conditions prevailing there due to the presence or absence of upward advection of air masses from the boundary layer in summer and winter, respectively [*Baltensperger et al.*, 1997; *Preunkert and Wagenbach*, 1998].

We also examined a high-resolution chemical record (470 samples) extracted from a Summit (central Greenland) ice core (Figure 3). The dating of this ice core indicates an annual snow accumulation close to 0.23 m w.e. and a possible error of two years over the time period from 1870 to 1992 [*Legrand and De Angelis,* 1996]. A specific difficulty dealing with the HCl record in ice cores extracted in polar regions characterized by low snow accumulation with respect to the situation at mid-latitudes glaciers comes from the fact that this species is present in the atmosphere in the gas phase which may be remobilized after deposition and during firnification [*De Angelis and Legrand*, 1995; *Legrand and Mayewski,* 1997]. It was shown that this process is particularly important at sites where the annual snow accumulation rate is as low as 0.03 to 0.05 m w.e. However, *Stanzick* [2001] investigated the spatial variability of pre-bomb ^{36}Cl levels and bomb ^{36}Cl inventories in central Greenland over a large snow accumulation range (down to 0.10 m w.e. per year) and found no significant losses. Since ^{36}Cl is expected to be deposited in the chemical form of HCl we may neglect re-emissions of this species at Summit. Based on the examination of the seasonal variations of sodium, ammonium and calcium contents and following previous works [*Whitlow et al.*, 1992; *Legrand and Mayewski*, 1997; *Fischer et al.*, 1998], we assigned three seasons: spring characterized by calcium maximum, summer by sodium and calcium minima, and winter by sodium maximum and ammonium minimum. At that site, the chloride level exhibits a winter/spring maximum (Figure 2) with a mean winter/spring to summer ratio close to two. Based on examination of seasonal variations in atmospheric transport pattern using a 44-year record of isobaric 10-day back trajectories at 500-hPa level, *Kahl et al.* [1997] suggested that air masses arriving at Summit in winter and spring correspond to a fast transport from North America extended upwind (westward) as far as Asia/Europe. Most of time in summer air masses arriving above Summit come from North America, these shorter trajectories being related due to a less vigorous circulation at 500 hPa in summer than in winter/spring.

3. Evaluation of HCl and Aerosol Derived Chloride Levels in Ice Cores

3.1 Evaluation of HCl Levels

Chloride is incorporated in precipitation as hydrochloric acid as well as various chloride containing aerosols. The most simple example is the case of a marine precipitation for which, as far as the aerosol input from continents can be neglected, it is legitimate to assume that

chloride is mainly provided as HCl and sea salt aerosol. In this case, the amount of HCl can be derived by subtracting the sea salt chloride contribution to total chloride as follows:

$$[HCl] = [Cl^-] - 1.8\ q\ [Na^+_m] \qquad (1)$$

Here Na^+_m is the marine sodium (identical to the total sodium in the absence of significant continental input) and q ($q \leq 1$) refers to the fractionation factor considering a possible deviation of the chloride to sodium ratio in sea salt aerosol from the respective seawater mass ratio (1.8).

In continental precipitation the sea spray chloride contribution is weaker, and the problem becomes much more complex since this use of sea-salt correction is biased by the presence of leachable sodium in continental input [*Legrand et al.*, 1988; *Legrand and Delmas*, 1988] and chloride containing aerosols may also originate from soil weathering and halide evaporites. Furthermore, it has been suggested [*Simeonov et al.,* 1999] that a significant fraction of chloride and sodium present in precipitation collected in central Austria comes from manure fertilized fields emissions which are rich in sodium and chloride (sodium to chloride mass ratio of 1.6) and poor in calcium and magnesium.

The aerosol derived chloride fraction in continental precipitation would depend on sodium and calcium levels, since sodium is mainly present in halide components (sea spray, evaporites, and manure fertilized fields emissions) and calcium in soils. We therefore examine the dependence of chloride to sodium and calcium contents in snow layers deposited before 1955 a period over which the anthropogenic chloride input as mostly related to coal combustion remained moderate (see section 4). This was done for snow layers deposited between 1925 and 1955 at CDD excluding samples containing saharan dust (see section 3.3) and between 1870 and 1955 at Summit excluding samples suspected to be contaminated by volcanic inputs (section 3.3). Over these time periods, the multiple regressions of chloride to sodium and calcium yield:

$[Cl^-] = 3.4 + 1.465\ [Na^+] + 0.0251\ [Ca^{2+}]$ ($R^2 = 0.8$ for 240 summer CDD samples) (2a)
with the following uncertainties on the regression coefficients: 1.465 ± 0.054 (denoted k_{Na}) and 0.0251 ± 0.0132 (denoted k_{Ca}),

$[Cl^-] = -0.5 + 1.74\ [Na^+] + 0.1399\ [Ca^{2+}]$ ($R^2 = 0.9$ for 69 winter CDD samples) (2b)
with k_{Na}= 1.74 ± 0.056 and k_{Ca}= 0.1399 ± 0.0873,

$[Cl^-] = 4.6 + 1.27\ [Na^+] + 0.0027\ [Ca^{2+}]$ ($R^2 = 0.8$ for 63 spring Summit samples) (2c)

with k_{Na}= 1.27 ± 0.08 and k_{Ca}= 0.0027 ± 0.067,

$[Cl^-] = 2.7 + 1.13\ [Na^+] + 0.40\ [Ca^{2+}]$ (R^2 = 0.36 for 63 summer Summit samples) (2d)
with k_{Na}= 1.13 ± 0.19 and k_{Ca}= 0.40 ± 0.15.

The knowledge of k_{Na} and k_{Ca} values permits then to evaluate the HCl level as follows:

$$[HCl] = [Cl^-] - (k_{Na}\ [Na^+] + k_{Ca}\ [Ca^{2+}]) \quad (3)$$

Because of the poor accuracy of the multiple regression for summer Summit snow layers (R^2 = 0.36, equation 2d) we used equation (2c) for calculating HCl levels in both spring and summer layers. The low sodium and calcium levels in summer layers (see Table 1) would however lead only to small differences on the HCl evaluation. Depending on sites and seasons, the k_{Na} values significantly differ from the chloride to sodium seawater ratio of 1.8 which was employed in the previous studies of HCl in ice cores. The use of the conventional sea salt correction (equation (1) with q = 1) produces a significant bias on the results. For instance, the mean HCl level of summer CDD layers calculated using this conventional correction is 3 ng g^{-1} lower than the one calculated by using equation (3).

Of a particular importance is the estimate of uncertainties when dealing with the low impurities content which characterizes deposition at remote regions. These uncertainties are usually dominated by the analytical accuracy (i.e., here Cl^-, Na^+, and Ca^{2+}) which accounts for 5% accuracy and blank standard deviations. An additional uncertainty in evaluating hydrochloric acid content is related to the uncertainties in the coefficients (k_{Na} and k_{Ca}) derived from equations (2a to 2c). The resulting errors have been estimated by state of the art error propagation calculations.

The estimated mean half year HCl levels of summer and winter CDD snow layers are plotted in Figure 4 along with their uncertainties. The uncertainties are typically close to ± 3.5 ng g^{-1} (± 2.7 ng g^{-1} when samples suspected to contain saharan dust are not considered) in summer and ± 1.5 ng g^{-1} in winter. In summer, they mainly result from analytical errors in the sodium and chloride determinations. Larger uncertainties are encountered for years during which samples suspected to contain saharan dust input are present (as in 1989, see Figure 4). In winter, due to lower chloride and sodium levels (Table 2), the uncertainties are resulting from both the accuracy of sodium and chloride determinations and the blank variability for these two species. Note that in spite of less samples containing saharan dust in the bottom of the CDD core, the standard error of HCl evaluation is there relatively high (± 3.5 ng g^{-1}) due to a

larger variability of chloride and sodium blank values. In Greenland, the uncertainties (not shown) are close to ± 1.5 ng g^{-1} in spring and ± 0.5 ng g^{-1} in summer due to the generally lower sodium and calcium levels to be corrected for.

3.2 Aerosol Derived Sodium and Chloride in Alpine and Greenland snow layers

In the following, we examine the meaning of the k_{Na} and k_{Ca} coefficients derived from the multiple regressions (equations 2a to 2c) in terms of origins of aerosol derived chloride and sodium present in snow layers deposited at the two drill sites. Using calcium and sodium as tracers of the input related to soil weathering and halide components (sea spray, evaporites, and possibly manure fertilized fields emissions), respectively, the chloride level of snow layers can be expressed as follows:

$$[Cl^-] = [HCl] + \gamma([Na^+] - \alpha\,[Ca^{2+}]) + \beta\,[Ca^{2+}]$$
$$= [HCl] + \gamma\,[Na^+] + (\beta - \gamma\alpha)\,[Ca^{2+}] \qquad (4)$$

where γ is the mean chloride to sodium mass ratio in the halide components, α and β are the sodium to calcium and chloride to calcium mass ratios in soils (leachable fractions), respectively.

At CDD in summer, comparison of equations (2a) and (4) indicates a chloride to sodium mass ratio γ (identical to k_{Na}) of 1.465. The examination of the relation between sodium and calcium in snow layers deposited at CDD in summer (Figure 5) shows that, in addition to the input related to soil weathering, other sodium sources (sea spray, evaporites from continents and possibly manure fertilized fields) contribute there to the sodium budget as suggested by the relatively low correlation coefficient (R^2 = 0.59) and the large y-intercept (~7 ng g^{-1}). Considering samples having a low sodium content with respect to calcium, the dashed line reported in Figure 5 suggests a typical sodium to calcium mass ratio in soils (α) of 0.11. This value and the k_{Ca} value derived from equation (2a) leads to a chloride to calcium ratio in soils (β) of 0.186. This value is consistent with the slope reported as a dashed line in Figure 5 which corresponds to the low envelop of the chloride to calcium correlation. Introducing α, β, and γ values in equation (4) we found that particulate chloride accounts for 79% (47 ± 24 % and 32 ± 22 % for halides and soils, respectively) of the total chloride level (30.4 ng g^{-1}, Table 2) of summer CDD snow layers deposited between 1925 and 1995. In addition to sea spray and evaporites, manure fertilized fields emissions may contribute to the halide aerosol budget at CDD, particularly in summer, when meteorological conditions favour the upward transport of air masses from the boundary layer. The high correlation coefficient (R^2 = 0.82) seen between magnesium and calcium summer levels (Figure 5) indicates that most of magnesium is related to soil weathering. In addition to this soil origin, magnesium is also

emitted with halides from evaporites and sea spray with a magnesium to sodium mass ratio close of 0.12 (i.e., the seawater ratio) whereas the presence of magnesium remaining negligible in manure fertilized fields emissions. In this way, the y-intercept of the correlation (~1 ng g^{-1}, Figure 5) would correspond to a sodium level of 8 ng g^{-1} related to sea spray and evaporites from continents. The y-intercept of the relation between sodium and calcium (Figure 5) indicates that, in addition to soils, halide components (sea spray, evaporites from continents and possibly manure fertilized fields) also contribute at the level of ~7 ng g^{-1} to the sodium budget. This value is close to the 8 ng g^{-1} of sodium from sea spray and evaporites derived from the magnesium- calcium relationship, suggesting an insignificant contribution of manure fertilized fields emissions at this site. Such a weak contribution of this source at high elevated Alpine site contrasts with its significant impact on precipitation at a low elevation European site reported by *Simeonov* [1999]. That suggests an inefficient upward transport of this material from the boundary layer to the free troposphere, likely related to its size distribution (coarse particles). In conclusion, chloride present in summer CDD snow layers originates from soils (32%) and halides (sea spray plus evaporites) (47%), the remaining fraction (21%) being related to the presence of HCl.

In winter at CDD, due to a lower input from soils as depicted by the calcium content of 6 ng g^{-1} (instead of 55 ng g^{-1} in summer, Table 2), the chloride coming with halide components dominates (78%) the total chloride level of 11.4 ng g^{-1}. Note again the non-soil Mg to non-soil Na ratio of 0.1 (i.e., close to the seawater value of 0.12) (Table 2) which suggests that the contribution from manure fertilized fields is also as expected insignificant at that season. The fraction of sodium coming with halide components is almost two times larger in summer than in winter (Table 2). Since sea spray emissions are higher in winter than in summer, the observed reverse seasonal change for the sea spray/evaporite sodium fraction suggests that in summer, as a result of an efficient upward transport from the continental boundary layer, halide (evaporite) emissions dominate this sodium fraction while in winter, due to a more active cyclogenis over the Atlantic ocean, sea spray likely dominates. Note that the γ value of 1.74 suggests a limited sea salt aerosol fractionation at that season. As depicted in Figure 2, the winter chloride level was two times larger over the 1985-1995 decade than between 1925 and 1955. The examination of the long term trend of chloride and sodium (not shown) indicates indeed that the chloride level, which fluctuated between 5 and 10 ng g^{-1} from 1925 to 1970, was enhanced to 18 ng g^{-1} over the 1975-1985 decade. Similarly the sodium level close to 5 ng g^{-1} from 1925 to 1970 reached 9 ng g^{-1} over the 1975-1985 decade suggesting an additional input of chloride mainly in the form of sodium chloride at that time. Such a recent increase of the sodium chloride content of winter CDD snow layers is possibly related to the growing use of salt for de-icing the roads in France (from 200 kilotons of sodium

chloride in the early 70s to 1200 kilotons in the 85s) and the subsequent spray of liquid by the car traffic.

In Greenland snow layers, the soil input is maximum in spring as depicted by the mean calcium level of 15 ng g^{-1} (Table 1). Using a sodium to calcium ratio (α) of 0.1 reported for dust input reaching Greenland by *De Angelis et al.* [1997] and *Mayewski et al.* [1993], we calculate from equations (2c and 4) a β value of 0.13. Chloride present in Summit snow layers originates in soils (12%) and halides (though to be dominated there by sea spray) (50%), the remaining part being related to HCl (38%). In summer Greenland snow layers, the sea spray and soil contribution is lower than in spring as depicted by the sodium and calcium contents (Table 1). As a result, the contribution of particulate chloride is weaker (29% for sea spray and 9% for soil) and two thirds of chloride are related to the presence of HCl at that season.

3.3. Impact of Saharan Dust in the Alps and Volcanic Eruptions in Greenland

Previous studies have shown that saharan dust plumes can sporadically reach the Alps and disturb the chemistry of snow deposits. Identified as calcium-rich layers having a negative acidity (i.e. alkaline samples) [*Wagenbach et al.*, 1996], 98 summer and 4 winter samples were found along the CDD core as contaminated by saharan dust by *Preunkert et al.* [in press].

To calculate the HCl levels in these layers, we need to know the amount of sodium and chloride present in saharan dust material reaching Alpine sites. *Talbot et al.* [1986] examined the water soluble mean composition of aerosols collected in saharan dust plumes present over the tropical North Atlantic for sodium (3704 ppm), potassium (1663 ppm), and chloride (3158 ppm). Since calcium was not measured by *Talbot et al.* [1986], we try to characterize the chemistry of saharan dust by checking the linear relationships between sodium, magnesium, potassium, and chloride versus calcium observed in summer CDD samples suspected to be contaminated by saharan dust. As seen in Table 3 soluble sodium is twice more abundant than soluble potassium in these snow layers what is in very good agreement with the composition reported by *Talbot et al.* [1986]. Based on sodium and chloride data from *Talbot et al.* [1986] and the observed sodium to calcium ratio of 0.071 in CDD dust events (Table 3), we can expect a chloride to calcium ratio close to 0.063. This value is twice lower than the slope of the correlation between chloride and calcium levels (0.11) reported in Table 3. Such a difference may be due to an additional uptake of chloride in the form of HCl by this alkaline aerosol during transport. Based on this evaluation, we corrected all samples suspected to be influenced by saharan dust from their terrigeneous contribution using sodium,

magnesium, potassium, and chloride to calcium mass ratios of 0.071, 0.045, 0.035, and 0.063, respectively.

As previously discussed by *Fischer et al.* [1998] and *Preunkert et al.* [submitted], the sulfate background level of Summit snow layers has been sporadically disturbed by well-identified volcanic eruptions. Annoted with a star in Figure 3, some of these events also appear to disturb the background chloride levels by a few tens of ng g^{-1}, in particular in 1873 (the Grimsvotn eruption in Iceland) and at the beginning of the 20^{th} century (several eruptions including the 1912/1913 Katmai one in Alaska). In the following all these snow layers were discarded in examining the long term trend.

4. The Alpine HCl Trends at Col du Dôme

4.1. CDD Summer Trend

To examine the long term summer trend of HCl we smoothed summer means reported in Figure 4 by using Single Spectrum Analysis (SSA) with a time window of five years (Figure 6). As discussed in detail by *Preunkert et al.* [submitted], in spite of a very uncertain dating between 90.3 and 95.3 m (w.e.) depth, the mean chemistry of CDD layers located reported in Table 4 closely reflects the pre-industrial condition at this site. An overall mean HCl level of 0.2 ± 2.7 ng g^{-1} is calculated for the pre-industrial summer CDD ice layers (Table 4). Out of twelve summer means, eight exhibit negative values (from -1 to -3 ng g^{-1} with an uncertainty of 3.5 ng g^{-1}) and four are positive (from 1 to 6 ng g^{-1}) of which two are significantly different from zero with respect to their uncertainties. That suggests the possible existence of a natural HCl background level of a few ng g^{-1}. From 1925 to 1965, smoothed values fluctuated between 3 and 9 ng g^{-1} (Figure 6), significantly exceeding the mean pre-industrial level of 0.2 ng g^{-1}. After 1965, HCl levels were sharply enhanced reaching a plateau value of 16-18 ng g^{-1} between 1972 and 1980. In the following we examine the role of anthropogenic processes having disturbed the natural HCl level of summer ice at high-elevated Alpine sites.

4.1.1. Coal Burning Contribution

Both sulfur and chloride are present at significant levels in coal. During combustion, most sulfur emitted to the atmosphere is in the form of SO_2 but a certain fraction of the sulfur content is retained in ash. For chloride, the amount of particulate versus HCl emissions is not well known and may depend of the combustion process [*Mc Culloch et al.,* 1999]. Also a fraction of chloride can be retained in ash. Assuming that a similar fraction of chloride and sulfur are retained in ash during the combustion and that chloride released into the atmosphere is mainly in the form of HCl, annual HCl emission (E_{Cl}) can be calculated from

the chlorine (C_{Cl}) and sulfur (C_S) contents of employed coal and from annual S coal burning emissions (E_S) following:

$$E_{Cl} = (C_{Cl}/C_S)\, E_S \qquad (5)$$

Comparing the long term trend of the anthropogenic sulfate fraction (evaluated by subtracting the natural background sulfate level of 80 ng g^{-1} from the total sulfate concentrations) in summer CDD layers with past SO_2 anthropogenic emissions in western Europe, *Preunkert et al.* [submitted] derived a main influence of SO_2 emissions from regions located within 700-1000 km from the Alps with a major contribution from France, Spain, Italy, and Switzerland. Chlorine and sulfur contents of employed hard and brown coals have been documented by *Mc Culloch et al.* [1999] and *Lefohn et al.* [1999]. For these four countries, the mean chlorine and sulfur contents are 0.11 ± 0.01 % and 0.7 ± 0.2 % in hard coal, respectively. For brown coal, the chlorine and sulfur content are 0.04 ± 0.02 % and 1.5 ± 0.5 %, respectively. *Lefohn et al.* [1999] also documented the annual sulfur emissions from hard and brown coal combustion in individual countries since 1850. Applying equation (5) to France, Italy, Spain, and Switzerland we derive annual HCl emissions (E_{Cl}) related to coal combustion. The contribution of coal combustion to HCl levels in CDD ice can be then estimated from the concentration of anthropogenic sulfate observed in summer CDD ice layers, the total anthropogenic annual sulfate emission including the liquid fuel contribution ($E_{sulfate}$ derived from *Mylona et al.* [1996]) and the annual chloride emission calculated from equation (5) following:

$$[HCl]_{coal} = E_{Cl}\, ([SO_4^{2-}] - 80)/\, \delta\, E_{sulfate} \qquad (6)$$

The δ factor refers to the change of the atmospheric HCl/SO_4 ratio between emission and deposition at the site. Since the atmospheric fate of HCl and SO_2 are not identical with respect to wet and dry deposition processes and considering the subsequent SO_2 to SO_4 conversion, the atmospheric HCl/SO_4 ratio is not conservative after emissions and the δ value would be higher than unit. As seen in Figure 6, using a δ value of 1, we calculated a coal burning contribution close to 8 ng g^{-1} in 1955 whereas the HCl level in the corresponding snow layers was close 5 ng g^{-1} suggesting a change of the HCl/SO_4 ratio between emission and deposition by at least a factor of 1.6. This δ value represents an upper estimate since the assumption made here that no other sources contribute to the HCl CDD levels is not necessarily valid (see section 4.1.2). *Preunkert et al.* [in press] proposed a change by a factor of 2.2 between emission and deposition for the fluoride to sulfate ratio which may be relevant for HCl as well, since a similar atmospheric lifetime for HCl and HF is realistic. Assuming a mean global tropospheric lifetime of 4 days for sulfate [*Chin et al.*, 1996] and considering the decrease of sulfate summer levels between the surface (with a typical value of SO_2 plus

sulfate of 14,000 ng m^{-3} of sulfate derived from the EMEP network in western Europe, *Schaug et al.* [1987]) and the CDD site (800 ng m^{-3} of sulfate, *Preunkert et al.* [submitted]), we calculate a mean transport time of air masses between the boundary layer and the CDD site of the order of 11 days. Based on this value, the δ value of 2.2 would imply a mean HCl lifetime of 3 days. That is consistent with a mean HCl lifetime of 1 to 2 days in the boundary layer and of one month in the free troposphere proposed by *Graedel and Keene* [1995]. Applied this δ value of 2.2 in equation (6), we calculated a mean coal burning contribution of 2.9 ± 0.6 ng g^{-1} to the HCl level of summer CDD layers deposited between 1925 and 1965. From 1965 to 1990, this contribution remained constant (2.6 ± 0.5 ng g^{-1}, Figure 6) with respect to the one from 1925 to 1965. This is in accordance with stabilized consumption of hard and brown coal in France, Italy, Spain and Switzerland.

4.1.2. Natural HCl Inputs

Over the 1925-1965 time period, the residual (non-coal burning) HCl fraction calculated by subtracting the coal burning contribution to the total level of HCl (Figure 6) is of 2.7 ± 1.7 ng g^{-1}. Prior 1965, the sole anthropogenic HCl source is coal burning and the residual HCl fraction would be of natural origin. Thus the examination of the bottom part of the CDD core as well as the trend between 1925 and 1965 suggests the significant contribution of a natural HCl source in summer at that site.

On a global scale, main natural sources of HCl include volcanoes, biomass burning, and sea salt dechlorination [*Keene et al.*, 1999]. It is unlikely that volcanoes significantly contribute to the HCl budget at high-elevated Alpine sites. For volcanic emissions, *Graedel and Keene* [1995] adopted an averaged global flux of 2 Mt yr^{-1} which remains two times lower than the annual release from coal burning in 1990 (4.6 Mt yr^{-1}, *McCulloch et al.* [1999]). Volcanic emissions take place far away from the Alps and even the Mount Etna (Sicily) was found to have no significant impact on the CDD fluoride record [*Preunkert et al.*, in press]. It is therefore unlikely that volcanic emissions represent the main natural source of HCl over the Alps. The sea salt dechlorination represents on a global scale a large source of HCl (50 Mt yr^{-1}, *Graedel and Keene,* 1995]). Due to larger amount of sea salt aerosol and high levels of HNO_3, SO_2, and N_2O_5 in winter than in summer, this source is likely more active in winter than in summer [*Erickson et al.*, 1999]. Given the low winter HCl levels in CDD ice (close to zero between 1925 and 1965, Figure 6), it is therefore unlikely that the natural sea salt dechlorination represents a major source for HCl present in summer Alpine ice.

Therefore, biomass burning which on a global scale would emit up to 6.3 Mt yr^{-1} of HCl [*Lobert et al.*, 1999] may be a possible candidate. Using estimates from *Lobert et al.* [1999]

for the 80s, we calculated an annual biomass burning HCl emission of 0.02 Mt provided by France, Spain, Italy and Switzerland. As argued by *Lobert et al.* [1999] very little quantitative information are available about long-term trend of biomass burning and recent data tend to suggest that biomass burning may currently not be increasing at all. Assuming such an absence of temporal trend in biomass burning at temperate latitudes, the 0.02 Mt of HCl annually emitted by biomass burning are six times weaker than annual emissions from coal combustion (~ 0.12 Mt) in 1955. However, biomass burning emissions may have a larger impact on HCl summer levels because they are more intense during the dry season at the opposite to coal burning emissions which were likely far more important in winter. The large interannual variability of residual HCl levels seen between 1925 and 1965 (also suggested by investigations made on the bottom part of the core) is consistent with the expected large interannual variability of this source. Note also that the large residual HCl levels seen in the late 40s (Figure 6) correspond to a period of unusually warm summer seasons in countries around the Alps [*Boehm et al.*, 2001].

Sanhueza [2001] proposed that the present-day chlorocarbons oxidation would produce up to 4.2 Mt of HCl per year in the background atmosphere, more than a half being related to the oxidation of methyl chloride. The author estimated that 50% of this HCl comes from anthropogenic sources of chlorocarbons. Since most of chlorocarbons are long lived species (1.5 years for CH_3Cl for instance) we would expect little interannual variability of this source. The residual HCl levels of summer snow layers deposited at CDD remained close to 1 ng g^{-1} over several years in the 30s and late 50s (Figure 6). Thus, if it exists, the natural contribution of chlorocarbon oxidation to the HCl budget would not exceed 1 ng g^{-1} in summer CDD snow layers.

4.1.3. Other Anthropogenic Inputs

Being close to 8 ng g^{-1} in 1965, HCl summer levels in CDD ice were enhanced to 17-18 ng g^{-1} between 1970 and 1980 and then decreased to 15 ng g^{-1} in 1990 (Figure 6). The present-day contribution of chlorocarbon oxidation would not exceed 2 ng g^{-1} referring to the upper limit of 1 ng g^{-1} derived for the 1925-1965 time period and assuming a doubling of chlorocarbon emissions between 1950 and present [*Sanhueza*, 2001]. Thus the increase seen in Figure 6 would be related to another anthropogenic input. The residual HCl levels were largely enhanced between 1973 and 1990, coinciding with the deployment of waste incineration whose PVC burning represents a large source of HCl. For 1983, *Lightowlers and Cape* [1988] estimated that France, Italy, Spain, and Switzerland together emitted 0.093 Mt of HCl from waste incineration, with more than a half (0.064 Mt) being emitted in France. Total amount of waste burned in France was insignificant in early 60s, reached 2.7 Mt in

1971, 4.3 Mt in 1975, 5.8 Mt in 1985 and 8.7 Mt in 1989. After 1985 the waste amount burned in France continued to increase (9.6 Mt in 1998) but corresponding HCl emissions likely started to decrease as a result of a progressive set up of flue gas scrubbers fitted to incineration units, all units having been equipped in 1995. Using data from *McCulloch et al.* [1999], we calculated an HCl emission from France, Italy, Spain and Switzerland of 0.064 Mt for 1990, with reduced emissions from France (from 0.024 Mt instead of 0.064 Mt in 1983) and Switzerland (from 0.0026 Mt instead of 0.012 Mt in 1983) and enhanced emissions from Spain (from 0.0022 Mt in 1983 [*Lightowlers and Cape*, 1988] to 0.017 Mt in 1990 [*McCulloch et al.*, 1999]). After 1995, the release of HCl from waste incineration continued to decrease due to the decreasing amount of burned PVC. Pit studies carried out at CDD indicate a mean HCl summer level of 6.2 ± 5.8 ng g^{-1} for 1998 to 2000 instead of 10 ng g^{-1} in 1995 (Figure 6). Thus, the change of HCl levels in summer CDD snow layers covering the 1965-2000 time period is very consistent with the expected course of HCl emissions from waste incineration in western Europe.

4.1.4. Comparison of the Various HCl Source Strength in Western Europe

In Table 5, we summarized the estimated contribution of biomass burning, coal combustion, waste incinerator and chlorocarbon oxidation to the summer budget of HCl in CDD snow layers deposited in the 80s. In the 80s, the mean HCl level of CDD snow layers was close to 15.5 ng g^{-1} of which 2.6 ng g^{-1} would be related to coal burning emissions. The HCl fraction related to waste incineration plus biomass burning emissions is close to 12.9 ng g^{-1}. Assuming a mean contribution of 2.7 ± 1.7 for biomass burning (i.e. similar to the one calculated for the 1925-1960 time period), that indicates that in the 80s the waste incineration contribution reached 10 ng g^{-1} if the chlorocarbon oxidation is neglected.

In Table 5, we report annual global emissions as well summertime emissions at the scale of western Europe (France, Italy, Spain, and Switzerland). For the latter we assumed that biomass burning emissions mainly take place in summer, coal burning emissions are two times larger in winter than in summer, and waste incineration emissions are well distributed over the year. Given the lifetime of several months of chlorocarbons and referring to a proposed lifetime of 1 to 2 month for HCl in the free troposphere [*Graedel and Keene*, 1995], we have assumed that the HCl production from the chlorocarbon oxidation is homogeneously distributed over the world.

The contribution of biomass burning and coal combustion to the HCl budget at CDD in summer are similar which remains consistent within a factor two with the estimates of summer emissions from these two sources over western Europe (Table 5). Note however that

the emission of 0.02 Mt from biomass burning is though to represent an upper limit [*Lobert et al.*, 1999]. The contribution from waste incineration is found to be three to four times larger than the coal burning emissions whereas summer emissions from waste incineration are estimated to be similar to the coal burning ones. Although the HCl production from the chlorocarbon oxidation is two to four times weaker than the ones from other sources located at the surface, we would expect a larger impact of this process. Since the chlorocarbon atmospheric burden is reasonably well known, such a discrepancy suggests that estimates of this source have overestimated the hydrochloric production in the employed chemical schemes.

4.2. CDD Winter Trend

Because of the lack of some individual means (Figure 4) we examined the winter trend by applying here a robust spline smoothing [*Bloomfield and Steiger*, 1983]. As seen in Figure 4, the HCl winter CDD level is most of time not significantly different from zero with respect to uncertainties. The smoothed profile (Figure 6) tends to suggest that, if it exists, the trend had mainly occurred after 1965. The contribution of coal combustion to the HCl level of winter CDD ice can be estimated from equation (6) using the natural background sulfate level of 21 ng g^{-1} (instead of 80 ng g^{-1} for summer) [*Preunkert et al.,* submitted]. $E_{sulfate}$ and E_{Cl} values used in equation (6) were calculated with respect to the source region apportionment derived by *Preunkert et al.* [submitted] for winter CDD snow layers (i.e. all countries of western and eastern Europe). As seen in Figure 6, the coal burning emissions only account for 0.3 ng g^{-1} to the HCl budget of winter CDD snow layers. Referring to the summer to winter ratio of anthropogenic sulfate levels seen in CDD (close to 10, *Preunkert et al.* [submitted], the 15 ng g^{-1} of residual HCl in summer between 1970 and 1980 would correspond to a winter level of 1.5 ng g^{-1} which is consistent with the observed winter levels at that time (Figure 6). Thus, although needed to be confirmed by further studies, the winter trend suggests a limited contamination of the free troposphere in winter by HCl waste incineration emissions.

However at the low level of a few ng g^{-1} encountered we may consider stratospheric HCl as a potential source to the inferred winter snow HCl concentrations as well. Since most of the modern stratospheric HCl inventory can be attributed to the CFC-degradation also a systematic increase of this contribution is expected after the 60s. We estimated the maximum fraction of stratospheric HCl deposited at high Alpine glacier sites via the cosmogenic ^{36}Cl radioisotope. ^{36}Cl is mainly produced in the stratosphere and mixed downward into the troposphere in the form of $H^{36}Cl$. Neglecting any tropospheric ^{36}Cl input at CDD (including re-emitted bomb ^{36}Cl, see section 2), an upper limit of the stratospheric Cl concentrations at this site ($[Cl_{strato}]$) may be simply calculated as:

$$[Cl_{strato}]_{CDD=} (Q_{HCl}/ \Gamma P) [^{36}Cl]_{CDD} \quad (7)$$

with $[^{36}Cl]_{CDD}$ denoting the mean ^{36}Cl concentration in CDD firn, Q_{HCl} the stratospheric HCl inventory ,P the ^{36}Cl production rate and Γ the mean residence time of ^{36}Cl in the stratosphere.

We derived a Q value of 4 10^{11} g from the vertical HCl profile given by *Zander et al.* [1990] for 1985 and deployed the global production rate (P) from latest compilation by *Masarik and Beer* [1999] of 3 10^{23} atoms per year. Using the global instead of the stratospheric P value mainly compensate for the tropospheric fraction contained in the mean ^{36}Cl ice core level. For the latter 700 atoms g^{-1} are obtained referring to recent data reported by *Synal et al.* [1997] from Fischerhorn (an Alpine ice core drill site with comparably high snow accumulation rate as at CDD) and by correcting these data from a small bomb-produced ^{36}Cl-excess via Greenland records [*Synal et al.*, 1990] extending into the pre-bomb era. Adopting a mean residence time Γ of one year we thus arrive at a typical Cl level at CDD derived from the stratosphere of around 0.9 ng g^{-1}. This crude estimate may be uncertain, at least, by a factor of two mainly arising from the production rate and the systematically different vertical profiles of HCl and ^{36}Cl in the stratosphere. We conclude therefore that $[HCl]_{strato}$ at CDD will be less than 1.8 ng g^{-1}. As seen in Figure 6 the mean winter HCl level observed over the 1998-2000 years (2.2 ± 0.6 ng g^{-1}) exceeds what is expected with regard to the corresponding level in summer (6.2 ± 5.8 ng g^{-1} instead of ~0.6 ng g^{-1}). Thus we cannot exclude the possibility that winter snow layers have already started to record the stratospheric changes related to the changing load of CFC in the stratosphere.

5. The HCl Greenland Records

5.1. The Natural HCl Input

The level of hydrochloric acid in spring and summer Summit snow layers remained close to 4 ng g^{-1} prior 1910 and was then enhanced to some 10 ng g^{-1} after 1970 (Figure 7). With respect to the situation at CDD, such a more moderate change over the 20th century indicates a more important contribution of natural HCl emissions there. With the aim to evaluate the representativeness of the Summit profile at the scale of the Greenland ice cap for this short lived species we examined the long term HCl trend in another Greenland ice core. *Fischer* [1995] investigated the chemical composition of snow layers deposited at another Greenland site (B18, located 400 km north from Summit) since 1500 AD on a mean biannual time

resolution. Calculating HCl levels from chloride, sodium, and calcium by using equation (2c) we obtained the long term trend reported in Figure 8. The smoothed HCl curve at B18 exhibits similar changes than those seen at Summit with a pre-industrial level close to 6 ng g^{-1} and an increase by a factor of two in the 70s. Thus the HCl long term Summit trend seen can be considered as well representative for the entire high elevated Greenland sites.

In spring we can assume that biomass burning is not a significant natural HCl contributor for Greenland snow layers. For summer, *Legrand and De Angelis* [1996] showed that the ammonium level of summer Summit snow layers is significantly influenced by biomass burning emissions from the boreal zone. *Savarino and Legrand* [1998] pointed out a higher frequency of biomass burning at the turn of the 19th century. Since no change of the HCl levels of summer Summit snow layers deposited at that time can be detected (Figure 7) we conclude that biomass burning is not the major natural source contributing to the HCl budget of pre-industrial Greenland snow layers.

In addition to biomass burning, the two other possible HCl natural sources are natural sea salt dechlorination and passively degassing volcanoes. On a global scale the volcanic source of HCl is estimated to be in the range of 2 Mt per year [*Graedel and Keene*, 1995] and remains weak compared to sea salt dechlorination emissions. However for Greenland, this contribution may be far larger due the rather high volcanic activity taking place in the high-northern latitude belt. *Legrand et al.* [1997] estimated that 12 ng g^{-1} of pre-industrial sulfate level at Summit are due to these passive quasi-permanent volcanic emissions. Based on this value and assuming a mean SO_2 to HCl mass ratio in passive volcanic emissions ranging from 1.8 to 18 (i.e., a sulfate to chloride mass ratio of 2.7 to 27) [*Symonds et al.*, 1987], we calculate a chloride contribution of this source between 4.5 and 0.45 ng g^{-1} in Summit snow layers. This estimate does not account for the scavenging process in the water-rich volcanic plumes and the fact that HCl is some 300 times more soluble in water than SO_2. For the 1912 Katmai eruption which injected the debris within the stratosphere, *De Angelis and Legrand* [1994] found that the HCl deposition of hydrochloric acid at Summit was three times lower than the sulfate one with respect emissions. Therefore the passive volcanic emissions would only account for 1.5 to 0.15 ng g^{-1} to the natural HCl level at Summit and very likely the natural HCl level of 4 ng g^{-1} is mainly related to the sea salt dechlorination.

5.2. The Anthropogenic Input

At Summit, the HCl level in spring snow layers, close to 3.7 ± 1.5 ng g^{-1} between 1870 and 1900, was enhanced to 5.5 ± 3.0 ng g^{-1} between 1920 and 1950 (Figure 7). The level was then rapidly enhanced up to 10 ng g^{-1} in the late 70s. Examining the source region apportionment

for sulfate in the Summit spring snow layers, *Preunkert et al.* [submitted] concluded that the source regions influencing the Greenland ice cap in spring include Eurasia (eastern Europe, former USSR, Japan and Korea) and North America. Based on that, the coal burning contribution calculated using equation (6) by considering a pre-industrial value of 38 ng g^{-1} [*Preunkert et al.*, submitted] and a δ value of 2.2 may account for up to 1.2 ng g^{-1} in spring Summit layers deposited in the late 60s. In contrast to the case of western Europe where coal burning and waste incineration HCl emissions are similar in amplitude, annual HCl emissions from Eurasia and North America in 1990 are dominated by coal combustion (~1.42 Mt) against only 0.34 Mt from waste incineration [*Mc Culloch et al.*, 1999]. Thus, growing emissions from coal burning and waste incineration may have accounted for ~ 1 ng g^{-1} to the observed trend of HCl in spring Summit snow layers. Due to a lower snow accumulation at Summit than at CDD, the estimated upper limit of the stratospheric HCl contribution in 1985 would be slightly higher there (~3 ng g^{-1} instead of 1.8 ng g^{-1} at CDD, see section 4.2). As seen in Figure 7, the spring Summit trend of 6 ng g^{-1} mainly took place between 1955 and 1970 whereas a significant contribution of stratospheric HCl is expected in the 80s. In contrast to spring levels, summer HCl levels remained unchanged and close to 4 ng g^{-1} until 1950 and were then increased by a factor of 2 in 1980 (Figure 7). We estimated that the coal burning contribution may account for up to 0.5 ng g^{-1} in summer Summit layers deposited in the late 60s. Finally the contribution of stratospheric HCl is expected to be lower in summer with respect to the spring situation in relation with less frequent intrusion of stratospheric air masses within the troposphere at that season.

Over the 20th century, the acidity of spring Summit layers have been enhanced from 1 ± 0.4 μEq L^{-1} at the beginning of the century to 2.3 ± 0.3 μEq L^{-1} between 1920 and 1950. In 1970, the acidity was close to 4.6 μEq L^{-1} (Figure 7). Such a change of the acidity of Greenland snow layers is related to the acidification of precipitation at high northern latitudes in response to enhanced emissions of SO_2 and NO_x [*Legrand and De Angelis*, 1996]. Note that the changes of acidity developed at the same time as the increase of HCl levels (Figure 7). In summer the acidity remained close to 1.7 μEq L^{-1} until 1950 and then was increased by a factor of two in 1980. As for spring snow layers, the change of the acidity is similar to the HCl trend in summer. These observations suggest that the spring and summer trends observed over the 20th century would be caused by an enhanced sea salt dechlorination in response to acidification of the atmosphere in these regions.

Assuming that the natural sea salt dechlorination is the main source of HCl in pre-industrial Greenland snow layers and referring to the change by a factor two to three between the pre-industrial time and the 90s, the estimate of 50 Mt of HCl annually emitted at present from sea

salt [*Graedel and Keene*, 1995] would imply that in the natural atmosphere this process produces some 17 to 25 Mt of HCl per year. Until recently, the dominant acid-displacement for the sea salt dechlorination were thought to be controlled by sulfuric acid and acids [*Sievering et al.*, 1995]. However, the study of *Erickson et al.* [1999] suggests that these processes produce only 7.2 Mt of HCl per year. Thus, other not well known processes (photolysis of dissolved organic compounds, and free radical reactions) (see *Keene et al.* [1999] and references therein) would account for the remaining production of 42 Mt per year. Interestingly, our finding of a change by a factor two between the pre-industrial era and present suggests that these dominant (not well-known) processes have also been enhanced by a factor of two over the 20th century.

6. Conclusions

This study of chloride, sodium, magnesium and calcium present in precipitation deposited at a high-elevated Alpine site and over Greenland revealed the complexity to calculate the amount of HCl present there. It is shown that an accurate evaluation of this HCl fraction requires a detailed examination of cations in order to evaluate the amount of chloride purely related to halide emissions (sea spray, evaporite) and soil weathering input which together represent some 80% of total chloride. The long term trend of HCl level in a high-elevated Alpine ice core suggests that in summer, although being highly variable from year to year, biomass burning is on average a significant natural source of HCl over the Alps. Coal burning emissions represented throughout the 20th century an additional (similar in intensity) source of HCl for these regions in summer. The main anthropogenic input comes from waste incineration which had a three to four times larger impact than coal burning at the scale of western Europe in the 70s and 80s. The contribution of chlorocarbon oxidation appears far lower than expected stimulating further investigation of the atmospheric fates of these species. Although needed to be confirmed by other ice core studies, the reincrease of winter levels in the late 90s may possibly reflect stratospheric HCl changes related to CFC degradation. The presence of HCl in Greenland ice cores is essentially related to sea salt dechlorination which was enhanced by a factor of two over the 20th century. If the recent finding that the acid displacement of sea salt by SO_2 and NO_x only accounts for 15% of the total sea salt dechlorination is correct, the Greenland data suggest that major (unknown) dominant sea salt dechlorination processes have also been enhanced by a factor of two over the 20th century.

Acknowledgements

This work has been supported by the European Environment and Climate program ALPCLIM. Funding was provided by the European Community via contract ENV4-CT97

(ALPCLIM) and ENV4-CT96-5051 (Environment and Climate Research Training), the Centre National de la Recherche Scientifique (programme PNCA), and the Ministery for Science and Research of Baden-Württemberg within the collaboration programme between Region Rhône-Alpes and Baden-Württemberg.

References

Baltensperger, U., H.W. Gaeggeler, D.T. Jost, M. Lugauer, M. Schwikowski, E. Weingartner, and P. Seibert, Aerosol climatology at the high-alpine site Jungfrauchjoch, Switzerland, *J. Geophys. Res.*, *102*, 19,707-19,715, 1997.

Bloomfield, P., W.L. Steiger, In *Last absolute deviations: Theory, Applications and Algoritms*, Birkhauser, Boston, 1983.

R. Boehm, I. Auer, M. Brunetti, M. Maugeri, T. Nanni, and W. Schöner, Regional temperature variability in the European Alps 1760-1998, *International Journal of Climatology*, in press.

Chin, M., D.J. Jacob, G. Gardner, M.S. Foreman-Fowler, and P.A. Spiro, A global three-dimensional model of tropospheric sulfate, *J. Geophys. Res.*, *101*, 18,667-18,690, 1996.

De Angelis, M., and M. Legrand, Origins and variations of fluoride in Greenland precipitation, *J. Geophys. Res.*, *99*, 1157-1172, 1994.

De Angelis, M., and M. Legrand, Preliminary investigations of post depositional effects on HCl, HNO_3, and organic acids in polar firn layers, in *Ice Core Studies of Global Biogeochemical Cycles, NATO ASI Ser. I*, vol. 30, edited by R.J. Delmas, pp. 361-381, Springer-Verlag, New York, 1995.

De Angelis, M., J.P. Steffensen, M. Legrand, H. Clausen, and C. Hammer, Primary aerosol (sea salt and soil dust) deposited in Greenland ice during the last climatic cycle: Comparison with East Antarctic records, *J. Geophys. Res.*, *102*, 26,681-26,698, 1997.

Eichler, A., M. Schwikowski, and H. Gäggeler, An Alpine ice-core record of anthropogenic HF and HCl emissions, *Geophys. Res. Lett.*, *27*, 3225-3228, 2000.

Erickson III, D.J., C. Seuzaret, W.C. Keene, and S.L. Gong, A general circulation model based calculation of HCl and $ClNO_2$ production from sea salt dechlorination: Reactive Chlorine Emissions Inventory, *J. Geophys. Res.*, *104*, 8347-8372, 1999.

Fischer, H., Spatial variability of ice core records from North-East Greenland: Reconstruction of climatic and atmospheric chemistry long-term trends since 1500 AD, Ph. D. dissertation, pp. 135, Univ. Heidelberg, Heidelberg, Germany, 1997.

Fischer, H., D. Wagenbach, and J. Kipfstuhl, Sulfate and nitrate firn concentrations on the Greenland ice sheet 1. Large-scale geographical deposition changes, *J. Geophys. Res.*, *103*, 21927-21934, 1998.

Graedel, T.E., and W.C. Keene, The tropospheric budget of reactive chlorine, *Global Biogeochem. Cycles*, *9*, 47-78, 1995.

Graedel, T.E., and W.C. Keene, The budget and cycle of Earth's natural chlorine, *Pure and Appl. Chem.*, *68*, 1689-1697, 1996.

Kahl, J.D., D.A. Martinez, H. Kuhns, C.I. Davidson, J.L. Jaffrezo, and J.M. Harris, Air mass trajectories to Summit: A 44-year climatology and some episodic events, *J. Geophys. Res.*, *102*, 26,861-26,875, 1997.

Keene, W.C., and 17 others, Composite global emissions of reactive chlorine from anthropogenic and natural sources: Reactive Chlorine Emissions Inventory, *J. Geophys. Res.*, *104*, 8429-8440, 1999.

Lefohn A.S., J.D. Husar, and R.B. Husar R.B., Estimating Historical Anthropogenic Global Sulfur Emission Patterns for the Period 1850-1990, *Atmos. Environ.*, *33*, 3435-3444, 1999.

Legrand M., C. Lorius, N.I. Barkov, and V.N. Petrov, Vostok (Antarctica) ice core: Atmospheric chemistry changes over the last climatic cycle (160,000 years), *Atmos. Environ.*, *22*, 317-331, 1988.

Legrand M., and R.J. Delmas, Formation of HCl in the antarctic atmosphere, *J. Geophys. Res.*, *93*, 7153-7168, 1988.

Legrand, M., M. De Angelis, and F. Maupetit, Field investigation of major and minor ions along Summit (central Greenland) ice cores by ion chromatography, *J. Chromatogr.*, *640*, 251-258, 1993.

Legrand, M., and De Angelis, M., Light carboxylic acids in Greenland ice: A record of past forest fires and vegetation emissions from the boreal zone, *J. Geophys. Res.*, *101*, 4129-4145, 1996.

Legrand, M., and P. Mayewski, Glaciochemistry of polar ice cores: A review, *Rev. of Geophys.*, *35*, 219-243, 1997.

Legrand, M., C. Hammer, M. De Angelis, J. Savarino, R. Delmas, H. Clausen, and S.J. Johnsen, Sulfur-containing species (methanesulfonate and SO_4) over the last climatic cycle in the Greenland Ice Core Project (central Greenland) ice core, *J. Geophys. Res.*, *102*, 26,663-26,679, 1997.

Lightowlers, P.J., and J.N. Cape, Sources and fate of atmospheric HCl in the U.K. and western Europe, *Atmos. Environ.*, 22, 7-15, 1988.

Lobert, J.M., W.C. Keene, J.A. Logan, and R. Yevich, Global chlorine emissions from biomass burning: Reactive Chlorine Emissions Inventory, *J. Geophys. Res.*, *104*, 8373-8389, 1999.

Masarik, J., and J. Beer, Simulation of particle fluxes and cosmogenic nuclides production in the Earth's atmosphere, *J. Geophys. Res.*, *104*, 12,099-13,112, 1999.

Mayewski, P., and 8 others, Greenland ice core «signal» characteristics: An expanded view of climate change, *J. Geophys. Res.*, *98*, 12,839-12,847, 1993.

McCulloch, A., and 6 others, Global emissions of hydrogen chloride and chloromethane from coal combustion, incineration and industrial activities: Reactive Chlorine Emissions Inventory, *J. Geophys. Res.*, *104*, 8391-8403, 1999.

Mylona, S., Sulphur dioxide emissions in Europe 1880-1991 and their effect on sulphur concentrations and deposition, *Tellus*, *48*, 662-689, 1996.

Preunkert, S., and D. Wagenbach, An automatic recorder for air/firn transfer studies of chemical aerosol species at remote glacier sites, *Atmos. Environ.*, *32*, 4021-4030, 1998.

Preunkert, S., D. Wagenbach, M. Legrand, and C. Vincent, Col du Dôme (Mt Blanc Massif, French Alps) suitability for ice core studies in relation with past atmospheric chemistry over Europe, *Tellus*, *52*, 993-1012, 2000.

Preunkert, S., M. Legrand, and D. Wagenbach, Causes of enhanced fluoride levels in Alpine ice cores over the last 75 years: Implications for the atmosphere fluoride budget, *J. Geophys. Res.*, in press.

Preunkert, S., M. Legrand, and D. Wagenbach, Sulfate Trends in a Col du Dôme (French Alps) Ice Core: A Record of Anthropogenic Sulfate Levels in the European Mid-Troposphere over the 20th Century, *J. Geophys. Res.*, submitted.

Sanhueza, E., Hydrochloric acid from chlorocarbons: A significant global source of background rain acidity, *Tellus*, *53*, 122-132, 2001.

Savarino, J., and M. Legrand, High northern latitude forest fires and vegetation emissions over the last millenium inferred from the chemistry of a central Greenland ice core, *J. Geophys. Res.*, *103*, 8267-8279, 1998.

Schaug, J., U. Pedersen, J.E. Skjelmoen, and I. Kvalvaagnes, Data report 1991. Part 2: Seasonal summaries. EMEP/CCC-Report 4/93. Norwegian Institute for Air Research, Lillestrom, Norway, 1987.

Simeonov, V., H. Puxbaum, S. Tsakovski, C. Sarbu, and M. Kalina, Classification and receptor modeling of wet precipitation data from central Austria (1984-1993), *Environmetrics*, *19*, 137-152, 1999.

Sievering, H., E. Gorman, T. Ley, A. Pszenny, M. Springer-Young, J. Boatman, Y. Kim, C. Nagamoto, and D. Wellman, Ozone oxidation of sulfur in sea-salt aerosol particles during the Azores marine Aerosol and Gas exchange experiment, *J. Geophys. Res.*, *100*, 23,075-23,081, 1995.

Stanzick, A., Spatio-temporal variations of ^{10}Be, ^{210}Pb, and ^{36}Cl in the Greenland firn cover: Air-firn transfer and recent trends (in German), Ph. D. Dissertation, pp. 118, Univ. Heidelberg, Heidelberg, Germany, 2001.

Symonds, R.B., W. Rose, and M.H. Reed, Contribution of Cl- and F-bearing gases to the atmosphere by volcanoes, *Nature*, *334*, 415-418, 1988.

Synal, H.A., J. Beer, G. Bonani, M. Suter, and W. Wolfli, Atmospheric transport of bomb produced ^{36}Cl, *Nuclear Instruments and Methods in Physik Research*, *52*, 483-488, 1990.

Synal, H.A., J. Beer, U. Schotterer, M. Suter, and L. Thompson, Bomb produced ^{36}Cl in ice core samples from mountain glaciers, In *Glaciers from the Alps: Climate and environmental archives*, PSI, Wengen/CH, 1997.

Talbot, R.W., R.C. Harriss, E.V. Browell, G.L. Gregory, D.I. Sebacher, and S.M. Beck, Distribution and geochemistry of aerosols in the tropical North Atlantic troposphere: Relationship to saharan dust, *J. Geophys. Res.*, *91*, 5173-5182, 1986.

Wagenbach, D., S. Preunkert, J. Schaefer, W. Jung, and L. Tomadin, Northward transport of saharan dust recorded in a deep Alpine ice core. In *The impact of African dust across the Mediterranean*, S. Guerzoni and R. Chester eds., Kluwer Academic Publishers, The Netherland, 291-300, 1996.

Whitlow, S., P. Mayewski, and J. Dibb, A comparison of major chemical species input timing and accumulation at South Pole and Summit, Greenland, *Atmos. Environ.*, *26*, 2045-2054, 1992.

Zander, R., M.R. Gunson, J.C. Foster, C.P. Rinsland, and J. Namkung, Stratospheric $ClONO_2$, HCl, and HF concentration profiles derived from atmospheric trace molecule spectroscopy experiment spacelab 3 observations: An update, *J. Geophys. Res.*, *95*, 20,519-20,525, 1990.

Tables

Table 1: Mean levels of sodium, non-soil sodium, chloride, hydrochloric acid, calcium, magnesium, and non-soil magnesium in spring and summer snow layers deposited at Summit between 1870 and 1993. For calculations of non-soil contributions of magnesium and sodium, as well as HCl, see text (section 3).

Species	Spring, ng g^{-1}	Summer, ng g^{-1}
Na^+	8.2 ± 4.7	2.2 ± 1.2
Non-soil-Na^+	6.7 ± 4.6	1.9 ± 1.2
Cl^-	16.6 ± 7.7	8.3 ± 5.2
HCl	6.2 ± 4.5	5.4 ± 4.8
Ca^{2+}	14.9 ± 7.5	3.1 ± 1.9
Mg^{2+}	2.6 ± 1.2	0.4 ± 0.3
Non-soil-Mg^{2+}	0.8 ± 0.8	-

Table 2: Same as Table 1 for summer and winter snow layers deposited at CDD between 1925 and 1995.

Species	Summer, ng g^{-1}	Winter, ng g^{-1}
Na^+	15.5 ± 12.7	5.7 ± 8.6
Non-soil-Na^+	9.4 ± 8.7	5.2 ± 8.1
Cl^-	30.4 ± 23.2	11.4 ± 16.0
HCl	6.4 ± 12.3	0.7 ± 3.3
Ca^{2+}	55 ± 63	5.9 ± 7.7
Mg^{2+}	7.2 ± 7.9	1.0 ± 0.9
Non-soil-Mg^{2+}	1.0 ± 3.3	0.5 ± 0.8

Table 3: Linear relationships between sodium, magnesium, potassium, and chloride versus calcium in CDD summer samples regarded as contaminated by saharan dust (see section 3.3).

Species	Linear Relationship	Number of samples	R^2
Na^+	$[Na^+] = 0.071\ [Ca^{2+}] + 20.8$	98	0.66
Mg^{2+}	$[Mg^{2+}] = 0.045\ [Ca^{2+}] + 9.2$	98	0.76
K^+	$[K^+] = 0.035\ [Ca^{2+}] + 12.5$	98	0.56
Cl^-	$[Cl^-] = 0.113\ [Ca^{2+}] + 34.6$	98	0.67

Table 4: Chemical composition of summer and winter layers located on the bottom part of the 1994 CDD core (between 90.3 and 95.3 m w.e.) which were estimated to span the 1906-1922 time period (see section 2). All data have been corrected from blank values (see section 2). Values refer to means after correction of samples (16 on a total of 111) suspected to contain saharan dust (see section 3.3).

Species	Winter, in ng g^{-1}	Summer, in ng g^{-1}
SO_4^{2-}	31 ± 8	64 ± 18
Ca^{2+}	21 ± 8	40 ± 10
Na^+	7 ± 3	13 ± 4
Cl^-	11 ± 3	20 ± 5
HCl	-1.0 ± 2.7	0.2 ± 2.7

Table 5: Estimates of the HCl fractions related to different processes contributing to the mean summer snow layers HCl level deposited at CDD in the 80s (15.5 ng g^{-1}). Comparison with the respective annual emission rates of these processes on a global scale and for summer over western Europe (see text).

Sources	Summer Emission in Western Europe, in Mt	HCl fraction in CDD summer, in ng g^{-1}	Global Emission, in Mt yr^{-1}	References
Volcanoes	-	-	2	*Graedel and Keene* [1995]
Biomass Burning	0.02	2.7	<6.3	*Lobert et al.* [1999]
Coal Burning	0.04	2.6	4.6 ± 4.3	*McCulloch et al.* [1999]
Waste Burning	0.046	8.2 - 10.2	2.0 ± 1.9	*McCulloch et al.* [1999]
Sea salt Dechlorination	-	-	50 ± 20	*Graedel and Keene* [1995]
Chlorocarbons Oxidation	0.01	0 to 2	4.2	*Sanhueza* [2001]

Figures

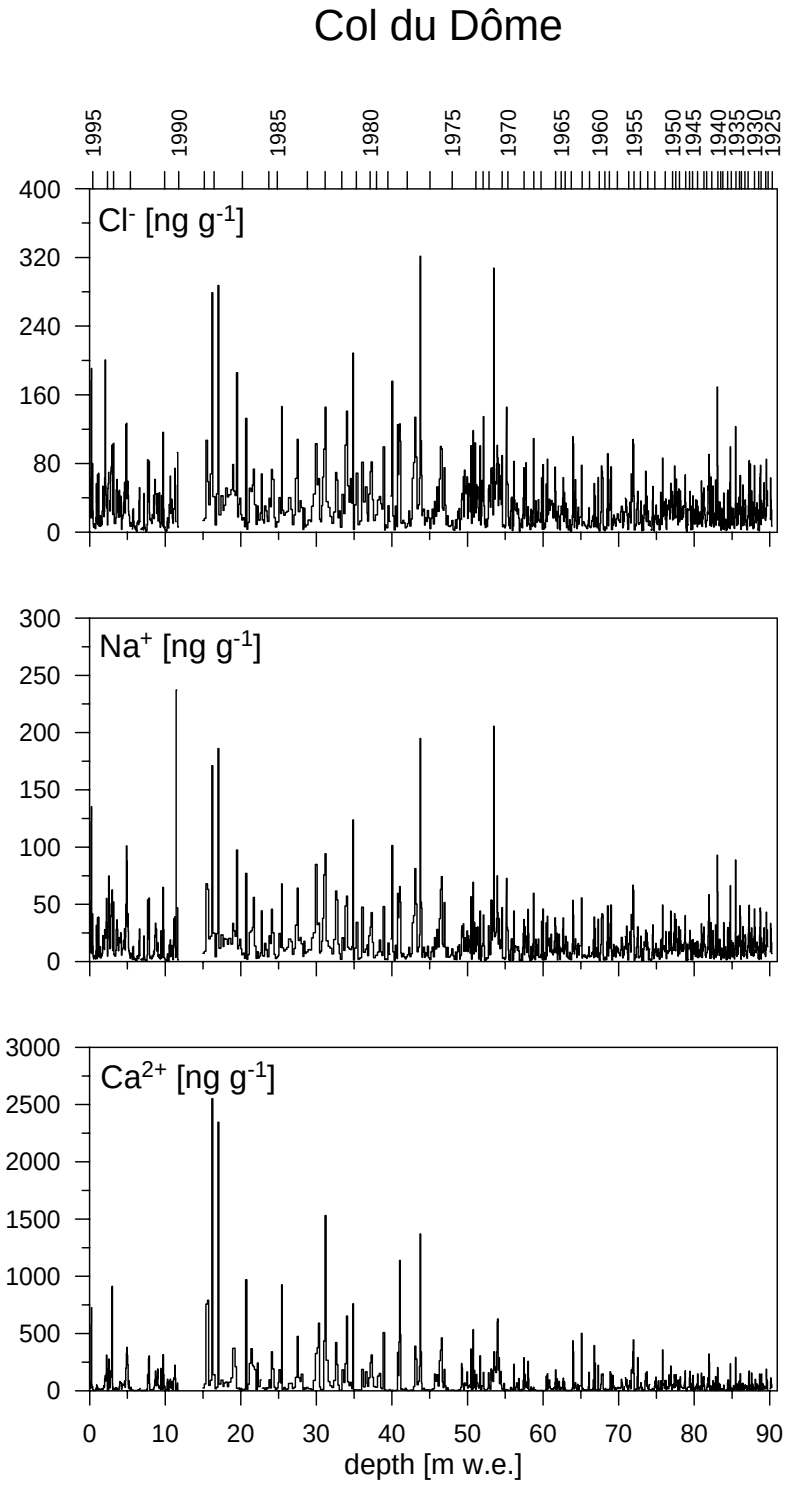

Figure 1: High-resolution depth profiles (in meters water equivalent) of chloride, sodium, and calcium along the upper 90 m w.e. of the 1994 CDD core. The dating reported on the top refers to Preunkert et al. [2000].

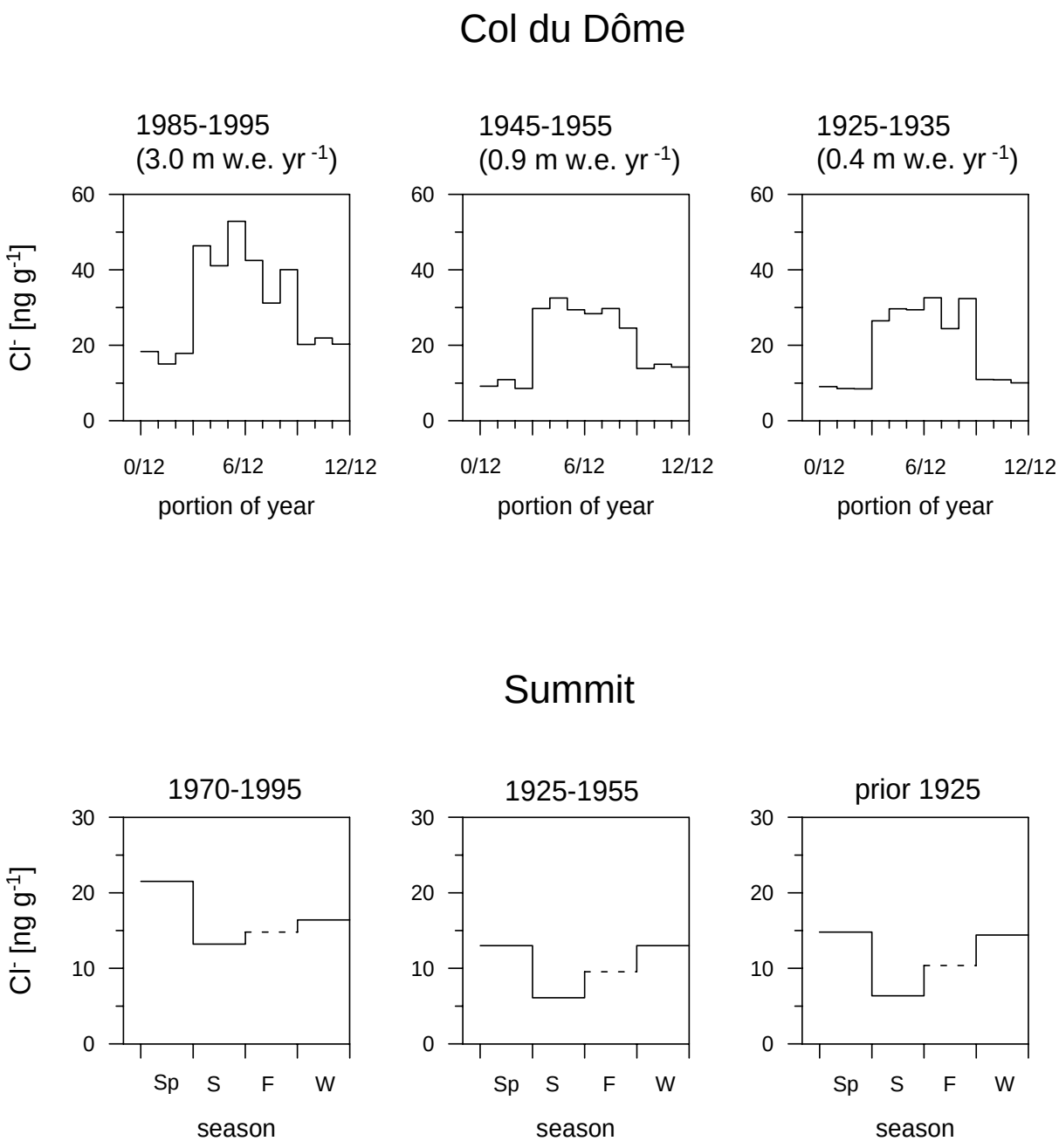

Figure 2: Mean seasonal cycle of chloride in snow layers deposited over various time periods at CDD (top) and Summit (bottom).

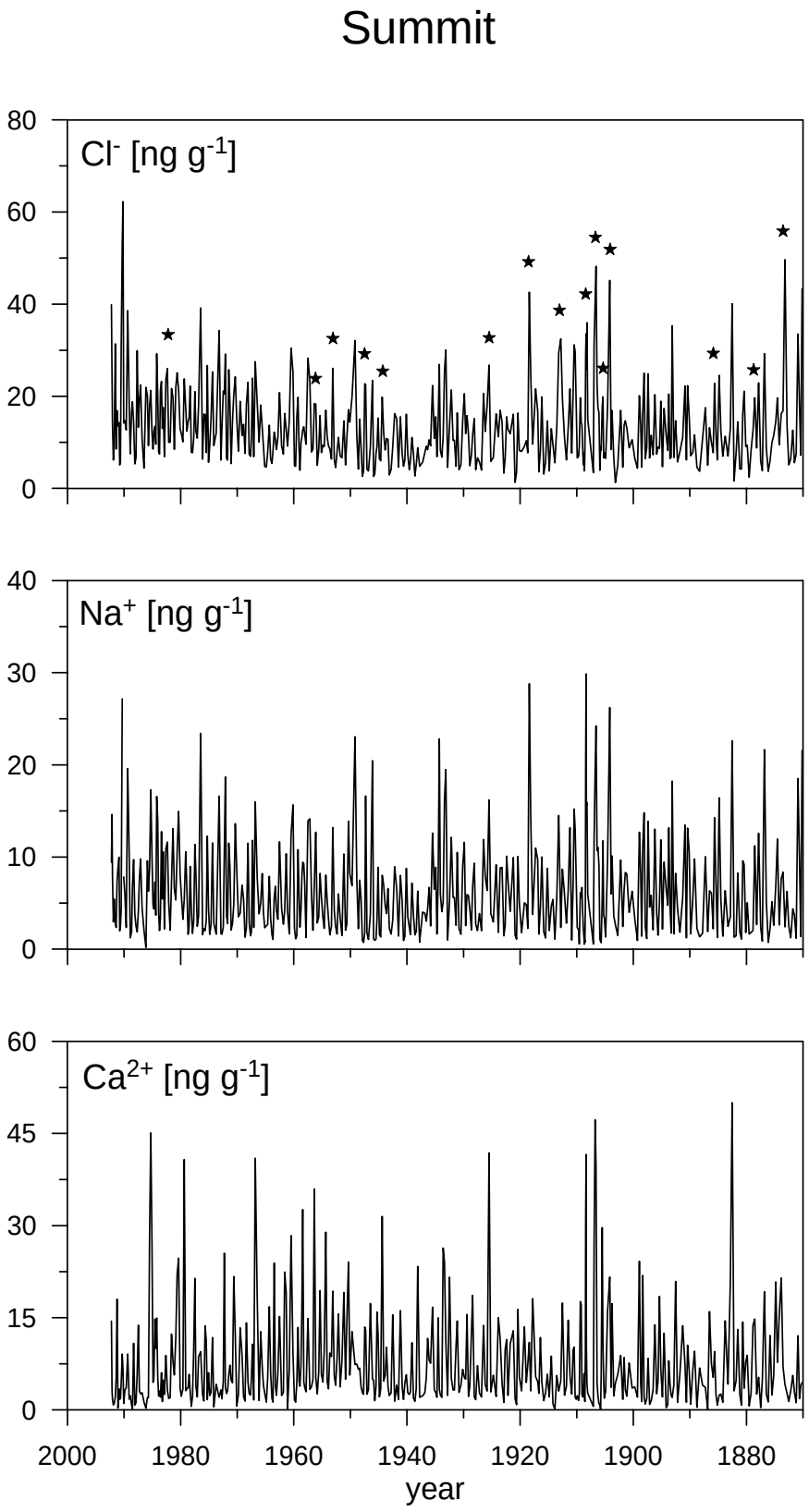

Figure 3: High-resolution profiles of chloride, sodium, and calcium along a Summit (central Greenland) ice core spanning the 1870-1993 time period. The dating of this core reported on the bottom refers to Legrand and De Angelis [1996]. Stars reported on the chloride profile refer to snow layers regarded as contaminated by volcanic inputs (see text).

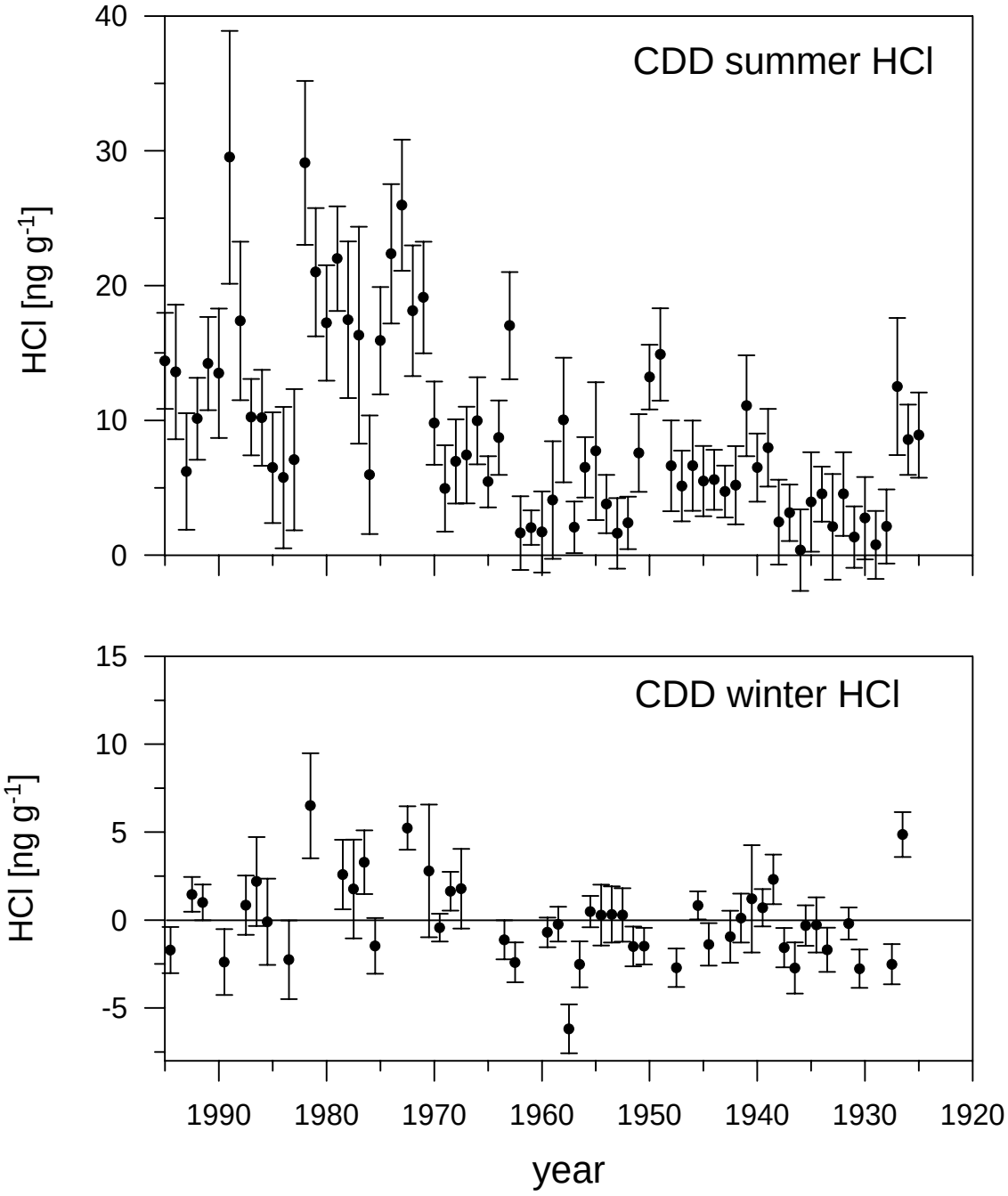

Figure 4: Annual summer (top) and winter (bottom) means of HCl in the CDD ice core. Vertical bars refer to the mean errors in evaluation the mean HCl annual levels.

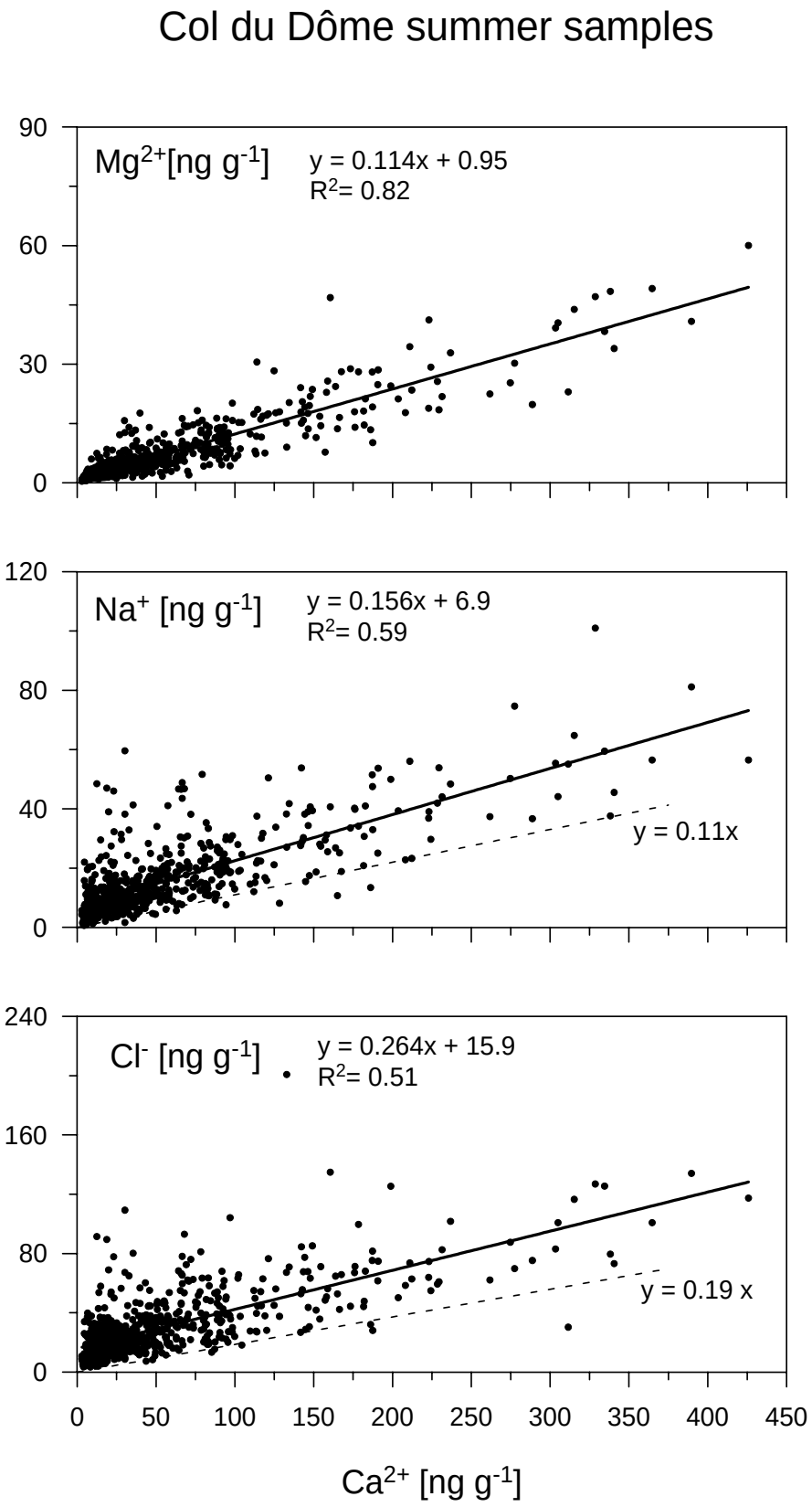

Figure 5: Magnesium (top), sodium (middle), and chloride (bottom) versus calcium in summer CDD layers excluding samples regarded as containing saharan dust (see section 3.3). The dashed lines reported on sodium and chloride plots refer to an estimate of the sodium to calcium (0.11) and chloride to calcium (0.186) mass ratios related to the input from soil weathering (see section 3).

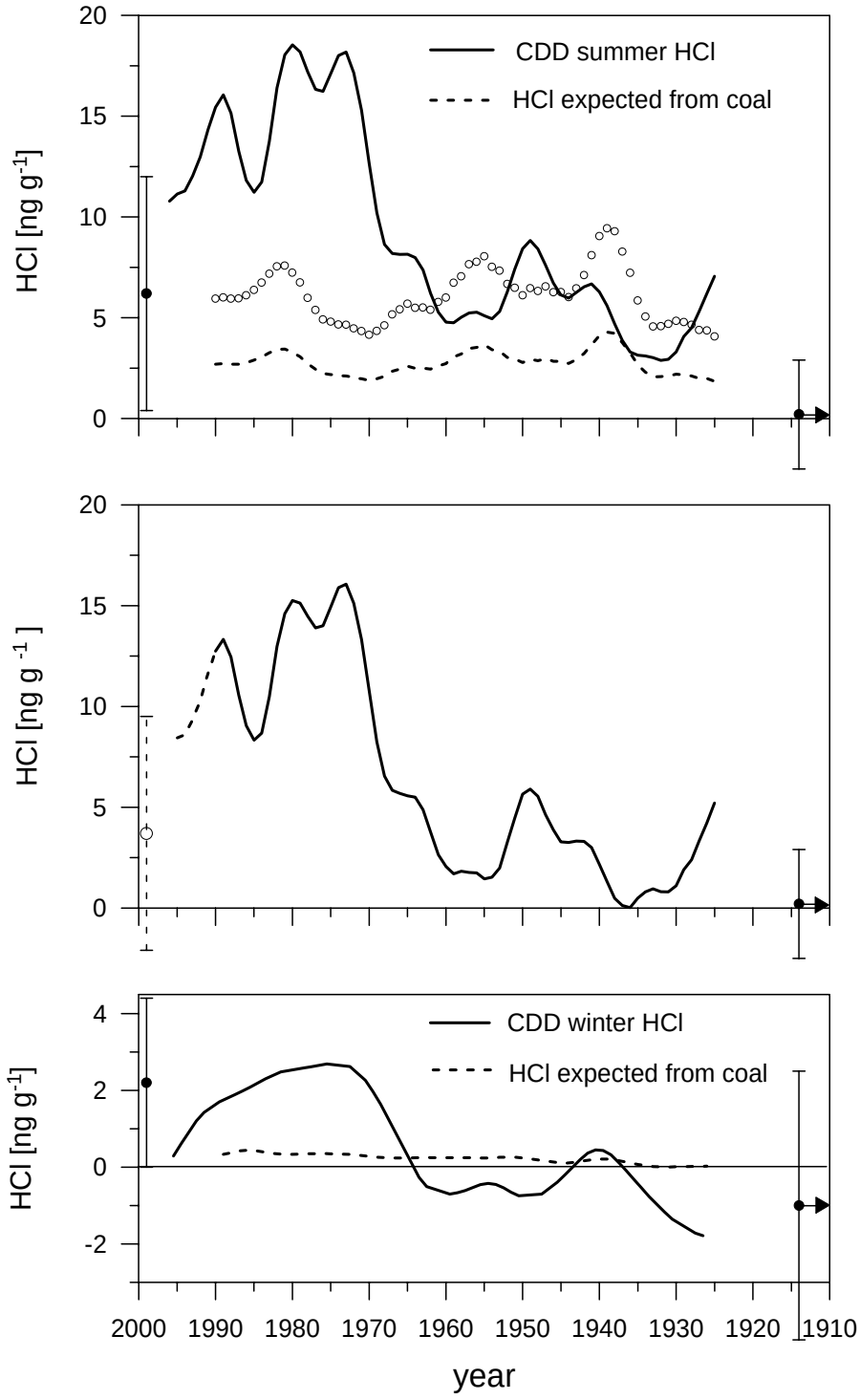

Figure 6: Summer (top) and winter (bottom) trends of HCl (solid lines) in the 1994 CDD ice core compared with the expected contribution of coal combustion (dashed lines). The expected contribution of coal burning is calculated from equation (6) (see section 4.1). The solid lines are the first SSA component with a 5-year time window and a robust spline for summer and winter means, respectively. The arrows on the right side refer to the mean level calculated in the bottom part of the core (Table 4). The arrows on the left side refer to the mean level calculated for snow layers sampled in snow pits covering the 1998, 1999, and 2000 years. The open circles refer to the coal contribution calculated when a δ value of 1 is applied in equation (6) (see section 4.1).

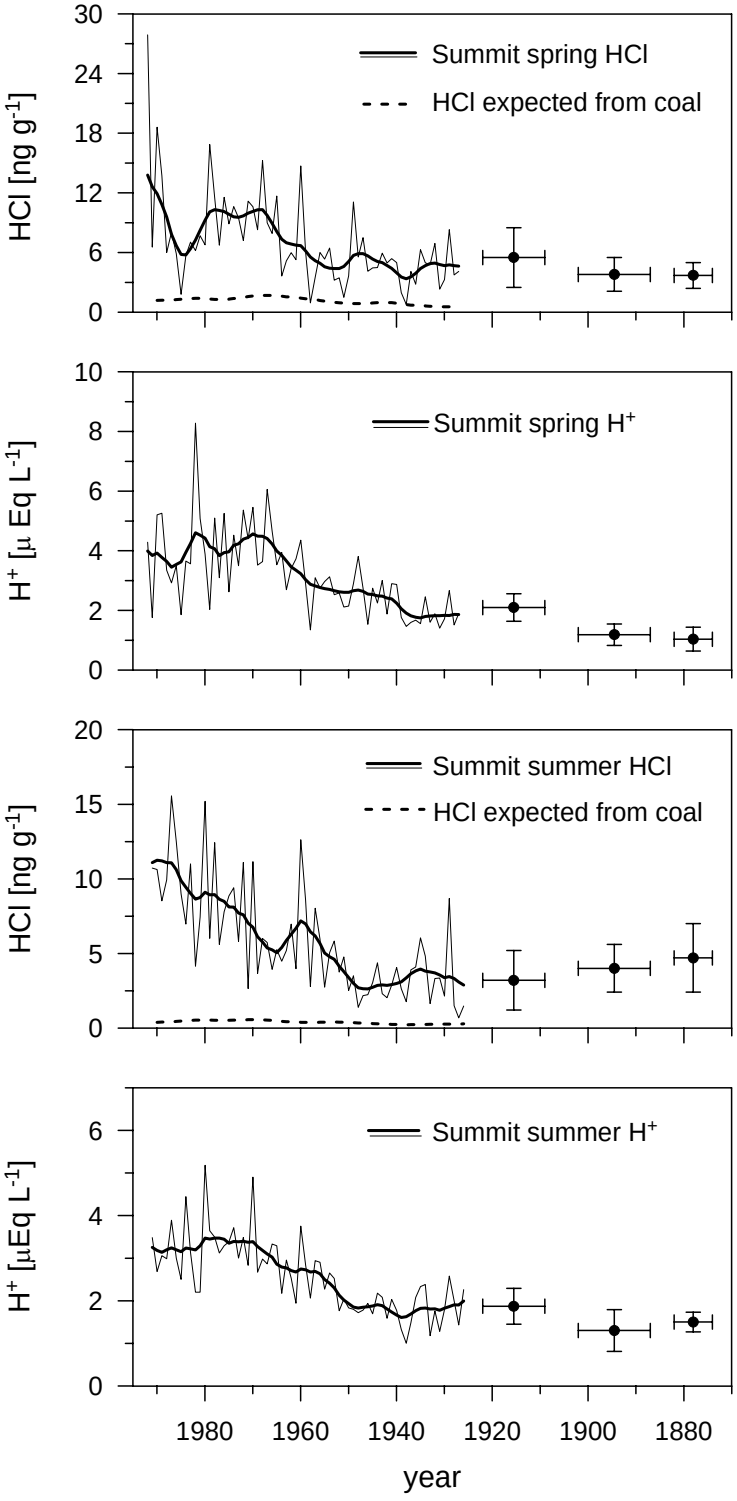

Figure 7: Summit HCl and acidity records over the 1870-1993 time period for spring (top) and summer (bottom) means. The solid smoothed curves represent the first SSA component with a 5-year time window. The three arrows reported on the right side refer to multiple-year means (1873-1881, 1886-1901, and 1908-1922) (horizontal bars are covered time periods, vertical bars refer to standard deviation). The dashed lines reported along with the HCl trends refer to the contribution of coal burning calculated with equation (6) (see section 4.1). The acidity has been calculated by checking the ionic balance following Legrand and De Angelis [1996].

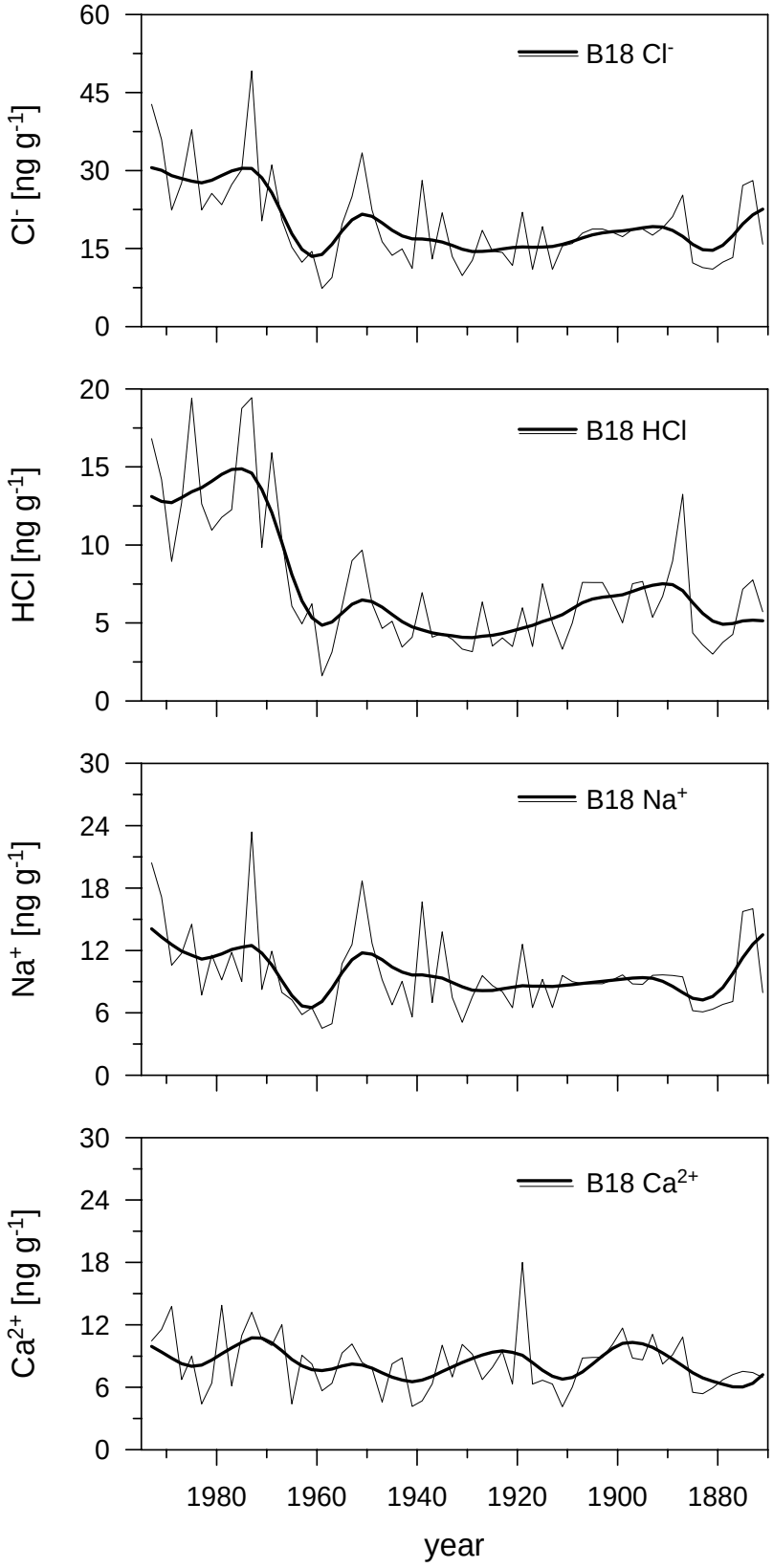

Figure 8: Records of chloride, HCl, sodium, and calcium at the B18 North Greenland site. Raw chloride, sodium and calcium data are from Fischer [1997]. HCl levels were evaluated in a same way than the one applied for the Summit snow layers using equation (2c) (see text).

Chapter VI

Temporal changes of carboxylic acids (formate, acetate, and oxalate) in CDD snow layers

6.1 Introduction

Present in all atmospheric phases (gas and liquid phases, aerosols), light carboxylic acids represent a significant fraction of the organic matter present in the atmosphere. They have been detected in the gas (Talbot et al., 1992; Khwaja, 1995) and particulate (Li and Winchester, 1989; Sempéré and Kawamura, 1994) phase as well as in rainwater and snow (Keene et al., 1983; Winiwarter et al., 1988; Legrand et al., 1992; Kumar et al., 1993), in high polluted continental sites as well as at remote marine regions of the world. The study of these species indicates that these carboxylic acids (particularly formic and acetic acids) can significantly contribute to the acidity of precipitation in urban and remote areas of the world (Galloway et al., 1982; Keene et al., 1983; Kawamura and Kaplan, 1983; Guiang et al., 1984; Keene and Galloway, 1984; Dayan et al., 1985; Norton, 1985; Chapman et al., 1986; Likens et al., 1987; Sanhueza et al., 1989; Gillet et al., 1990). For instance, Keene et al. (1983) estimated that carboxylic acids contribute up to 64% of the free acidity of the precipitation in non urban environments. Although different sources of monocarboxylic and dicarboxylic acids in the atmosphere have been identified, their relative importance for the global budget remains highly uncertain.

Mono-carboxylic acids sources include direct releases into the atmosphere by anthropogenic and/or biogenic activities, and photochemical oxidation of organic precursors in the gas or aqueous phases (Su et al., 1980; Chameides and Davis, 1983; Duce et al., 1983; Calvert and Stockwell, 1983; Atkinson and Lloyd, 1984; Jacob, 1986; Jacob and Wofsy, 1988(b); Madronich and Calvert, 1990). Direct emissions include biomass burning (Talbot et al., 1990; Lacaux et al., 1992), vehicular exhaust emissions (Kawamura and Kaplan, 1985; Talbot et al., 1988), emissions from soil and vegetation (Servant et al., 1991; Kesselmeier and Staudt, 1999), and possibly marine biogenic emissions (Graedel and Weschler, 1981). Photochemical gas-phase oxidation of hydrocarbons and of their degradation products such as aldehydes is believed to be a major pathway of the carboxylic acid secondary production (Keene and Galloway, 1988). Aldehydes themselves are directly emitted during combustion of hydrocarbons. Other important mechanisms producing carboxylic acids are the ozone-olefin reactions (Calvert and Stockwell, 1983), the oxidation of formaldehyde by hydroxyl radical (Jacob, 1986; Chameides, 1984), and the photochemical decomposition of isoprene (Jacob and Wofsy, 1988a). Finally, biogenic emissions (direct and secondary) from

vegetation have been hypothesized as important natural sources for formic and acetic acids particularly during the growing season (Keene and Galloway, 1986).

Sources of dicarboxylic acids in the atmosphere are determined at present even more uncertain than those of mono-carboxylic acids. Direct emissions from motor exhausts and soils have been identified as sources of oxalic acid (Kawamura and Kaplan, 1987; Grosjean, 1989), although the major sources of this acid is assumed to be the degradation of higher diacids, produced by ozonolysis of cycloolefins and aliphatic diolefins (Hatakeyama et al., 1985, 1987).

Due to their low chemical reactivity, formic and acetic acids, mainly present in the gas phase, are mainly removed from the atmosphere by wet and dry depositions. Oxalic acid is mostly present in the atmosphere in the aerosol phase although a recent study (Limbeck et al., 2001) pointed out its semivolatile behaviour.

Investigations of past atmospheric changes of carboxylic acids are limited to ice core studies performed on Greenland ice cores by Legrand et al. (1992), Legrand and De Angelis (1995 and 1996), and Savarino and Legrand (1998). Legrand and De Angelis (1996) pointed out an anthropogenic increase for acetate whereas rather unchanged levels for formate and oxalate were observed in Greenland snow layers deposited since 1780. These Greenland studies revealed that the levels of formate and acetate have been very often enhanced in the past following forest fire events taking place in Canada (Savarino and Legrand, 1998). Apart from these sporadic events, the natural background level of formate appears to be influenced by vegetation emissions from the boreal zone (Legrand and De Angelis, 1996) whereas another source (possibly marine) is suspected to also influence the natural budget of acetate.

In this work we will examine the long term trends of carboxylic acids (acetate, formate, and oxalate) along the deep CDD ice core. Hereby the discussion will be focused to examine in what extend such records are useful to get an idea about the relative importance of the different sources of these species for free tropospheric conditions over Europe, and in particular to examine how important are anthropogenic emissions versus natural sources.

6.2 The dicarboxylic acid oxalate

The long term trends of oxalate in CDD summer and winter snow layers are reported in Figure 6.1. The smoothed curves were achieved by applying SSA and robust spline protocols on summer and winter records, respectively (see section 3.2.4). The summer record shows no significant trend over the last 70 years except a sharp decrease of levels having took place from 1955 to 1960 followed by a re-increase from 1970 to 1980. The winter trend also exhibits a minimum of concentrations around 1965. To examine the spatial representativeness of these temporal changes, we investigated the oxalate level in samples from a Colle Gnifetti ice core in which in addition to summer snow layers a few snow layers were representative of winter snow precipitation (Figure 6.1). The mean summer and winter concentrations of

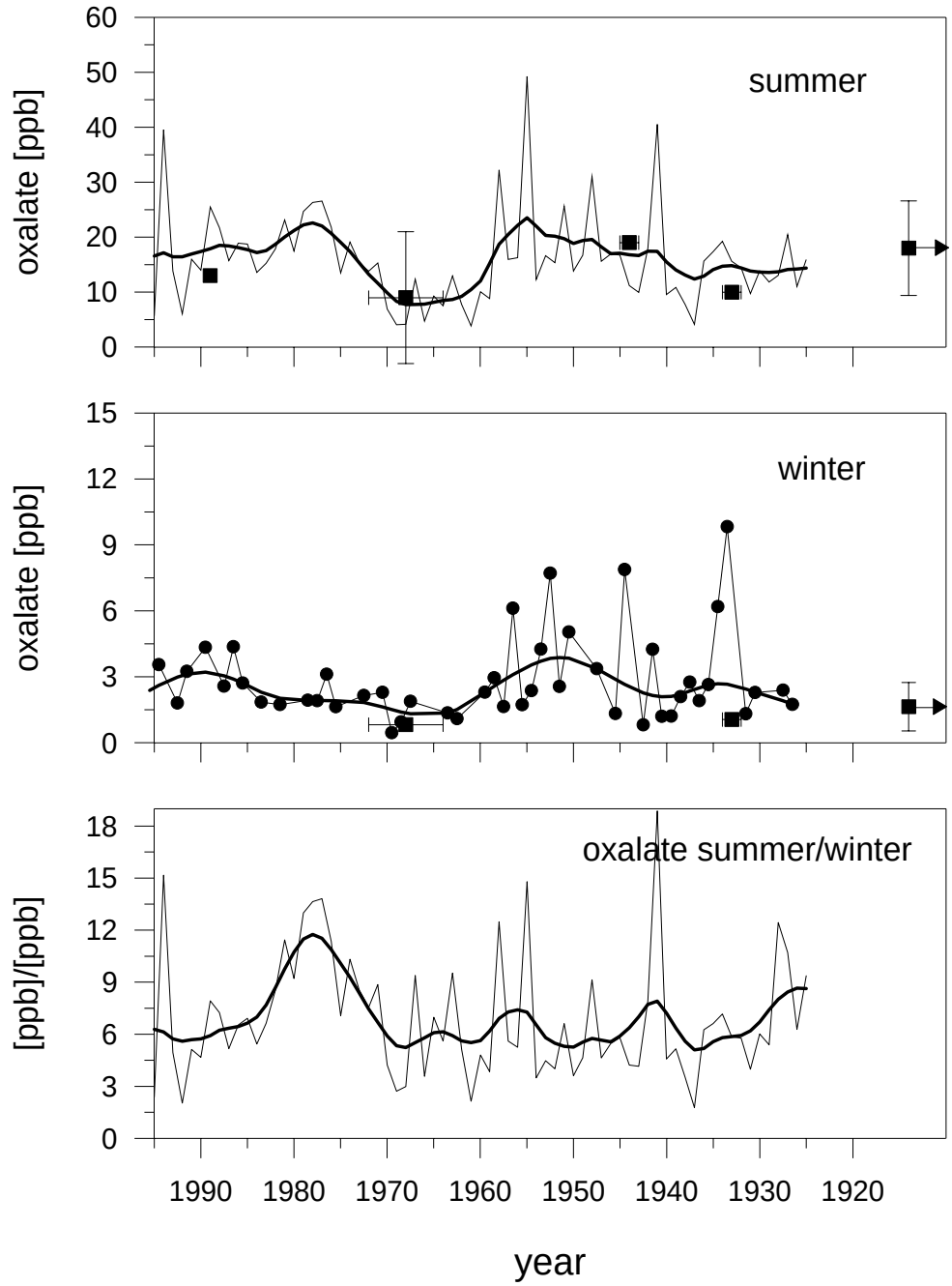

Figure 6.1: Summer and winter long term records of oxalate in the C10 ice core along with temporal changes of the summer to winter ratio. Reported are individual summer and winter means (thin lines) and smoothed time trends (thick lines) derived by SSA (first component) in summer and robust spline smoothing in winter. Filled squares mark winter and summer oxalate levels obtained in Colle Gnifetti snow layers corresponding to different time periods (horizontal bars indicate the covered time periods, vertical bars refer to standard deviation of individual half year means). The arrows on the right site refer to the mean pre-industrial levels (≈ 1850 ± 10 years).

oxalate obtained in these summer and winter Colle Gnifetti snow layers exhibit changes which are very consistent with those we found at CDD, including the low values found between 1966 and 1972. Therefore we conclude that the oxalate levels and their temporal changes observed at the CDD site are representative of the Alpine massif. Except between 1972 and 1983 the summer to winter ratio of oxalate levels fluctuates between 5 and 8. This is in the same order of magnitude of what is observed for other mineral species such as nitrate and sulfate.

With a mean summer level of 17 ppb (i.e., 0.4 μEq/l) in recent snow layers (Figure 6.1), oxalate contributes for less than 4.5% to the total acidity of CDD snow layers. The mean summer oxalate level of 17 ppb corresponds to ~5 ppb of C and referring to the pilot study of dissolved organic carbon (DOC) (personal communication, S. Greilich) corresponds to ≈ 3% of DOC (≈160 ppbC) in CDD snow layers. Note that this is in good agreement with the oxalate contribution to the total organic input of 6 % reported for cloud water samples at Sonnblick Observatory (Löflund et al., submitted).

Oxalate is generally found to be the most abundant dicarboxylic acid present in the aerosol phase in various regions. Atmospheric oxalate concentrations range from low values in the marine atmosphere (24 ng m^{-3}, Baboukas et al., 2000) to 80 ng m^{-3} at rural sites (Limbeck et al., 2001), 160 ng m^{-3} in air masses contaminated by biomass burning (Lefer et al., 1994) and 440 ng m^{-3} at Los Angeles (Kawamura and Kaplan, 1987). A few measurements made at the Sonnblick Observatory (3106 m asl, Austrian Alps) indicate a mean value in spring of 150 ng m^{-3}. Note that these atmospheric oxalate levels confirm the dominance of continental sources and the contribution of biomass burning and fossil fuel burning. As seen in section 1.3 (*6.1*), the mean summer oxalate atmospheric level at the Vallot Observatory is of 44 ng m^{-3}STP. In recent summer CDD snow layers we found a typical concentration of 17 ppb. This value is some 35 times lower than the level of sulfate (600~ppb, see Chapter 2) and is consistent with the sulfate to oxalate ratio of 20 observed in cloud water at Sonnblick in spring (7850 and 380ppb of sulfate and oxalate, respectively). The mean oxalate values found in summer (≈16 ± 8 ppb) and winter (≈2.8 ± 1.9 ppb) at Col du Dôme over the last 70 years are largely higher than the annual mean oxalate levels (≈0.3 ± 0.2 ppb) found in Greenland snow layers over this time period (Legrand and De Angelis, 1996). That is in agreement with the fact that oxalate sources are thought to be mainly located over continents.

To evaluate the pre-industrial oxalate level in high Alpine snow layers, we investigated Colle Gnifetti ice samples covering about 10 years around 1850 ± 10 years (see Figure 6.1). The CG oxalate concentrations (summer: 21 ± 8 ppb, winter: ≈1.5 ppb) are very close to those found in 1925 to 1930 (summer: 15 ± 4 ppb, winter: ≈2 ppb) at CDD. Theses values indicate an absence of an anthropogenic increase of oxalate levels in high Alpine snow layers. Note that a similar absence of anthropogenic trend has been observed in a Greenland

ice core by Legrand and De Angelis (1996). Such an absence of an anthropogenic trend suggests that biogenic emissions are mainly controlling the oxalate levels at high Alpine sites while direct anthropogenic oxalate sources (fuel combustion and/or motor exhausts, Kawamura and Kaplan, 1987), as well as secondary ones (photochemical oxidation of organic compounds like cyclic olefins emitted from anthropogenic sources, Grosjean et al., 1978) do not significantly influence tropospheric air conditions at 4300 m asl over Europe. Biogenic sources of oxalate include direct emissions (biomass burning, soils and vegetation) and secondary productions. A more detailed estimation of the relative contribution of these different biogenic sources to high Alpine snow deposits would be possible in the future, based on current investigation on black and organic carbon. We here present therefore only a brief preliminary discussion. Although the overall correlation between calcium and oxalate levels is rather poor ($R^2 = 0.38$, not shown), we have to emphasize that the minimum of oxalate level of 7 ppb seen in 1965 (Figure 6.1) coincide with the well marked minimum of the calcium trend (35 ppb compared to a mean level of 55 ppb between 1925 and 1995). That would suggest that soils represent one of the biogenic sources of oxalate for the CDD site. Further; as discussed in section 5.5 (*4.1.2*), the late 1940's are supposed to be marked by biomass burning (HCl input), and since the oxalate level in 1948 reached a rather high value of 30 ppb (Figure 6.1) a biomass burning contribution to the oxalate budget at CDD likely exists. Finally, comparing oxalate levels measured at the high Alpine site Sonnblick Observatory (3106 m asl, Austrian Alps) with the ones obtained at the urban site Vienna, Limbeck and Puxbaum (1999) concluded that the secondary oxalate production taking place in the troposphere contributes significantly to the overall oxalate budget.

In conclusion, the study of oxalate which represents a few percents of the organic aerosol species present in the atmosphere surprisingly indicates no major change in response to man made activities. If we assume that the oxalate to total organic aerosol ratio has not changed over the past, this absence of an oxalate trend suggests that, in contrast to the present-day situation where both anthropogenic sulfate and organic aerosol contribute similarly to the total aerosol load of the atmosphere, organic aerosol largely dominated the atmospheric aerosol load at the beginning of the 20th century. Implications for climate are here very important.

6.3 The monocarboxylic acids (acetate and formate)

6.3.1 Post depositional effects

Formate and acetate long term changes in CDD summer and winter snow layers obtained following the data processing protocol described in Chapter 3 are reported in Figure 6.2. They indicate a slight increase of acetate levels whereas formate levels remain

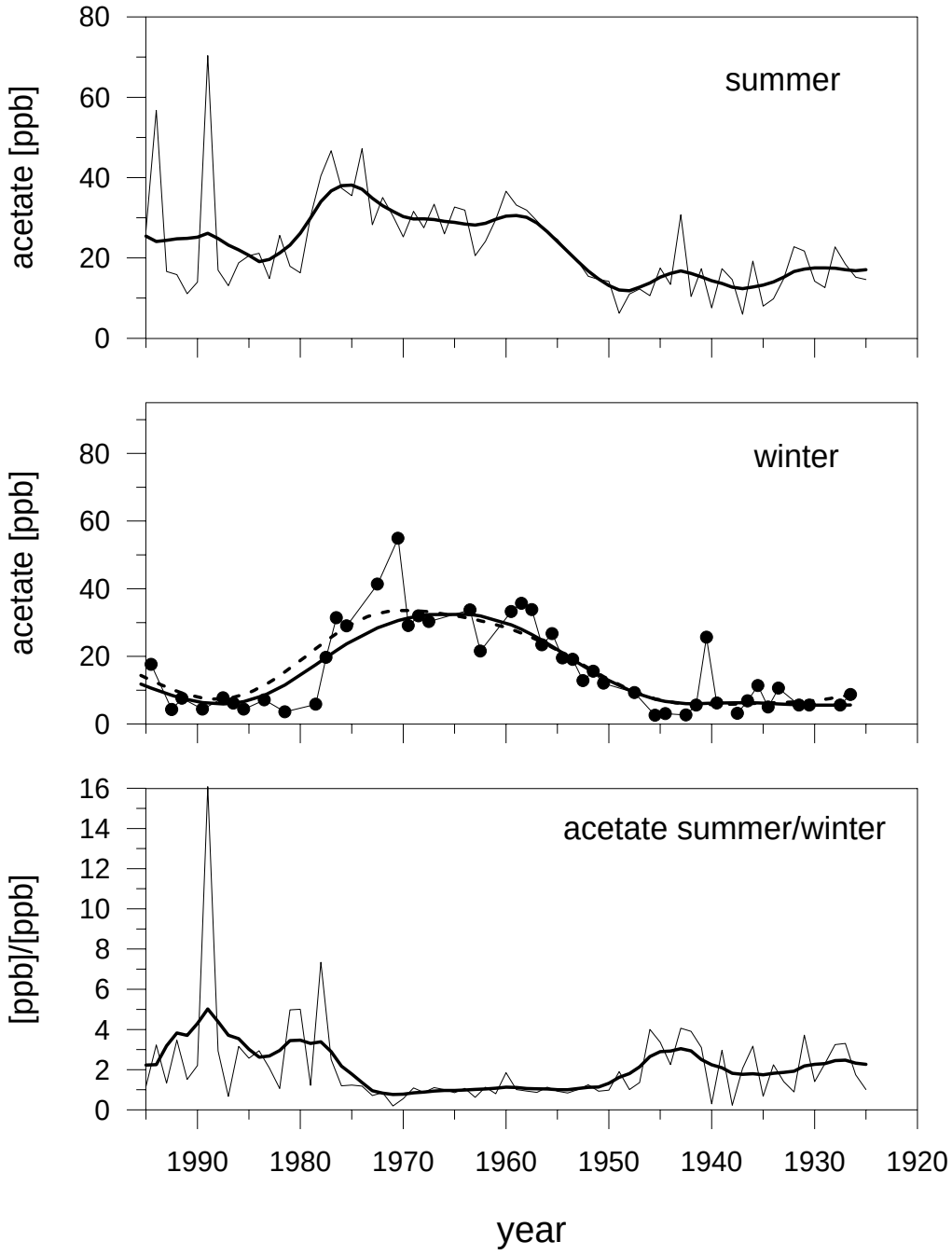

Figure 6.2a: Summer and winter long term records along with temporal evolution of summer to winter ratio of acetate in C10 snow layers. Reported are individual summer and winter means (thin lines) and smoothed time trends (thick lines) derived from SSA (first component) in summer and robust spline smoothing in winter. In addition to the winter (background) data, the smoothed spline corresponding to total winter layers is reported as thin dashed line.

unchanged over the last 70 years. A striking pattern appears for the winter trends of both species with a large increase of winter values over the 1946-1978 time period for acetate and over the 1955-1982 time period for formate. As a result, the summer to winter contrast was

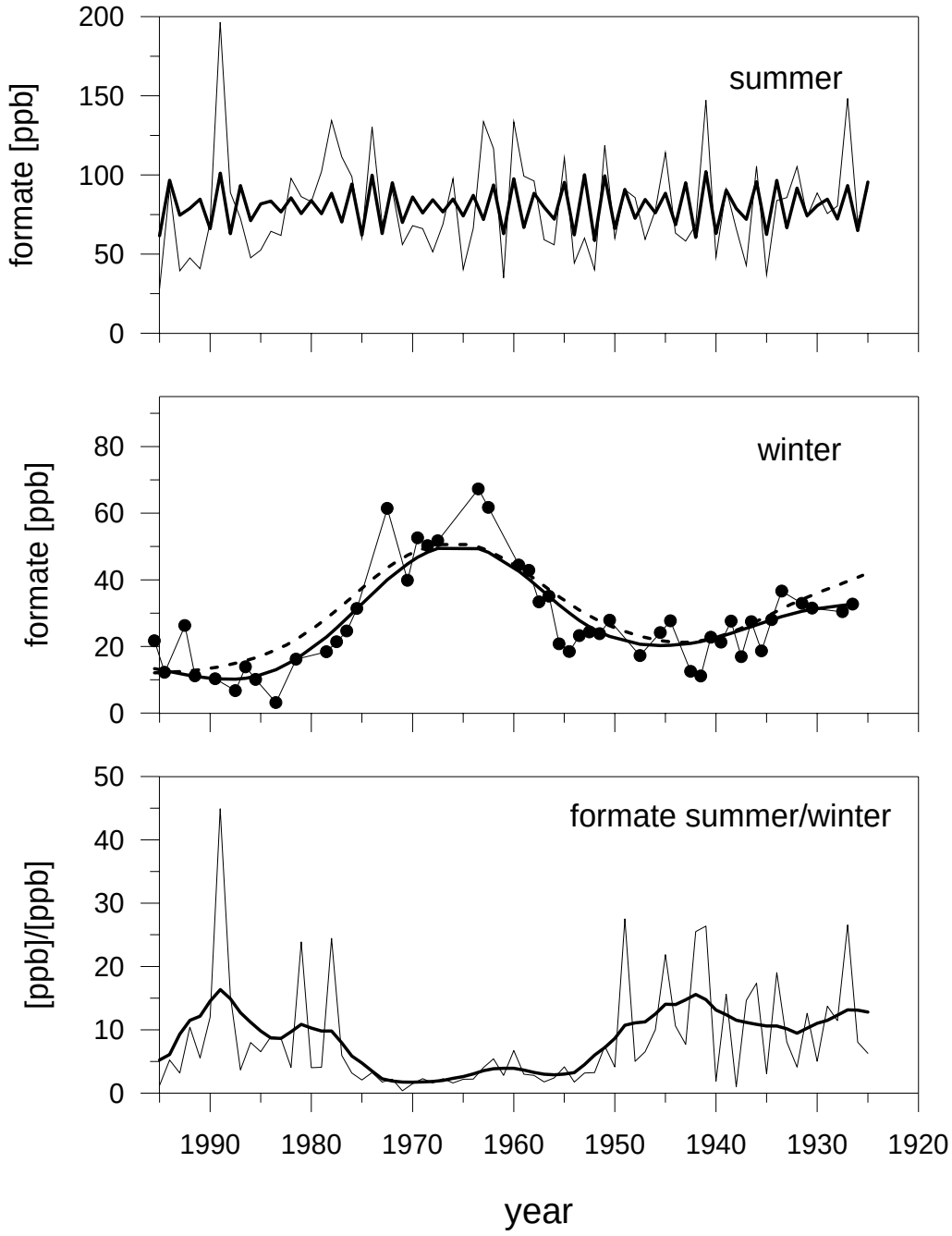

Figure 6.2b: Summer and winter long term records along with temporal evolution of summer to winter ratio of formate in C10 snow layers. Reported are individual summer and winter means (thin lines) and smoothed time trends (thick lines) derived from SSA (first component) in summer and robust spline smoothing in winter. In addition to the winter (background) data, the smoothed spline corresponding to total winter layers is reported as thin dashed line.

strongly decreased for formate and totally vanished for acetate over this time period (see Figure 6.2). In their Greenland study, Legrand and De Angelis (1995) noted a very weak summer/winter contrast for acetate and formate. Since a strong seasonality is expected for the

atmospheric levels of these species whose sources are here vegetation emissions from the boreal zone, such a weak seasonality in snow layers suggests that these species are diffusing quite rapidly after deposition in Greenland snow layers. Since natural and anthropogenic sources of these two species at high Alpine sites are likely mainly of continental origin (as for nitrate, sulfate, and ammonium), we can expect (as it was seen for these latter species) a strong summer maximum driven by the efficient upward transport in summer. Since a change of the formate and acetate seasonality at the CDD site is not expected to take place over the past, we suspect that this phenomena of a decreased seasonal contrast is a consequence of post depositional effects.

To elucidate the cause of this possible post depositional effect and its changes along the CDD ice core, we report in Figure 6.3 the temporal variations of glaciological properties and acidity down the length of the C10 ice core. The period over which we observed a decreased summer to winter contrast ended in 1977 and corresponds to the depth of 44 m w.e. (i.e., at the transition between firn and ice in the C10 core) where the corresponding surface snow accumulation rate as well as the summer to winter accumulation ratio ($A_{w/s}$) start to decrease significantly and the thinning of snow layers by glacier flow increases rapidly (Figure 6.3). The consequence of these changes is that the thickness of winter snow layers decreases rapidly at that time (from ≈1.6 m w.e. in 1980 to ≈0.6 m w.e. in 1970). That provides the conditions for which a diffusion of volatile species between summer and winter layers could lead to a significant decrease of the summer to winter contrast. If so, we would expect that the phenomena continues further core-down which is not the case. At the opposite, the summer to winter contrast recovers at a depth of 76 m w.e. (≈1950). Thus the observed effect can not be explained exclusively by these glaciological parameters and therefore an additional parameter likely controls the intensity of diffusive processes of formate and acetate along the C10 ice core.

Formic and acetic acids have a significant vapour pressure over the ice and since they are weak acids, we can suspect that the acidity of snow layers acts as the driving force of diffusion processes. In Figure 6.3 we report the change of the acidity (made up by ions which are assumed to be largely free of diffusive processes) in summer and winter snow layers. Higher acidity is seen in summer than in winter in snow layers deposited between 1950 and present, whereas before 1950 the acidity of winter snow is slightly higher than in summer snow layers. This suggests that the relative strong summer/winter acidity difference seen within snow layers deposited after 1950 could have acted as a force which tends to remove acetate and formate, originally deposited in summer layers, to the less acidic winter snow layers. A more detailed examination of the covariation between monocarboxylic acids and acidity in C10 snow layers and within snow deposits sampled rapidly after their deposition (snow pit study, see section 2.3) confirms the idea that the acidity of snow layers is acting as a driving force of diffusive processes within the C10 ice core. Indeed, while in snow samples

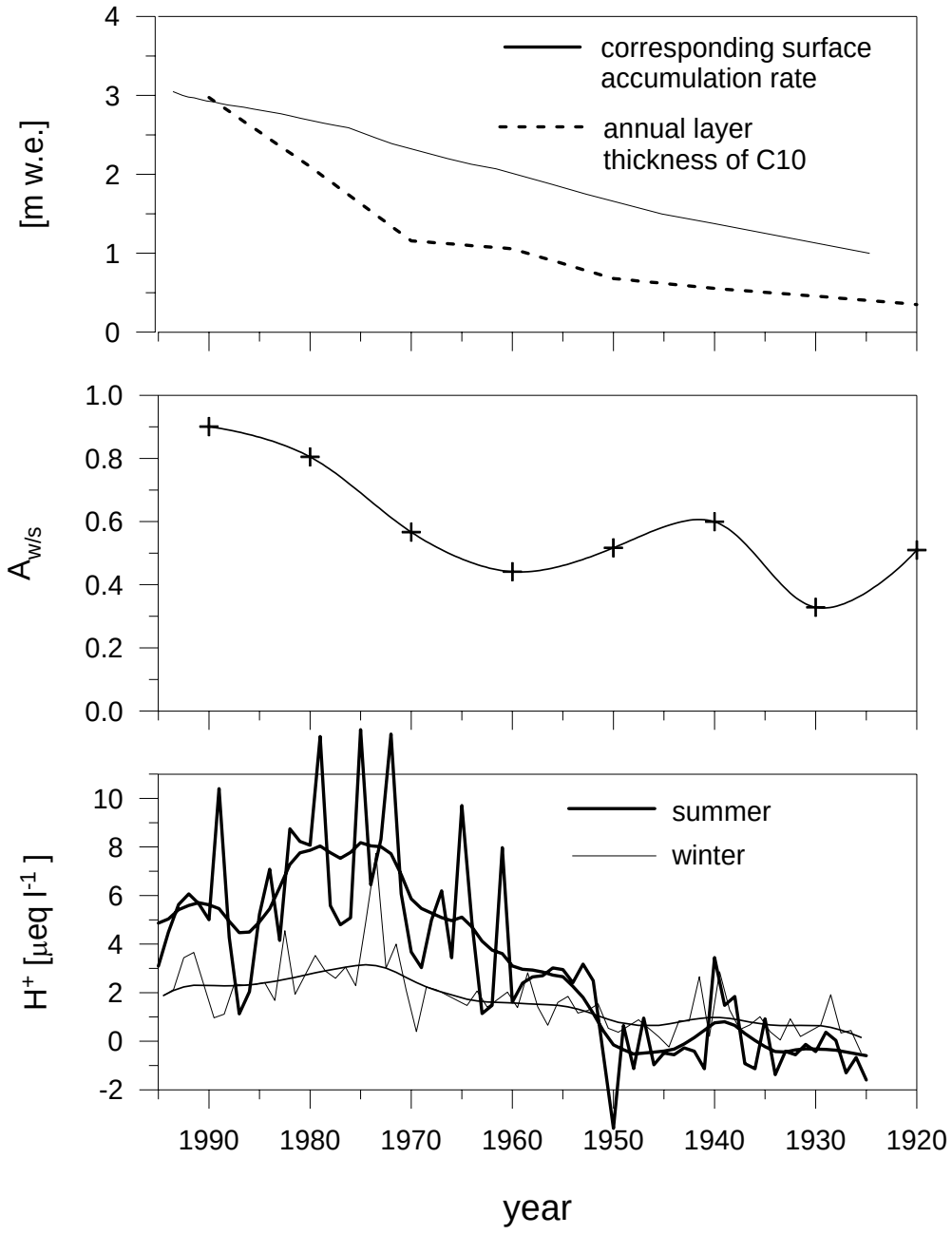

Figure 6.3: Glaciological parameters and acidity along the C10 ice core versus time. (Top) Annual layer thickness (see also Figure 9 in section 2.4) together with the respective corresponding surface accumulation rate (estimated by applying the glacier flow model of Vincent et al., 1997). (Middle) summer to winter snow accumulation rate (Aw/s) versus time (see also Figure 9 in section 2.4). (Bottom) Variation of the acidity calculated from the contents of F^-, Cl^-, NO_3^-, SO_4^{2-}, $C_2O_4^{2-}$,Na^+, NH_4^+, K^+, Mg^{2+} and Ca^{2+} in summer (thick lines) and winter (thin lines) in snow deposits of C10. Reported are individual half year mean and by SSA (summer) and robust spline smoothing (winter) derived tends

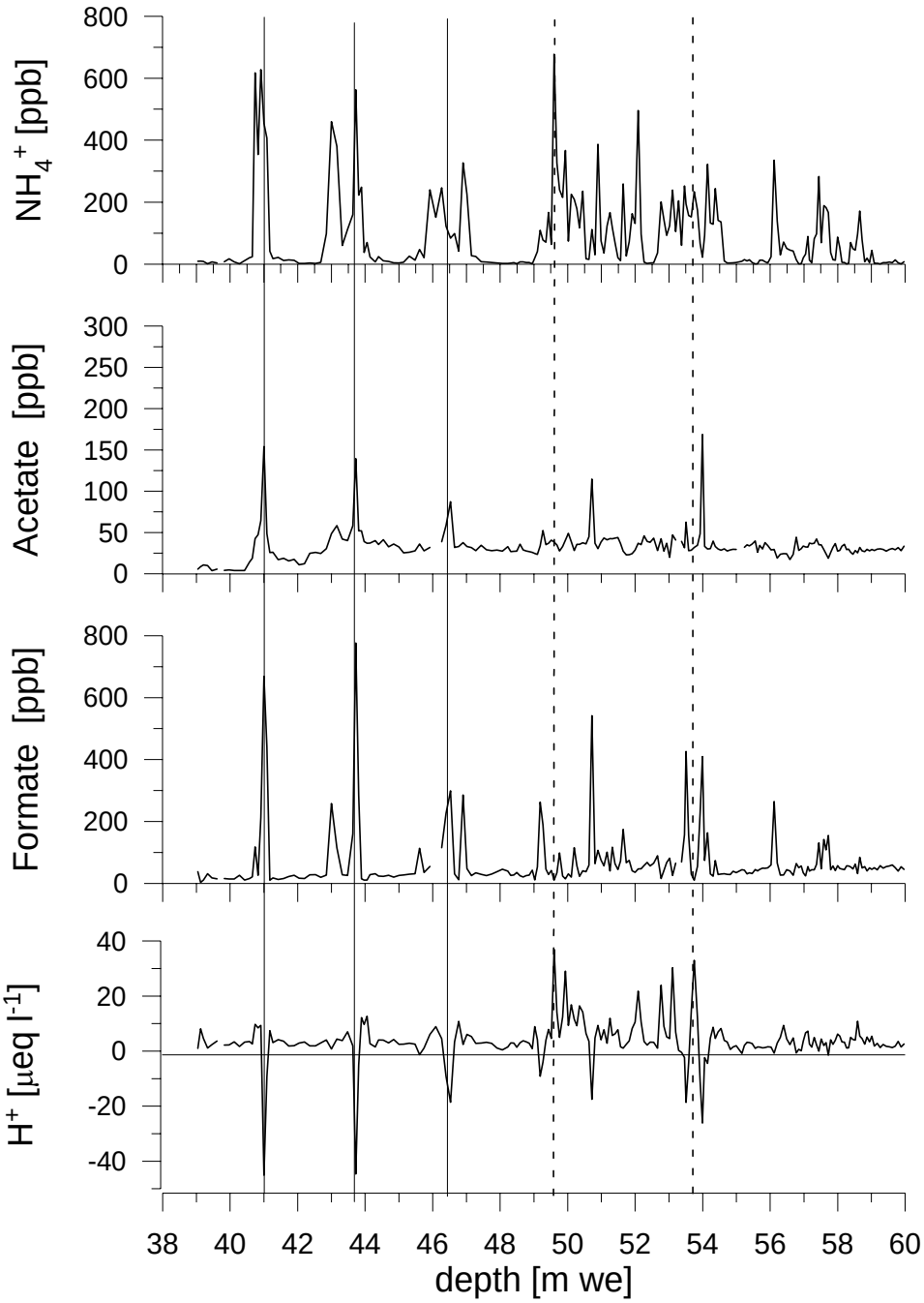

Figure 6.4: C10 raw data profiles of NH_4^+, acetate, formate and acidity calculated from F^-, Cl^-, NO_3^-, SO_4^{2-}, $C_2O_4^{2-}$,Na^+, NH_4^+, K^+, Mg^{2+} and Ca^{2+} levels from 39 m w.e. to 60 m w.e. depth (corresponding to the 1967-1979 time period). To guide the eye, examples of extremely high and low acidic snow layers are marked with solid and dashed horizontal lines, respectively.

collected in the snow pit acetate (and to a lesser extend formate) peaks together with the acidity level (see Figure 2.3d), this is not the case within snow layers stored for several years within the CDD glacier site (see Figure 6.4). Here, acetate and formate peaks are almost exclusively observed when the snow is strongly alkaline.

Another parameter which can modulate the intensity of diffusion processes versus depth along the C10 ice core is the close-off ice age (age after which a deposited snow layer becomes ice) and its variability upstream the C10 drill site. The concrete effect of this factor on the diffusion mechanism within the C10 ice core remains difficult to evaluate since the change of the close-off age upstream the C10 drill site is rather unknown. Close-off age determinations on the flow line upstream the C10 ice core (which do not fit however with the model estimations from Gagliardini and Meyssonnier (1997)) indicate close-off ages of 10 to 40 years about 130 m upstream of C10, 5 to 8 years about 200 m upstream to C10 and more than 50 years about 270 m upstream of C10 (at the summit position of the Dôme du Gouter). Applying the ice flow model from Vincent et al. (1997), ice layers originally deposited within 10 m around the point for which the lowest close off age (5 to 8 years) was determined, are assumed to appear within C10 at the depth of 75 to 84 m we (i.e. 1952 – 1937), means nearby the depth where the diffusive effect becomes to be weaker (negligible) and the seasonal variations re-appear. Although needed to be confirmed by further investigations, we cannot exclude the idea that the variability of the close-off age upstream the C10 drill site also influence the strength of diffusive processes observed along the C10 ice core.

In summary we conclude that due to glaciological upstream effects (as decreased accumulation rates and winter snow contributions, and variation of the close-off age) and the enhanced acidity of summer layers if compared to winter ones in recent times, originally during summer deposited formate and acetate diffuse in surrounding winter snow layers. As a consequence an "artificial" but significant enhancement of acetate and formate concentrations is observed in some corresponding winter snow layers of C10.

To correct formate and acetate summer trends from this non atmospheric effect, we assumed that atmospheric winter conditions of acetate and formate have not significantly changed over the last 80 years. With that, we applied to individual mean summer levels corresponding to the 1947-1994 time period (C_{so}^{snow}) the following correction:

$$C_{so}^{corr} = C_{so}^{snow} + A_{w/s}(C_{wi}^{snow} - C_{wi}^{back}) \qquad (6.1)$$

C_{wi}^{back} denotes the winter snow level seen in snow pits (8 ppb for acetate, 10 ppb for formate) which is assumed to be representative from recent times back to 1947, C_{wi}^{snow} denotes the individual total winter means of acetate and formate (for definition of the "total winter mean" see section 3.2.2).

The corrected summer trend of acetate and formate derived from equation (6.1) are given in Figures 6.8a and 6.8b. In Table 6.1 the mean winter levels of acetate and formate observed in the CDD snow layers are reported for time periods over which the summer to winter contrast is not too far away from what was observed in the snow pit samples. For acetate our assumption of constant winter level seems to be realistic if we assume that winter

Table 6.1: Mean acetate and formate winter levels for time periods over which a clear seasonal contrast was observed for acetate and formate levels in the C10 ice core and winter levels observed in the snow pit. Means and standard deviations of the C10 core are derived on the base of annual means, while means and standard deviation of the snow pit samples are calculated from individual samples.

	1997 – 2000 (snow pit)	1994 – 1978 (C10 core)	1947 – 1925 (C10 core)
acetate (ppb)	8.0 ± 2.9	8.3 ± 6.2	7.3 ± 5.7
formate (ppb)	10 ± 6.3	13.7 ± 6.6	25.2 ± 7

levels deposited before 1947 are mostly free of post depositional effects. Legrand and De Angelis (1996) reported however an increase of acetate by a factor of 2 over the last century in Greenland. If correct also for CDD winter conditions, the winter levels observed before 1947 are also influenced by diffusive processes and in this case our corrected summer trend would be about 2 ppb (≈ 13%) underestimated over this time period. Formate levels are enhanced by a factor of two over the 1925-1947 time period compared to winter levels observed in recent times. For Greenland snow deposits a decreasing trend with factor 1.5 was observed (Legrand and De Angelis, 1996). If this is also true for CDD winter levels our correction is correct. If the enhanced winter values observed before 1947 are however due to diffusive processes, our corrected summer trend would be systematically underestimated by about 6ppb (≈ 8%) over the time period before 1947.

Note that since summer layers are expected to contain significantly higher acetate and formate concentrations than winter ones, a reverse diffusive process from winter to summer snow layers is rather unlikely, but can however not be excluded in particular during years or time periods for which the winter acidity is higher than summer one. If this effect would have appeared for snow layers deposited before 1950 our corrected acetate and formate summer trends would correspond to a lower limit of formate and acetate summer levels for the 1925-1947 time period, what will however not hamper a qualitative discussion of the trends.

6.3.2 Acidity dependence of monocarboxylic acid incorporation in precipitation

In contrast to oxalic acid, formic and acetic acids are mainly (more than 90%) present in the gas phase (Andreae et al., 1988; Talbot et al., 1988; see section 1.2 (*Table2)*). The incorporation of monocarboxylic acids in solid precipitation remains still not well understood but likely would depend on the occurrence of two major scavenging mechanisms, namely the riming and the co-condensation with water vapour during diffusion growth. Legrand and De Angelis (1995) discussed the incorporation processes of acetic and formic acids during riming and diffusion growth in Greenland snow flakes. They concluded that the presence of these

two light carboxylic acids in solid precipitation is mainly related to their incorporation in cloud supercooled liquid droplets where the scavenging efficiency is pH dependent, and their co-condensation along with water during the growth of snowflakes by water diffusion. Since riming is thought to represent a major scavenging mechanism for Alpine summer precipitation (Kalina and Puxbaum, 1994), we here summarize the theory related to the pH dependence of the incorporation of these carboxylic acids in water following the presentation from Legrand and De Angelis (1995). The partition of formic and acetic acids between the gas and aqueous phase is strongly dependent on the acidity of the cloud droplet because of the acid-base equilibrium in liquid water of these weak acids. The gas/liquid water partitioning is driven by the pseudo-Henry's law constant (K^*_H) (Schwartz, 1984), which takes into account the gas-liquid equilibrium as well as the equilibrium of the acid in the liquid phase:

$$K_H^* = K_H(1 + K_a/[H^+]) \qquad (6.2)$$

where K_H and K_a are the Henry's law constant and the acid dissociation constant, respectively.

Expressions of the temperature dependence of the Henry's law constant (Winiwarter et al., 1988) and dissociation constants (Wagman et al., 1965; Chao and Zwolinsky, 1978) for formic and acetic acids are :

HCOOH: $K_H = 5527 \exp(5736\ (1/T - 1/298))$
$K_a = 1.8 \times 10^{-4} \exp(151\ (1/T - 1/298))$

CH_3COOH: $K_H = 8685 \exp(6391\ (1/T - 1/298))$
$K_a = 1.7 \times 10^{-5} \exp(50\ (1/T - 1/298))$

Using the ideal gas law, the fraction of carboxylic acid incorporated into solution (ε) can be expressed as a function of K^*_H, the absolute temperature (T) and the liquid water content of cloud (L in grams of water per cubic meter of air) (Warneck, 1986):

$$\varepsilon = 1/(1 + \frac{12 \cdot 10^6}{K_H^* \cdot T \cdot L}) \qquad (6.3)$$

The corresponding concentration in the aqueous phase (c_s in grams per litre) may be related to the gas phase concentration (c) following:

$$c_s = \frac{10^3 \varepsilon \cdot c \cdot P \cdot M}{R \cdot T \cdot L} \qquad (6.4)$$

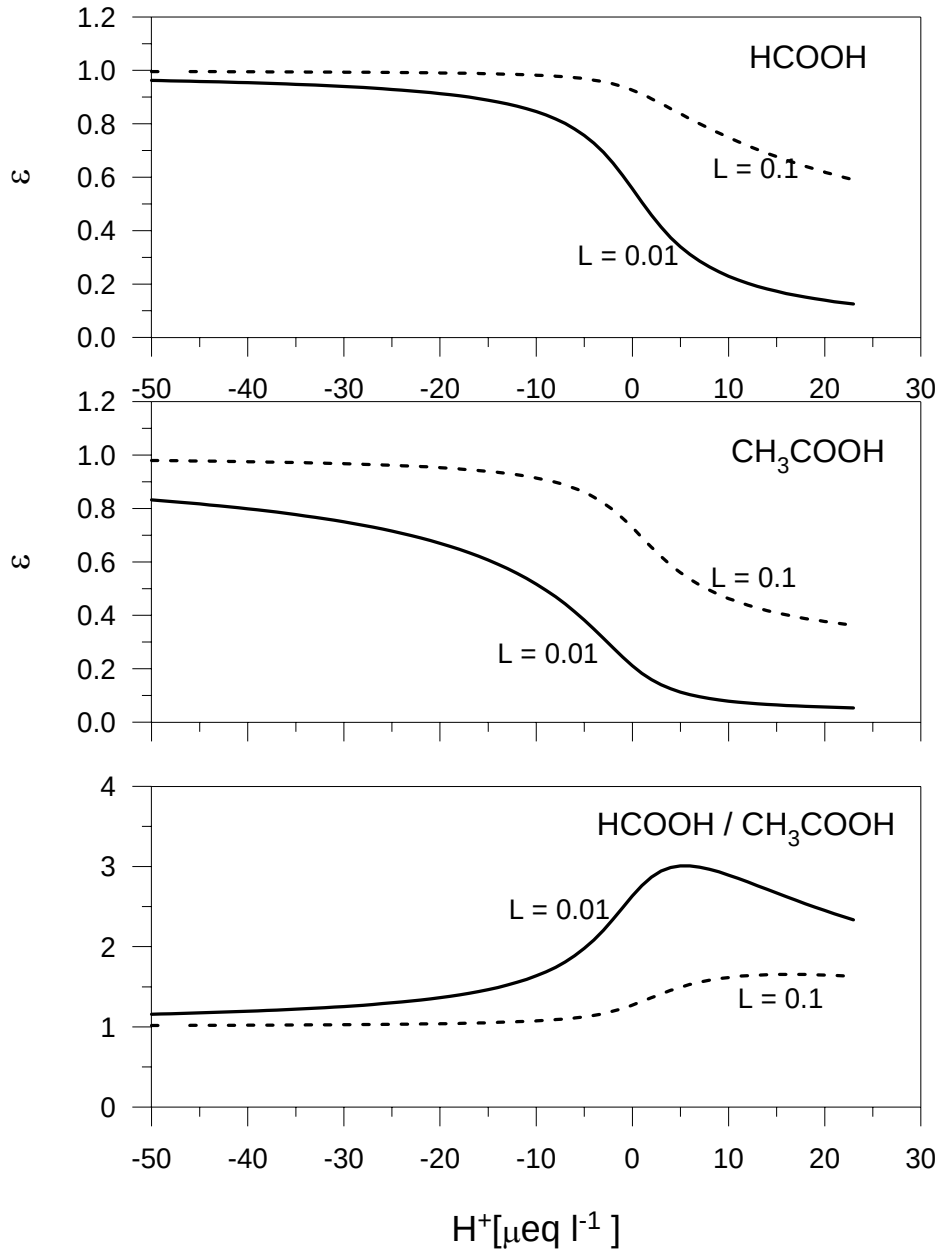

Figure 6.5a: Fraction of formic and acetic acids incorporated in solution (ε) together with ratio of ε-formate to ε-acetate versus the acidity. The incorporation coefficient (ε) is calculated following equation (6.3), assuming 263 K and liquid water contents of 0.1 and 0.01 g/m3.

with R is the gas constant (8.3 x 10^{-5} m^3 bar deg^{-1} mol^{-1}), M the molecular weight of the carboxylic acid, and P the atmospheric pressure (in bars) at cloud level. Assuming a temperature of –10°C and a cloud liquid water content ranging from 0.01 to 0.1 g/m^3, the incorporation into solution (ε) as function from the acidity is reported in Figure 6.5a. With similar values of the temperature and of the cloud liquid water content as those assumed for

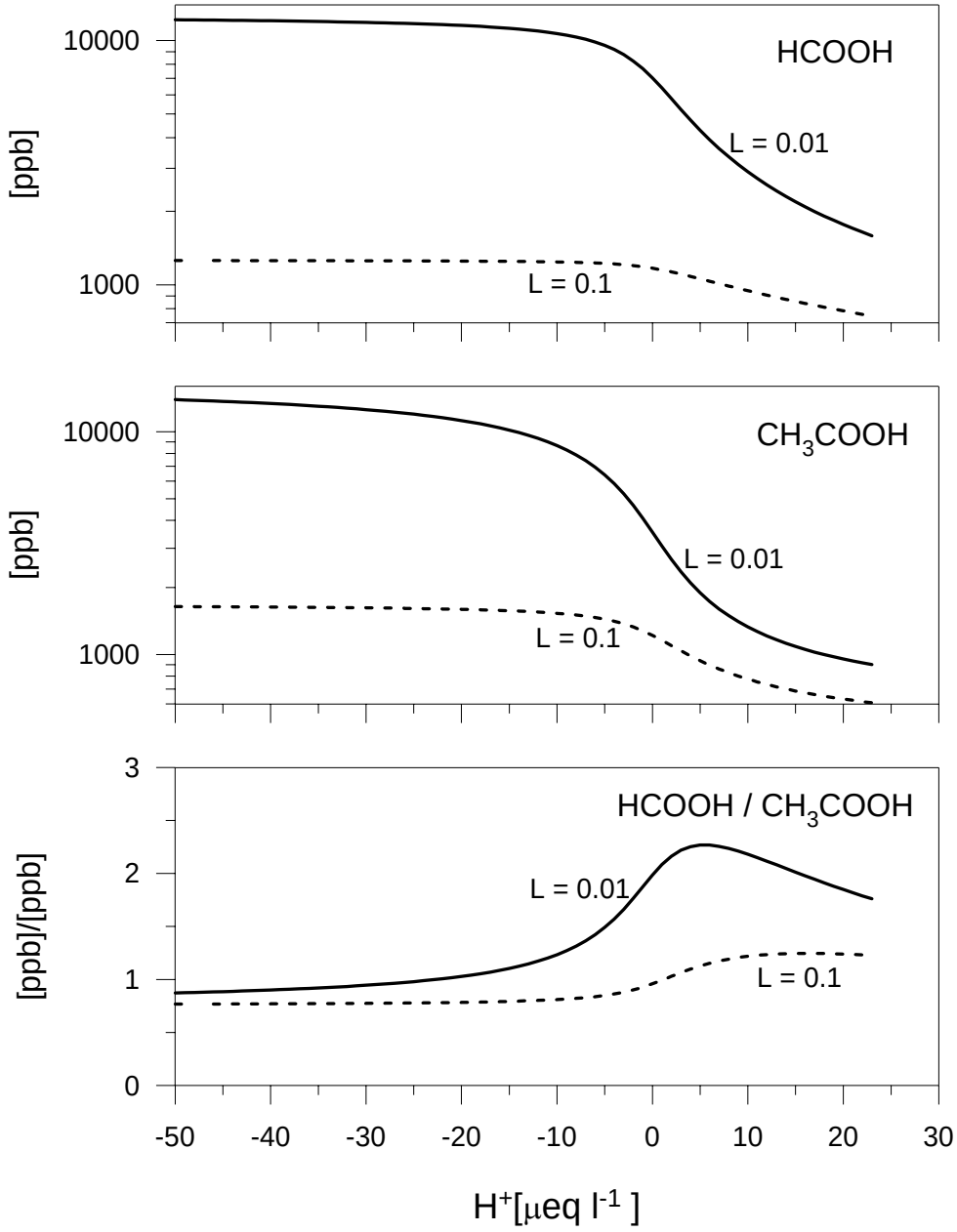

Figure 6.5b: Formic and acetic acid contents and corresponding weight ratios in water as function of the acidity, for water liquid contents of 0.01 and 0.1 g/m3, respectively. Calculations are made on the base of equation (6.4), assuming a 100 pptv gas phase mixing ratio for both formic and acetic acids.

Figure 6.5a, Figure 6.5b shows the concentration in the aqueous phase (c_s) corresponding to a gas phase mixing ratio of 100 pptv (as measured at the high Alpine site Refuge Cosmiques (see section 1.3 (*Table3*)). Note that to translate the acidity into pH values ($[H^+]$ in equation (6.2)), we took into account the buffer effect of CO_2 assuming a CO_2 mixing ratio of 375 ppbv (Stumm and Morgan, 1970).

At low acidity formic and acetic acids are expected to be similarly uptaken into the cloud water as suggested by the formic to acetic ratio close to unit (Figure 6.5b). At higher acidity ($[H^+] > 10$ μEq/l) formic acid becomes more efficiently incorporated (up to more than a factor 2 for $L = 0.01$) in cloud water compared with acetic acid, in particular when a low cloud water content is assumed.

This acidity dependence of the incorporation of carboxylic acids during the riming process has to be considered when discussing their trend in the solid precipitation of the C10 ice core since the acidity of the C10 snow layers have been changed over the last 75 years. That means that the recent trends of monocarboxylic acids seen in CDD snow layers result from changes in their atmospheric levels (source effect) as well as changes in the efficiency of their incorporation into the solid precipitation. In order to assess the role of acidity on the acetate and formate changes in the C10 summer snow layers, we examined the relationship between formate and acetate levels and the acidity within summer snow samples collected in a CDD snow pit covering the 1997-2000 years (see section 2.3). We here have preferred to examine such a relationship within the snow pits instead of in the C10 ice core since in the latter data set this relationship is likely biased by post depositional diffusion effects (see section 6.3.1).

Figure 6.6 shows the relationship between acetate and formate levels versus acidity in summer snow layers of the CDD snow pit. While no evidence of a dependence of levels to the acidity can be detected for acetate, formate levels are significantly reduced when the acidity is enhanced. Following this observation, we have assumed that acetate levels are not pH dependant what was also previously observed by Legrand and De Angelis (1995) for Greenland snow deposits. Conversely, it appears that the summer snow trend of formate is likely biased by the change of the acidity over the last 80 years. With the aim to correct the CDD formate trend from this effect, formate concentrations of summer snow pit samples were normalized to their mean value (102 ppb) and the line reported in Figure 6.7 is aimed to reflect the mean relation between the acidity and the fraction of formate which is incorporated in solid precipitation. The equation of this line is:

$$[HCOO^-]/[HCOO^-]_{mean} = -0.15\ [H^+] + 2 \qquad (6.5)$$

with $[HCOO^-]_{mean}$ =102 ppb, denoting the mean formate level of summer snow pit samples.

Note that the overall relationship between acidity and the formate content is theoretically not linear (see the theoretical relationship between formate content of the liquid phase and H^+ concentration reported in Figure 6.5b) but seems however a good approximation (at the first order) for acidity values ranging between -10 and + 10 μEq/l. Based on equation (6.5), the decrease of formate levels is in the order of a factor of 2 for an increase of the acidity by 3.3 μEq/l, while Legrand and De Angelis (1995) obtained a reduction by a factor of

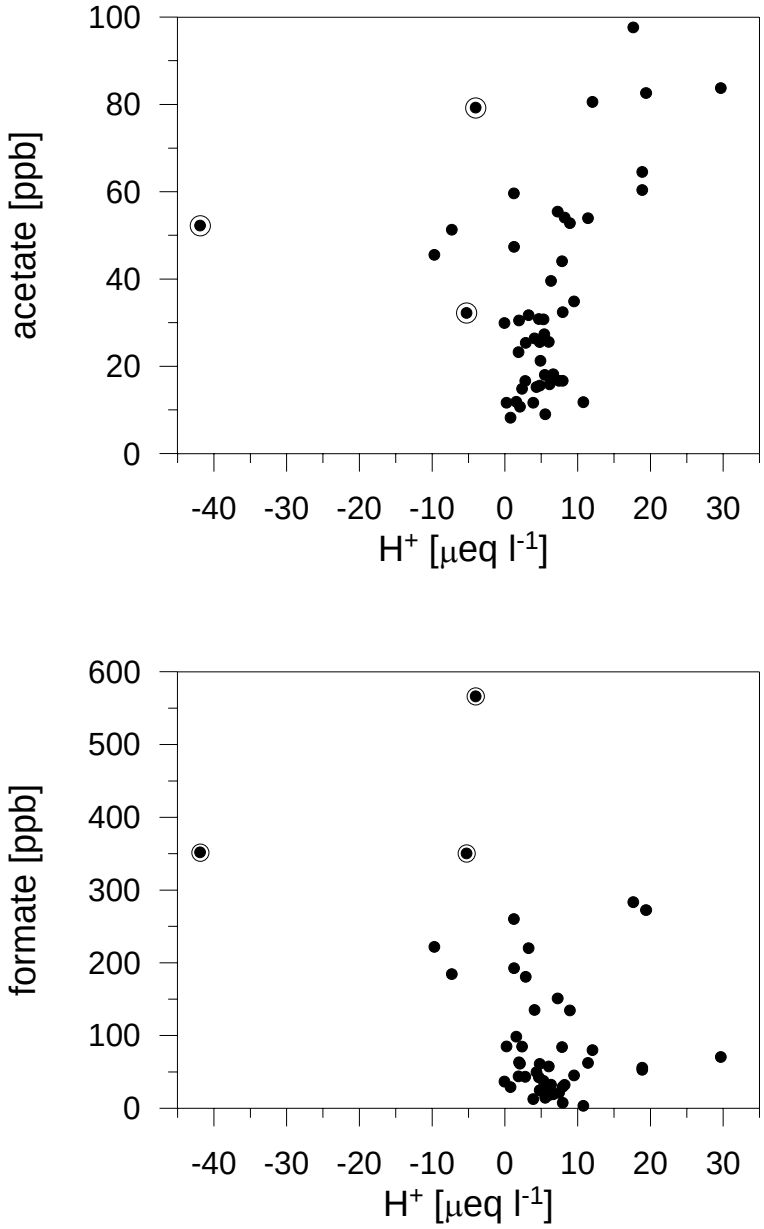

Figure 6.6: Acetate (top) and formate (bottom) versus H^+ concentrations of summer snow pit samples spanning the 1997–2000 time period (see also Figure 2.3). Samples regarded as influenced by Saharan dust input are denoted with open circles around dots.

2 of formate levels when the acidity increases by 4.8 μEq/l in Greenland firn layers. This stronger formate/acidity dependence found for CDD snow layers would be due to the expected higher contribution of riming to solid precipitation formation in summer at high Alpine sites compared to the Greenland one over all the year. Note that at the latter site the dominant mode of precipitation formation during winter is assumed to be by diffusion growth (Legrand and De Angelis, 1995).

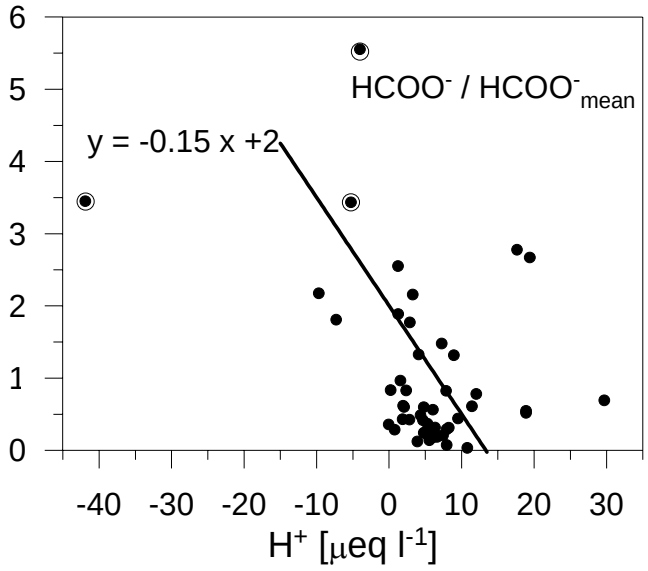

Figure 6.7: Formate concentrations of summer snow pit samples covering the 1997–2000 time period relative to their mean value ($HCOO^-/HCOO^-_{mean}$) versus H^+ levels. Samples regarded as influenced by Saharan dust input are denoted with open circles around dots. The straight line is an estimate of the mean relation of $HCCO^-/HCCO^-_{mean}$ versus the acidity (see text).

An additional bias effect also related to the acidity dependence of the formate incorporation in solid precipitation might be related to the sporadic Saharan dust inputs observed in summer snow layers at high Alpine sites (see section 3.2.1) since they lead to a significantly decreased acidity of the respective precipitation events. Though theoretically the formate dependence of the acidity should become weaker at lower acidity values (see Figure 6.5), significant larger formate increases as expected with decreasing acidity were observed in precipitation at Greenland and at the PO Valley (Legrand and De Angelis, 1995; Winiwarter et al., 1988). Thus Saharan dust inputs might sporadically enhance formate levels of corresponding snow layers, and depending on their frequency they can bias the overall long term trends of formate revealed by the C10 ice record. As seen in Figure 6.6, formate levels of samples suspected to contain dust inputs are indeed increased compared to the other (undisturbed) summer samples, while for acetate this effect again cannot be detected. Note that however both monocarboxylic acids are initially present in Saharan dust plumes in a similar amount (see Table 3.2). This apparent relative enhancement of formate versus acetate in Saharan dust inputs is also depicted by the linear relationship between formate and acetate versus Ca^{2+} which suggests a 3 times more abundant formate than acetate in Saharan dust contaminated snow layers (see Table 3.2). To evaluate the impact of Saharan dust on the long term trends of formate and acetate, we report in Figure 6.8a and 6.8b the formate and acetate trends (with and without correction from diffusion effects) which are obtained by applying the

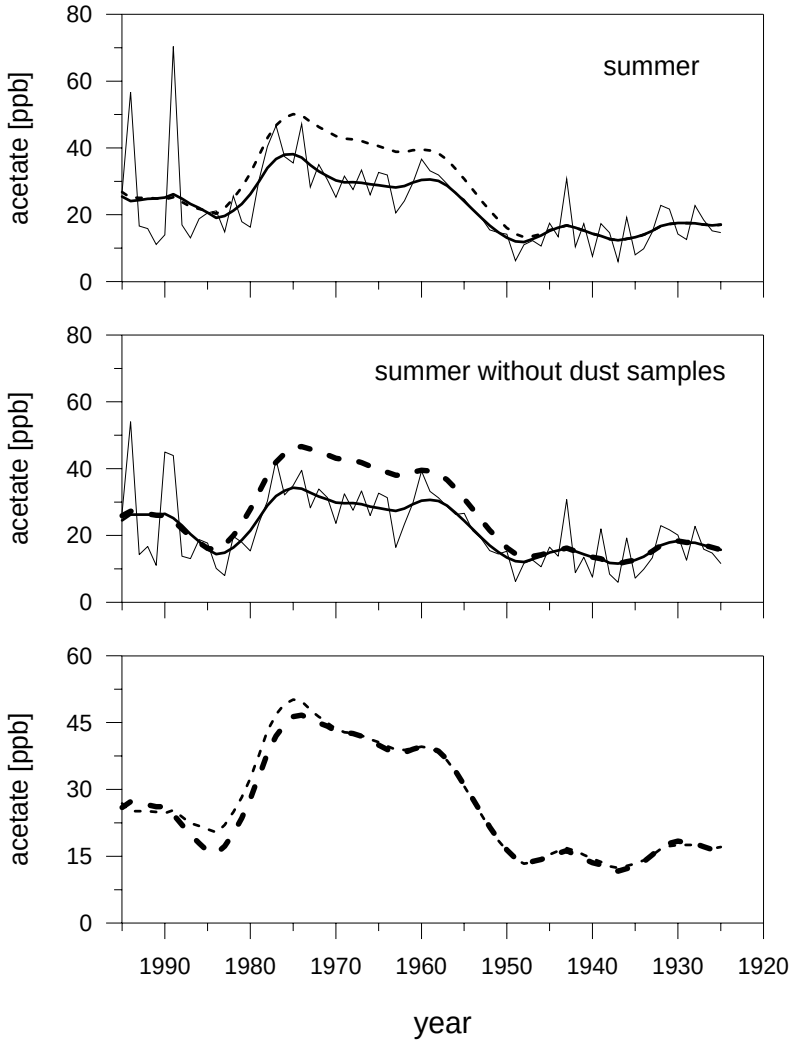

Figure 6.8a: CDD summer trends of acetate after correction from diffusion effects. (Top) Acetate summer trend as reported in Figure 6.2a (thick and thin line). The dashed line denotes the respective acetate trend corrected from diffusive effects (see text). (Middle) CDD summer trend of acetate in which Saharan dust influenced samples have been excluded. Reported are individual summer means (thin lines) and smoothed time trends (thick lines) derived by SSA (first component). The dashed line denotes the respective acetate trend corrected from diffusive effects (see text). (Bottom) Comparison of from diffusion effects corrected acetate summer trends obtained when Saharan dust inputs are considered and excluded, respectively (dashed lines from top and middle).

standard protocol described in section 3.3 (also reported in Figure 6.2) together with the respective formate and acetate trends obtained having discarded samples containing Saharan dust inputs. While for acetate almost no difference can be seen between the two curves (meandifference of ≈ 10% between 1975 and 1990), for formate the trends show a mean concentration difference of ≈ 40% between 1975 and 1990 and a significantly different pattern over this time period. If we assume that the acetate levels are not acidity dependent,

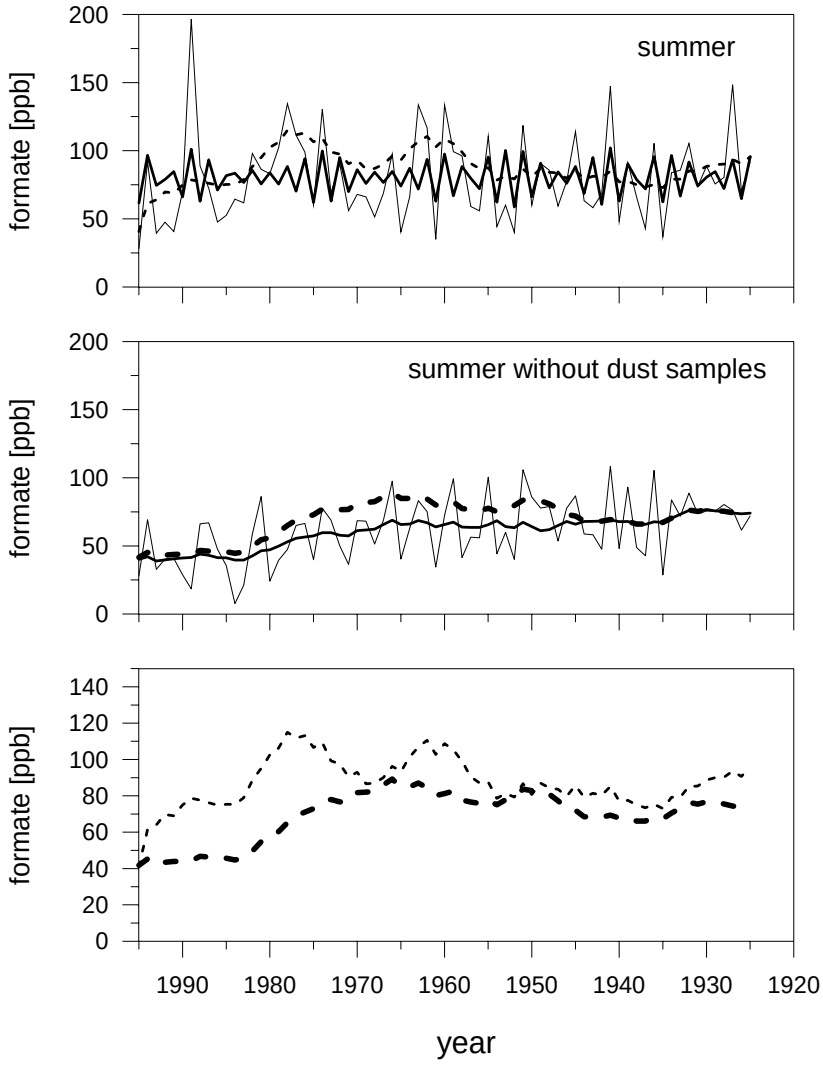

Figure 6.8b: CDD summer trends of formate after correction from diffusion effects. (Top) Formate summer trend as reported in Figure 6.2b (thick and thin line). The dashed line denotes the respective formate trend corrected from diffusive effects (see text). (Middle) CDD summer trend of formate in which Saharan dust influenced samples have been excluded. Reported are individual summer means (thin lines) and smoothed time trends (thick lines) derived by SSA (first component). The dashed line denotes the respective formate trend corrected from diffusive effects (see text). (Bottom) Comparison of from diffusion effects corrected formate summer trends obtained when Saharan dust inputs are considered and excluded, respectively (dashed lines from top and middle).

the small difference seen for acetate between the two trends (including and excluding Saharan dust events) could be attributed to an external mixing of the dust plume (scavenging of acetic acid by this alkaline material) but also to post depositional diffusive effects. The large differences between the two formate summer trends are likely mainly due to external mixing and incorporation effects of formic acid in cloud droplets containing alkaline dust material. In the

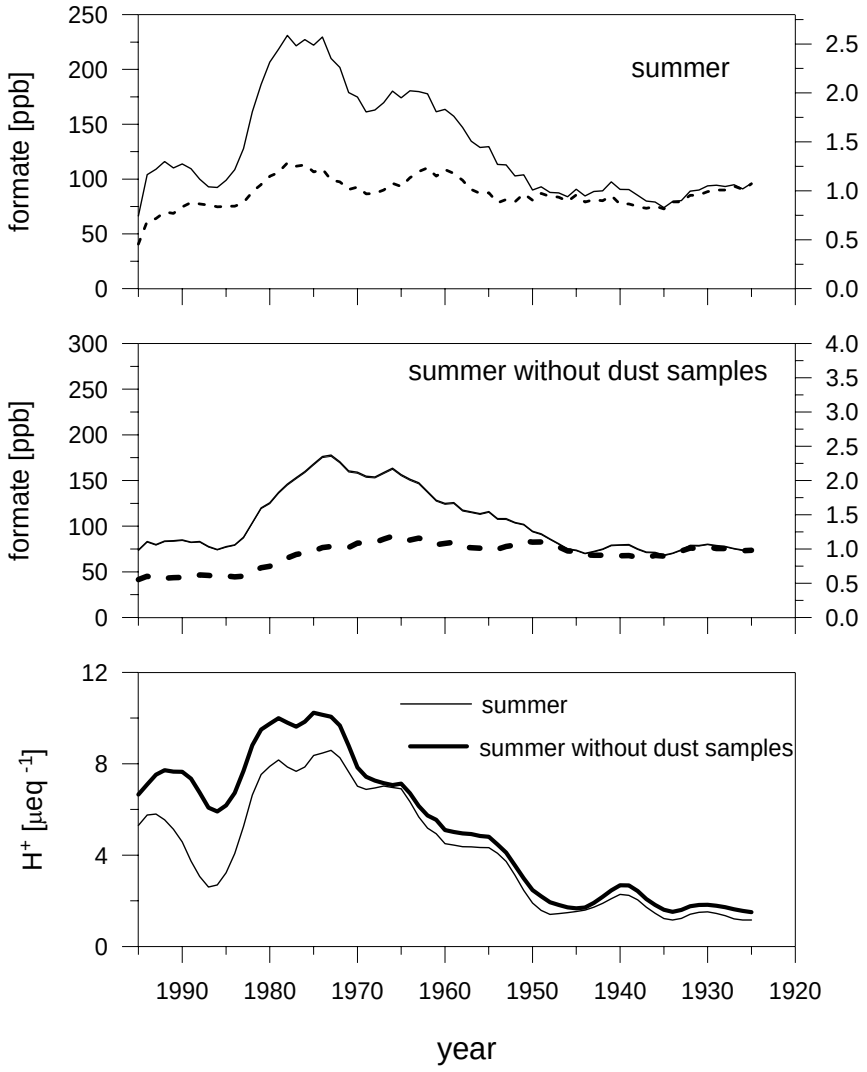

Figure 6.9: Formate trends corrected from the acidity dependant formate incorporation in precipitation (see text). (Top) From diffusive effects corrected formate concentration levels in snow deposits (including Saharan dust samples) as reported in Figure 6.8b (dashed line). The thin solid line corresponds to the respective formate trend corrected (following equation (6.6)) for changing acidity with respect to the situation between 1925 and 1935. Formate levels are given on an absolute (left) and on a to 1925 – 1935 relative (right) scale. (Middle) Same as top for the data set in which Saharan dust samples were not considered. (Bottom) Smoothed acidity time trends (first component SSA) derived from data sets in which dust samples were considered (thin line) and excluded (thick line), respectively.

following we consider therefore the two formate trends which would be representative as lower and upper limits of past atmospheric changes.

Finally these upper and lower limit formate summer trends were corrected from their long term acidity dependence assuming that the acidity correction factor (slope of equation (6.5)) did not change with time. In Figure 6.9 the with equation (6.1) obtained C10 summer

formate trend (C_{for}^{depo}) was corrected with respect to the mean acidity level observed over the time period from 1925 – 1935 (H^+_0: acidity including Saharan dusts: 1.12 ± 0.9 μEq/l; acidity excluding Saharan dusts: 1.53 ± 0.63 μEq/l) following:

$$C_{for}^{corr} = C_{for}^{depo} + (0.15 \cdot ([H^+] - H_0^+) \cdot C_{for}^{depo}) \qquad (6.6)$$

where $[H^+]$ denotes the acidity including, excluding Saharan dust inputs, respectively.

6.3.3 Atmospheric relevant changes of formate and acetate summer levels at CDD

Figure 6.10 summarizes the corrected acetate and formate trends of CDD summer snow layers which are assumed to be of representative of atmospheric changes of formic and acetic acid levels over the last 75 years. In addition to the CDD data, the pre-industrial levels of both species observed in pre-industrial ice from Colle Gnifetti (see also section 6.2) are reported. The formate concentrations obtained at Colle Gnifetti have been corrected with regard to the deviation of their mean acidity levels versus the ones found in CDD snow layers corresponding to the 1925–1935 time period. The Colle Gnifetti summer snow levels of acetate and formate are significantly lower than the respective ones measured from 1925 to 1935 at the Col du Dôme site. Since they are significantly higher than the corresponding (Colle Gnifetti) winter values (a factor of ≈2.5 – 4 for acetate and of ≈8 – 11 for formate), it is assumed that, if existing, diffusion processes are limited in these CG ice core sections. Given the complexity of factors controlling the incorporation mechanism of acetate and formate in solid precipitation (cloud and precipitation microphysics, dust content), the difference observed between the 1925-1935 CDD snow layers and the pre-industrial CG ones (60% and 40% lower for acetate and formate, respectively, see Figure 6.10) cannot be easily discussed. However, the fact that similar CG levels for acetate and formate were observed in 1933-1935 and in pre-industrial time (towards 1850 ± 10 years), respectively, suggests that the concentration levels of acetate and formate have not changed significantly from pre-industrial times to the 1930's within high Alpine summer snow deposits. Note that this has been also observed for Greenland snow deposits (Legrand and De Angelis, 1996). From this discussion, we conclude that formate and acetate levels were not significantly increased above their pre-industrial level (≈77 ± 25 ppb and ≈15 ± 5 ppb for formate and acetate, respectively) before 1950 in the CDD summer snow layers. In 1950 acetate summer CDD snow levels started to increase, reaching a maximum (≈ 50 ppb) in 1975. After this increase by about a factor of 3.3, a sharp decrease occurred between 1975 and 1985, leading to recent (1985–1995) levels close to ≈25 ± 20 ppb. On the contrary, the long term trend of formate summer snow layers differs largely from the acetate one. After 1950, formate summer CDD snow layers tend to decrease by a factor of 1.2-1.7, reaching a recent level of ≈ 45–70 ppb. However the corrected formate

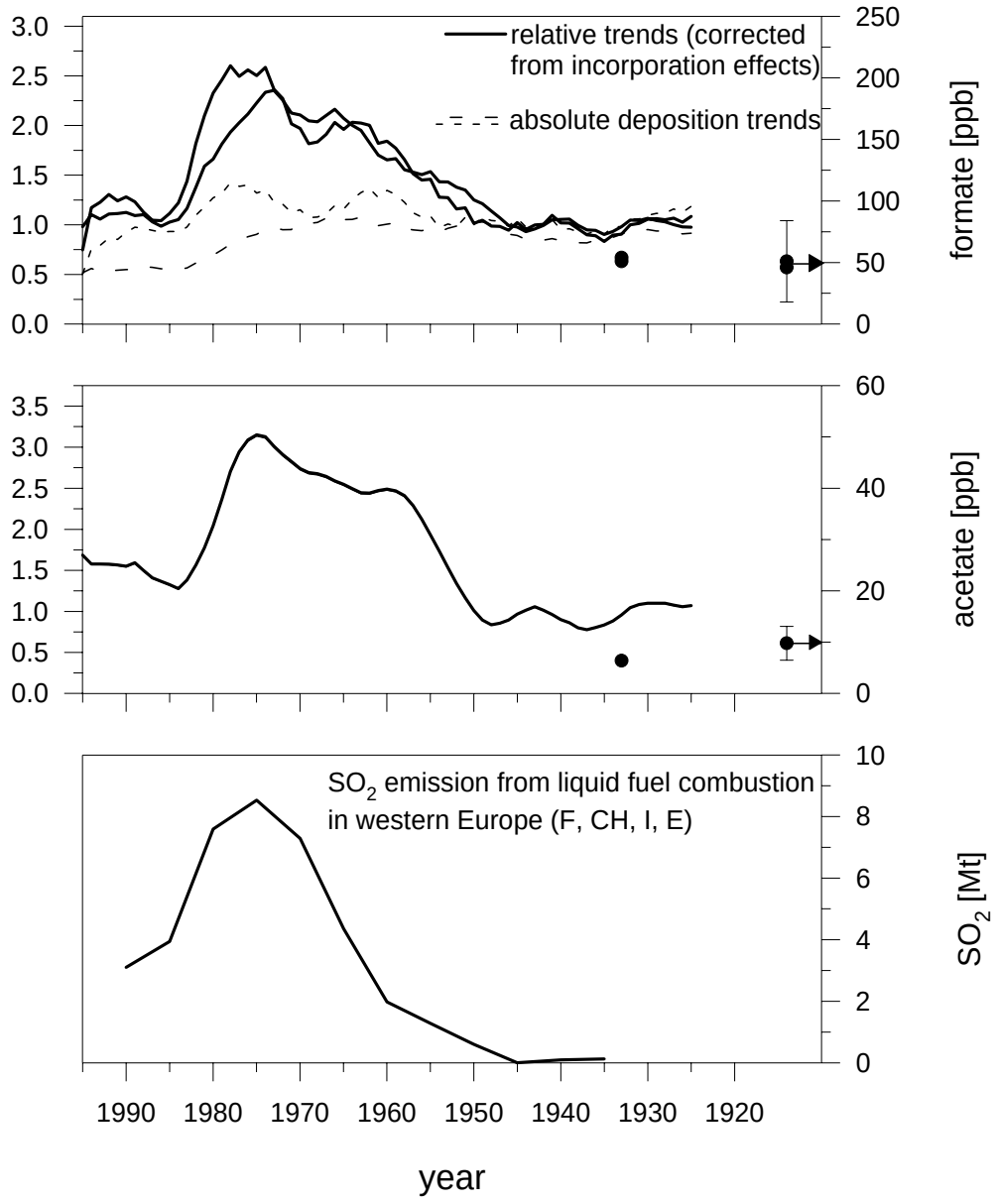

Figure 6.10: (Top and middle) CDD trends of formate and acetate assumed to be relevant for past atmospheric conditions changes (see text). For formate the temporal evolutions of the formate trends corrected from incorporation effects are given relative to the situation in 1925-1935 (thick lines) along with the absolute levels of the respective (corrected from diffusion effects) summer snow deposits (dashed lines) (see also Figure 6.9). For acetate the mean temporal evolution of snow deposition levels is reported on a relative (normalized on 1925-1935) and an absolute scale (see also Figure 6.8a). Dots mark summer formate and acetate levels obtained from Colle Gnifetti ice layers. The arrows on the right site refer to the mean pre-industrial levels. (Bottom) SO_2 emissions due to liquid fuel combustion in France, Switzerland, Italy, and Spain over the 1935-1990 time period (data from Mylona., 1993).

trend reported in Figure 6.10 which is thought to be more representative for past atmospheric formate changes indicates that, similarly to acetate, the formate level would have been enhanced from 1950 to 1975/1980 by a factor of ≈2.4 and then decreases to reach nearly its pre 1950 level. Note that in Greenland snow layers an increase of acetate by a factor of 2 was observed after 1950, whereas, even corrected from the recent increase of the acidity, the Greenland snow layers indicates no recent changes of formate (Legrand and De Angelis, 1996).

Formate and acetate were found to represent an important contributor (up to 65%) to the present-day free acidity in remote areas (Galloway et al., 1982). In recent CDD summer snow layers, due to the high levels of sulfate and nitrate, formate and acetate only contribute for ≈8% of the acidity in 1990. With respect to the change of acidic species over the last 75 years, formate and acetate are found to account for ≈10% in 1980, ≈20% in 1925 and ≈30% in pre-industrial times to the free acidity. CDD acetate and formate levels are found to contribute significantly to the dissolved organic carbon (DOC) present in recent snow layers (≈30%). For comparison, based on DOC data from S. Greilich and M. Schock (personal communication) and formate and acetate levels obtained by Legrand and De Angelis (1996), that is three times higher than what is seen in Greenland snow.

As described above, summer snow levels of acetate as well as the corrected formate trends show a clear increase after 1950. These changes remain however limited to a factor of two to three respectively. That suggests that direct and/or secondary natural (biogenic) emissions of formic and acetic acid (soil and vegetation emissions, photochemical degradation of isoprene and monoterpenes; see Chebbi and Carlier (1996) for a review) dominated the atmospheric budget of these species before 1950, while afterwards anthropogenic derived inputs contributed to up to ≈70% and ≈60% to the total atmospheric formate and acetate budget at high Alpine sites, respectively. Since the shape of the temporal trends is similar in both formate and acetate, it is likely that their anthropogenic sources are closely related, if not identical. As summarized in section 6.1, anthropogenic sources of formic and acetic acids include direct emissions (combustion of biomass, burning of wood and motor exhaust emission) and secondary production resulting from the ozone oxidation of olefins produced by biomass burning, vehicular exhaust, various industrial emissions, and/or the photochemical gas phase oxidation of hydrocarbons and their degradation products released for example during the combustion of hydrocarbon fuels. Since biomass combustion did probably not significantly change over the last 70 years and waste incineration started to became important only after 1965 (see section 5.5 (*4.1*), these sources may contribute to the anthropogenic input observed at CDD but not in a large extend. In Figure 6.10, we compare the CDD formate and acetate trends with the SO_2 emissions due to liquid fuel combustion from France, Italy, Spain, and Switzerland (WE4 countries, see also Chapter 4) over the last 70 years (Mylona, 1993). The temporal evolution of anthropogenic formate and acetate inputs

at CDD fits rather well with the temporal evolution of these SO_2 emissions, which started to increase after 1950 and sharply decreased after 1980 due to an improvement in the quality of fuel and emission abatements. Since the emission abatement mainly concern acidic gases like SO_2 and other acids, such a covariation between the SO_2 emissions from liquid fuel combustion and carboxylic acids would suggest that the anthropogenic acetate and formate trends observed at CDD are mainly related to direct acetate and formate emissions from fuel combustion. On the other hand Puxbaum et al. (1988) proposed on the base of atmospheric acetic and formic acid measurements at semi-rural and rural sites in Austria an important input of secondary produced organic acids in the atmosphere. If true also for the high elevated CDD site, the strong decrease of acetate and formate seen in CDD records cannot only be attributed to fuel combustion releases, since releases of hydrocarbons by liquid fuel combustion which can act as precursors for organic acids were not reduced by the scrubbers set up in the 1980's. Thus although a part of the trend of formate and acetate could be the result of growing liquid fuel consumption, other anthropogenic processes that we have not yet identified may have also contributed to these changes.

The ratio of formic to acetic acid in atmosphere is sometimes used as an indicator of the relative importance of direct emissions (low ratio) and secondary production by photochemical processes (high ratio) (Khwaja, 1995). Several atmospheric studies (e.g. Kawamura and Kaplan, 1985; Talbot et al., 1988) claimed for example that direct emissions from motor vehicular are enriched in acetic compared to formic acid (i.e. a weighted formic to acetic ratio of less than 1.3). Applying this criteria on our data set to decide whether formate and acetate at CDD are possibly derived by direct emissions of monocarboxylic acids is however not evident in view of the complex incorporation mechanism of monocarboxylic acids in precipitation and the respective corrections made for the CDD formate data set (see section 6.3.2). Following equation (6.6), the correction of the formate trend relative to 1925-1935 (see Figure 6.9) would propose for example weighted formate to acetate ratios of ≈5.5 before 1950 and ≈4 afterwards. In contrast, a correction of the formate trend relative to recent times (1985-1994) would deliver weighted formate to acetate ratios of ≈1.6–2.3 in recent times, ≈2.1–3.2 from 1980–1970, and ≈0.7–2.2 from 1925–1935.

Restricting therefore our discussion to the weighted acetate to formate ratio in recent snow, we observe values of 1.2 in winter (snow pit samples) and about 1.8 – 2.7 for the CDD summer snow layers deposited over the 1985-1994 time period (the respective value in snow pit samples is 2.5). Note that these values as well as the seasonal contrast are in quite good agreement with observations made before in continental precipitation, where mean weighted acetate to formate ratios of 1.1 and 2.0 were found in winter and in summer, respectively (Keene and Galloway, 1986). Taking in addition into account that formate becomes likely more efficient incorporated (up to a factor of 2 or more) in precipitation than acetate for recent times mean acidity levels which range between 5 and 8 μEq/l at CDD (see Figure 6.5),

we can not exclude that direct anthropogenic acetate and formate emissions contribute significantly to recent atmospheric conditions and summer snow deposits at CDD. To gain however more accurate information on past atmospheric changes of acetate and formate from the ice core records, detailed investigations are needed to characterize and quantify the respective air/snow/ice relations (including post depositional effects) for these species at the CDD ice core drill site.

Conclusions et prospectives

L'objectif de ce travail était d'étudier de manière approfondie le potentiel que représente les carottes de glace des Alpes pour reconstruire en détail les changements de la composition chimique de l'atmosphère survenus aux moyennes latitudes de l'hémisphère Nord depuis l'époque pré-industrielle. Ce travail montre que des informations relatives à la composition chimique de l'atmosphère peuvent être extraites des enregistrements glaciaires au site du Col du Dôme avec une résolution saisonnière au moins sur les 80 dernières années. Ce travail, associé aux études menées au Colle Gnifetti qui donnent accès à une période de temps plus longue mais avec une résolution temporelle moindre, permettent de conclure que la glace des Alpes a archivé des informations importantes concernant les changements passés de la composition de l'atmosphère. L'étude des tendances « long terme » résolues à l'échelle de la saison montre que le fluage de la glace qui est important sur ces glaciers de petite dimension peut perturber de manière significative les enregistrements chimiques en liaison avec le changement de la quantité respective de neige déposée en été et en hiver en amont du site de forage. Cet effet glaciologique peut induire des erreurs d'interprétation des profils en terme de changement de la chimie de l'atmosphère.

Sur la base des enregistrements saisonniers obtenus dans la glace déposée au Col du Dôme au cours des 70 dernières années, nous discutons les changements observés au cours du 20^{ième} siècle. L'augmentation d'un facteur 10 des concentrations de sulfate observée dans la neige déposée en été entre la période pré-industrielle et l'époque actuelle suit assez fidèlement l'évolution des émissions anthropiques de SO_2 liées aux émissions des zones sources situées dans un rayon de 700 à 1000 km autour des Alpes. Par opposition l'évolution des concentrations dans les couches d'hiver (une augmentation d'un facteur 4 entre l'ère pré-industrielle et l'époque actuelle) corresponds à une contamination plus limitée de la troposphère libre mais qui par opposition à la situation en été se produit à une plus large échelle géographique (l'ensemble de l'Europe). En utilisant la relation entre la composition de l'air et de la neige que nous avons établi sur le site de l'Observatoire Vallot en période estivale comme en période hivernale, nous avons pu pour la première fois inverser les signaux enregistrés dans la glace en terme de changements de la composition de l'atmosphère à 4300 m d'altitude au dessus de l'Europe. A partir de cela nous avons pu montré que de telles données constituent des contraintes importantes au vu de l'incertitude actuelle des simulations des modèles « chimie-transport » visant à modéliser la distribution du sulfate d'origine anthropique et son effet sur le bilan radiatif à l'échelle européenne.

L'évolution des teneurs en nitrate au cours du 20^{ième} siècle a été étudié dans la carotte du Col du Dôme. L'importante accumulation annuelle de neige à l'endroit du forage fait que le lissage des variations saisonnières avec la profondeur est ici un phénomène limité. Les tendances lon-terme des teneurs en nitrate d'été et d'hiver sont en bon accord avec la

croissance des anthropiques émissions de NO en provenance de l'Europe de l'Ouest (en été), de toute l'Europe (en hiver). Probablement plus important constitue l'estimation que nous avons pu faire des niveaux pré-industriels en été comme en hiver qui suggèrent que les émissions naturelles de NO représentent près de 20% du budget du nitrate pour la période actuelle (les estimations antérieures variant de 1 à 20%).

Tandis que les teneurs en ammonium de la glace du Col du Dôme ne révèlent aucune tendance au cours du 20^{ième} siècle en hiver, les concentrations d'été indiquent une augmentation significative depuis le début du siècle. Tout comme ce qui avait déjà été observé dans les carottes de glace du Colle Gnifetti (tendances non résolues saisonnièrement), cette tendance de l'ammonium en été au Col du Dôme est plus forte que la croissance estimée des émissions d'ammoniac d'origine anthropique. Ces données sont des informations importantes sur l'évolution des composés azotés réduits dans la troposphère au dessus de l'Europe en été.

L'examen du budget du fluor et de son évolution dans le passé que nous avons pu faire nous a permis de discuter l'origine du fluor naturel et sa perturbation par l'impact de différentes sources anthropiques dont les rejets de fluor par l'industrie de l'aluminium, la combustion du charbon, et contribution du réservoir stratosphérique (dégradation des CFCs).

Peu d'études antérieures traitent de l'évolution des tendances passées en acide chlorhydrique. Le calcul des teneurs en HCl dans les couches de neige d'été au Col du Dôme est particulièrement complexe car nous avons montré que les aérosols contenant du chlore émis sur les continents représentent près de 80% du chlore qui y est présent. Nous avons pu montré que la majorité de HCl présent dans la neige avant 1960 vient des combustions de biomasse et de la combustion du charbon, tandis qu'après 1960 l'incinération des déchets représente une contribution majeure aux teneurs en acide chlorhydrique de l'atmosphère au dessus de l'Europe.

La première étude des acide carboxyliques dans la glace des Alpes que constitue notre travail a montré des résultats surprenants. Tout d'abord, les teneurs en oxalate, une espèce chimique qui constitue une fraction de l'aérosol organique atmosphérique, ne montrent aucune tendance depuis le début du 20^{ième} siècle. Cet espèce étant émis par les combustions (combustible fossile et de biomasse), cette absence de changement suggère que les processus naturels d'émission (sols biogéniques, feux de biomasse, production secondaire à partir de précurseurs biogéniques naturels) dominent le budget atmosphérique de cette espèce. Les tendances long-terme de l'acétate et du formate (après correction de l'effet du changement de pH de la précipitation sur son incorporation dans la neige) indiquent une augmentation d'un facteur deux après 1950 et une tendance à la décroissante entre 1980 et 2000. Ces changements suggèrent que le budget de ces deux espèces a été modifié par la combustion des combustibles liquides mais que leur budget atmosphérique restent pour moitié d'origine naturelle.

Dans le futur, les résultats obtenus au Col du Dôme pourront servir de contraintes pour les modèles de chimie-transport à l'échelle de l'Europe et pour réduire les incertitudes portant sur les inventaires d'émissions existants. De plus une utilisation conjointe des carottes du Colle Gnifetti et Col du Dôme devraient permettre l'étude détaillée de la variabilité naturelle (pré-industrielle) de l'atmosphère au dessus de l'Europe. Par ailleurs il est clair que l'étude des acides carboxyliques que nous avons initié devra être étendue à d'autres fractions de l'aérosol organique (cela fait partie d'un des objectifs principaux du futur programme Européen CARBOSOL). La question clé est ici de savoir si l'importante augmentation de la charge en sulfate de l'atmosphère Européenne a été ou non (comme le suggère ici notre étude de l'oxalate) accompagnée par une modification similaire de la charge en aérosol organique. De la réponse à cette question dépendra l'importance du rôle joué par les aérosols sur le climat au dessus d'un continent fortement industrialisé comme l'Europe.

Le collecteur automatique d'aérosol que nous avons développé et mis en place à l'Observatoire Vallot a fonctionné correctement en dépit des conditions météorologiques difficiles qui y sévissent. Il sera important de maintenir cette activité sur plusieurs années et de lui associée des mesures de la hauteur de neige afin d'augmenter la précision dans l'évaluation de la relation « air-neige » que nous avons proposé ici à partir d'une série de mesure couvrant une année. De plus des améliorations du dispositif sont encore nécessaires pour certaines espèces atmosphériques comme les grosses particules. Enfin si le matériel utilisé (filtres, supports de filtres) peut être adapté, une extension des collectes à d'autres espèces (organiques en particulier) est envisageable.

Ces études de la glace du Col du Dôme ainsi que les études atmosphériques à l'Observatoire Vallot montrent l'intérêt de ce site pour l'étude de la troposphère Européenne. Dans le futur la poursuite du monitoring des espèces aérosol (sulfate, ammonium, oxalate) devront être étendu au travers de campagne intensive à d'autres composantes de l'aérosol (espèces minérales mineure, composés organiques) ainsi qu'à des études sur la fraction gazeuse.

Au cours de ce travail, nous avons également participé à des études prospectives (mesure radar de l'épaisseur de glace, mesure de l'accumulation en surface, et étude de petits carottages) visant à localiser d'autres points de forage sur le site de Col du Dôme avec comme objectif d'étendre la période de temps couverte par les enregistrements (75 ans actuellement) à 130 voir 200 ans, et ce avec une résolution temporelle permettant encore de différencier couches d'été et couches d'hiver. En fin 1999, deux nouveaux forages ont été effectués jusqu'au socle dont un de 39 m au sommet du Dôme du Goûter. A cet endroit, la faible accumulation (19 cm d'eau equivalent, F. Pinglot, communication personnelle) devrait permettre de remonter le temps sur plusieurs siècles, complémentant ainsi l'étude des carottes du Colle Gnefetti. Notons que le faible écoulement de la glace en ce point devrait permettre de mieux documenter les enregistrements de trace gazeuses (méthane) dans cette région. Le

deuxième forage (103 m) a été réalisé dans la pente sous l'Observatoire Vallot. Les premières mesures indiquent une accumulation de 80 cm d'eau équivalent (F. Pinglot, communication personnelle) ce qui devrait permettre de couvrir beaucoup plus que les 75 dernières années obtenues sur la carotte de 1994.

Dans le futur il serait également intéressant d'explorer ces carottes du CDD pour d'autres espèces comme (1) le plomb et d'autres métaux lourds pour lesquels n'existent actuellement que des profiles non résolus saisonnièrement, (2) différents composés ou groupe de composés organiques (carbone suie, carbone organique, formaldéhyde) pour lesquels rappelons que le rôle de l'anthropique par rapport aux processus naturels restent une inconnue majeure de la chimie de l'atmosphère de bruit de fond continentale.

Summary and outlook

The objective of this study was to investigate in detail the suitability of Alpine ice cores to reconstruct accurately the history of atmospheric changes occurred at the scale of mid-northern latitudes since the pre-industrial era. In this work we demonstrate that information related to the atmospheric chemistry can be extracted in seasonal (winter/summer) resolution from Col du Dôme ice core records at least over the last 80 years. This work together with studies carried out at the Colle Gnifetti glacier site which permit investigations over longer time periods but with a poorer time resolution, permit to conclude that detailed long term atmospheric information is stored in high elevated Alpine ice cores. The examination of seasonally resolved chemical long term trends at Col du Dôme revealed that the glacier flow can significantly disturb annual mean long term ice core records from small scaled glacier sites due to changed summer to winter snow accumulation rates upstream to the drill site. Due to this glaciological effect, misleading interpretation of long term Alpine ice core records in term of atmospheric chemistry changes can occur.

Based on seasonally resolved Col du Dôme ice core records spanning the last 75 years, the temporal evolution of several chemical species over the course of the 20th century was discussed. It was found that the Col du Dôme summer sulfate change (an increase by a factor of ten between the pre-industrial era and present) follows closely the course of growing anthropogenic SO_2 emissions from source regions located within 700–1000 km around the Alps. In contrary, the Col du Dôme winter trend (an increase by a factor of four since the pre-industrial era) reflects a limited contamination of the free European troposphere which, in contrast to summer, occurs at a larger scale (total Europe). The use of the within this work established relationship between present-day concentrations in air and snow at the Col du Dôme site, allowed for the first time to invert ice core trends (winter and summer), and to reconstruct present and past atmospheric sulfate concentrations at 4300 m asl over Europe. These data are shown to constitute an useful constraint for the current uncertainties of transport-chemistry models dealing with the sulfur cycle and its climatic implication (radiative forcing) at the scale of Europe.

The temporal change of nitrate over the 20th century was investigated in seasonal resolution in the Col du Dôme deep ice core. Due to a sufficient high snow accumulation rate here, the smoothing of seasonal variation of this volatile species (nitric acid) with depth remains a limited phenomena. The temporal changes of summer and winter nitrate levels at the Col du Dôme are in fair agreement which the growth of anthropogenic NO_x emissions in western Europe and total Europe, respectively. Probably more important is the estimation which was made for the rather unknown pre-industrial nitrate summer and winter levels, and which shows that natural NO emissions contribute up to 20% to the present-day summer budget (previous estimates varying between 1 and 20 %).

While ammonium winter levels at Col du Dôme show no significant temporal change over the 20th century, the summer ones reveal a significant increase since the beginning of the 20th century. In agreement with what was already revealed in non-seasonally resolved high Alpine ice cores from Colle Gnifetti, this summer increase is significantly stronger than what is predicted by existing ammonia emission estimates. That provides therefore new insight on the temporal evolution of tropospheric conditions of reduced nitrogen species during the summer season.

The examination of the fluoride budget and its temporal evolution in the Col du Dôme ice core permitted to discuss natural fluoride sources for the free troposphere over Europe and the recent impact of anthropogenic sources such as release from aluminium smelters, coal burning, and contributions of the stratospheric reservoir built up from the chlorofluorocarbon degradation.

Very rare are studies of the HCl content in polar ice cores. The evaluation of the HCl content in Col du Dôme summer snow deposits was particularly complex since it was found that continental chloride aerosol emissions account for 80% to the budget of total chloride. The HCl content in Col du Dôme snow layers was found to be dominated by biomass burning and coal emissions until the late 1960's, while more recently waste incineration in western Europe has strongly disturbed the atmospheric HCl budget.

First investigations of light carboxylic acids (formate, acetate, and oxalate) in an Alpine ice core have shown some unexpected findings. First the levels of oxalate, a species which constitutes a part of the atmospheric organic aerosol, show no significant change since the beginning of the 20th century. Although this species is emitted during combustion (fossil fuel and biomass burning), this absence of trend suggests that natural processes (biogenic soil emissions, biomass burning, secondary production from other biogenic compounds) are still dominating its atmospheric budget at this altitude. The long term trends of acetate and formate (after correction from the pH effect of its incorporation in the precipitation) show an increase by a factor of two after 1950 and a decrease after 1980. Such a pattern suggests that the budget of theses species has been significantly influenced by emissions from liquid fuel combustion whereas natural sources account for a half of their budget even in 1980.

In addition to further applications of the data gained in this study such as their future use in constraining atmospheric chemistry models at the scale of Europe and assessing past emission inventory estimates, further works examining seasonal resolved long-term trends at Col du Dome and Colle Gnifetti are mandatory to investigate in more detail the natural (pre-industrial) conditions in the mid-troposphere over Europe. Furthermore, our preliminary study of light carboxylic acids, which represent only a minor fraction of the organic matter present in the atmosphere, has to be extended to other organic groups and species (partly included in the forthcoming European research project: CARBOSOL). The key question is here to investigate whether the dramatic change of sulfate aerosol load in the European atmosphere

has been accompanied by a similar change of organic aerosol or not (as suggested in this work for oxalate). Depending of these forthcoming findings the contribution of organic aerosol to the climate forcing over continental industrialized areas would need to be reconsidered.

The newly developed aerosol device set up at the Vallot Observatory was shown to work well in spite of the persisting harsh environmental conditions at this site. With regard to the temporal limited data set which was gained during this study, future routine aerosol sampling at Vallot Observatory along with more regular measurements of the snow height will be very helpful to establish a statistically more reliable air snow relationship for key aerosol species. To achieve also reliable air firn relationship of supermicronic aerosols (dust particles), further field experiments are needed to estimate more carefully the sampling efficiency of the device for these species. That would permit to extend the preliminary attempt to invert ice core signals into atmospheric changes made for sulfate, ammonium and oxalate within this study. If filter material and filter holders can be adapted, an extension of continuous aerosol sampling for other (e.g. organic) species can be envisaged.

Ice core and atmospheric data gained in this study suggest that the Col du Dôme glacier site (including the Vallot Observatory) experiences year round undisturbed tropospheric background conditions representative on a spatial scale of western and total Europe. Thus, the continuous documentation of key aerosol species, and regular discontinuous atmospheric measurements of minor aerosol species and gaseous compounds at the Vallot Observatory would offer the unique possibility to gain rock stable information about the chemical composition and its temporal variability of the atmosphere at 4361 m asl over Europe.

From 1997 to 1999 glaciological investigation including radar measurements (personal communication, S. Sutter), snow accumulation measurements (personal communication, C. Vincent) and shallow ice core drillings have been performed at the Col du Dôme glacier site to locate further drill sites aimed to obtain ice core records covering a maximal time period, seasonally resolved ice core records which extend back to the pre-industrial era (i.e. covering the last 130 to 200 years), respectively. In 1999 two deep ice cores were drilled almost to bedrock at Col du Dôme from which one (39 m length) was recovered at the Dome (summit) position of the Dôme du Gouter. At this site the rather low snow accumulation rate (≈ 19 cm w.e.; personal communication, F. Pinglot) would permit to have snow layers deposited over the last few centuries which will complement ice core records already obtained at Colle Gnifetti (Schaefer, 1995; Wagenbach et al., 1996; Schwikowski et al., 1999). Note that since glacier flow effects are assumed to be rather low at this drill site, trace gas investigations on this core could be worthwhile in view to assess already existing high Alpine trace gas data sets (Blunier, 1995; Blanchard, 1998). The second deep ice core drilled in 1999 is located on the slope of the Vallot Observatory (103 m length). First measurements reveal a mean snow

accumulation rate of 80 cm w.e. over the 1963–1999 period (personal communication, F. Pinglot) at this site. A glaciochemical study of this ice core would likely permit to examine in detail the natural (pre-industrial) chemical snow composition and its temporal variability.

With regard to the accessibility of a seasonal resolved and atmospheric relevant glacier archive at the Col du Dôme glacier site, it would be useful to extend the here presented seasonally resolved ice core study on other climatic and environmental relevant species as e.g. (1) lead and other heavy metals for which only non-seasonally resolved long term ice core records exist (Wagenbach and Preunkert, 1996; Van de Velde, 1999), (2) total organic carbon and other specific organic components (formaldehyde and others) for which almost nothing is known at present concerning the respective role of natural versus anthropogenic processes over the past.

References **(publications related to this work are not included)**

Alean, J., Haeberli, W. and Schaedler, B., 1983. Snow accumulation, firn temperature and solar radiation in the area of the Colle Gnifetti core drilling site (Monte Rosa, Swiss Alps): distribution patterns and interrelationships. *Z. Gletscherkd. Glazialgeol*. **19**, 131-147.

Andreae, M.O., Talbot, R.W., Andreae, T.W. and Harriss, R.C., 1988. Formic and acetic acids over the central Amazon region. *J. Geophys. Res.* **93**, 1616-1624.

Armbruster, M., 2000. *Stratigraphische Datierung hoch-alpiner Eisbohrkerne über die letzten 1000 Jahre*. MS-Thesis, Institut für Umweltphysik der Universität Heidelberg, 72p.

Asman, W.A.H., Drukker, B. and Janssen, A.J., 1988. Modelled historical concentrations and depositions of ammonia and ammonium in Europe. *Atmos. Environ*. **22**, 725-735.

Atkinson, R. and Lloyd, A.L., 1984. Evaluation of kinetic and mechanistic data for modeling of photochemical smog. *J. phys. Chem. ref. Data* **13**, 315-444.

Aymoz, G., 1999. *Etude de la composition chimique de la neige de surface de Groenland*. MS-Thesis, Laboratoire de Glaciologie et Géophysique de l'Environnement, University Joseph Fourier, Grenoble 1, 45p.

Baboukas, E.D., Kanakidou, M. and Mihalopoulos, N., 2000. Carboxylic acids in gas and particulate phase above the Atlantic Ocean. *J. Geophys. Res.* **105**, 14459-14471.

Bales, R.C. and Wolff, E.W., 1996. Interpreting natural climate signals in ice cores. *EOS* **76**, 477, 482-483.

Baltensperger, U., Gaeggeler, H. W., Jost, D.T., Lugauer, M., Schwikowski, M., Weingartner, E. and Seibert, P., 1997. Aerosol climatology at the high-alpine site Jungfraujoch, Switzerland. *J. Geophys. Res*. **102,** 19707-19715.

Barnola, J.M., Raynaud, D., Korotkevitch,Y.S. and Lorius, C., 1987. Vostok ice core provides 160,000-year record of atmospheric CO_2. *Nature* **329**, 408-414.

Barrett, K., Seland, O., Foss, A., Mylona, S., Sandnes, H., Styve, H. and Tarrason, L., 1995. *European transboundary acidifying air pollution. Ten years calculated fields and budgets to the end of the first sulphur protocol*. EMEP/MSC-W Rep. 1/95, Meteorol. Syn. Cent.-West, Norw. Meteorol. Inst., Oslo, 71p.

Blanchard, R., 1998. *Evolution de la teneur en methane et en monoxyde de carbon de la glace du Col du Dôme (Mont Blanc) au cours de la periode industrielle*. MS-Thesis, Laboratoire de Glaciologie et Géophysique de l'Environnement, University Joseph Fourier, Grenoble 1, 40p.

Bloomfield, P. and Steiger, W.L., 1983. In *Last absolute deviations: Theory, Applications and Algoritms*. Birkhauser, Boston.

Blunier, T., 1995. Methanmessungen aus Arktis, Antarktis und den Walliser Alpen, Interhemisphärischer Gradient und Quellenverteilung. PhD-Thesis, Universität Bern, Abteilung für Klima und Umweltphysik.

Blunier, T., Chappellaz, J., Schwander, J., Stauffer, B. and Raynaud, D., 1995. Variations in atmospheric methane concentration during the Holocene epoch. *Nature* **374**, 46-49.

Briat, M., 1978. Evaluation of levels of Pb, V, Cd, Zn and Cu in the snow of Mt Blanc during the last 25 years. In: *Studies in the Environmental Science,* vol.1 (ed. M.M. Benarie). Elsevier, Amsterdam, 225-228.

Buijsman, E., Maas, H.F.M. and Asman, W.A.H., 1987. Anthropogenic NH_3 emissions in Europe. *Atmos. Environ*. **21**, 1009-1022.

Calvert, J.G. and Stockwell, W.R., 1983. Acid generation in the troposphere by gas-phase chemistry. *Envir. Sci. Technol*. **17**, 428A-443A.

Chameides, W.L. and Davis, D.D., 1983. Aqueous-phase source of formic acid in clouds. *Nature* **304**, 427-429.

Chameides, W.L., 1984. The photochemistry of the remote marine stratiform cloud. *J. Geophys. Res*. **89**, 4739-4755.

Chao, J. and Zwolinski, B.J., 1978. Ideal gas thermodynamic properties of methanoic and ethanoic acids. *J. Phys. Chem. Ref. Data* **7**, 363-377.

Chapman, E.G., Sklarew, D.S. and Flickinger, J.S., 1986. Organic acids in springtime Wisconsin precipitation samples. *Atmos. Environ*. **20**, 1717-1726.

Chappellaz, J., Barnola, J.M., Raynaud, D., Korotkevich, Y.S. and Lorius, C., 1990. Ice-core record of atmospheric methane over the past 160,000 years. *Nature* **345**, 127-131.

Chappellaz, J., Blunier, T., Kints, S., Dallenbach, A., Barnola, J.M., Schwander, J., Raynaud, D. and Stauffer, B., 1997. Changes in the atmospheric CH_4 gradient between Greenland and Antarctica during the Holocene. *J. of Geophys. Res.* **102**, 15987-15997.

Chebbi, A. and Carlier, P., 1996. Carboxylic acids in the troposphere, occurrence, sources, and sinks: A review. *Atmos.Environ.* **30**, 4233-4249.

Cicerone, R., 1981. Halogens in the atmosphere. *Reviews of Geophysics* **19**, 123-139.

Dansgaard, W., 1954. The oxygen-18 abundance in fresh water. *Geochim. Cosmochim. Acta* **6**, 241-260.

Dansgaard, W., Johnsen, S.J., Clausen, H.B. and Gundestrup, N., 1973. Stable isotope glaciology. *Meddelelser om Gronland* **197** (2), 5-53.1973

Dansgaard, W., Johnsen, S.J., Clausen, H.B., Dahl-Jensen, D., Gundestrup, N.S., Hammer, C.U., Hvidberg, C.S., Steffensen, J.P., Sveinbjornsdottir, A.E., Jouzel, J. and Bond, G.,

1993. Evidence for general instability of past climate from a 250-kyr ice-core record. *Nature* 364, 218-221.

Davidson, E.A. and Kingerlee, W., 1997. A global inventory of nitric oxide emissions from soils. *Nutr. Cycling Agroecosys.* **48**, 91-104.

Dayan, U., Miller, J.M., Keene, W.C. and Galloway, J.N., 1985. An analysis of precipitation chemistry data from Alaska. *Atmos. Environ*. **19**, 651-657.

De Angelis, M. and Gaudichet, A., 1991. Saharan dust deposition over Mont Blanc (French Alps) during the last 30 years. *Tellus* **43B**, 61-75.

De Angelis, M. and Legrand, M., 1994. Origins and variations of fluoride in Greenland precipitation. *J. Geophys. Res.* **99**, 1157-1172.

De Angelis, M. and Legrand, M., 1995. Preliminary investigations of post depositional effects on HCl, HNO_3, and organic acids in polar firn layers. In: *Ice Core Studies of Global Biogeochemical Cycles, NATO ASI Ser. I*, vol. 30 (ed. R.J. Delmas). Springer-Verlag, New York, 361-381.

Delmas,R.J., 1992. Environmental information from ice cores. *Reviews of Geophysics* **30**, 1-21.

Delmas, R.J., Ascencio, J.M. and Legrand, M., 1980. Polar ice evidence that atmospheric CO_2 20,000yr BP was 50% of present. *Nature* **284**, 155-157.

Dibb, J.E., Talbot, R.W. and Bergin, M., 1994. Soluble acidic species in air and snow at Summit, Greenland. *Geophys. Res. Lett.* **21**, 1627-1630.

Dignon, J. and Hameed, S., 1989. Global emissions of nitrogen and sulfur oxides from 1860 to 1980. *JAPCA* **39**, 180-186.

Döscher A., Gäggeler, H.W., Schotterer, U. and Schwikowski, M., 1995. A 130 years deposition record of sulfate, nitrate and chloride from a high-Alpine glacier. *Water, Air and Soil Pollution* **85**, 603-609.

Döscher, A., Gäggeler, H.W., Schotterer, U. and Schwikowski, M., 1996. A historical record of ammonium concentrations from a glacier in the Alps. *Geophys. Res. Lett*. **23**, 2741-2744.

Duce, R.A., Mohen, V.A., Zimmerman, P.R., Grosjean, D., Cautreels, W., Chatfield, R., Jaenicke, R., Ogren, J.A., Pellizzari, E.D. and Wallace, G.T., 1983. Organic material in the global troposphere. *Reviews of Geophysics* **21**, 921-952.

Eichler, A., Schwikowski, M. and Gäggeler, H., 2000. An Alpine ice-core record of anthropogenic HF and HCl emissions. *Geophys. Res. Lett.* **27**, 3225-3228.

Etheridge, D.M., Steele, L.P., Francey, R.J. and Langenfelds, R.L., 1998. Atmospheric methane between 1000 AD and present: Evidence of anthropogenic emissions and climatic variability. *J. Geophys. Res*. **103**, 15979-15993.

Fischer, H., 1997. *Räumliche Variabilität in Eiskernzeitreihen Nordostgrönlands - Rekonstruktion klimatischer und luftchemischer Langzeittrends seit 1500 A.D.*. PhD-Thesis, Institut für Umweltphysik der Universität Heidelberg, 135p.

Fischer, H., Wagenbach, D. and Kipfstuhl, J., 1998a. Sulfate and nitrate firn concentrations on the Greenland ice sheet 1. Large-scale geographical deposition changes. *J. Geophys. Res*. **103**, 21927-21934.

Fischer, H., Wagenbach, D. and Kipfstuhl, J., 1998b. Sulfate and nitrate firn concentrations on the Greenland ice sheet 2. Temporal anthropogenic deposition changes. *J.Geophys.Res*. **103**, 21935–21942.

Flückiger, J., Dällenbach, A., Blunier, T., Stauffer, B., Stocker, T.F., Raynaud, D. and Barnola, J.M., 1999. Variations in atmospheric N_2O concentration during abrupt climatic changes. *Science* **285**, 227-230.

Fuhrer, K., Neftel., A., Anklin, M., Staffelbach, T. and Legrand, M., 1996. High-resolution ammonium ice core record covering a complete glacial-interglacial cycle. *J. Geophys. Res*. **101**, 4147-4164.

Funk, M., 1993. Possible Alpine ice-core drilling sites, an overview. In: *Proceedings of the ESF/EPC workshop: Greenhouse gases, isotopes and trace elements in glaciers as climatic evidence for Holocene time* (ed. W. Haeberli and B. Stauffer). Report of the ESF/EPC Workshop, Zürich 27.-28.10.1992, Arbeitsheft Nr. 14, VAW-ETH-Zürich, 40-44.

Gagliardini, O. and Meyssonnier, J., 1997. Flow simulation of a firn-covered cold glacier. *Ann. of Glaciol.* **24**, 242-248.

Galloway, J.N., Likens, G.E., Keene, W.C. and Miller, J.M., 1982. The composition of precipitation in remote areas of the world. *J. Geophys. Res*. **87**, 8771-8786.

Georgii, H.W. and Lenhard, U., 1978. Contribution to the atmospheric NH_3 budget. *Pure Appl. Geophys*. **116**, 385-391.

Gillet, R.W., Ayers, G.P. and Noller, B.N., 1990. Rainwater acidity at Jabiru, Australia, in the wet season of 1983/84. *Sci. total. Envir*. **92**, 129-144.

Graedel, T.E. and Weschler, C.J., 1981. Chemistry within aqueous atmospheric aerosols and raindrops. *Review of Geophysics* **19**, 505-539.

Graedel, T.E. and Keene, W.C., 1995. The tropospheric budget of reactive chlorine. *Global Biogeochem. Cycles* **9**, 47-78.

Graedel, T.E. and Keene, W.C., 1996. The budget and cycle of Earth's natural chlorine. *Pure and Appl. Chem.* **68**, 1689-1697.

Grosjean, D., Van Cauwenberghe, K., Schmid, J.P., Kelly, P.E. and Pitts, J.N., 1978. Identification of C_2-C_{10} aliphateic dicorboxylic acids in airborne matter. *Envir. Sci. Technol*. **12**, 313-316.

Grosjean, D., 1989. Organic acids in southern California air: Ambient concentrations, mobile source emisions, in situ formation and removal processes. *Environ. Sci. Technol*. **23**, 1506-1514.

Guiang, S.F., Krupa, S.V. and Pratt, G.C., 1984. Measurement of S(IV) and organic anions in Minnesota rain. *Atmos. Environ*. **18**, 1677-1682.

Haeberli, W., Schotterer, U., Wagenbach, D., Haeberli-Schwitter, H. and Bortenschlager, S., 1983. Accumulation characteristics on a cold, high-alpine firn saddle from a snow-pit study on Colle Gnifetti, Monte Rosa, Swiss Alps. *J. Glaciol*. **29**, 260-271.

Hatakeyama, S., Tanonaka, T., Weng, J., Bandow, H., Takagi, H. and Akimoto, H., 1985. Ozone-cyclohexene reaction in air: Ouantitative analyses of particulate products and the reaction mechanism. *Environ. Sci. Technol*. **19**, 935-942.

Hatakeyama, S., Ohno, M., Weng, J., Takagi, H. and Akimoto, H., 1987. Mechanism for the formation of gaseous and particulate products from ozone-cycloalkene reactions in air. *Environ. Sci. Technol*. **21**, 52-57.

Holdsworth, G. and Peak, E., 1985. Acid content of snow from a mid-troposphere sampling site on Mount Logan, Yukon Territory. *Ann. of Glaciol.* **7**, 153-160.

Horvath., L. and Sutton, M.A., 1998. Long-term record of ammonia and ammonium concentrations at K-Puszta, Hungary. *Atmos. Environ*. **32**, 339-344.

Hov, O., Allegrini, I., Beilke, S., Cox, R.A., Eliassen, A., Elshout, A.J., Gravenhorst, G., Penkett, S.A. and Stern, R., 1987. *Evaluation of atmospheric processes leading to acid deposition in Europe*. Vol. 10 of *Air pollution research report*. Commission of the European Communities, 179p.

Jacob, D.J., 1986. Chemistry of OH in remote clouds and its role in the production of formic acid and peroxymonosulphate. *J. Geophys. Res*. **91**, 9807-9826.

Jacob, D.J. and Wofsy, S.C., 1988a. Photochemistry of biogenic emission over the Amazon forest. *J. Geophys. Res*. **93**, 1477-1486.

Jacob, D.J. and Wofsy, S.C., 1988b. Photochemical production of carboxylic acids in a remote continental atmosphere. In: *Acid Deposition Processes at High Elevation Site*s (ed. M.H. Unsworth). D. Reidel, Hingham, MA, 73-92.

Jaffrezo, J.L. and Davidson, C.I., 1993. The Dye 3 gas and aerosol sampling program (DGASP): An overview. *Atmos. Environ*. **27A**, 3029-3036.

Jaffrezo, J.L., Davidson, C.I., Kuhns, H.D. and Strader, R.. Seasonal variations in aerosol chemical species on the Greenland ice sheet. *Atmos. Environ.*, submitted.

Johnsen, S.J., Dansgaard, W. and Clausen, H.B., 1972. Oxygen isotope profiles through the Antarctic and Greenland ice sheets. *Nature* **235**, 429-434.

Jouzel, J., Legrand, M.R., Pinglot, J.F., Pourchet, M. and Reynaud, L., 1984. Chronologie d'un carottage de 20 m au Col du Dôme (Massif du Mont-Blanc). *Houille Blanche* **1984**, 491-497.

Jouzel, J., Lorius, C., Genthon, C., Barkov, N.I., Kotlyakov, V.M. and Petrov, V.N., 1987. Vostok ice core: A continuous isotope temperature record over the last climatic cycle (160,000 years). *Nature* **329**, 403-409.

Jung, W., 1993. *Hundertjährige Zeitreihen der Aerosoldeposition auf einem hochalpinen Gletscher*. MS-Thesis, Institut für Umweltphysik der Universität Heidelberg, 71p.

Kahl, J.D., Martinez, D.A., Kuhns, H., Davidson, C.I., Jaffrezo, J.L. and Harris, J.M., 1997. Air mass trajectories to Summit: A 44-year climatology and some episodic events. *J. Geophys. Res.* **102**, 26861-26875.

Kalina, M.F. and Puxbaum, H., 1994. A study of the influence of riming of ice crystals on snow chemistry during different seasons in precipitating continental clouds. *Atmos. Environ*. **28**, 3311-3328.

Kasper, A. and Puxbaum, H., 1998. Seasonal variation of SO_2, HNO_3, NH_3 and selected aerosol components at Sonnblick (3106 m asl*). Atmos. Environ*. **32**, 3925-3939.

Kasper-Giebl, A., Kalina, M.F. and Puxbaum, H., 1999. Scavenging ratios for sulfate, ammonium and nitrate determined at Mt. Sonnblick (3106 m a.s.l.). *Atmos. Environ.* **33**, 895-906.

Kawamura, D. and Kaplan, I.R., 1983. Organic compounds in rainwater of Los Angeles. *Envir. Sci. Technol*. **17**, 497-501.

Kawamura, K. and Kaplan, I.R., 1985. Determination of organic acis (C_1-C_{10}) in the atmosphere, motor exhaust, and engine oils. *Environ. Sci. Technol.* **19**, 1092-1086.

Kawamura, K. and Kaplan, I.R., 1987. Motor exhaust emissions as primary source for dicarboxylic acids in Los Angeles ambient air. *Environ. Sci. Technol.* **21**, 105-110.

Keene, W.C., Galloway, J.N. and Holden, J.D., 1983. Measurement of weak acidity in precipitation from remote areas of the world. *J. Geophys. Res*. **88**, 5122-5130.

Keene, W.C. and Galloway, J.N., 1984. Organic acidity in precipitation of North America. *Atmos. Environ*. **18**, 2491-2497.

Keene, W.C. and Galloway, J.N., 1986. Considerations regarding sources for formic and acetic acids in the troposphere. *J. Geophys. Res*. **91**, 14466-14474.

Keene, W.C. and Galloway, J.N., 1988. The biogeochemical cycling of formic and acetic acids through the troposphere: An overview of current understanding. *Tellus* **40B**, 322-334.

Kesselmeier, J. and Staudt, M., 1999. Biogenic volatile organic compounds (VOC): An overview on emission, physiology and ecology. *J. Atmos. Chem*. **33**, 23-88.

Khwaja, H.A., 1995. Atmospheric concentrations of carboxylic acids and related compounds at a semiurban site. *Atmos. Environ*. **29**, 127-139.

Koerner, R.M., 1977. Devon Island Ice Cap: Core stratigraphy and paleoclimate. *Science* **196,** 15-18.

Kumar, N., Kulshrestha, U.C., Saxena, A., Kumari, K.M. and Srivastava, S.S, 1993. Formate and acetate in monsoon rainwater of Agra, India. *J. Geophys. Res*. **98**, 5135-5137.

Laceaux, J.P., Loemba-Mdembi, J., Lefeivre, B., Cros, B. and Delmas, R., 1992. Biogenic emissions and biomass burning influences on the chemistry of the fogwater and stratiform precipitations in the african equatorial forest. *Atmos. Environ*. **26A**, 541-551.

Lefer, B.L. and 13 others, 1994. Enhancement of acidic gases in biomass burning impacted air masses over Canada. J. Geophys. Res., 1721-1737.

Lefohn, A.S., Husar, J.D. and Husar, R.B., 1999. Estimating Historical Anthropogenic Global Sulfur Emission Patterns for the Period 1850-1990. *Atmos. Environ.* **33**, 3435-3444.

Legrand, M., De Angelis, M., Staffelbach, T., Neftel, A. and Stauffer, B., 1992. Large perturbations of ammonium and organic acids content in the Summit-Greenland ice core, Fingerprint from forest fires? *Geophys. Res. Lett*. **19**, 473-475.

Legrand, M., De Angelis, M. and Maupetit, F., 1993. Field investigation of major and minor ions along Summit (central Greenland) ice cores by ion chromatography. *J. Chromatogr*. **640**, 251-258.

Legrand, M. and De Angelis, M., 1995. Origins and variations of light carboxylic acids in polar precipitation. *J. Geophys. Res.* **100**, 1445-1462.

Legrand, M. and De Angelis, M., 1996. Light carboxylic acids in Greenland ice: A record of past forest fires and vegetation emissions from the boreal zone. *J. Geophys. Res*. **101**, 4129-4145.

Legrand, M. and Mayewski, P., 1997. Glaciochemistry of polar ice cores: A review. *Reviews of Geophysics* **35**, 219-243.

Lenhard, U., 1977. Messungen von Ammoniak in der unteren Troposphäre und Untersuchung der NH_3 Quellstärke von Böden. MS-Thesis, Institut für Meteorologie und Geophysik der Universität Frankfurt/Main.

Li, S.M. and Winchester, J.W., 1989. Geochemistry of organic and inorganic ions of a late winter Arctic aerosols. *Atmos. Environ*. **23**, 2401-2415.

Likens, G.E., Keene, W.C., Miller, J.M. and Galloway, J.N., 1987. Chemistry of precipitation from a remote, terrestrial site in Australia. *J. Geophys. Res*. **92**, 13299-13314.

Limbeck, A. and Puxbaum, H., 1999. Organic acids in continental background aerosols. *Atmos. Environ*. **33**, 1847-1852.

Limbeck, A., Puxbaum, H., Otter, L. and Scholes, M.C., 2001. Semivolatile behavior of dicarboxylic acids and other polar organic species at a rural background site (Nylsvley, RSA). *Atmos. Environ.* **35**, 1853-1862.

Löflund, M., Kasper-Giebl, A., Schuster, B., Giebl, H., Hitzenberger, R. and Puxbaum, H.. Formic, acetic, oxalic, malonic and succinic acid concentrations and their contribution to organic carbon in cloud water. *Atmos Environ.,* submitted.

Logan, J.A., 1983. Nitrogen oxides in the troposphere: Global and regional budgets. *J. Geophys . Res*. **88**, 10785-10807.

Lorius, C., Jouzel, J., Ritz, C., Merlivat, L., Barkov, N.I., Korotkevich, Y. and Kotlyakov, V.N., 1985. A 150,000 year climatic record from Antarctic ice. *Nature* **346**, 258-260.

Madronich, S. and Calvert, J.G., 1990. Permutation reactions of organic peroxyradicals in the troposphere. *J. Geophys. Res*. **95D**, 5697-5715.

Maupetit, F., 1992. *Chimie de la neige de très haute altitude dans les Alpes Francaises*. PhD-Thesis, Paris 7 University, publication no. 745 of the Laboratoire de Glaciologie et Géophysique de l'Environnement, 246 p.

Maupetit, F. and Delmas, R., 1994. Snow chemistry of high altitude glaciers in the French Alps. *Tellus* **46B**, 304-324.

Maupetit, F., Wagenbach, D., Weddeling, P. and Delmas, R., 1995. Recent chemical and isotopic properties of high altitude cold Alpine glaciers. *Atmos. Environ*. **29**, 1-9.

Mayewski, P., Lyons, W.B., Spencer, M.J., Twickler, M., Dansgaard, C., Koci, B., Davidson, C.I. and Honrath, R.E., 1986. Sulphate and nitrate concentrations from the south Greenland ice core. *Sience* **232**, 975-977.

McCulloch, A., Aucott, A.M.L., Benkovitz, C.M., Graedel, T.E., Kleiman, G., Midgley, P.M. and Li, Y.F. 1999. Global emissions of hydrogen chloride and chloromethane from coal combustion, incineration and industrial activities: Reactive Chlorine Emissions Inventory. *J. Geophys. Res.* **104**, 8391-8403.

Minikin, A., 1994. *Spurenstoff-glaziologische Untersuchung von Eisbohrkernen des Filchner-Ronne-Schelfeises, Antarktis: Bestimmung der Tiefenverteilung und der Kontinentaleffekte ionischer Aerosolkomponenten*. PhD-Thesis, Institut für Umweltphysik der Universität Heidelberg, 219p.

Mylona, S., 1993. *Trends of sulfur dioxide emissions, air concentrations, and deposition of sulfur in Europe since 1880.* EMEP/MSC-W Rep. 2/93, Meteorol. Syn. Cent.-West, Norw. Meteorol. Inst., Oslo, 35p.

Mylona, S., 1996. Sulphur dioxide emissions in Europe 1880-1991 and their effect on sulphur concentrations and deposition. *Tellus* **48**, 662-689.

Neftel, A., Beer, J., Oeschger, H., Zurcher, H. and Finkel, F., 1985. Sulphate and nitrate concentrations in snow from south Greenland 1895-1978. *Nature* **314**, 611-613.

Norton, R.B., 1985. Measurements of formate and acetate in precipitation at Niwot Ridge and Boulder, Colorado. *Geophys. Res. Lett.* **12**, 769-772.

Pain, B.F., Van der Weerden, T.J., Chambers, B.J., Phillips, V.R. and Jarvis, S.C., 1998. A new inventory for ammonia emissions from U.K. agriculture. *Atmos. Environ*. **32**, 309-313.

Preunkert, S., 1994. *Glazio-chemische Verhältnisse des Colle Gnifetti im Vergleich zu seiner regionalen Umgebung*. MS-Thesis, Institut für Umweltphysik der Universität Heidelberg, 88p.

Preunkert, S. and Wagenbach, D., 1998. An automatic recorder for air/firn transfer studies of chemical aerosol species at remote glacier sites. *Atmos. Environ*. **32**, 4021-4030.

Puxbaum, H., Rosenberg, C., Gregori, M., Lanzerstorfer, C., Ober, E. and Winiwarter, W., 1988. Atmospheric concentrations of formic and acetic acid and related compounds in eastern and northern Austria. *Atmos. Environ*. **22**, 2841-2850.

Puxbaum, H., Haumer, G., Moser, K. and Ellinger, R., 1993. Seasonal variation of HNO_3, HCl, SO_2, NH_3 and particulate matter at a rural site in northeastern Austria (Wolkersdorf, 240 m asl). *Atmos. Environ*. **27A**, 2445-2447.

Sanhueza, E., Elbert, W., Randon, A., Arias, M.C. and Hermoso, M. (1989). Organic and inorganic acids in rain from a remote site of the Venezuelan savanna. *Tellus* **41B**, 170-176.

Savarino, J. and Legrand, M., 1998. High northern latitude forest fires and vegetation emisions over the last millennium inferred from the chemistry of a central Greenland ice core. *J. Geophys. Res*. **103**, 8267-8279.

Schäfer, J., 1995. *Rekonstruktion bio-geochemischer Spurenstoffkreisläufe anhand eines alpinen Eisbohrkerns*. MS-Thesis, Institut für Umweltphysik der Universität Heidelberg, 105p.

Schajor, R., 1993. *Zeitliche Entwicklung der Schwermetallkonznetration in hochalpinen Niederschlägen (Monte rosa Masiv, Schweiz).* MS-Thesis, Institut für Umweltphysik der Universität Heidelberg, 105p.

Schwartz, S.E., 1984. Gas-aqueous reactions of sulfur and nitrogen oxides in liquid water clouds. In: *SO_2, NO and NO_2 Oxidation Mechanisms: Atmospheric Considerations* (ed. J.G. Calvert). Butterworth Stoneham, Mass., 173-208.

Schwikowski, M., Döscher, A., Gäggeler, H.W. and Schotterer, U., 1999a. Anthropogenic versus natural sources of atmospheric sulphate from an alpine ice core. *Tellus* **51**, 938-951.

Schwikowski, M., Bruetsch, S., Gäggeler, H.W. and Schotterer, U., 1999b. A high-resolution air chemistry record from an Alpine ice core: Fiescherhorn glacier, Swiss Alps. *J. Geophys. Res.* **104**, 13709-13719.

Seinfeld, J.H., 1986. *Atmospheric Chemistry and Physics of Air Pollution*. Wiley, New York.

Simeonov, V., Puxbaum, H., Tsakovski, S., Sarbu, C. and Kalina, M., 1999. Classification and receptor modeling of wet precipitation data from central Austria (1984-1993). *Environmetrics* **19**, 137-152.

Sempéré, R. and Kawamura, R., 1994. Comparative distribution of dicarboxylic acids and related polar compounds in snow, rain, and aerosols from urban atmosphere. *Atmos. Environ*. **28**, 449-459.

Servant, J., Kouadio, G., Gros, B. and Delmas, R., 1991. Carboxylic monoacids in the air of Mayombe forest (Congo): Role of the forest as a source or sink. *J. Atmos. Chem.* **12**, 367-380.

Simpson, D., Olendrzynski, K., Semb, A., Storen, E. and Unger, S., 1997. Photochemical oxidant modelling in Europe: multi-annual modelling and source-receptor relationships. EMEP/MSC-W Rep. 3/97, Meteorol. Syn. Cent.-West, Norw. Meteorol. Inst., Oslo, 55p.

Simpson, D. and 16 others, 1999. Inventorying emissions from nature in Europe. *J. Geophys. Res.* **104**, 8113-8152.

Skiba, U., Fowler, D. and Smith, K.A., 1997. Nitric oxide emissions from agricultural soils in temperate and tropical climates: Sources, controls and mitigation options. *Nutr. Cycling Agroecosys.* **48**, 139-153.

Stumm, W. and Morgan, J.J, 1970. *Aquatic Chemistry*. Wiley Interscience, New York, 583p.

Su, F., Calvert, J.G. and Shaw, J.H., 1980. An FTIR spectroscopic study of the ozone ethene reaction mechanism in O_2-rich mixtures. *J. phys. Chem*. **84**, 239-246.

Talbot, R.W., Harriss, R.C., Browell, E.V., Gregory, G.L., Sebacher, D.I. and Beck, S.M., 1986. Distribution and geochemistry of aerosols in the tropical North Atlantic troposphere: Relationship to saharan dust *J. Geophys. Res.* **91**, 5173-5182.

Talbot, R.W., Beecher, K.M., Harris, R.C. and Cofer, W.R., 1988. Atmospheric geochemistry of formic and acetic acids at a mid-latitude temperate site. *J. Geophys. Res*. **93**, 1638-1652.

Talbot, R.W., Andreae, M.O., Barresheim, H., Jacob, D.J. and Beecher, K.M., 1990. Sources and sinks of formic, acetic, and pyruvic acids over Central Amazonia: 2. Wet seson. *J. Geophys. Res*. **95**, 16799-16811.

Talbot, R.W., Vijgen, A.S. and Harris, R.C., 1992. Soluble species in the Arctic summer troposphere: Acidic gases, aerosols, and precipitation. *J. Geophys. Res*. **97**, 16531-16543.

Thompson , L.G., Xiaoling, W., Mosley-Thompson, E. and Zichu, X., 1988. Climatic records from the Dunde Ice Cap, China. *Ann. of Glaciol.* **10**, 178-182.

Thompson, L.G., Mosley-Thompson, E., Davis, M.E., Lin, P.N., Mikhalenko, V. and Dai, J., 1995a. A 1000 year ice core climate record from the Guliya Ice Cap, China and its relationship to global climate variability. *Ann. of Glaciol.* **21**, 175-181.

Thompson, L.G., Mosley-Thompson, E., Davis, M.E., Lin, P.N., Henderson, K.A., Cole-Dai, J., Bolzan, J.F. and Liu, K.B., 1995b. Late glacial stage and holocene tropical ice core records from Huascaran, Peru. *Science* **269**, 46-50.

Van de Velde, K., 1999. *Les neiges et glaces de haute altitude des Alpes archives de lèhitoire de la pollution atmospherique en metaux lourds en Europe au cours des deux dernier siecles*. PhD-Thesis, Laboratoire de Glaciologie et Géophysique de L'Environnement, University Joseph Fourier, Grenoble 1, 270p.

Van der Hoek, K.W., 1998. Estimating ammonia emission factors in Europe: summary of the work of the UNECE ammonia expert panel. *Atmos. Environ*. **32**, 315-316.

Vautard, R., Yiou, P. and Ghil, M., 1992. Singular spectrum analysis: A toolkit for short, noisy, chaotic signals. *Physica* **58**, 95-126.

Vincent, C., Vallon, M., Pinglot, F., Funk, M. and Reynaud, L., 1997. Snow accumulation and ice flow at Dôme du Goûter (4300 m), Mont Blanc, French Alps. *J. Glaciol*. **43**, 513-521.

Wagenbach, D., Münnich, K.O., Schotterer, U. and Oeschger, H., 1988. The anthropogenic impact on snow chemistry at Colle Gnifetti, Swiss Alps. *Ann. of Glaciol.* **10**, 183-187.

Wagenbach, D., 1989. Environmental records in alpine glaciers. In: *The environmental record in glaciers and ice sheets* (ed. H. Oeschger and C.C. Langway). Dahlem Konferenzen, John Wiley and Sons, Chichester, 69-83.

Wagenbach, D., 1993a. Special problems of mid latitude glacier ice core research. In: *Proceedings of the ESF/EPC workshop: Greenhouse gases, isotopes and trace elements in glaciers as climatic evidence for Holocene time* (ed. W. Haeberli and B. Stauffer). Report of the ESF/EPC Workshop, Zürich 27.-28.10.1992, Arbeitsheft Nr. 14, VAW-ETH-Zürich, 10-14.

Wagenbach, D., 1993b. Results from the Colle Gnifetti ice-core programme. In: *Proceedings of the ESF/EPC workshop: Greenhouse gases, isotopes and trace elements in glaciers as climatic evidence for Holocene time* (ed. W. Haeberli and B. Stauffer). Report of the ESF/EPC Workshop, Zürich 27.-28.10.1992, Arbeitsheft Nr. 14, VAW-ETH-Zürich, 19-22.

Wagenbach, D. and Preunkert, S., 1996. The History of European Pollution Recorded in Alpine Ice Cores. In: *Proceedings of the EUROTRAC Symposium 1996, G.-Partenkirchen* (ed. P.M. Borell et al.). Computational Mechanics Publications, Southampton, 273-281.

Wagenbach, D., Preunkert, S., Schaefer, J., Jung, W. and Tomadin, L., 1996. Northward transport of Saharan dust recorded in a deep Alpine ice core. In: *The impact of African dust across the Mediterranean* (ed. S. Guerzoni and R. Chester). Kluwer Academic Publishers, The Neetherlands, 291-300.

Wagman, D.D, Evans, W.H., Parker, V.B., Halow, I., Bailey, S.M. and Schumm, R.H., 1965. Selected values of chemical thermodynamic properties. *NBS Tech. Note* **207-3**, Natl. Inst of Stand. and Technol., Gaithersburg, Md.

Wåhlin, P., 1996. One year's continuous aerosol sampling at Summit in central Greenland. In *Chemical Exchange Between the Atmosphere and Polar Snow* (ed. E.W. Wolff and R.C. Bales). Springer, New York, 131-143.

Warneck, P., 1986. The equilibrium distribution of atmospheric gases between the two phases of liquid water clouds. In: *Chemistry of Multiphase Atmospheric Systems* (ed. W. Jaeschke). Springer-Verlag, New York, 473-499.

Warneck, P., 1988. *Chemisrty of the natural atmosphere*. Vol. 41 in *International Geophysics Series*. Academic press, inc., San Diego, 753p.

Winiwarter, W., Puxbaum, H., Fuzzi, S., Facchini, M.C., Orsi, G., Beltz, N., Enderle, K. and Jaeschke, W., 1988. Organic acid gas and liquid phase measurements in Po valley Fall-Winter conditions in the presence of fog. *Tellus* **40B**, 348-357.

Pergamon

Annex1

Atmospheric Environment Vol. 32, No. 23, pp. 4021–4030, 1998

Printed in Great Britain

PII: S1352–2310(97)00146–5

1352–2310/98 $19.00 + 0.00

AN AUTOMATIC RECORDER FOR AIR/FIRN TRANSFER STUDIES OF CHEMICAL AEROSOL SPECIES AT REMOTE GLACIER SITES

SUSANNE PREUNKERT and DIETMAR WAGENBACH

Institut für Umweltphysik, University of Heidelberg

(*First received* 30 *May* 1996 *and in final form* 26 *March* 1997. *Published September* 1998)

Abstract—In order to gain year round information on the relationship between major ions in atmospheric aerosol and deposited snow at ice core drill sites, an automatic station for filter pack sampling and for monitoring of snow height changes by vertical temperature profile readings was developed. The station was deployed for two years at a high elevation ice core drill site in the Alps (Colle Gnifetti, 4450 m asl) and thoroughly tested during several unattended campaigns for its long term reliability. Both devices showed a good long-term field performance, despite harsh environmental conditions, with the exception of data logger break downs induced by strong thunderstorms. Snow height evaluations from the vertical temperature profiles and their temporal changes provided a depth resolution of less than 5 cm and agreed well with concurrent readings from an ultra-sonic distance meter. Measurement of major ions in the autonomously sampled filter packs revealed (1) enhanced field blanks for nearly all species but no important increase of the NH_4^+ to SO_4^{2-} ratio during storage of exposed filters, (2) a nearly complete remobilisation of NO_3^-, Cl^- and Br^- from the front quartz filters and (3) a sufficiently large retention of gaseous NO_3^-, Cl^- and Br^- species on the back up nylon filters to allow quantification of the total concentration of these ions. Except for Na^+, K^+ and Mg^{2+} the (field blank controlled) detection limits allowed to evaluate year round atmospheric concentrations although mid-winter levels have been as low as in central Greenland during summer. The pattern and summer–winter means of atmospheric concentrations were found to be consistent with year round observations performed at a lower Alpine site as well as with the chemical snow properties at Colle Gnifetti.

1. INTRODUCTION

Permanent snow fields constitute vast natural receptacles for atmospheric aerosol particles and associated precursor gases. Provided that they are situated in the "dry snow zone", the glacier masses successively formed from them may thus provide a genuine archive of past air chemical changes. Until now, several ice core studies performed at polar ice sheets (Oeschger and Langway, 1989; Delmas, 1995) and in a few cases also on non-temperated mountain glaciers (Wagenbach, 1989) have revealed important glacio-chemical changes over various time scales.

Presently, one of the most crucial shortcomings of these studies concern the interpretation of the chemical ice core signals in terms of the corresponding change in the local atmospheric loads (Bales and Wolff, 1996). For example, the interannual and even the interdecadal variability of mayor ions (Mayewski *et al*., 1986) and other particulate species observed in ice cores is generally much larger than what might be expected for the respective mean atmospheric levels. Furthermore, very strong seasonal cycles of chemical aerosol components prevail at both, polar and mid-latitudinal glacier sites (Dams and De Jonge, 1976; Mosher *et al*., 1993; Wagenbach, 1996) which, in conjunction with a possible seasonality of the net snow accumulation, may severely bias the net atmospheric information of glacio-chemical ice core records (Wagenbach, 1993a; Dibb, 1996).

Therefore, year round observations at the relevant ice core drill sites are urgently needed, to establish an empirical relationship between the variability of atmospheric loads and the resulting chemical firn stratigraphy. However, due to logistical constraints such information is presently only available through the DGASP campaign (Jaffrezo and Davidson, 1993) at Dye 3 (South Greenland) and, limited to the summer season, for the central Greenland position Summit (Jaffrezo *et al*., 1995). At the latter site, weekly year round records on the elemental aerosol composition are actually recovered by an automatic striker sampler (Heidam *et al*., 1993). PIXE-analyses applied here provide, however, only semiquantitative results on Cl and Na, no information on nitrogen species and no speciation of sulphur components.

We attempted to partly overcome this information lack by developing an automatic field station which is

able to collect aerosol samples on filters for subsequent major ion analyses and to faithfully record the snow pack evolution unattended throughout the year. Here, we describe the technical design of this station along with the principal field experience gained so far from deploying the prototype device at the Alpine ice core drill site Colle Gnifetti (CG).

2. TECHNICAL DESIGN

2.1. *System requirements*

The collection of aerosol samples should allow to establish a quasi-continuous record of major ion species commonly measured in ice cores. This means that also gas phase nitric acid, which may contribute significantly to the total nitrate deposited onto remote glaciers (Legrand and Kirchner, 1990) and may partly evaporate from inert aerosol filters (Zhang and McMurry, 1992) has to be collected as well. A maximum sampling interval of 1 month appears appropriate, since reworking of the snow surface limits the time resolution of chemical firn profiles generally to 1–2 months at best. Furthermore, the strong seasonal aerosol cycle observed at polar (Wagenbach *et al.*, 1988) and mountain (Baltensperger *et al.*, 1991) glacier sites may still be resolved by consecutive monthly means.

The automatic monitoring of snow height changes is primarily aimed to recognize events leading to a substantial net snow accumulation, which remained ultimately preserved. In this way, the monitor is primarily used as a dating tool, to elucidate the approximate deposition date of firn samples, subsequently recovered from a nearby snow pit. Daily readings with a depth resolution of several cm (which is in the range of the surface undulation shown by small sastrugies) is believed to be sufficient for this purpose. Employing the automatic station at ice core drill sites would require unattended runnings over up to nine months in an extremely harsh environment. Thus the station design outlined below was based mainly on the following technical demands:

- reduction of the energy consumption and the oversnow equipment,
- protection against heavy accretion of supercooled cloud droplets, internal water vapour condensation and high snow creeping rates,
- appropriate long-term performance of air pumps, flow meter and data memory,
- long-term preservation of aerosol samples and blank substrates,
- low-temperature working range of all delicate parts.

2.2. *Aerosol collection device*

The concept of the aerosol sampling system (outlined in Fig. 1) is essentially based on the use of multiple units, each consisting of an inline filter holder and a small air pump. As the pumps are consecutively activated for a (constant) preselected sampling time, the risk of a total system break down by failure of a central pump unit is greatly reduced. Furthermore, the use of troublesome (and energy consuming) magnetic valves can be avoided here. In order to reduce particle losses and water vapour condensation in the sampling lines, the housing of the filterholders was arranged close to the air intake head, which was mounted on the top of a rugged tripod (Fig. 1).

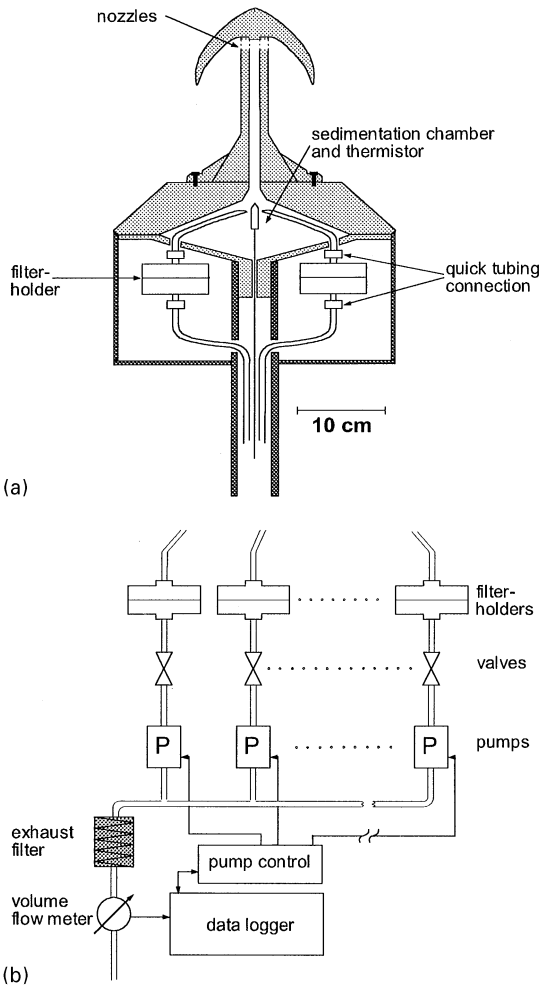

Fig. 1. Design of the sampling head (a) and the arrangement of filter pack units (b) of the automatic aerosol sampler.

In the present version, air is sucked through an all-PTFE sampling head into a 1 ℓ chamber serving as sedimentation sink for ice crystals and cloud droplets. The chamber is connected via 8 cm Teflon tubings (inner diameter 7 mm) to ten individual aerosol sampling units. Each unit consists of a 47 mm inline filter holder equipped with quick tubing connections, a miniature vacuum pump and a (one way) valve. The pump was found to be the most critical component in view of its reliable long term performance at low temperatures. After extensive testings we selected

a carbon vane pump (Brey, FRG, 2.4 ℓ min^{-1}, maximum pressure difference 160 mbar) which is driven by an electronically commutated 12 V DC motor. For the central flow meter, we found a micro processor controlled vane wheel sensor (Höntzsch, FRG) most suitable. Calibration of this volumetric flow meter was performed in the field through a constant air flow provided by a pressurized air tank which was accurately weighted before and after the calibration procedure. To protect the flow meter from the carbon particle exhaust of the pumps, a large area exhaust filter capsule was used. For this *single flow meter configuration* one-way valves are needed for each sampling unit to avoid any inverse by-pass flow through the stand by aerosol filters. For this purpose a pneumatic valve (Fürgut, FRG) being already activated at a pressure drop of 2 mbar turned out to be well suited. A specifically rugged pump control was accomplished via a programmable data logger (Datataker, Australia), transmitting a 5 V initializing pulse to an electro-mechanical counting switch. This arrangement was found to be much more insensitive towards malfunctions by static electricity than a more sophisticated electronic timer/counter device.

The flow rate was recorded regularly at 1 h intervals along with the pump current, the latter serving as surrogate flow information in case of a flow meter break down. Using a quartz filter, followed by a nylon membrane filter as sampling substrates (see Section 3.3), a typical flow rate of 2 ℓ STP min^{-1} is achieved. The total energy consumption then amounts to 5 W (pump 3 W, flow meter 0.6 W, and data logger 1.3 W). If data acquisition is performed non-continuously the overall power supply may be reduced to slightly more than 3 W. For application at mid-latitude glaciers we installed a 50 W solar panel backed up with a 100 Ah buffer battery to ensure continuous sampling.

Negative sampling artefacts of supra-micron aerosol particles arising from anisokinetic sampling and losses inside the device are difficult to assess under realistic field conditions. The effect of particle settling within the sedimentation chamber may be roughly estimated, however, from the chamber dimensions, the volume flow rate and from the particle settling velocity by

$$\frac{c_{\text{out}}}{c_{\text{a}}} = \frac{\tau_{\text{s}}}{\tau_{\text{s}} + \tau_{\text{a}}}$$

(c_{out} and c_{a} denote the particle concentration in the chamber out flow and ambient air, respectively, τ_{a} the air residence time in the chamber, and τ_{s} the particle live time against sedimentation). At our flow rate, for example, 20% of 2.5 μm particles (i.e. the mass mean diameter (MMD) of mineral dust aerosol at Colle Gnifetti (Wagenbach and Geis, 1989)) would be lost by internal sedimentation, whereas 4.5 μm particles (i.e. the MMD of long-range transported desert dust at this site) would be decreased by 40%. Similar results were obtained in the laboratory by optical particle counter readings showing a 60% depletion of particles larger than 5 μm. In view of additional losses arising from particle impacting on external surfaces at the air intake in the case of high wind speeds, the above numbers may be regarded as lower limits. We expected, therefore, that the large particle aerosol fraction made up by mineral dust, sea salt and associated nitrate is systematically underestimated by the automatic sampling station (which would be important for alpine and coastal Antarctic sites only). Using an inertial preseperator (i.e. impactor stage) to achieve a better defined sampling cut off is not applicable here because much powerful pumps would be required.

2.3. *Snow height monitor*

Our preferred technique to record snow height changes at remote glacier sites is based on regular readings of the vertical temperature profile taken across the snow/air interface. The actual snow surface is expected to be marked in the individual profiles by the position of a significant temperature gradient. Alternatively, readings which were accumulated over a time interval, may be inspected for a strong decrease in the temporal variability to identify those sensors sitting below the snow/air interface. The advantage of these relatively simple methods over the commonly used ultra-sonic echo sounding (Gubler, 1981) is their minimal energy consumption and the fact, that no delicate electronic devices need to be installed above the snow surface. A further aspect to promote the temperature profiling method here, arises from the perspective to additionally gain seasonal records of the temperature gradient developed in the surface snow layer. Among others, this key parameter driving the diffusional energy and mass transfer within the snow pack (Giddings and LaChapelle, 1962) may possibly give some hints on periods showing a high probability for substantial frost deposition, sublimation loss or depth hoar formation.

For the temperature readings we used a series of 19 thermistors (PT-100) fixed on a massive, white polyethylene rod (see Fig. 2). According to the deployment on a high elevation Alpine glacier, spacing of the temperature probes was chosen to be 10 cm. The sensors are alternately connected to two programmable data loggers, equipped with memory cards (serving as a data back up). This arrangement ensures that after the failure of one logger unit, double spaced profiles may still be recovered. In order to profit from the strong diurnal temperature cycle, particularly prevailing on mid-latitude glaciers (radiative cooling during night, insolation induced warming of the overs snow sensors) daily data acquisition was set at midnight and noon. To assess the reliability of the inferred snow heights we also deployed the conventional ultrasonic reflection method. These supplementary measurements were performed concurrently to the temperature readings using a commercially available distance meter (Grieshaber, Switzerland). This particularly selected type is specified for a temperature

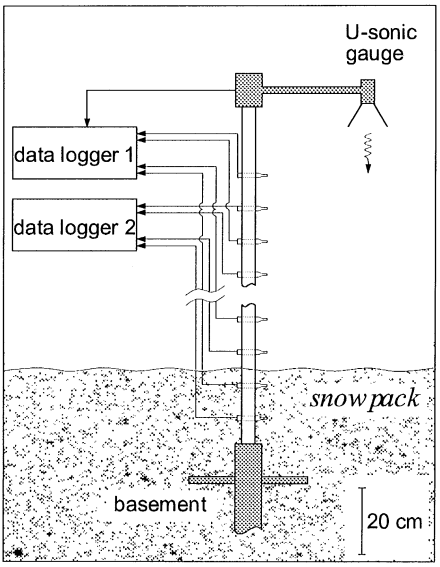

Fig. 2. Principle assembly of the snow height gauges (fixation by the tripod not shown).

working range down to $-30°C$ due to its transmitter/receiver system being equipped with a metal rather than a polymer membrane. In order to minimize the possibility of misreading arising from weak reflection signals during high wind speed or soft surface snow conditions, a stainless-steel cone was fixed in front of the transmitter/receiver unit. Since data acquisition and running of the ultrasonic gauge was activated only twice a day for several seconds, the average daily energy consumption of the system is very low (4.2 mW for ultrasonic gauge and 3.6 mW for each data logger unit).

3. FIELD EXPERIENCE

3.1. *Test site*

The first application of the automatic station was accomplished on a high elevation Alpine firn saddle (Colle Gnifetti, 4450 m asl), which we are using extensively for recovering several ice cores drilled to bed rock (Wagenbach *et al.*, 1985; Wagenbach, 1993b, 1996). This extremely exposed hanging glacier is characterized by the following glacio-meteorological conditions (mainly derived from our automatic weather station operated there):

- 10 m firn temperature $-14.5°C$ (Haeberli and Funk, 1991),
- net annual snow accumulation range: 20–80 cm water equivalent (w.e.),
- daily mean air temperature extremes -5 to $-35°C$,
- hourly wind speed maximum of 25 m s^{-1}

For specific reasons we separated the aerosol collection unit from the snow height gauges and installed the latter on a tripod in the northern sattle slope at the position of a deep drill hole (annual snow accumulation: 15–30 cm w.e.), while the solar panel powered aerosol sampling device was positioned in the south slope of the saddle.

3.2. *Snow height monitor*

Technical inspections of the snow gauges after unattended runnings over one to eight months revealed that the only serious malfunction has been regular breakdowns of one or both data logger units induced by the strong lightning activity at the CG site (see also following section). We realized, however, no signs of melt water percolation along the whitened rod or mechanical distortion of the thermistor chain by snow creeping or compaction. Note that the total annual precipitation at this site may exceed the annual net snow accumulation of 25 cm w.e. by up to a factor of ten. Evaluation of the air/snow interface by the temperature profiling method was possible from almost all readings. Weak or even disappearing temperature gradients occurred during heavy snow drift events, especially in cases when snow temperature sensors covered only a limited depth (~ 30 cm). As illustrated in Fig. 3, no dramatic difference in the distinctness of the gradient signals acquired during summer and winter, at noon and midnight or during fair and overcast weather conditions has been found.

Our first approach for the data evaluation is to screen the temperature readings downwards and to place the air/snow interface midway between the first two sensors showing a significant deviation from the mean oversnow temperature. Refining and cross checking of these preliminary results is achieved by inspecting the standard deviation of each sensor derived from several daily readings for a clear, systematic decline (see Fig. 4(a)). Again going downwards, the first sensor exhibiting a significantly damped variability is then placed closely below the air/snow interface. Where possible, combining both methods gives much confidence in the reliability of the results. In view of using the temperature profiling at ice sheet positions, during the polar night, evaluation of the temporal standard deviation records appears to be the preferred method to recognize significant snow height changes. This is illustrated in Fig. 4 by two vertical variance profiles taken at CG from a series of midnight readings and by the temporal changes shown up by selected sensors.

Concurrent daily measurements with the ultrasonic distance meter has been subject to a 12% rate of misreadings due to weak or highly erroneous reflection signals. This rate has to be compared with the 20% of ambiguous evaluations of daily temperature profiles which have led to unsystematic mismatches with the ultrasonically derived surface snow position of maximal ± 10 cm. Also within the clear temperature profile readings we found no systematic deviation from the ultrasonic data (providing a long-term reproducibility of ± 1.3 cm on flat, wind crusted

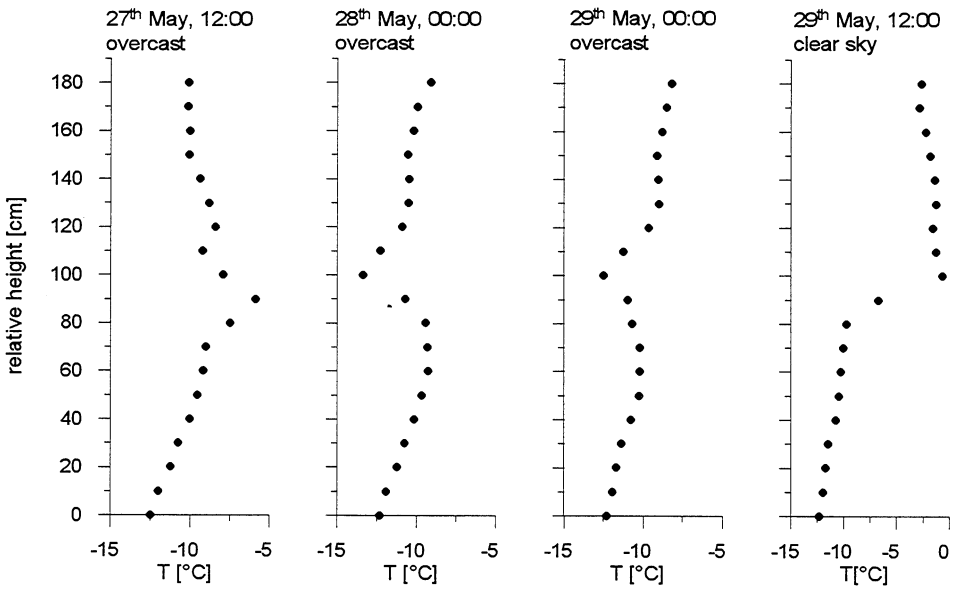

Fig. 3. Vertical temperature profiles consecutively obtained at the end of a bad weather period at C.G. with previous fresh snow accumulation.

snow surfaces) but a surprisingly good agreement of both methods within 5 ± 4 cm. Unfortunately, exceptional high winter snow erosion rates and the lightning induced losses of summer data prevented an immediate comparison of firn impurity records with the concurrent atmospheric observations presented in Section 3.3. We may, however, conclude that the accuracy as well as the depth resolution (less than half the sensor spacing) achieved here are quite sufficient to infer precise dating of (bi)-annual snow pits also in central Greenland and in high snow accumulation areas of Antarctica (particularly if two thermistor chains are installed near by). Regular dispersing of various tracers (Braaten, 1995) would be an attractive alternative to our method if its technical reliability for long-term deployments will be proven. However, as is the case with ultrasonic distance meters, no additional information on the thermal regime near the snow surface (see e.g. Fig. 4b) would be obtained.

3.3. *Aerosol collection device*

For aerosol sampling, we decided to use high-purity quartz fibre filters (Whatman QM-A) due to their low pressure drop compared to Teflon membranes, their high collection efficiency and their less serious sampling artefacts if compared to other fibre filters (Appel *et al.*, 1984; Bardwell *et al.*, 1990). Since a good deal of total atmospheric nitrate was expected to be made up by nitric acid or may be remobilized from the aerosol filter (Goldan *et al.*, 1983; Talbot *et al.*, 1990), a single nylon membrane filter (Gelman, Nylosorb) was placed downstream the quartz filter for the collection of gas-phase nitrate.

Both filter types were thoroughly cleaned in the laboratory by several soakings in deionized (18 MΩ) —water, dried in a clean air stream (free of particles, NH_3, HNO_3, SO_2) and loaded within a laminar hood into the inline filter holders. Sealing of the filter pack was achieved by specially designed Teflon o-rings which reduce the diameter of the exposed filter area to 36 mm. The loaded filter holders were capped and stored in double sealed polyethylene bags until they were exchanged in the field by the exposed ones. The data logger was then programmed to start the sampling procedure on a preselected date (normally after retreat from the site by helicopters) and to leave one filter pack unit unexposed for evaluating the overall blank contributions.

The filter samples were transported back at below 0°C and stored at -20°C until processing for ion chromatography analyses. After discarding the unexposed area, the filters were ultrasonically extracted into 20 ml high purity water. In the case of nylon filters, the extraction solution was adjusted to pH 8 by Na(OH). Subsequent analyses of the solutions for Cl^-, Br^-, NO_3^-, SO_4^{2-}-, NH_4^+, Na^+, K^+, Mg^{2+}, Ca^{2+} were based on our protocol for suppressed (gradient and isocratic) ion chromatography established for alpine and polar snow samples (Minikin *et al.*, 1994; Fischer and Wagenbach, 1996; Wagenbach *et al.*, this issue). Standard matching in the case of alkaline nylon filter extract was found to be not necessary.

The aerosol sampling station has been run unattended over 4 periods, ranging from one to eight months and covering individual collection intervals between 4 and 20 days. These test series proved the excellent reliability of all system components, except the data loggers. The latter had been partly destroyed in several cases by the strong lightning activities regularly occurring during mid summer at Colle Gnifetti.

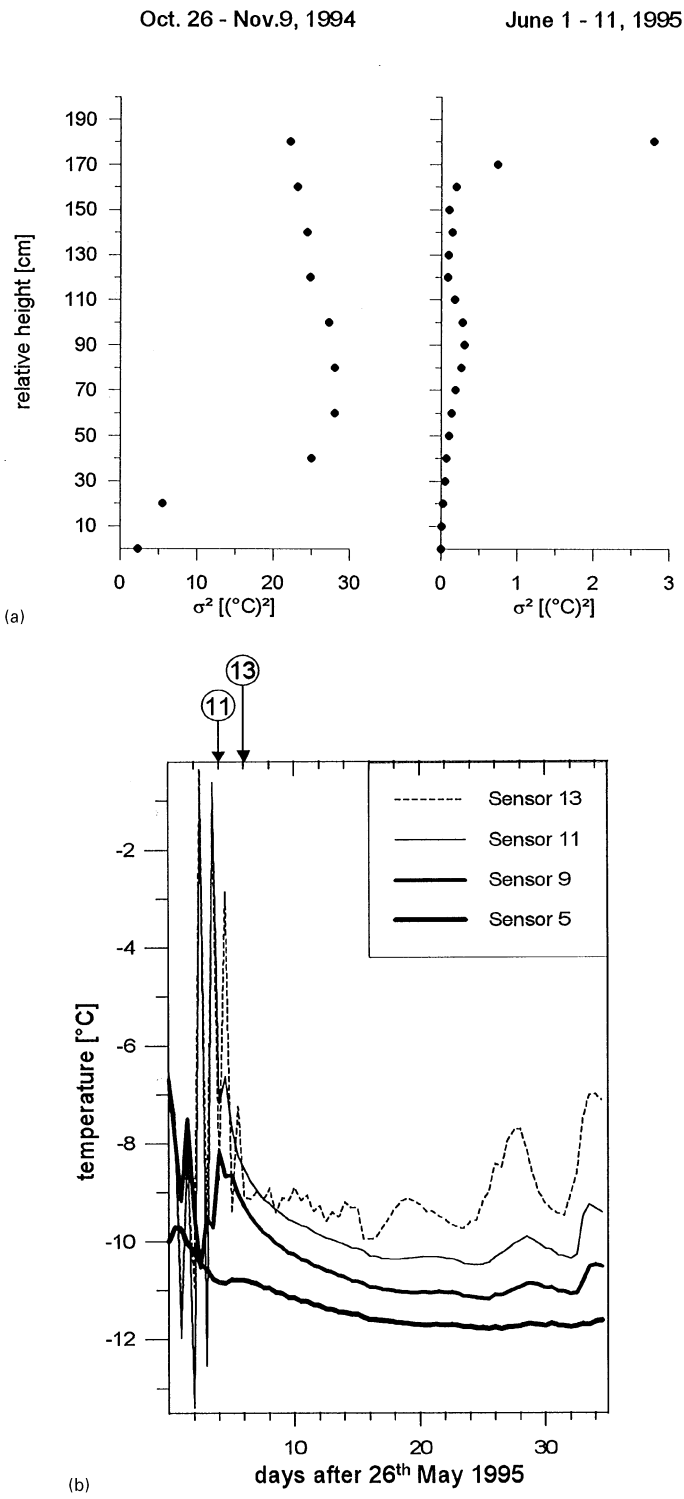

Fig. 4. (a) Vertical profiles of the temperature variance taken during midnight over 15 and 10 days, respectively, (b) temperature records of selected sensors (with No. 13 the uppermost one) recorded over a period with significant accumulation during the first 6 days. Arrows and numbers indicate the date when the respective sensors submerged.

The atmospheric electricity pulses were obviously guided by the lines connecting the multiplexer unit to the external wind and insolation sensors. In one case, static electricity presumably build up by strong snow drift, may have been responsible for the logger malfunction. Since there is no access to ground potential

Table 1. Mean field filter blanks with standard deviation SD and their relative enhancement above laboratory filter blanks ($\Delta c/c_F$) derived from 5 sampling campaigns at CG. Detection limits (DL) refer to bi-weekly sampling intervals corresponding to 40 m^3 STP

Species	$C_F \pm$ SD (ng)	$\Delta C/C_F$ (%)	DL (ng m^{-3})
47 mm filter		Quartz	
NO_3^-	270 ± 120	52	5
SO_4^{2-}	240 ± 190	65	8
NH_4^+	440 ± 290	42	13
Cl^-	100 ± 110	50	5
Na^+	2000 ± 590	1.3	26
Ca^{2+}	220 ± 59	6	3
Mg^{2+}	41 ± 16	33	0.7
K^+	110 ± 120	0	5
Br^-	<10 ± 3	24	< 1.5
47 mm filter		Nylon	
NO_3^-	320 ± 150	51	7
SO_4^{2-}	690 ± 520	78	23
Cl^-	630 ± 540	80	24
Br^-	26 ± 12	57	0.6

on a cold glacier, we tried to accomplish lightning protection by electronic means leading, however, to no substantial improvement in the case of strong thunderstorms. On the other side, inspection of the regular flow rate readings gave no evidence for any irregularities of the pumps, valves or the flow sensor. Apart from an insignificant diurnal cycle of the flow rate (introduced by the solar panel power supply) flow rates of individual sampling units remained essentially constant as was the case with the calibration of the flow sensor. This suggests, that blocking of the air intake or wetting of the aerosol filters did not occur (also, no substantial ice crystal deposits were observed by visual inspections inside the system).

Since all stand by filter packs are not totally separated from ambient air (see Fig. 1), passive sampling may play an important role for the sample preservation and for the amount and variability of the filter blanks. Since the latter generally controls the overall detection limits, a total of 17 blank filter stacks were stored in the automatic station during 5 field runs, lasting 1, 1.5, 4.7 and 8 months, respectively. Grand average field blank values and their typical fraction not linked with the previously cleaned filter matrix are given in Table 1. On the average all species (except Na^+ and Ca^{2+}, *a priori* showing relatively high blank levels) are significantly enhanced over their respective laboratory values. We were unable, however, to derive a conclusive picture on the source apportionment of these blank enhancements (i.e. passive sampling versus random contamination). An univocal increase of the field blanks with the exposure interval was only evident for SO_4^{2-} and NO_3^- of the nylon filters (roughly 270 ± 170 ng and 130 ± 70 ng per month, respectively), whereas in some cases also a slight depletion of Cl^-, NH_4^+ and K^+ was noted for the field blanks. We gained no clear indications about passive sampling by (or losses from) loaded filter packs during storage in the sampler except for NH_4^+. This species is shown by Silvente and Legrand (1993) to be passively accumulated on acidic filter loads leading to erroneously high NH_4^+ to SO_4^{2-} ratios. The molar ratios found at CG are 1.5 ± 0.5 in summer and 0.8 ± 0.3 in winter which corresponds well with the respective ratios in Alpine snow above 4000 m asl (Maupetit *et al.*, 1995; Wagenbach *et al.*, this issue). They are even slightly lower than those observed by Kasper and Puxbaum (1998) at the Alpine Sonnblick Observatory (3050 m asl, Eastern Alps) on daily aerosol samples (see Table 2). At least for NH_4^+ no dramatic storage effect on loaded aerosol filters may be expected, therefore.

The relative detection limits given in Table 1 were estimated from three times of the blank variability and refer to a collection period of two weeks (40 m^3 STP). Since they also include the variability between different sampling campaigns (i.e. different filter

Table 2. Mean summer (May–August 1993–1994) and mid-winter (December–February 1994/1995) concentrations derived from automatic aerosol collection at CG (summer means of previous atmospheric observation (Wagenbach *et al.*, 1985) in parentheses) as well as representative seasonal snow impurity levels at CG and atmospheric data (1991–1993) from the Sonnblick Observatory (Kasper *et al.*, 1998)

	Colle Gnifetti (4450 m asl)				Sonnblick (3106 m asl)	
	Air (ng m^{-3} STP)		Snow (ng g^{-1})		Air (ng m^{-3} STP)	
Species	Summer	Winter	Summer	Winter	Summer	Winter
SO_4^{2-}	630 (1000)	110	360	120	2400	290
part. NO_3^-	26 (–)	6	—	—	410	35
total NO_3^-	420 (330)	83	190	120	750	150
NH_4^+	180 (–)	20	90	10	730	68
total Cl^-	86 (–)	19	45	11	—	—
Na^+	26 (25)*	<15	30	10	—	—
Ca^{2+}	37 (24)*	4.3	130	37	—	
total Br^-†	6.6 (1.5*)	1.2	—	—	—	—

† Tentative values.
* Total element concentrations.

batches and processings) somewhat lower limits were achieved during individual campaigns. The sensitivity of the present device (referring to total concentrations in the case of NO_3^-, Cl^- and Br^-) was well above the pollution levels prevailing at CG except during the mid-winter season where K^+, Mg^{2+} and Na^+ could not be quantified.

Exposed filters showed virtually no chloride on the quartz but significant net amounts on all nylon filters. The same behaviour was found for Br^-. Also particulate nitrate appears to be relatively low on the quartz filter and contributes on the average only 6% to total nitrate. The strong mobilization of halogen and particulate nitrate species (as HNO_3, HCl and HBr) from the front aerosol filter may be possibly favoured by the long collection times associated with the relatively low filter face velocity of 5 cm s^{-1} (Goldan *et al.*, 1983). On nylon filters we found in addition to nitrate, chloride and bromide a minor fraction of sulphate presumably collected as SO_2 (Cadle and Mulawa, 1987), and, surprisingly, in few cases also some ammonium. A break through test performed at a five fold higher flow rate (10 ℓ min^{-1}) in the field with a double nylon filter pack (open face) revealed that 90 and close to 100% of Cl^- and NO_3^-, respectively, but less than 70% of SO_2 and Br^- was retained on the first nylon filter (36 h sampling of 20 m^3 under stormy and foggy conditions). Along with this test, four filter packs of the automatic station (already stored for 1 month in the device) were loaded concurrently by 4 m^3 STP. Where possible, comparison of these results with the open face sampling system showed excellent agreement for sulphate, a 30% deficit for total nitrate (presumably due to losses at internal surfaces not yet equilibrated with ambient HNO_3) and a surplus of 85% for (total) chloride and 68% for ammonium (the latter two findings are hard to assess in view of the relatively large blank contribution involved here). The 36 h samplings showed NO_3^- to HNO_3 ratios of 0.4 to 0.5, which are far above those we obtained from all other (long-term) collections. This suggests that the strong, negative NO_3^- artefacts seen otherwise are mainly due to the relatively long sampling times of up to three weeks (similar findings are obtained for Br^- and Cl^-). Concerning the typical time scale of more than one month relevant in ice core related air to snow transfer studies the total concentrations of NO_3^-, Cl^- and Br^- obtained here are sufficient, however, in depicting an effective air to snow concentration ratio.

Four successful sampling campaigns were evaluated for all particulate species found on the quartz filters as well as for total nitrate, total chloride and total bromide (sum of quartz and nylon nitrate). Due to the highly uncertain and variable SO_2 collection efficiency of nylon filters (Chan *et al.*, 1986) no quantification was made here. Figure 5 illustrates the evolution of sulphate, total nitrate and ammonium in the course of the summer half-year 1994 in comparison with the respective mean winter level in

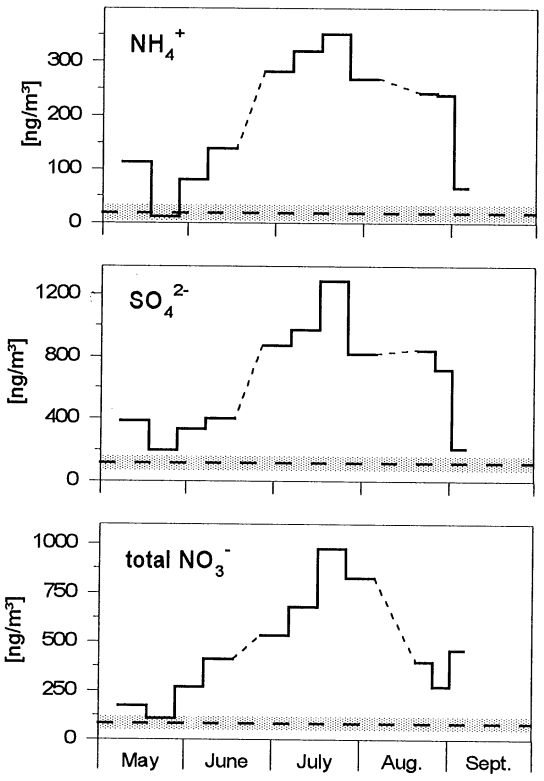

Fig. 5. Seasonal pattern of NH_4^+, SO_4^{2-} and total nitrate observed at CG during summer 1994. Dashed horizontal lines and shaded area denotes the mean levels and ranges, respectively, obtained by three-weekly samplings during the subsequent mid winter period.

1994/1995. The seasonal pattern as well as the summer/winter contrast *quantitatively* agree with the seasonally changing snow chemistry at high Alpine sites (Table 2; Maupetit *et al.*, 1995; Wagenbach *et al.*, this issue), but also with the multi-years epiphaniometer readings (a surrogate for the sub-micron aerosol surface concentration) performed by baltensberger *et al.* (1991) at the Jungfraujoch Observatory (3454 m asl, Western Alps).

Presently, the only reliable, year round records of chemical aerosol (and associated precursor gases) from a high Alpine site are those obtained by Kasper and Puxbaum (this issue) via multi-stage filter sampling at the Sonnblick observatory (SBO). For quantitative comparison, mean winter and summer levels are compiled for both sites (see Table 2) showing a general tendency towards significantly lower levels at Colle Gnifetti. This may be explained by the 1400 m elevation difference, the increasing atmospheric pollution levels towards the eastern part of the Alps (Puxbaum and Wagenbach, 1994) and possibly by a stronger influence of local contaminants at the Sonnblick station, like tourist activities. Referring to the daily SBO data, particulate nitrate collected over 1–3 weeks by the automatic station at CG appears indeed to be plagued by strong negative sampling artefacts

(see above), allowing to evaluate total nitrate only. Within all species examined total nitrate shows, however, the lowest depletion relative to SBO which suggests no dramatic sampling losses of HNO_3 inside the automatic station.

Further evidence for the reliability of our CG data comes from a series of 20 daily high volume aerosol samplings (open face, Whatman 41 filter) which we performed between May and August 1982 at CG (Wagenbach *et al*., 1985). The mean summer levels obtained here for sulphate, nitrate, the total concentrations of bromine, calcium and sodium are also included in Table 2. The agreement between both data sets is surprisingly good, especially if the changed pollution levels at Colle Gnifetti (Wagenbach *et al*., this issue) and the different filter media used, are taken in account. The summer–winter mean snow impurity concentrations given for comparison in Table 2 are compiled from shallow ice cores drilled at CG, and are supplemented by true mid-winter snow pit samples gathered over 4 years near CG at the 3500–3900 m altitude range (Wagenbach *et al*., 1997). They are quite consistent with the respective atmospheric observation in terms of mean seasonal scavenging ratios observed on other high Alpine sites (Kasper, 1994) providing further evidence for the usefulness of the automatic aerosol sampling device.

Concerning the deployment of the present sampler on drill sites at the polar ice sheets it is worth to note, that the aerosols and trace gases accumulated during two weeks on the filter pack are roughly equivalent to the respective amount contained in 20–80 g of snow. If the typical air (or snow) pollution levels are considered at these sites, the bi-weekly detection limits (referring to total concentrations in the case of NO_3^- and Cl^-) would place the following restrictions on the deployment of the present sampler at ice sheet positions:

Central Greenland (Jaffrezo *et al*., 1995; Silvente and Legrand, 1995; Dibb, 1996): Not to be quantified are crustal species almost throughout the year, sea salt during summer and presumably NH_4^+ as well as total Cl^- during winter.

Coastal Antarctica (Wagenbach, 1996): Not detectable are crustal species throughout the year and NH_4^+ during the austral mid-winter season.

Central Antarctica (Maenhaut and Zoller, 1979; Silvente and Legrand, 1993): Below detection limit are mineral dust components, sea salt and ammonium throughout the year and possibly SO_4^{2-} during the mid-winter season.

However, an improvement of the detection limits in the range of a factor 5–10 may be expected by (1) replacing the quartz- by PTFE-filters leading to much lower blanks (especially for Na^+, Ca^{2+} and K^+) and (2) by brackening each filter pack via two specially designed magnetic valves operating in a flip-flop mode and thus consuming energy only during the switching phase. The latter development would greatly reduce the potential shortcomings with passive pre- or post-sampling effects as well. Provided that the actual field blank levels for major ions are decreased by a factor of five, year round observation on a bi-weekly basis would be possible at ice sheet positions in both hemispheres for all species (presumably, except for NH_4^+ in Central Antarctica).

Acknowledgements—This work is a contribution to the EUROTRAC subproject ALPTRAC and was funded by the German Ministry for Education and Research. We thank N. Beck and K. Geis for their commitment during many pilot investigations as well as H.G. Junghans, R. Fletterer and the work shop staff of the institute for invaluable help in constructing the device. We particularly acknowledge the logistical support provided by the Club Alpino Italiano, Air Zermatt and the Meteorological Observatory Locarno.

REFERENCES

Appel, B. R., Tokiwa, Y., Haik, M. and Kothny, E. L. (1984) Artifact particulate sulphate and nitrate formation on filter media. *Atmospheric Environment* **18**, 409–416.

Bales, R. C. and Wolff, E. W. (1995) Interpreting natural climate signals in ice cores. *Eos* **76**, 477,482–483.

Baltensperger, U., Gäggeler, H. W., Jost, D. T., Emenegger, M. and Nägeli, W. (1991) Continous background aerosol monitoring with the Epiphaniometer. *Atmospheric Environment* **25A**, 629–634.

Bardwell, C. A., Maben, J. R., Hurt, J. A., Keene, W. C., Galloway, J. N., Boatman, J. F. and Wellman, D. L. (1990) A technique using high-flow, dichotomous filter packs for measuring major atmospheric chemical constituents. *Global Biogeochemical Cycles* **4**, 151–163.

Braaten, D. A. (1995) A new technique to provide high time resolution snowpack dating for stratigraphy and chemistry assessments. *Atmospheric Environment* **29**, 2535–2539.

Cadle, S. H. and Mulawa, P. A. (1987) The retention of SO_2 by nylon filters. *Atmospheric Environment* **21**, 599–603.

Chan, W. H., Orr, D. B. and Chung, D. H. S. (1986) An evaluation of artifact SO_4^{2-} formation on nylon filters under field conditions. *Atmospheric Environment* **20**, 2397–2401.

Dams, R. and De Jonge, J. (1976) Chemical composition of Swiss aerosol from the Jungfraujoch. *Atmospheric Environment* **10**, 1079–1084.

Delmas, R. J. (ed.) (1995) *Ice Core Studies of Global Biogeochemical Cycles*. NATO-ASI Series, Series I: *Global Environmental Change*, Vol 30, Springer, Berlin.

Dibb, J. E. (1996) Overview of field data on the deposition of aerosol-associated species to the surface snow of polar glaciers (Emphasizing recent work in Greenland). In *NATO ARW Workshop: Process of Chemical Exchange Between the Atmosphere and Polar Snow* (Il Chiocco, Italy 1995), eds. E. Wolff and R. Bales, NATO-ASI Series I: Chemical Exchange Between the Atmosphere and Polar Snow, Vol. 43, pp. 249–274. Springer, Berlin.

Fischer, H. and Wagenbach, D. (1996) Large scale spatial trends in recent firn chemistry along an east-west transect through central Greenland. *Atmospheric Environment* **30**, 3227–3238.

Giddings, J. C. and LaChapelle, E. (1962) The formation rate of depth hoar. *Journal of Geophysical Research* **67**, 2377–2382.

Goldan, P. D., Kuster, W. C., Albritton, L., Fehsenfeld, F. C., Connell, P. S.,Norton, R. B. and Huebert, B. (1983) Calibration and tests of the filter-collection method for measuring clean-air, ambient levels of nitric acid. *Atmospheric Environment* **17**, 1355–1364.

Gubler, H. (1981) An inexpensive remote snow-depth gauge based on ultrasonic wave reflection from the snow surface. *Journal of Glaciology* **27**, 157–163.

Haeberli, W. and Funk, M. (1991) Borehole temperatures at the Colle Gnifetti core-drilling site (Monte Rosa, Swiss Alps). *Journal of Glaciology* **37**, 37–46.

Heidam, N. Z., Wåhlin, P. and Kemp, K. (1993) Arctic aerosols in Greenland. *Atmospheric Environment* **27A**, 3029–3036.

Jaffrezo, J. L. and Davidson, C. I. (1993) The Dye 3 gas and aerosol sampling program (DGASP): An overview. *Atmospheric Environment* **27A,** 2703–2707.

Jaffrezo, J. L., Dibb, J. E., Bales, R. C. and Neftel, A. (1995) Current status of atmospheric studies at summit (Greenland) and implications for further research. In *Ice Core Studies of Global Biogeochemical Cycles*, ed. R. J. Delmas, NATO-ASI Series, Series I: Global Environmental Change, Vol 30, pp. 427–458, Springer, Berlin.

Kasper, A. (1994) Saisonale Trends atmosphärischer Spurenstoffe sowie deren Austauschverhalten an der Hintergrundmeßstelle Hoher Sonnblick. Ph.D. thesis, Technical University of Vienna.

Kasper, A. and Puxbaum, H. (1998) Seasonal variation of SO_2, HNO_3, NH_3 and selected aerosol components at Sonnblick (3106 m asl). *Atmospheric Environment* **32**, 3925–3939.

Legrand, M. R. and Kirchner, S. (1990) Origins and variations of nitrate in south polar precipitation. *Journal of Geophysical Research* **95**, 3493–3507.

Maenhaut, W. and Zoller, W. H. (1979) Determination of the chemical composition of the South Pole aerosol by instrumental neutron activation analysis. *Journal of Radioanalytical Chemistry* **37**, 637–650.

Maupetit, F., Wagenbach, D., Weddeling, P. and Delmas, R. J. (1995) Recent chemical and isotopic properties of high altitude cold Alpine glaciers. *Atmospheric Environment* **29**, 1–9.

Mayewski, P. A., Lyons, W. B., Spencer, M. J., Twickler, M., Dansgaard, W., Koci, B., Davidson, C. I. and Honrath, R. E. (1986) Sulfate and nitrate concentrations from a South Greenland ice core. *Science* **232**, 975–977.

Minikin, A., Wagenbach, D., Graf, W. and Kipfstuhl, J. (1994) Spatial and seasonal variations of the snow chemistry at the central Filchner-Ronne Ice Shelf, Antarctica. *Annals of Glaciology* **20**, 283–290.

Mosher, B. W., Winkler, P. and Jaffrezo, J. L. (1993) Seasonal aerosol chemistry at Dye 3, Greenland. *Atmospheric Environment* **27A**, 2761–2772.

Oeschger, H. and Langway, C. C. eds. (1989), *The Environmental Record in Glaciers and Ice Sheets*. Dahlem Konferenzen. Wiley, Chichester.

Puxbaum, H. and Wagenbach, D. (1994) High alpine precipitation chemistry. In *The Proceedings of EUROTRAC Symposium* 1994, eds. P. M. Borell *et al*., pp. 597–605. SPB Academic Publishing bv, The Hague, The Netherlands.

Silvente, E. and Legrand, M. (1993) Ammonium to sulphate ratio in aerosol and snow of Greenland and Antarctic regions. *Geophysical Research Letters* **20**, 687–690.

Silvente, E. and Legrand, M. (1995) A preliminary study of the air snow relationship for nitric acid in Greenland. In *Ice Core Studies of Global Biogeochemical Cycles*, ed. R. J. Delmas, NATO-ASI Series, Series I: *Global Environmental Change*, Vol. 30, pp. 225–240. Springer, Berlin.

Talbot, R. W., Vijgen, A. S. and Harriss, R. C. (1990) Measuring tropospheric HNO_3: Problems and prospects for nylon filter and mist chamber techniques. *Journal of Geophysical Research* **95**, 7553–7561.

Wagenbach, D. (1989) Environmental records in alpine glaciers. In *The Environmental Record in Glaciers and Ice Sheets*, eds. H. Oeschger, and C. C. Langway, Dahlem Konferenzen, pp. 69–83. Wiley, Chichester.

Wagenbach, D. (1993a) Special problems of mid latitude glacier ice core research. In *Proceedings of the ESF/EPC Workshop*: *Greenhouse Gases*, *Isotopes and Trace Elements in Glaciers as Climatic Evidence for Holocene Time*, eds. W. Haeberli and B. Stauffer, Report of the ESF/EPC Workshop, Zürch 27–28. October 1992, Arbeitsheft Nr. 14, VAW-ETH-Zürich, pp. 10–14.

Wagenbach, D. (1993b) Results from the Colle Gnifetti icecore program, In *Proceedings of the ESF/EPC Workshop*: *Greenhouse Gases*, *Isotopes and Trace Elements in Glaciers as Climatic Evidence for Holocene Time*, eds. W. Haeberli and B. Stauffer, Report of the ESF/EPC Workshop, Zürch 27–28. October 1992, Arbeitsheft Nr. 14, VAW-ETH-Zürich, pp. 19–22.

Wagenbach, D. (1996) Coastal Antarctica: Atmospheric chemical composition and atmospheric transport. In *NATO ARW Workshop*: *Process of chemical exchange between the atmosphere and polar snow* (*Il Chiocco*, *Italy* 1995), eds. E. Wolff and R. Bales, NATO-ASI Series I: Chemical Exchange Between the Atmosphere and Polar Snow, Vol 43, pp. 173–199. Springer, Berlin.

Wagenbach, D., Görlach, U., Haffa, K., Junghans, H. G., Münnich, K. O. and Schotterer, U. (1985) A long-term aerosol deposition record in a high-altitude alpine glacier. *WMO Technical Conference on Observation and Measurement of Atmospheric Contaminants* (*TECOMAC*) *Vienna*, WMO Report No. 647, pp. 623–631.

Wagenbach, D., Görlach, U., Moser, K. and Münnich, K. O. (1988) Coastal Antarctic aerosol: the seasonal pattern of its chemical composition and radionuclide content. *Tellus* **40B**, 426–436.

Wagenbach, D. and Geis, K. (1989) The mineral dust record in a high altitude glacier (Colle Gnifetti, Swiss Alps). In *Paleoclimatology and Paleometeorology*: *Modern and Past Patterns of Global Atmospheric Transport*, eds. M. Leinen, and M. Sarnthein, pp. 543–564. Kluwer Academic Publishers, Dordrecht.

Wagenbach, D., Geis, K., Hebestreit, K., Jung, W., Preunkert, S., Schäfer, J., Schajor, R., Ulshöfer, V. and Weddeling, P. (1997) Retrospective and present state of the anthropogenic aerosol deposition at a high altitude alpine glacier. In *Cloud Multi-phase Processes and High Alpine Air and Snow Chemistry*, eds. S. Fuzzi and D. Wagenbach, pp. 228–233. Springer, Berlin.

Wagenbach, D., Preunkert, S., Hebestreit, H., Schäfer, J., Kovac, J., Ulshöfer, V., Schajor, R. and Jung, W. (1998) Recent decadal changes of pollutant deposition recorded in a High Alpine cold glacier. *Atmospheric Environment* (submitted).

Zhang, X. and McMurry, P. H. (1992) Evaporative losses of fine particulate nitrates during sampling. *Atmospheric Environment* **26A**, 3305–3312.

Annex II

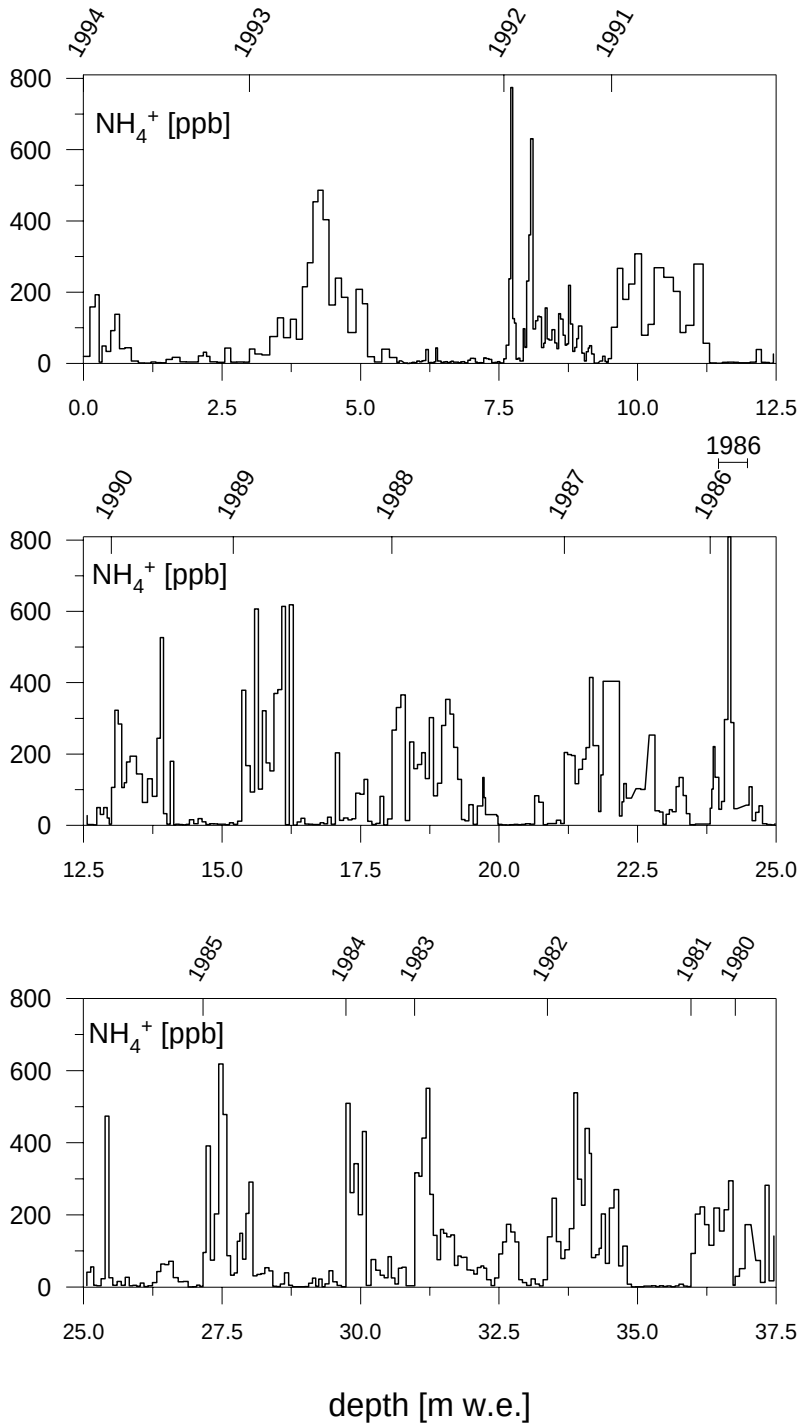

Figure A1a: NH_4^+ raw data profile of the Col du Dôme C10 ice core from the surface to 37.5 m w.e. depth, corresponding to the time period from 1994 to 1980.

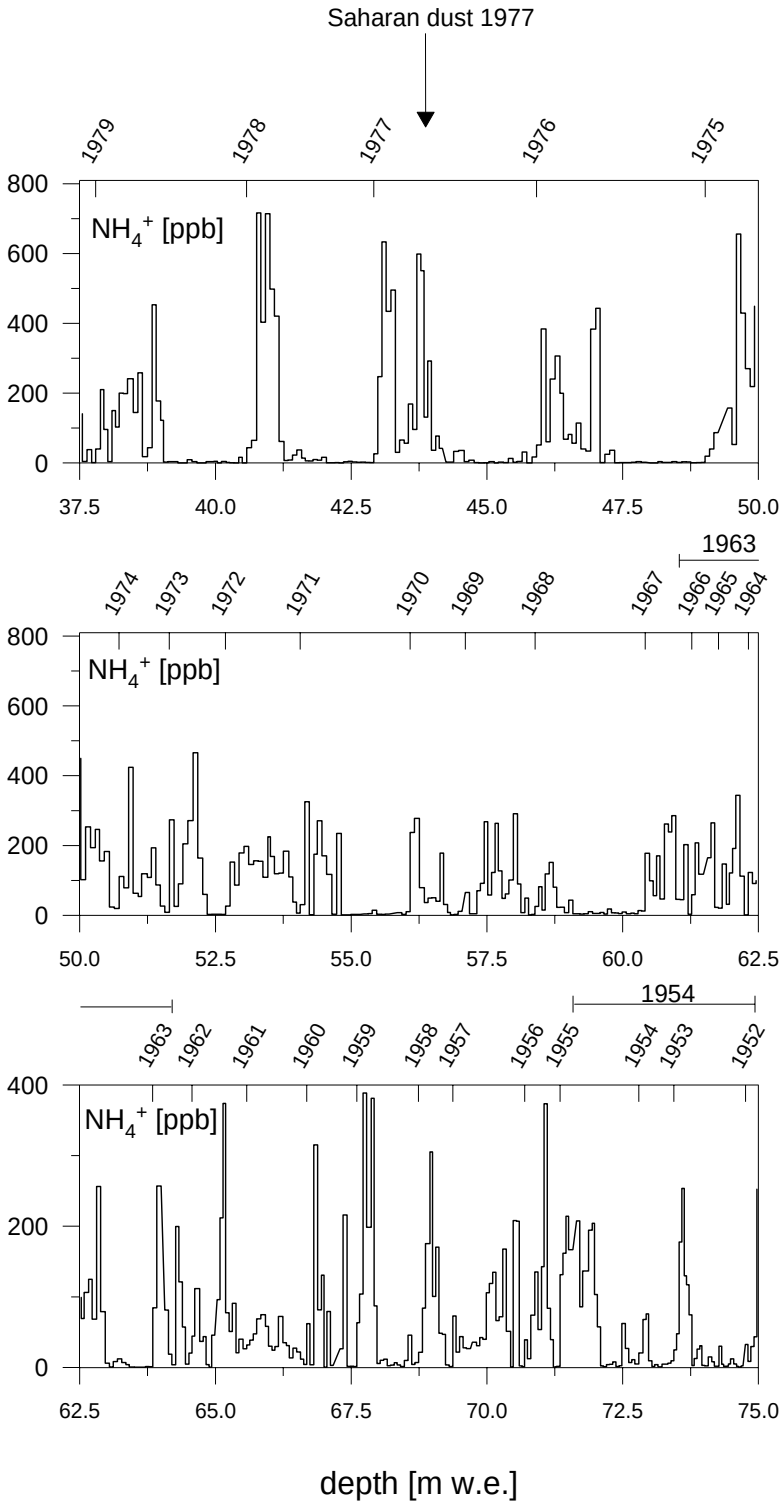

Figure A1b: NH_4^+ raw data profile of the Col du Dôme C10 ice core from 37.5 m w.e. to 75 m w.e. depth, corresponding to the time period from 1979 to 1952.

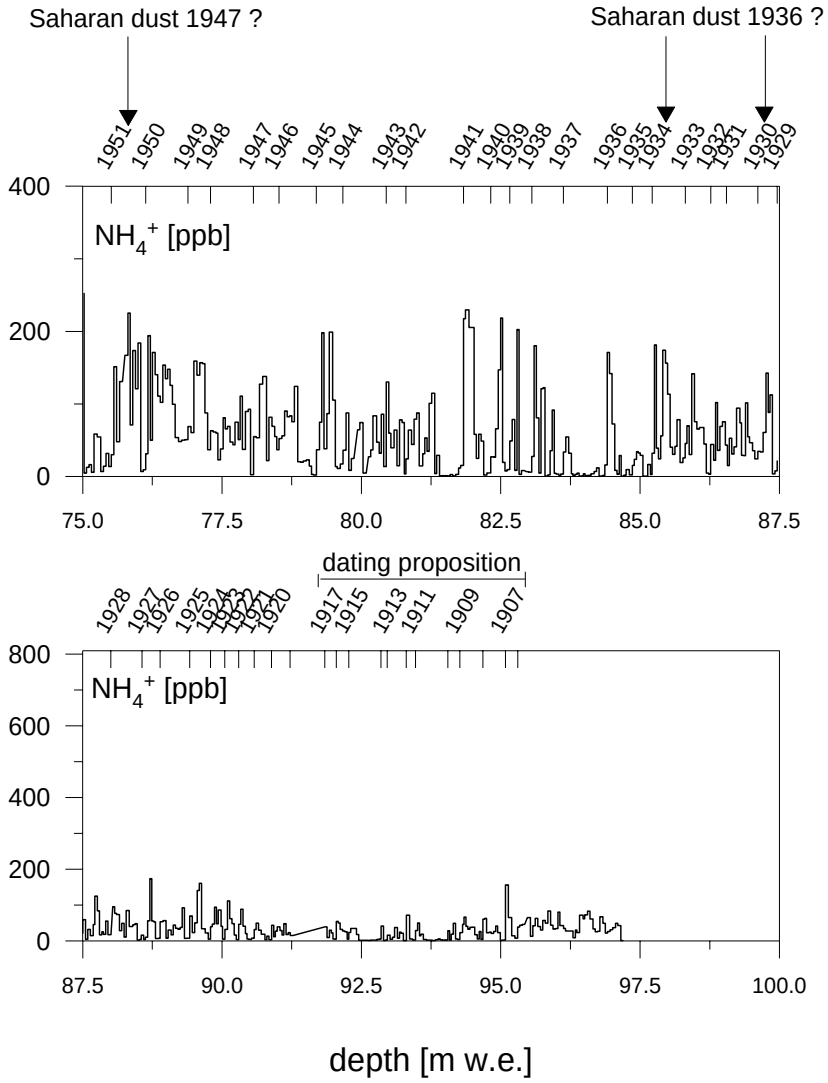

Figure A1c: NH_4^+ raw data profile of the Col du Dôme C10 ice core from 75 m w.e. to 97 m w.e. depth, corresponding to the time period from 1951 to ≈1900.

Acknowledgements

That's it, finally also this thesis has come to an end. For outstanding persons it might appear to be a harmless pile of written DIN A4 paper which weights nearly 1000 g. But this is far from reality and insiders know that the final arrangement of this pile of paper was preceded by many traps, as e.g. an IC device which was low in mind, a cold room which did not care if fingers and feats got frozen, a lonely aerosol sampling device which used to ask a lot of attention to remain in a good mood, and finally insidious data sets which made their deciphering as hard as possible, even sometimes not possible at all. With that it becomes clear that I couldn't end up in any way without the help of numerous humans. Thanks a lot to all of them.

Since my first contact with Alpine ice core studies dates back to a few years before starting this thesis, I want first of all to address my special thanks to Dietmar Wagenbach, from who I learned a lot about Alpine glacio-chemistry during the last nine years, and who was and is always disposable for me to discuss with and give advise in any scientific question. Actually it was him who opened the way for me to perform this thesis, and who acted during the last four years as a kind of unofficial co-supervisor.
Likewise I want to address my sincere thanks to my supervisor Michel Legrand. First for his efforts to make this thesis possible, for his confidence and the space he gave me to realize my scientific, technical and logistical ideas, but also for very fruitful discussions which were indispensable for interpreting the data finally in a scientific relevant geo-chemical way.
I want to thank also to Hans Puxbaum and Eric Wolff for accepting to review the thesis although this implied long travels for both of them, and to Michel Campillo for presiding the jury.

Further deep thanks go to many colleagues from the LGGE Grenoble but also to some of the IUP Heidelberg, the ETH Zürich and the IUP Bern for their indispensable help during the last four years. Unfortunately, to list all of them would explode the frame of this acknowledgement. On the other hand there are a few specimen which I do want to list here anyway.
Thanks a lot, Bruno, for you extensive help in "Fontanil", in the "Salle blanche", but in particular at "Vallot", and that even in times in which you had normally no minute free to do other things than working on your own thesis.
Likewise, this thesis wouldn't have been feasible without Alain and Claude who drilled in 1994 at Col du Dôme the principal ice core of this work, and who went "up there "again a few times with me in the last 4 years. Additional thanks to them and to Jean Philippe for their help to realize the "gold version" of the aerosol sampler ROBERTA.

However ROBERTA GOLD wouldn’t have been born without the ingenious electro technical ideas from Hans Georg Junghans (IUP Heidelberg) and Stephan Grabert. Many thanks for your help!
All the field work performed within this thesis wouldn’t have been possible without the logistical help and the commitment in the field of Christian, Delphine, Gilles, Phillipe, Jean Robert, Urs, Patric, Laurent, Marc, Raphaël, Danièle, Louis and certainly others which I missed here. Thanks a lot for your man power and the pleasant working atmosphere at 4400 m asl.
The deep drilling in 1999 couldn’t have been realized without the extensive help of our Swiss colleagues Stephan Sutter and Henry Rufli. Thank to radar measurements done by Stephan appropriate drill places could be found, at which Henry and this ice core auger drilled two nice ice cores down to bedrock. Thanks a lot to both of you for your support, which made this drilling action a pleasant affair.
Beside that, thanks a lot also to Francis for the complement ^{210}Pb and ^{137}Cs measurements, to Martine for all her efforts to keep the IC devices running, to Jocelyne for supporting me and making me surviving in the claws of French administration, and to Sophie for the help to find the right stuff within the labyrinth of “marchés publics”.
Not to forget, thanks a lot to Pascal, Corrado and Nadine from CMBH–Helicopters, for taking us up to and down from Col du Dôme whenever we needed although weather conditions were sometimes rather dubious.
The funding from Europe via the contracts ENV4-CT96-5051 (Environment and Climate Research Training) and ENV4-CT97 (ALPCLIM), from the CNRS, and the Ministry for Science and Research of Baden Württemberg is here also sincerely acknowledged.

But work is far away to be all to stand life and make it pleasant.
I am very grateful to all the colleagues of the LGGE who made the work there agreeable, but in particular to the “No Name band” who provided occasions of very pleasant beer and pastis breaks before and during the redaction of this thesis.
Further deep thanks to the community of the “Château" at 2, rue Béranger, and the “Atmosphere gang”. Their existence and presence made me feel at home in Grenoble.
On the other hand, I could not stand without some “ever lasting” friends form Heidelberg, Schwäbisch Hall and Zürich, which showed me that 700 km distance will not hamper any friendship.
Finally I am very, very grateful to my parents who supported and encouraged me in all the “plans“ and “studies” I followed during the last 33 years, and who had always confidence in the decisions I made.